International Journal of Bifurcation and Chaos, Vol. 17, No. 9 (2007) 2839–3012

A NONLINEAR DYNAMICS PERSPECTIVE OF WOLFRAM'S NEW KIND OF SCIENCE. PART VII: ISLES OF EDEN

LEON O. CHUA, JUNBIAO GUAN*,
VALERY I. SBITNEV and JINWOOK SHIN
Department of Electrical Engineering and Computer Sciences,
University of California at Berkeley,
Berkeley, CA 94720, USA
**Department of Mathematics,*
Shanghai University,
Shanghai 200436, P. R. China

Received February 5, 2007; Revised June 12, 2007

This paper continues our quest to develop a rigorous *analytical* theory of 1-D cellular automata via a nonlinear dynamics perspective. The 18 yet uncharacterized local rules are henceforth partitioned into ten *complex Bernoulli* σ_τ-shift rules and eight *hyper Bernoulli* σ_τ-shift rules, the latter including such famous rules $\boxed{30}$ and $\boxed{110}$. All exhibit a bizarre *composite wave dynamics* with arbitrarily large Bernoulli *velocity* σ and Bernoulli *return time* τ as the length $L \to \infty$.

Basin tree diagrams of all ten complex Bernoulli σ_τ-shift rules are exhibited for lengths $L = 3, 4, \ldots, 8$. Superficial as it may seem, these basin tree diagrams suggest general qualitative properties which have since been proved to be true in general. Two such properties form the main results of this paper; namely,

- Rule $\boxed{90}$ has *no Isles of Eden.*
- Rules $\boxed{105}$ and $\boxed{150}$ are composed of nothing but *Isles of Eden* for all string lengths L not divisible by 3.

Explicit global state transition formulas are given for local rules $\boxed{90}$, $\boxed{105}$ and $\boxed{150}$. Such formulas led to the rigorous proof of several surprising *periodicity constraints* for rule $\boxed{90}$, and to the discovery of a new global, *quasi-equivalence* class, defined via an *alternating transformation.* In particular, local rules $\boxed{105}$ and $\boxed{150}$ *are globally quasi-equivalent* where corresponding space-time patterns can be derived from each other by simply complementing every other row.

Another important result of this paper is the discovery of a *scale-free phenomenon* exhibited by the local rules $\boxed{90}$, $\boxed{105}$ and $\boxed{150}$. In particular, the *period* "T" of all *attractors* of rules $\boxed{90}$, $\boxed{105}$ and $\boxed{150}$, as well as of all *isles of Eden* of rules $\boxed{105}$ and $\boxed{150}$, increases *linearly with unit slope*, in logarithmic scale, with the length L.

Keywords: Cellular automata; nonlinear dynamics; attractors; Isles of Eden; Bernoulli shift; shift maps; basin tree diagram; Bernoulli velocity; Bernoulli return time; complex Bernoulli shifts; hyper Bernoulli shifts; rule 90; rule 105; rule 150; binomial series; scale-free phenomena.

1. Recap of Main Results from Parts I to VI

A rigorous *analytical* theory of one-dimensional cellular automata composed of $L \triangleq I + 1$ identical cells, as shown in Fig. 1, has been studied in the following series of papers from a *nonlinear dynamics* perspective[1]:

Part I: Threshold of Complexity [Chua *et al.*, 2002]
Part II: Universal Neuron [Chua *et al.*, 2003]
Part III: Predicting the Unpredictable [Chua *et al.*, 2004]
Part IV: From Bernoulli shift to $1/f$ spectrum [Chua *et al.*, 2005a]
Part V: Fractals everywhere [Chua *et al.*, 2005b]
Part VI: From Time-reversible attractors to the arrow of time [Chua *et al.*, 2006]

1.1. *Local rules and Boolean cubes*

Observe that the "zeros" and "ones" in Wolfram's truth tables [Wolfram, 2002] are symbolic variables denoting a logic "Yes" or "No" state, or a "high" or "low" state in digital electronic circuit implementations. In order to exploit powerful mathematical tools from nonlinear dynamics, it is necessary to work with *real* numbers. Consequently, in the papers cited above, the *symbolic* truth table shown in Fig. 1(c) is converted into the *numeric* truth table shown in Fig. 1(d).

One could also redefine the "0" and "1" in the symbolic truth tables as *real* numbers, instead of changing "0" to "−1". There are two reasons why we opted for the latter choice. First, each of the 256 local rules can be implemented on a cellular neural network (CNN) chip [Chua & Roska, 2002] with at least three orders of magnitude faster speed than computing on standard digital computers. Such CNN implementations require that the truth tables be formulated in terms of "1" and "−1" [Chang & Muthuswamy, 2007]. The second reason is that the numeric truth table shown in Fig. 1(d) can be conveniently represented by merely coloring the eight vertices of a "unit Boolean cube" whose center is located at the origin of the (u_{i-1}, u_i, u_{i+1}) — input space, as shown in Fig. 1(e). Such a representation in turn leads to simple visualizations of many rotational symmetrical transformations [Chua *et al.*, 2003]. Each of the 256 local rules corresponds to exactly one Boolean cube in Table 1 (extracted from [Chua *et al.*, 2003]). Observe that the number N printed under each cube corresponds to the local rule number in [Wolfram, 2002]. This number is easily obtained by adding the "vertex weights" of all *red* vertices in the Boolean cube, where the vertex weight for vertex k is equal to 2^k, as specified in Fig. 1(e), as well as in the lower part of Table 1.

1.2. *Threshold of complexity*

Observe also that the identification number N of each Boolean cube is colored in *red*, *blue* or *green*, depending on whether the red vertices can be segregated and separated from each other by $\kappa = 1, 2$, or 3 parallel planes, where κ is called *the index of complexity* of the local rule N [Chua *et al.*, 2002]. Table 2 lists all 256 local rules along with their index of complexity.

The *index of complexity* κ is *not* a *definition* of complexity. Rather it measures the relative number of electronic devices needed to implement each local rule. A $\kappa = 1$ local rule requires the smallest number of transistors. More transistors *must* be added to realize a $\kappa = 2$ local rule. Still more transistors are required to implement a $\kappa = 3$ local rule. In other words, the index of complexity κ measures the relative "cost" of hardware (Chip) implementations.

While the *asymptotic* qualitative *behaviors* of all $\kappa = 1$ local rules, and all $\kappa = 3$ local rules, have been completely understood and characterized in [Chua *et al.*, 2006], and in this paper (for Rules $\boxed{105}$, and $\boxed{150}$), there are some $\kappa = 2$ local rules that have not yet been characterized, including rules $\boxed{110}$, $\boxed{124}$, $\boxed{137}$ and $\boxed{193}$ [Chua *et al.*, 2004]. Since these four rules are universal Turing machines, they can never be completely characterized. In other words, it seems that $\kappa = 2$ can be considered as the *threshold of complexity*, in the sense articulated in [Wolfram, 2002].

[1]These 6-part papers have been republished, with errors corrected, in two recent edited books [Chua, 2006] and [Chua, 2007].

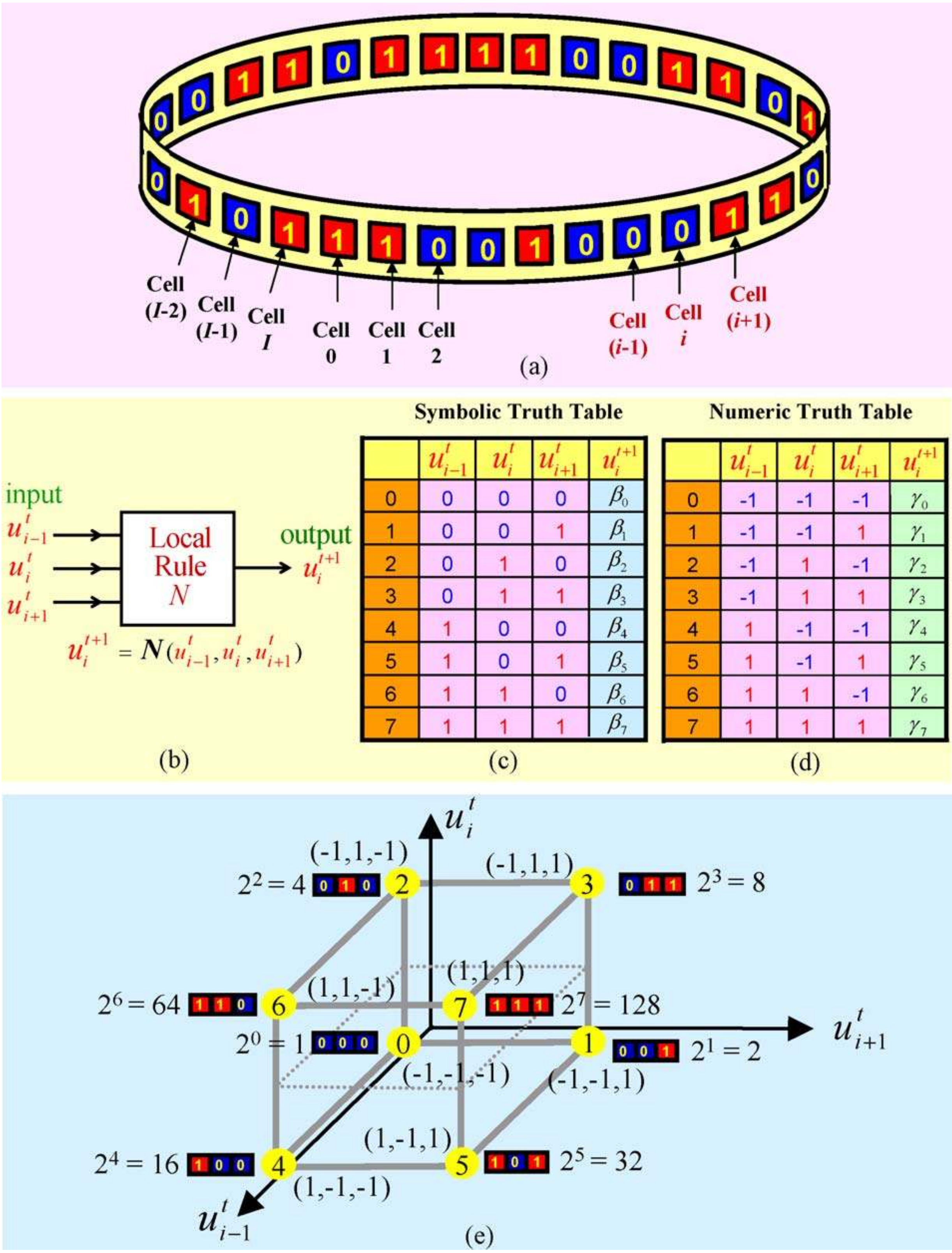

	u_{i-1}^t	u_i^t	u_{i+1}^t	u_i^{t+1}
0	0	0	0	β_0
1	0	0	1	β_1
2	0	1	0	β_2
3	0	1	1	β_3
4	1	0	0	β_4
5	1	0	1	β_5
6	1	1	0	β_6
7	1	1	1	β_7

	u_{i-1}^t	u_i^t	u_{i+1}^t	u_i^{t+1}
0	-1	-1	-1	γ_0
1	-1	-1	1	γ_1
2	-1	1	-1	γ_2
3	-1	1	1	γ_3
4	1	-1	-1	γ_4
5	1	-1	1	γ_5
6	1	1	-1	γ_6
7	1	1	1	γ_7

Fig. 1. (a) A one-dimensional Cellular Automata (CA) made of $L = I + 1$ identical cells with a periodic boundary condition. Each cell "i" is coupled only to its left neighbor cell $(i - 1)$ and right neighbor cell $(i + 1)$. (b) Each cell "i" is described by a local rule N, where N is a decimal number specified by a binary string $\{\beta_0, \beta_1, \ldots, \beta_7\}$, $\beta_i \in \{0, 1\}$. (c) The symbolic truth table specifying each local rule N, $N = 0, 1, 2, \ldots, 255$. (d) By recoding "0" to "-1", each row of the symbolic truth table in (c) can be recast into a numeric truth table, where $\gamma_k \in \{-1, 1\}$. (e) Each row of the numeric truth table in (d) can be represented as a *vertex* of a Boolean Cube whose color is red if $\gamma_k = 1$, and blue if $\gamma_k = -1$.

Table 1. Encoding 256 local rules defining a binary 1D CA onto 256 corresponding "Boolean Cubes".

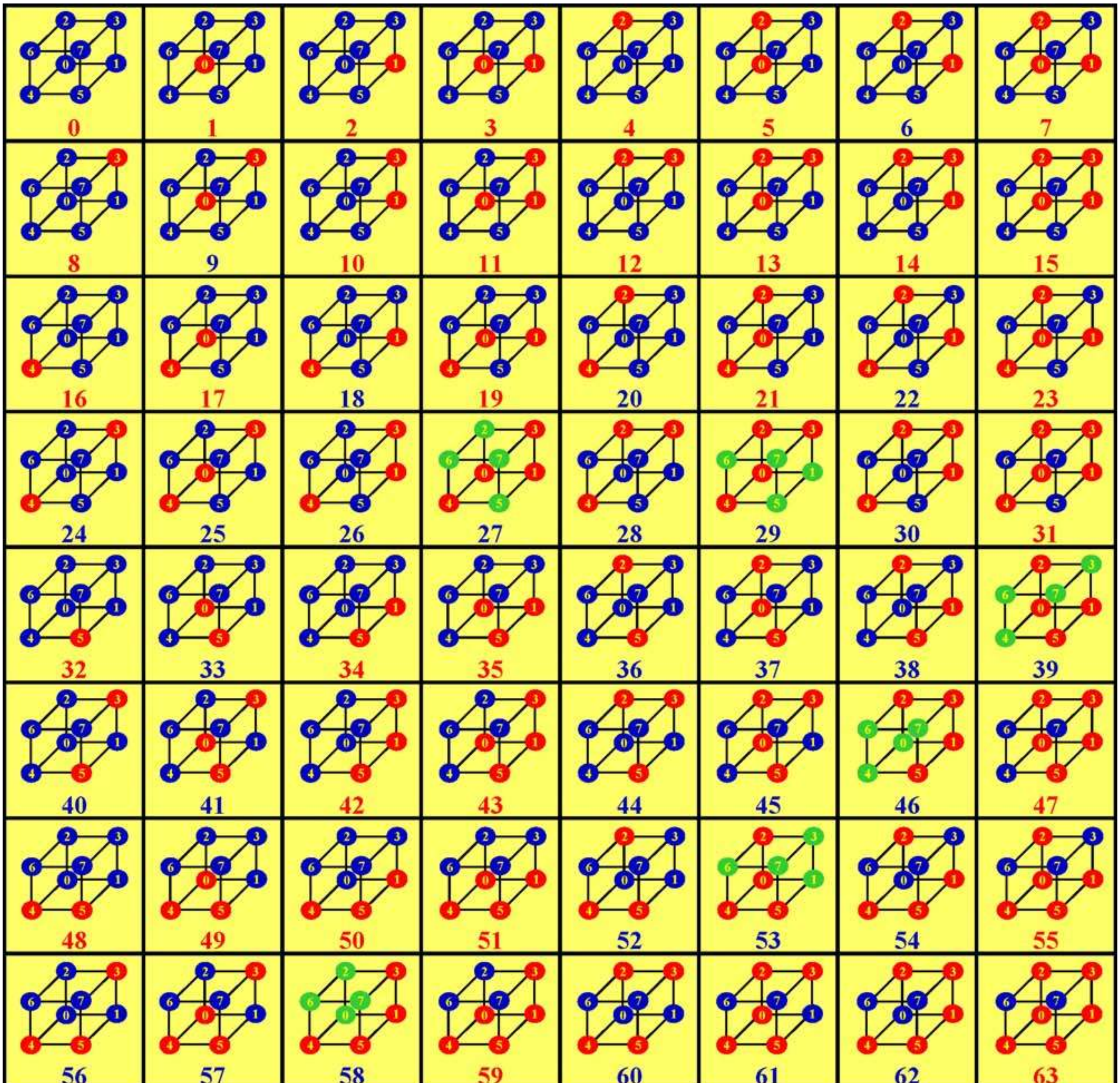

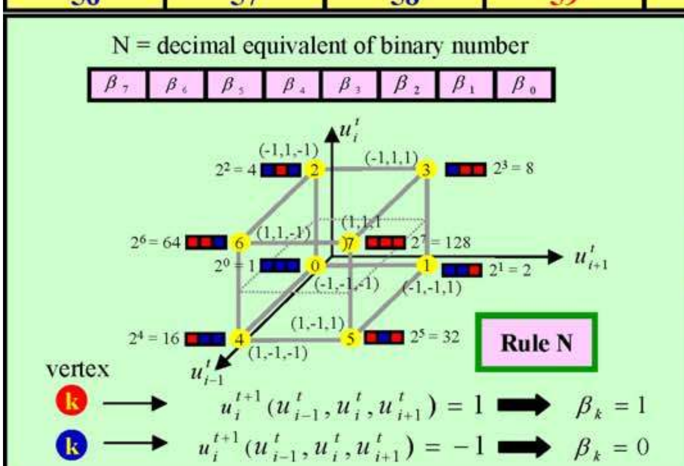

vertex (k)	u_{i-1}^t	u_i^t	u_{i+1}^t	u_i^{t+1}
0	-1	-1	-1	γ_0
1	-1	-1	1	γ_1
2	-1	1	-1	γ_2
3	-1	1	1	γ_3
4	1	-1	-1	γ_4
5	1	-1	1	γ_5
6	1	1	-1	γ_6
7	1	1	1	γ_7

Table 1. (*Continued*)

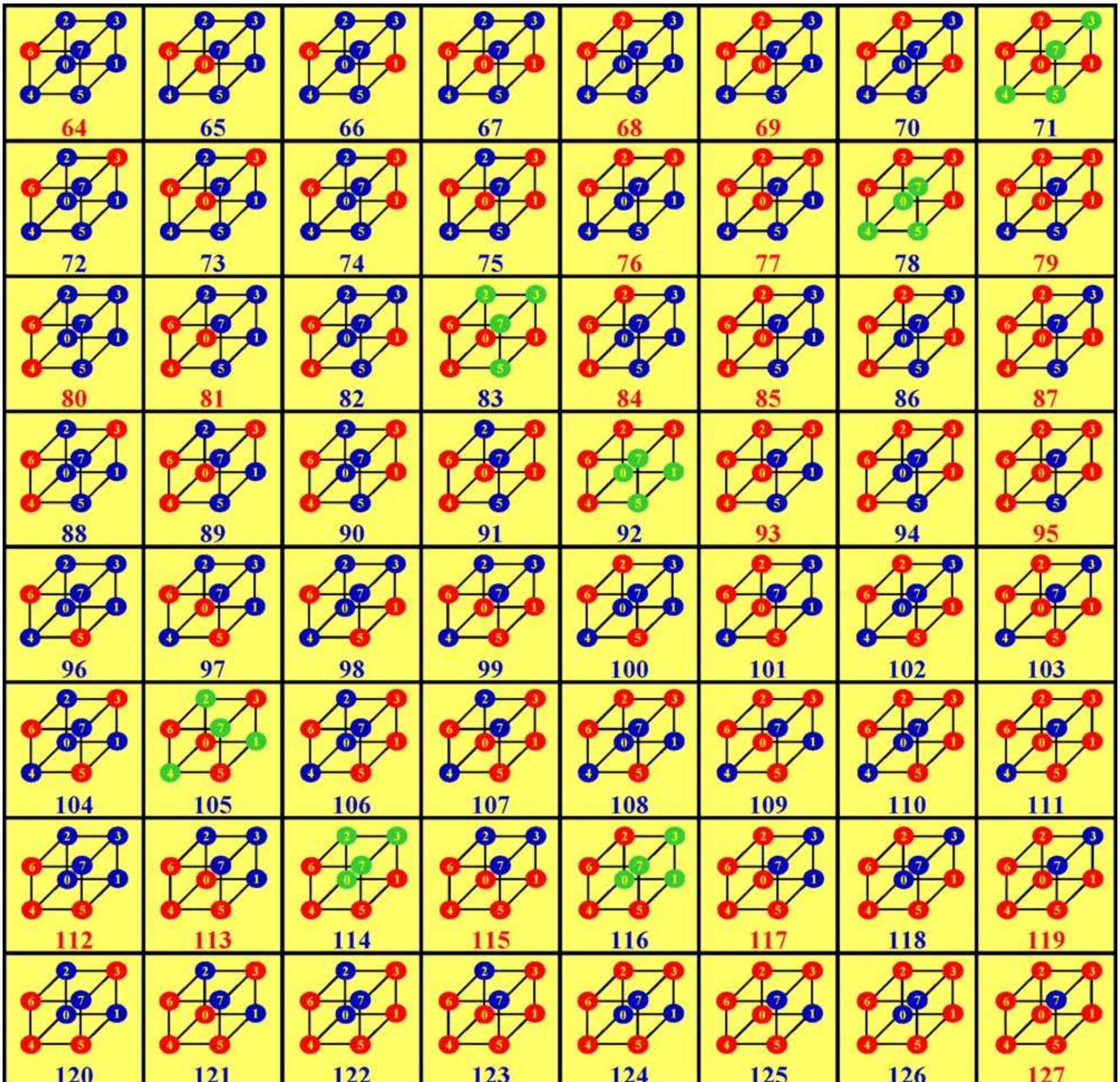

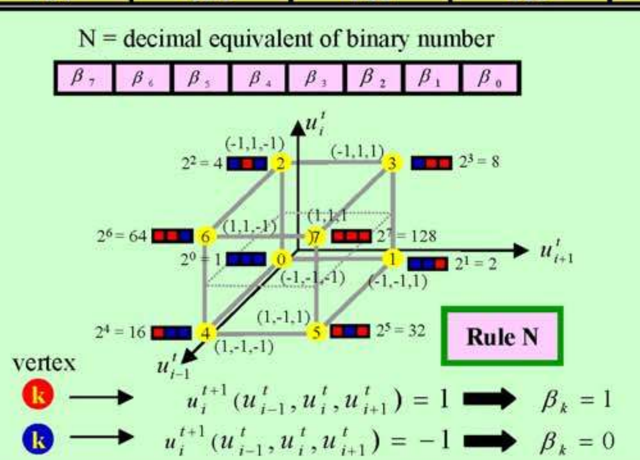

vertex (k)	u_{i-1}^t	u_i^t	u_{i+1}^t	u_i^{t+1}
0	-1	-1	-1	γ_0
1	-1	-1	1	γ_1
2	-1	1	-1	γ_2
3	-1	1	1	γ_3
4	1	-1	-1	γ_4
5	1	-1	1	γ_5
6	1	1	-1	γ_6
7	1	1	1	γ_7

Table 1. (*Continued*)

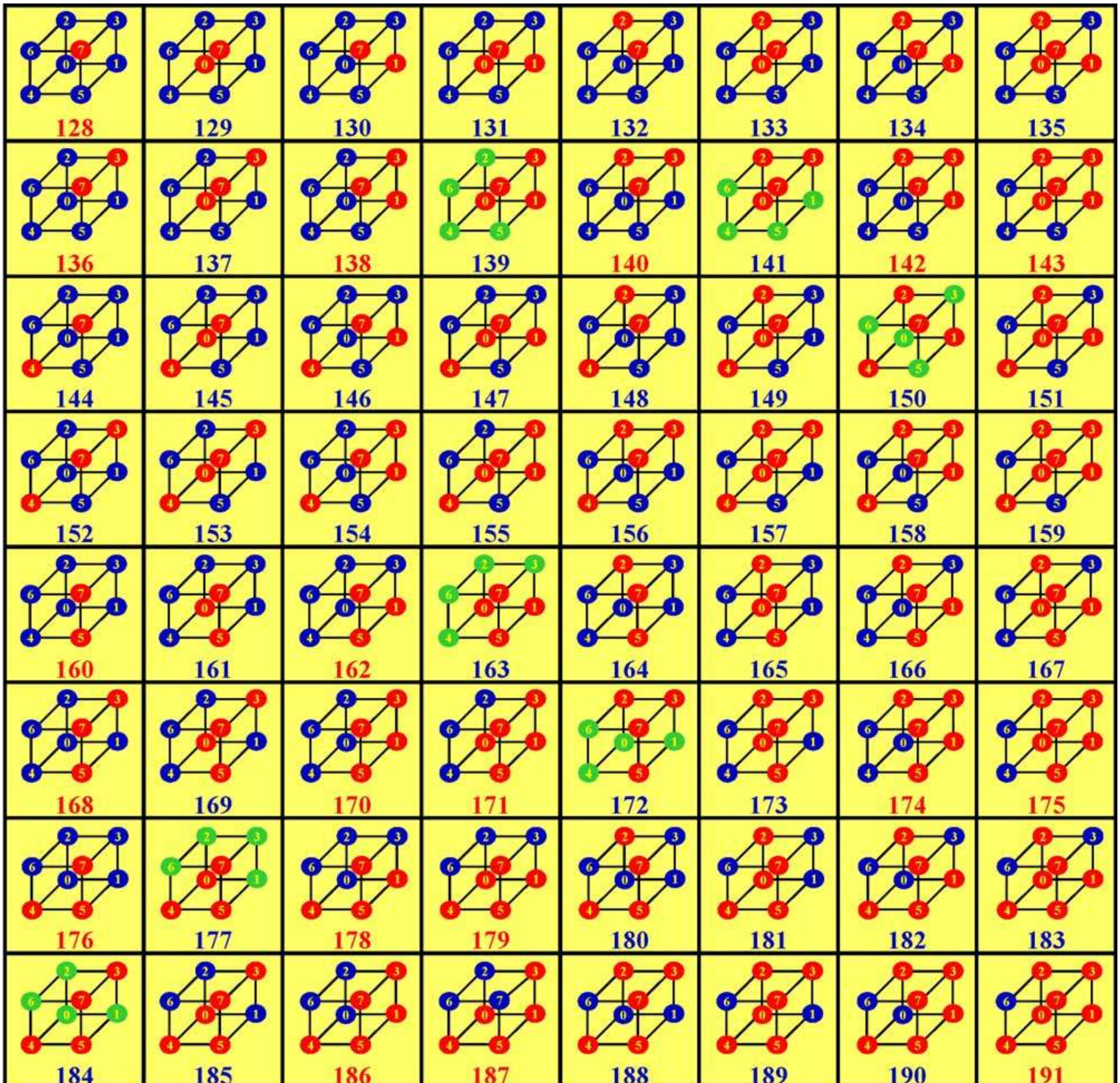

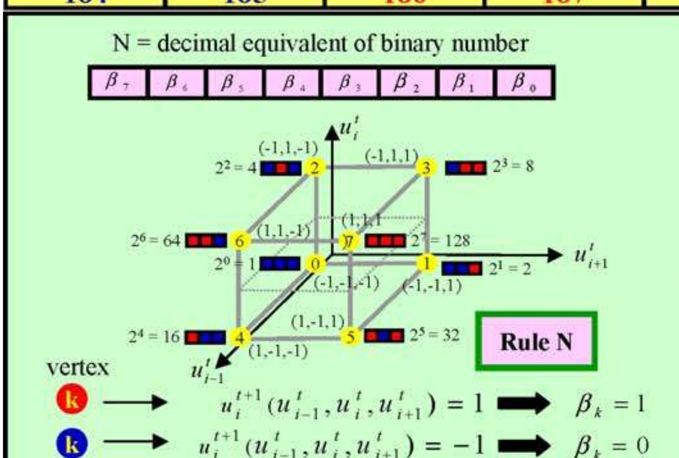

vertex (k)	u_{i-1}^t	u_i^t	u_{i+1}^t	u_i^{t+1}
0	-1	-1	-1	γ_0
1	-1	-1	1	γ_1
2	-1	1	-1	γ_2
3	-1	1	1	γ_3
4	1	-1	-1	γ_4
5	1	-1	1	γ_5
6	1	1	-1	γ_6
7	1	1	1	γ_7

Table 1. (*Continued*)

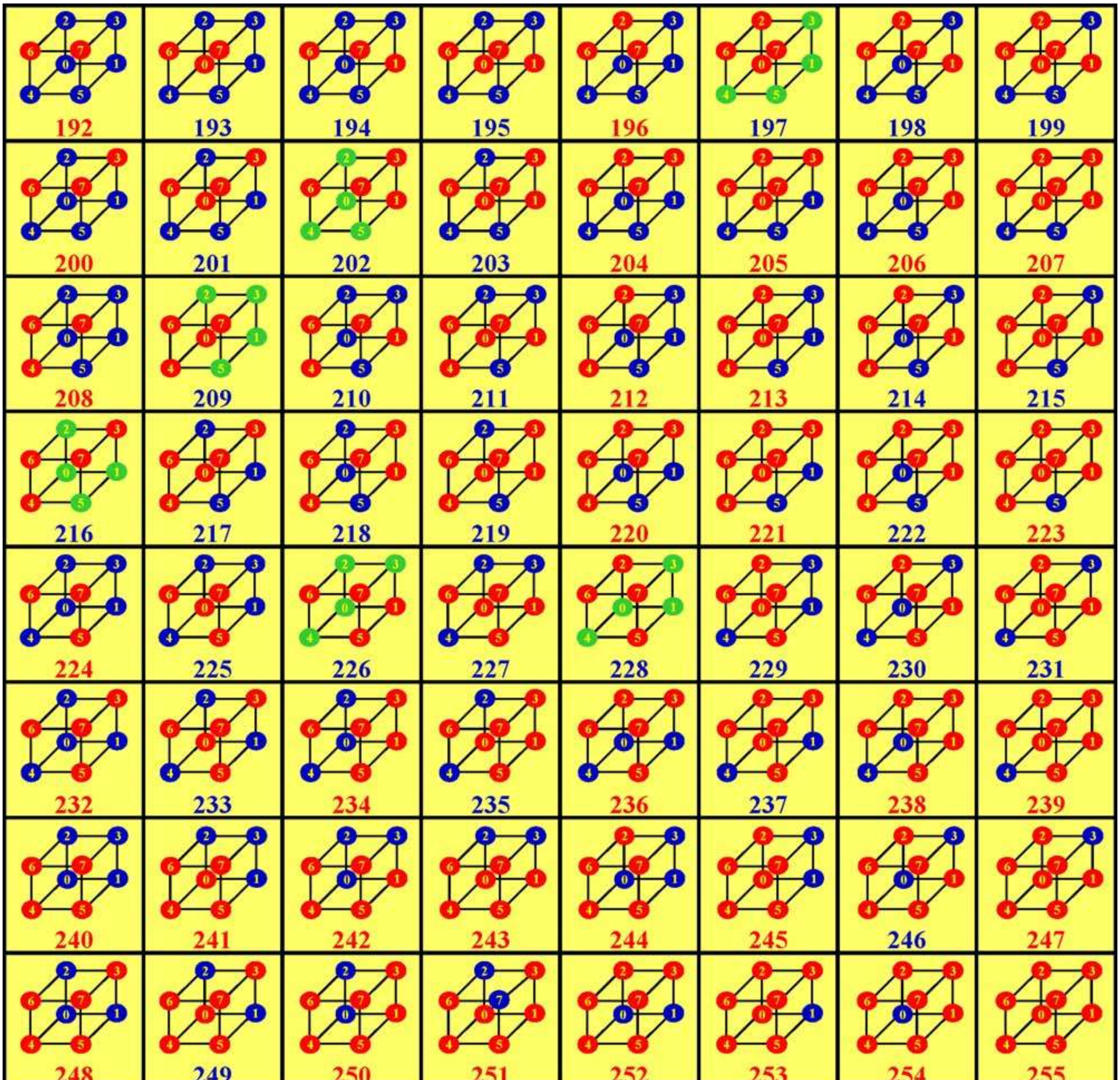

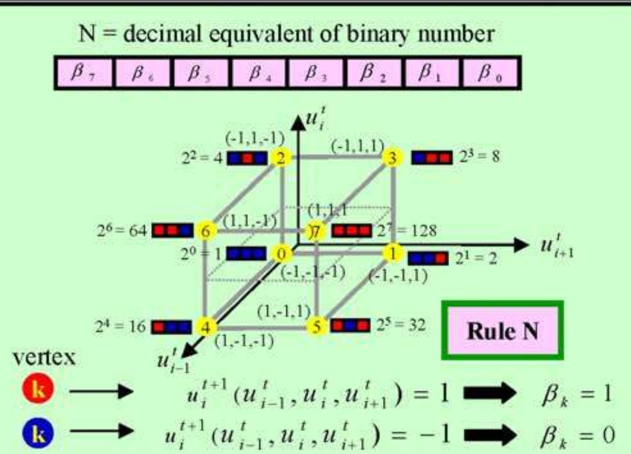

vertex k	u_{i-1}^t	u_i^t	u_{i+1}^t	u_i^{t+1}
0	-1	-1	-1	γ_0
1	-1	-1	1	γ_1
2	-1	1	-1	γ_2
3	-1	1	1	γ_3
4	1	-1	-1	γ_4
5	1	-1	1	γ_5
6	1	1	-1	γ_6
7	1	1	1	γ_7

Table 2. List of 256 local rules with their complexity index coded in red ($\kappa = 1$), blue ($\kappa = 2$) and green ($\kappa = 3$), respectively.

0	1	2	3	4	5	6	7	8	9	10	11	12	13	14	15
16	17	18	19	20	21	22	23	24	25	26	27	28	29	30	31
32	33	34	35	36	37	38	39	40	41	42	43	44	45	46	47
48	49	50	51	52	53	54	55	56	57	58	59	60	61	62	63
64	65	66	67	68	69	70	71	72	73	74	75	76	77	78	79
80	81	82	83	84	85	86	87	88	89	90	91	92	93	94	95
96	97	98	99	100	101	102	103	104	105	106	107	108	109	110	111
112	113	114	115	116	117	118	119	120	121	122	123	124	125	126	127
128	129	130	131	132	133	134	135	136	137	138	139	140	141	142	143
144	145	146	147	148	149	150	151	152	153	154	155	156	157	158	159
160	161	162	163	164	165	166	167	168	169	170	171	172	173	174	175
176	177	178	179	180	181	182	183	184	185	186	187	188	189	190	191
192	193	194	195	196	197	198	199	200	201	202	203	204	205	206	207
208	209	210	211	212	213	214	215	216	217	218	219	220	221	222	223
224	225	226	227	228	229	230	231	232	233	234	235	236	237	238	239
240	241	242	243	244	245	246	247	248	249	250	251	252	253	254	255

$\kappa = 1$ (Red) 104 rules

$\kappa = 2$ (Blue) 126 rules

$\kappa = 3$ (Green) 26 rules

1.3. *Only 88 local rules are independent*

Among the 256 local rules, only 88 are dynamically *independent*[2] from each other in the sense that the dynamics and solutions (space-time diagrams) of any one of the remaining 168 local rules can be derived *exactly* from one of the 88 *globally equivalent* rules, listed in Table 3 [Chua *et al.*, 2004], via one of the following three topological conjugacies:

3 Global Equivalence Transformations	1. *left-right transformation* $T^{\dagger}$ 2. *global complementation* $\overline{T}$ 3. *left-right complementation* T^{*}

For the reader's convenience, each of the 256 local rules is listed in the *left-most* column in Table 4, along with its equivalent local rule with respect to each of the above three global equivalence transformations. Observe that due to symmetries possessed by certain rules, some rules have only two *distinct* equivalent rules (e.g. $T^{\dagger}(\boxed{1}) = \boxed{1}$ and $\overline{T}(\boxed{1}) = T^{*}(\boxed{1}) = \boxed{127}$; $T^{\dagger}(\boxed{29}) = \overline{T}(\boxed{29}) = \boxed{71}$ and $T^{*}(\boxed{29}) = \boxed{29}$; $T^{\dagger}(\boxed{15}) = T^{*}(\boxed{15}) = \boxed{85}$ and $\overline{T}(\boxed{15}) = \boxed{15}$). Such rules are *identical twins*. There are altogether 72 identical twin local rules, as listed in Table 5. A few

[2] We thank Andy Adamatzky [Adamatzky, 2007] for suggesting possible intersections of our work with [Wuensche & Lesser, 1992]. We thank Andy Wuensche for informing us that the concept of global equivalence classes was first mentioned in [Walker, 1971]. The 88 equivalence classes of local rules were listed in [Walker & Aadryan, 1971] and [Wuensche & Lesser, 1992], using differing numbering schemes. It is likely that other results published, or yet to be published, in our series of *tutorial expositions* on "Wolfram's New Kind of Science" may also intersect, if not contained, in other works. We apologize to all such authors for not citing their publications, and we will appreciate their informing us of any such intersections so that future acknowledgments can be made. Being novice on the mature subject of *cellular automata*, the high probability of such inadvertent omissions is what prompted the authors to publish their papers as *expositions* for a nonspecialist audience, and not as original papers, in the *Tutorial-Review* section of this journal.

Table 3. The first 88 *globally-independent* local rules among the 256 listed in Table 2.

88 Global Equivalence Classes

0	1	2	3	4	5	6	7
8	9	10	11	12	13	14	15
18	19	22	23	24	25	26	27
28	29	30	32	33	34	35	36
37	38	40	41	42	43	44	45
46	50	51	54	56	57	58	60
62	72	73	74	76	77	78	90
94	104	105	106	108	110	122	126
128	130	132	134	136	138	140	142
146	150	152	154	156	160	162	164
168	170	172	178	184	200	204	232

local rules are endowed with additional symmetries such that $T^{\dagger}(\boxed{N}) = \overline{T}(\boxed{N}) = T^{*}(\boxed{N}) = \boxed{N}$. Such rules are *identical quadruplets*. There are only eight identical quadruplet rules, as listed in Table 6.

1.4. *Robust characterization of 70 independent local rules*

By virtue of the three *global equivalence* transformations derived in [Chua *et al.*, 2004] it suffices to conduct an in-depth analysis of *only* the 88 local rules listed in Table 3, out of 256, a saving of nearly 70% of otherwise wasted man hours! By using *random* bit strings (with at least $L = 400$ bits) as *testing* signals, we have found via extensive computer simulations, and supplemented by analytical studies [Chua *et al.*, 2006], that the *robust time asymptotic* dynamics of 70, out of 88, local rules can be characterized by only one of four *steady-state* behaviors.

1.4.1. *Steady-state behavior 1: Period-1 attractors or period-1 isles of Eden*

Table 7 lists 26 local rules from Table 3 which exhibit a robust *period-1* steady-state behavior corresponding to *fixed points* of the *time-1 characteristic function* $\chi^1_{\boxed{N}}$ of local rule $\boxed{N}$ [Chua *et al.*, 2004]. Except for rule $\boxed{204}$ where all orbits are period-1 *isles of Eden*, the *generic* steady-state behavior of the other 25 rules in Table 7 are all *period-1 attractors*. This asymptotic behavior holds for *almost all* initial random bit strings, and for *arbitrary length* $L \triangleq I + 1$.

1.4.2. *Steady-state behavior 2: Period-2 attractors or period-2 isles of Eden*

Table 8 lists 13 local rules from Table 3 which exhibit a robust *period-2* steady-state behavior corresponding to *fixed points* of the *time-2 characteristic* function $\chi^2_{\boxed{N}}$ of local rule $\boxed{N}$ [Chua *et al.*, 2006]. Except for rule $\boxed{51}$ where all orbits are period-2 *isles of Eden*, the *generic* steady-state behavior of the other 12 rules in Table 8 are all *period-2 attractors*. This asymptotic behavior holds for almost all initial random bit strings, and for arbitrary L.

1.4.3. *Steady-state behavior 3: Period-3 attractors*

There is only one rule from Table 3 which exhibits a robust *period-3 attractor*, namely, rule $\boxed{62}$. As demonstrated in, Figs. 5–14 of [Chua *et al.*, 2006], almost all initial bit strings of $\boxed{62}$ converge to a *period-3 orbit* corresponding to *fixed points* of the *time-3* characteristic function $\chi^3_{\boxed{62}}$ of local rule $\boxed{62}$ [Chua *et al.*, 2006]. The other attractors of $\boxed{62}$ have a relatively small *basin of attraction*. The period-3 isles of Eden of $\boxed{62}$ have no basins of attraction and therefore require an initial bit string falling exactly on one of the three bit strings forming an isle of Eden.

1.4.4. *Steady-state behavior 4: Bernoulli σ_τ-shift attractors or isles of Eden*

Table 9 lists 30 local rules from Table 3 which exhibit a robust Bernoulli σ_τ-shift steady-state behavior corresponding to a *period-T attractor* or a *period-T isle of Eden*, where $T \le \tau L$. The three parameters (σ, τ, β) characterizing each Bernoulli rules are listed in Table 10 for each of the 30 robust Bernoulli rules listed in Table 9.[3] We will henceforth call "σ" the *Bernoulli Shift Velocity*, "τ" the *Bernoulli Return Time* and "β" the *Bernoulli Complementation sign*, or simply Bernoulli

[3]Table 10 is constructed from Table 16 of [Chua *et al.*, 2005, pp. 1159–1162].

Table 4. Table of globally equivalent local rules. All local rules in each row are globally equivalent to each other. Rows with red, blue, or green background colors denote local rules with a *complexity index* $\kappa = 1, 2$, or 3, respectively.

Rule Number N	Left — Right Transformation $T^{\dagger}[N]$	Global Complementation $\bar{T}[N]$	Left — Right Complementation $T^{*}[N]$
0	0	255	255
1	1	127	127
2	16	191	247
3	17	63	119
4	4	223	223
5	5	95	95
6	20	159	215
7	21	31	87
8	64	239	253
9	65	111	125
10	80	175	245
11	81	47	117
12	68	207	221
13	69	79	93
14	84	143	213
15	85	15	85
16	2	247	191
17	3	119	63
18	18	183	183
19	19	55	55
20	6	215	159
21	7	87	31
22	22	151	151
23	23	23	23
24	66	231	189
25	67	103	61
26	82	167	181
27	83	39	53
28	70	199	157
29	71	71	29
30	86	135	149
31	87	7	21
32	32	251	251
33	33	123	123
34	48	187	243
35	49	59	115
36	36	219	219
37	37	91	91
38	52	155	211
39	53	27	83
40	96	235	249
41	97	107	121
42	112	171	241
43	113	43	113
44	100	203	217
45	101	75	89
46	116	139	209
47	117	11	81
48	34	243	187
49	35	115	59
50	50	179	179
51	51	51	51
52	38	211	155
53	39	83	27
54	54	147	147
55	55	19	19
56	98	227	185
57	99	99	57
58	114	163	177
59	115	35	49
60	102	195	153
61	103	67	25
62	118	131	145
63	119	3	17

Table 4. (*Continued*)

Rule Number N	Left — Right Transformation $T^{\dagger}[N]$	Global Complementation $\bar{T}[N]$	Left — Right Complementation $T^{*}[N]$
64	8	253	239
65	9	125	111
66	24	189	231
67	25	61	103
68	12	221	207
69	13	93	79
70	28	157	199
71	29	29	71
72	72	237	237
73	73	109	109
74	88	173	229
75	89	45	101
76	76	205	205
77	77	77	77
78	92	141	197
79	93	13	69
80	10	245	175
81	11	117	47
82	26	181	167
83	27	53	39
84	14	213	143
85	15	85	15
86	30	149	135
87	31	21	7
88	74	229	173
89	75	101	45
90	90	165	165
91	91	37	37
92	78	197	141
93	79	69	13
94	94	133	133
95	95	5	5

Rule Number N	Left — Right Transformation $T^{\dagger}[N]$	Global Complementation $\bar{T}[N]$	Left — Right Complementation $T^{*}[N]$
96	40	249	235
97	41	121	107
98	56	185	227
99	57	57	99
100	44	217	203
101	45	89	75
102	60	153	195
103	61	25	67
104	104	233	233
105	105	105	105
106	120	169	225
107	121	41	97
108	108	201	201
109	109	73	73
110	124	137	193
111	125	9	65
112	42	241	171
113	43	113	43
114	58	177	163
115	59	49	35
116	46	209	139
117	47	81	11
118	62	145	131
119	63	17	3
120	106	225	169
121	107	97	41
122	122	161	161
123	123	33	33
124	110	193	137
125	111	65	9
126	126	129	129
127	127	1	1

Table 4. (*Continued*)

Rule Number N	Left — Right Transformation $T^{\dagger}[N]$	Global Complementation $\bar{T}[N]$	Left — Right Complementation $T^{*}[N]$
128	128	254	254
129	129	126	126
130	144	190	246
131	145	62	118
132	132	222	222
133	133	94	94
134	148	158	214
135	149	30	86
136	192	238	252
137	193	110	124
138	208	174	244
139	209	46	116
140	196	206	220
141	197	78	92
142	212	142	212
143	213	14	84
144	130	246	190
145	131	118	62
146	146	182	182
147	147	54	54
148	134	214	158
149	135	86	30
150	150	150	150
151	151	22	22
152	194	230	188
153	195	102	60
154	210	166	180
155	211	38	52
156	198	198	156
157	199	70	28
158	214	134	148
159	215	6	20
160	160	250	250
161	161	122	122
162	176	186	242
163	177	58	114
164	164	218	218
165	165	90	90
166	180	154	210
167	181	26	82
168	224	234	248
169	225	106	120
170	240	170	240
171	241	42	112
172	228	202	216
173	229	74	88
174	244	138	208
175	245	10	80
176	162	242	186
177	163	114	58
178	178	178	178
179	179	50	50
180	166	210	154
181	167	82	26
182	182	146	146
183	183	18	18
184	226	226	184
185	227	98	56
186	242	162	176
187	243	34	48
188	230	194	152
189	231	66	24
190	246	130	144
191	247	2	16

Table 4. (*Continued*)

Rule Number N	Left — Right Transformation $T^{\dagger}[N]$	Global Complementation $\bar{T}[N]$	Left — Right Complementation $T^{*}[N]$
192	136	252	238
193	137	124	110
194	152	188	230
195	153	60	102
196	140	220	206
197	141	92	78
198	156	156	198
199	157	28	70
200	200	236	236
201	201	108	108
202	216	172	228
203	217	44	100
204	204	204	204
205	205	76	76
206	220	140	196
207	221	12	68
208	138	244	174
209	139	116	46
210	154	180	166
211	155	52	38
212	142	212	142
213	143	84	14
214	158	148	134
215	159	20	6
216	202	228	172
217	203	100	44
218	218	164	164
219	219	36	36
220	206	196	140
221	207	68	12
222	222	132	132
223	223	4	4
224	168	248	234
225	169	120	106
226	184	184	226
227	185	56	98
228	172	216	202
229	173	88	74
230	188	152	194
231	189	24	66
232	232	232	232
233	233	104	104
234	248	168	224
235	249	40	96
236	236	200	200
237	237	72	72
238	252	136	192
239	253	8	64
240	170	240	170
241	171	112	42
242	186	176	162
243	187	48	34
244	174	208	138
245	175	80	10
246	190	144	130
247	191	16	2
248	234	224	168
249	235	96	40
250	250	160	160
251	251	32	32
252	238	192	136
253	239	64	8
254	254	128	128
255	255	0	0

Table 5. List of 72 identical twin rules.

0	1	4	5	250	251	254	255
15	18	19	22	233	236	237	240
29	32	33	36	219	222	223	226
37	43	50	54	201	205	212	218
55	57	71	72	183	184	198	200
73	76	85	90	165	170	179	182
91	94	95	99	156	160	161	164
104	108	109	113	142	146	147	151
122	123	126	127	128	129	132	133

Table 6. List of eight identical quadruplet rules.

23	51	77	105	150	178	204	232

velocity, *time*, and *sign*, respectively. Observe that local rules $\boxed{6}$, $\boxed{9}$, $\boxed{11}$, $\boxed{14}$, $\boxed{27}$, $\boxed{35}$, $\boxed{38}$, $\boxed{43}$, $\boxed{56}$, $\boxed{57}$, $\boxed{58}$, $\boxed{134}$, $\boxed{142}$, and $\boxed{184}$ have two robust Bernoulli attractors, whereas local rules $\boxed{25}$ and $\boxed{74}$ have three robust Bernoulli attractors.

Observe from Table 10 that only five rules listed in Table 10 ($\boxed{11}$, $\boxed{14}$, $\boxed{15}$, $\boxed{43}$ and $\boxed{142}$) have a *negative* sign for β. The *space-time* evolution patterns of these five rules are generated by following the same procedures as the other rules (*shift left* by σ bits if $\sigma > 0$, or *shift right* by $|\sigma|$ bits if $\sigma < 0$, every τ iterations), and then *complementing* (change color of all bits) the resulting bit string. In fact, except for rule $\boxed{15}$, only one of two Bernoulli attractors from the other four rules have a negative sign for β.

Observe that any Bernoulli (σ, τ, β) rule with $\beta < 0$ is equivalent to iterating the rule with *twice* the *velocity* and *return time without* complementation, i.e.

$$(\sigma, \tau, \beta) = (2\sigma, 2\tau, |\beta|), \quad \text{if } \beta < 0 \qquad (1)$$

For examples illustrating this equivalence, see Table 5 (pp. 2393) for $\boxed{15}$ in [Chua *et al.*, 2003], Fig. 29(a_2) for $\boxed{11}$, Fig. 29(b_2) for $\boxed{14}$, Fig. 29(d_2) for $\boxed{43}$, and Fig. 29(i_2) for $\boxed{142}$ in [Chua *et al.*, 2006].

In general, $T = \tau L$ if $T_0 \triangleq \tau L/|\sigma|$ is not an integer. If T_0 is an integer, then $T = \tau L/|\sigma|$ for $|\sigma| \geq 2$. If each bit string in the period-T orbit consists of a concatenation of m identical substrings, then the period T is reduced further to T/m.

Each Bernoulli rule listed in Table 9 can possess up to three robust Bernoulli attractors, as depicted in Table 29A of [Chua *et al.*, 2006, pp. 1293–1297] for rules $\boxed{74}$, $\boxed{88}$, $\boxed{173}$ and $\boxed{229}$. Each of these attractors has a large enough basin of attraction that different random initial bit strings could converge to one of these robust Bernoulli σ_τ-shift attractors. This steady-state behavior does *not* depend on the length $L \triangleq I + 1$ of the bit string. Except for local rule $\boxed{15}$ and $\boxed{170}$, whose orbits are all *isles of Eden*, all other *generic* steady states converge to a Bernoulli σ_τ-shift attractor.

1.4.5. *There are ten complex Bernoulli and eight hyper Bernoulli shift rules*

Together, Tables 7–9, plus the period-3 rule $\boxed{62}$, made up 70, out of the 88, local rules from Table 3. The robust steady-state behaviors of these 70 local rules have been completely characterized in [Chua *et al.*, 2006]. The remaining 18 rules listed in Table 3 that have not yet been characterized are listed in Table 11, dubbed *complex Bernoulli-shift* rules, and Table 12, dubbed *hyper Bernoulli-shift rules*. It will be clear from the sequel that all of these 18 yet uncharacterized rules are also identified with *Bernoulli shifts* because they behave like Bernoulli σ_τ-shifts from Table 9 except that the number of attractors is no longer bounded by 3, but increases

Table 7. List of 26 robust Period-1 local rules.

26 Topologically-Distinct Period-1 Rules

0	4	8	12	13
32	36	40	44	72
76	77	78	94	104
128	132	136	140	160
164	168	172	200	204
232				

Table 8. List of 13 robust Period-2 local rules.

13 Topologically-Distinct Period-2 Rules

1	5	19	23
28	29	33	37
50	51	108	156
178			

Table 9. List of 30 robust Bernoulli σ_τ-shift local rules.

30 Topologically-Distinct Bernoulli σ_τ -shift Rules

2	3	6	7	9
10	11	14	15	24
25	27	34	35	38
42	43	46	56	57
58	74	130	134	138
142	152	162	170	184

with the length $L \triangleq I + 1$ of the bit strings. The ten complex Bernoulli shift rules in Table 11 are *bilateral*, and correspond to those listed in column 1 of Table 17 of [Chua *et al.*, 2006, pp. 1176]. The eight hyper Bernoulli-shift rules in Table 12 are *nonbilateral*, and correspond to those listed in column 1 of Table 18 of [Chua *et al.*, 2006]. Table 13 gives a composition of the asymptotic behaviors of all 88 dynamically-independent local rules listed in Table 3.

In this paper (Part VII) only the ten *complex Bernoulli-shift rules* from Table 11 will be studied. The remaining eight *Hyper Bernoulli-shift rules* from Table 12 will be studied in Part VIII.

2. Basin Tree Diagrams of Ten Complex Bernoulli Shift Rules

For binary bit strings

$$\boldsymbol{x}^n = (x_0^n \quad x_1^n \quad x_2^n \quad \cdots \quad x_{L-1}^n) \tag{2}$$

at *time* n with *finite* L and periodic (or fixed) boundary conditions, the evolution

$$\boldsymbol{x}^n \mapsto \boldsymbol{\chi}^1_{\boxed{N}}(\boldsymbol{x}^n) \triangleq \boldsymbol{x}^{n+1} \tag{3}$$

under local rule $\boxed{N}$ must converge to either a *fixed point*

$$\boldsymbol{x}^* = (x_0^{n^*} \quad x_1^{n^*} \quad x_2^{n^*} \quad \cdots \quad x_{L-1}^{n^*}) \tag{4}$$

or to a *periodic orbit* $\Gamma_T(\boxed{N})$ of period $T \leq T_{\max}$, at some *finite* time $n^* = T_{\text{transient}} + T$, where

$$\boldsymbol{\chi}^1_{\boxed{N}} : \sum \to \sum \tag{5}$$

is the *time-1 characteristic function* defined in [Chua *et al.*, 2005a], and

$$T_{\max} \triangleq 2^L \tag{6}$$

is the number of distinct binary bit strings of length L.

2.1. *Basin of attraction and basin trees*

In general, many initial bit strings can converge to one of several *period-T orbits*, including period-1 orbits (i.e. fixed points of $\chi^1_{\boxed{N}}$).

Definition 1. Basin of attraction $B(\Gamma_T(\boxed{N}))$ of $\Gamma_T(\boxed{N})$.

The *union* of all bit strings which converge to a period-T orbit $\Gamma_T(\boxed{N})$ of local rule $\boxed{N}$, *including* all bit strings belonging to $\Gamma_T(\boxed{N})$, is called the *basin of attraction* $\mathcal{B}(\Gamma_T(\boxed{N}))$ of $\Gamma_T(\boxed{N})$.

Table 10. Bernoulli Parameters σ (Bernoulli shift *velocity*), τ (Bernoulli return *time*), and β (Bernoulli complementation *sign*) associated with the 30 Robust Bernoulli Rules from Table 9.

N	σ	τ	β
2	1	1	+
3	-1	2	+
6	2	2	+
	-2	2	+
7	-1	2	+
9	-2	2	+
	2	3	+
10	1	1	+
11	1	1	+
	-1	1	−
14	1	1	+
	-1	1	−
15	-1	1	−
24	-1	1	+
25	-1	2	+
	3	3	+
	2	5	+
27	-1	2	+
	2	2	+
34	1	1	+
35	-1	2	+
	1	1	+
38	2	2	+
	2	2	+
42	1	1	+
43	1	1	+
	-1	1	−
46	1	1	+
56	1	1	+
	-1	1	+
57	1	1	+
	-1	1	+
58	1	1	+
	-1	2	+
74	1	1	+
	2	2	+
	-3	3	+
130	1	1	+
134	2	2	+
	-2	2	+
138	1	1	+
142	1	1	+
	-1	1	−
152	-1	1	+
162	1	1	+
170	1	1	+
184	1	1	+
	-1	1	+

Table 11. List of ten complex Bernoulli-shift rules.

18	22	54	73	90
105	122	126	146	150

Table 12. List of eight Hyper Bernoulli-shift rules.

26	**30**	**41**	**45**
60	**106**	**110**	**154**

Table 13. Steady-state characterization of 88 dynamically-independent local rules.

Topological Classifications of 88 Equivalence Classes

Topologically-distinct Rules	Number
Period-1 Rules	26
Period-2 Rules	13
Period-3 Rules	1
Bernoulli σ_τ-Shift Rules	30
Complex-Bernoulli-Shift Rules	10
Hyper Bernoulli-Shift Rules	8
Total	**88**

More precisely,

$$\mathcal{B}\left(\Gamma_T\left(\boxed{N}\right)\right) \triangleq \cup\left\{x \in \sum : \rho^n_{\boxed{N}}(x) \in \Gamma_T\right\} \tag{7}$$

where $\rho^n_{\boxed{N}}(x) \triangleq \underbrace{\rho^1_{\boxed{N}} \circ \rho^1_{\boxed{N}} \circ \cdots \circ \rho^1_{\boxed{N}}(x)}_{n \text{ times}}$

is the *time-n map* of $\boxed{N}$ [Chua *et al.*, 2005a] $\rho^n_{\boxed{N}} : x^0 \mapsto x^n$, where n depends in general on $\boldsymbol{x}$.

Definition 2. Basin Trees $\Im(\Gamma_T)$. The set of all bit strings which converges to a period-T orbit $\Gamma_T(\boxed{N})$, *excluding* $\Gamma_T(\boxed{N})$, is called the *basin trees* of $\Gamma_T(\boxed{N})$.

More precisely,

$$\Im(\Gamma_T) \triangleq \mathcal{B}\left(\Gamma_T\left(\boxed{N}\right)\right) \backslash \Gamma_T\left(\boxed{N}\right) \tag{8}$$

An example of a basin tree is shown in Fig. 3(g) of [Chua *et al.*, 2006] for rule $\boxed{62}$ with $L = 9$. In this case, $\Gamma_T = \Gamma_1(\boxed{62}) = 0$, and

$$\begin{aligned}\Im(\Gamma_T) &= \Im\left(\Gamma_1\left(\boxed{62}\right)\right) \\ &= \{73, 85, 146, 149, 165, 169, \\ &\qquad 170, 292, 298, 330, 338, 340, 511\}\end{aligned}$$

$$\mathcal{B}\left(\Gamma_T\left(\boxed{62}\right)\right) \triangleq \Im(\Gamma_1) \cup 0 \tag{9}$$

Observe from Fig. 3(g) that the *digraph* of $\Im(\Gamma_1(\boxed{62}))$ is a *directed tree* from *graph theory*.

Another example of a basin tree is shown in Fig. 6 of [Chua *et al.*, 2006]. Consider the period-3 orbit

$$\Gamma_3\left(\boxed{62}\right) \triangleq \{3, 38, 61\} \tag{10}$$

in Fig. 6(a)-i. The basin tree of $\Gamma_3(\boxed{62})$ is the set of bit strings

$$\Im(\Gamma_3) \triangleq \{40, 23, 60, 1, 35, 22\} \tag{11}$$

In this case, one can associate the basin tree $\Im(\Gamma_3)$ as two subtrees $\{40\}$ and $\{23, 60, 1, 35, 22\}$ emerging from the period-3 orbit $\Gamma_3(\boxed{62})$, which is analogous to a *cluster of roots*. For large L, a basin tree in general is made of many topologically similar subtrees, such as Fig. 11 of [Chua *et al.*, 2006]. In this case, we have a period-14 orbit

$$\begin{aligned}\Gamma\left(\boxed{62}\right) = \{&59, 102, 93, 51, 110, 89, 55, \\ &108, 91, 54, 109, 27, 118, 77\}\end{aligned} \tag{12}$$

and the basin tree $\Im(\Gamma_{14}(\boxed{62}))$ of $\Gamma_{14}(\boxed{62})$ is made of seven subtrees having identical topologies.

2.2. *Garden of Eden*

Definition 3. Garden of Eden. A bit string

$$\boldsymbol{x} = (x_0 \quad x_1 \quad x_2 \quad \ldots \quad x_{L-1})$$

is said to be a *garden of Eden* of a local rule $\boxed{N}$ iff its *preimage* is an empty set.

More precisely,[4] a bit string $\boldsymbol{x}$ is a *garden of Eden* of $\boxed{N}$ iff it has no *predecessors* in the sense

[4]Under Definition 3, a *fixed point* x^* of $\chi^1_{\boxed{N}}$, i.e. a *period-1 orbit*, is not a garden of Eden of $\boxed{N}$ because $\chi^{-1}(x^*) = x^*$.

that there *does not exist* a bit string y such that $\boldsymbol{x} = \chi^1_{\boxed{N}}(y)$.

Many examples of gardens of Eden can be found in [Chua *et al.*, 2006]. In particular, all *gardens of Eden* of $\boxed{62}$ are identified by a *pink* color in Figs. 3, 6, 8, 9, 11–14, in [Chua *et al.*, 2006]. Observe that they are just the *terminus* of subtrees.

2.3. *Isle of Eden*

A cursory inspection of the basin of attractions of the period-3 orbits $\Gamma_3(\boxed{62})$ of rule $\boxed{62}$ in Figs. 5(a)–5(f) in [Chua *et al.*, 2006] reveals that there are no basin trees converging to any node (i.e. bit string) belonging to these period-3 orbits! Such orbits are indeed special, and except for rules $\boxed{15}$, $\boxed{85}$, $\boxed{45}$, $\boxed{105}$, $\boxed{150}$, $\boxed{154}$, $\boxed{170}$, and $\boxed{240}$, they are isolated period-T orbits which are *buried* amidst neighboring bit strings belonging to basin trees of other periodic orbits. We will see in Part VIII that for large L, these isolated period-T orbits could have extremely long periods and hence are very, very hard to find,[5] like well-hidden *Easter eggs*! Moreover, such rare objects *cannot* exist in $\mathbb{R}^n$ in view of the *Zubov–Ura–Kimura Theorem* [Garay & Hofbauer, 2003], which implies that "no compact isolated invariant sets in $\mathbb{R}^n$ can be an isle of Eden". These objects can be either *isolated* or *dense*, and are called *Isles of Eden* in [Chua *et al.*, 2005b] and [Chua *et al.*, 2006]. It's time to give a formal definition.

Definition 4. Isle of Eden.

A bit string

$$\boldsymbol{x} = (x_0 \quad x_1 \quad x_2 \quad \cdots \quad x_{L-1})$$

is said to be a *period-n isle of Eden* of a local rule $\boxed{N}$ iff its *preimage* under $\chi^n_{\boxed{N}}$ is *itself*, where $\chi^n_{\boxed{N}}$ is the *time-n characteristic function* of $\boxed{N}$.

More precisely, $\boldsymbol{x}$ is a *period-n isle of Eden* of a local rule $\boxed{N}$ iff

$$\chi^{-n}_{\boxed{N}}(\boldsymbol{x}) = \boldsymbol{x} \tag{13}$$

Proposition 1. *A bit string $\boldsymbol{x}$ is a period-n isle of Eden of $\boxed{N}$ $\Leftrightarrow$ $\boldsymbol{x}$ belongs to a period-n orbit $\Gamma_n(\boxed{N})$ with an empty basin tree; i.e.*

$$\Im(\Gamma_n(\boxed{N})) = \emptyset \tag{14}$$

when $\emptyset$ denotes the empty set.

Proof. Follows directly from Definitions 2 and 4. ■

Corollary 1. *A bit string $\boldsymbol{x}$ is a period-n isle of Eden of $\boxed{N}$ $\Leftrightarrow$ the orbit through $\boldsymbol{x}$ is a period-n orbit $\Gamma_n(\boxed{N})$ where each bit string $\boldsymbol{x}$, $\chi^1_{\boxed{N}}(\boldsymbol{x}), \chi^2_{\boxed{N}}(\boldsymbol{x}), \ldots, \chi^{n-1}_{\boxed{N}}(\boldsymbol{x})$ has a unique preimage.*

Proof. Follows from Eq. (14) and Proposition 1. ■

Remarks

1. To avoid clutter, we will usually refer to *all* bit strings belonging to the orbit of a *period-n isle of Eden* also as an *isle of Eden*.
2. Every bit string belonging to a period-n isle of Eden has exactly one *incoming* and one *outgoing* bit string, for all $n \geq 2$.

2.4. *Gallery of basin tree diagrams*

The collection of all *period-n orbits* $\Gamma_n(\boxed{N})$ of all possible periods $n = 1, 2, \ldots$ and their associated *basin trees* $\Im(\Gamma_n(\boxed{N}))$ of an L-bit cellular automata under local rule $\boxed{N}$ is called a *basin tree diagram* of local rule $\boxed{N}$. An examination of such diagrams, even for a relatively small L, can reveal certain characteristic qualitative behaviors of the space-time patterns of many local rules. These empirical characteristics can sometimes be proved to be true in general, as will be illustrated for the *complex Bernoulli shift* rules $\boxed{105}$ and $\boxed{150}$ in this paper, and for the *hyper Bernoulli shift* rules $\boxed{45}$ and $\boxed{154}$ in Part VIII.

A *gallery* of such *basin tree diagrams* for the ten *complex Bernoulli shift* rules listed in Table 11 is exhibited in Tables 14–23 for $L = 3, 4, 5, 6, 7$ and 8, respectively. Each table displays the periodic orbits and their basin trees, where each bit string is displayed in color along with its *decimal* identification number, calculated from the decimal equivalent of the binary bit string as in Fig. 6 of [Chua *et al.*, 2006]. For example, for $L = 3$, the two binary bit strings and in Gallery 18-1 from Table 14 would be identified by the decimal numbers[6]

$$1 \bullet 2^2 + 0 \bullet 2^1 + 0 \bullet 2^0 = 4$$

[5] Every isolated long-period isle of Eden is a gem worth digging for. They would provide ideal havens for cryptographic systems. Any one who discovers a long-period isle of Edens earns the right of naming it after himself for posterity reasons!

[6] Each page of the basin tree diagrams listed under Tables 14–23 will be called a *gallery*, and identified by a *Gallery number* $N - k, k = 1, 2, \ldots$, where N is the local rule number.

Table 14. Basin tree diagrams for rule $\boxed{18}$.

Basin tree diagrams for Rule $\boxed{18}$

$\boxed{18}$, $L = 3$ (a) Period-1 Attractor : $\rho_1 = \frac{8}{8} = 1$

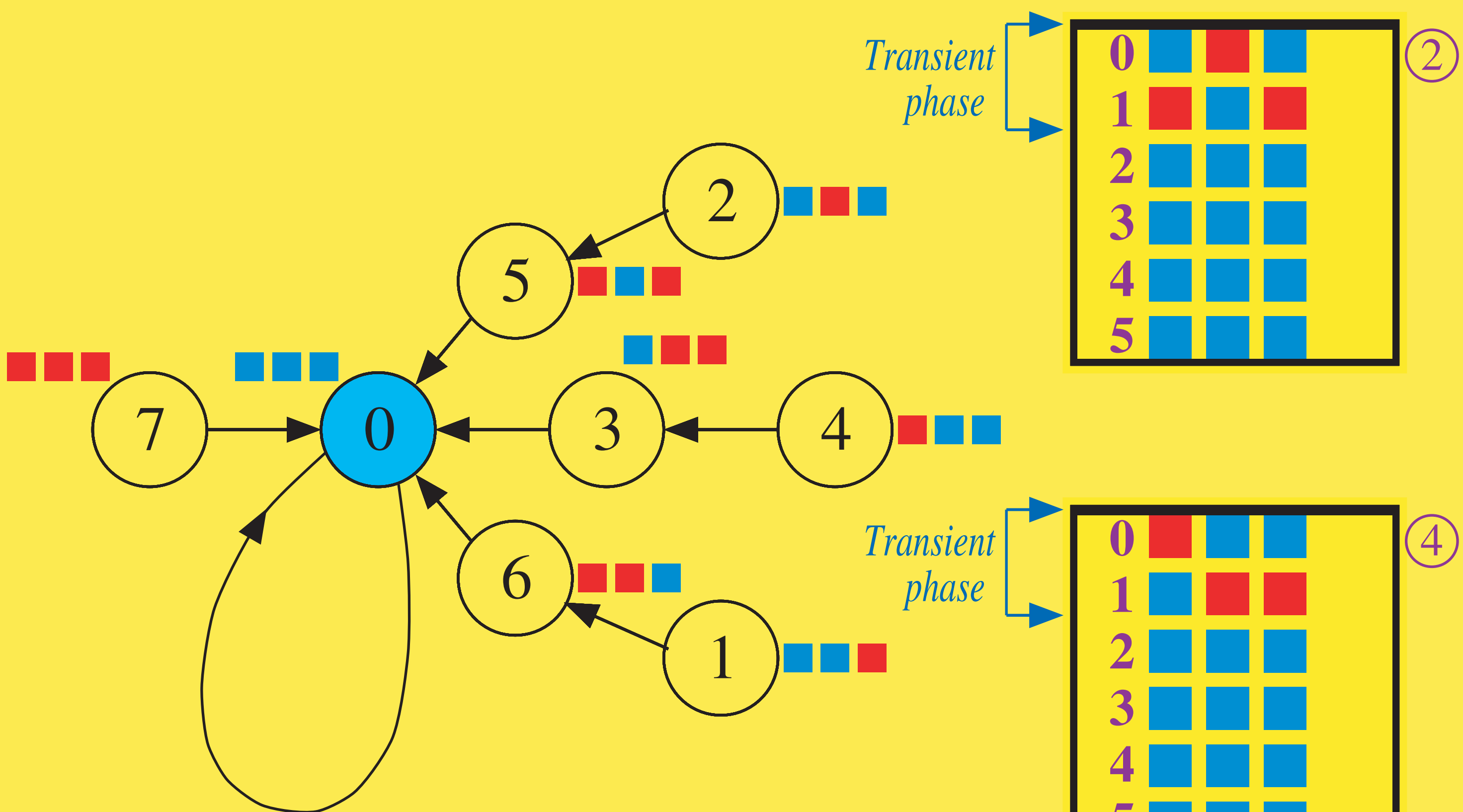

Gallery 18 -1

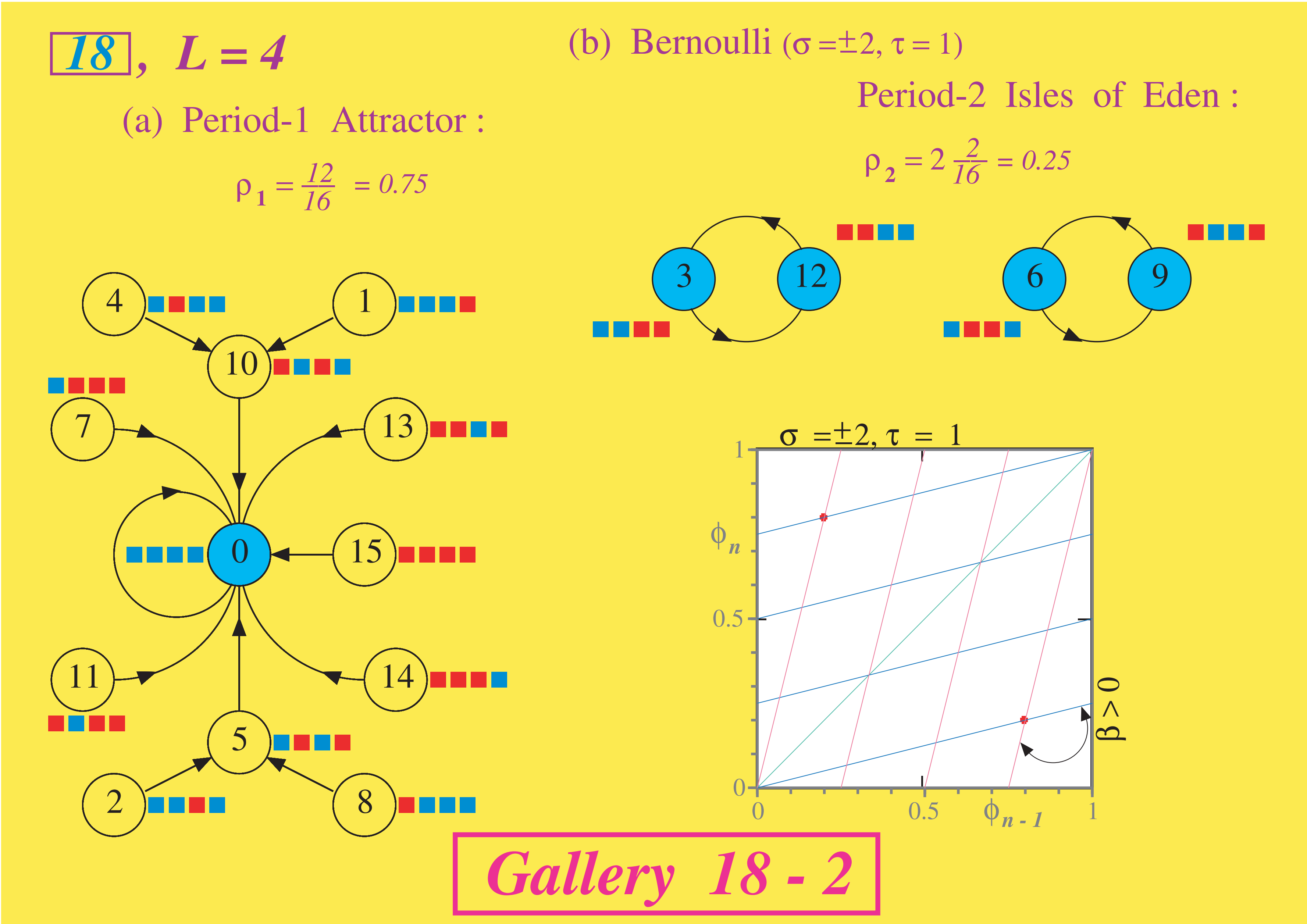

18, L = 4
(a) Period-1 Attractor :
ρ1 = 12/16 = 0.75
4
1
10
7
13
0
15
11
14
5
2
8
(b) Bernoulli (σ = ±2, τ = 1)
Period-2 Isles of Eden :
ρ2 = 2 2/16 = 0.25
3
12
6
9
σ = ±2, τ = 1
φn
φn-1
β > 0
0
0.5
1
Gallery 18 - 2

$\boxed{18}$, $L = 5$

(a) Period-1 Attractor : $\rho_1 = \frac{12}{32} = 0.375$

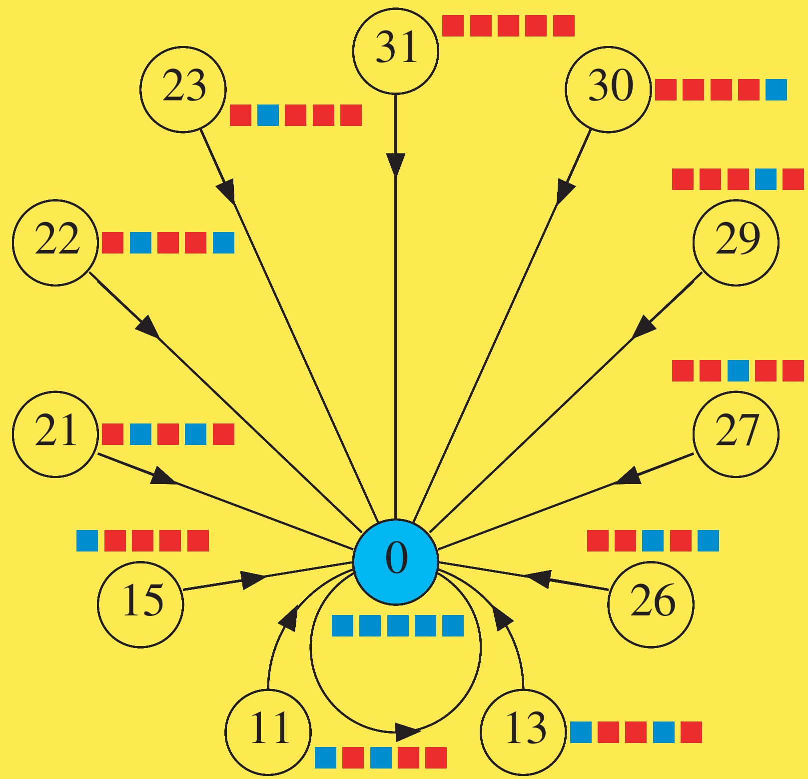

Gallery 18 - 3

$\boxed{18}$, $L = 5$ (b) Bernoulli ($\sigma = \pm 5, \tau = 2$) Period-2 Attractors : $\rho_2 = 5\,\frac{4}{32} = 0.625$

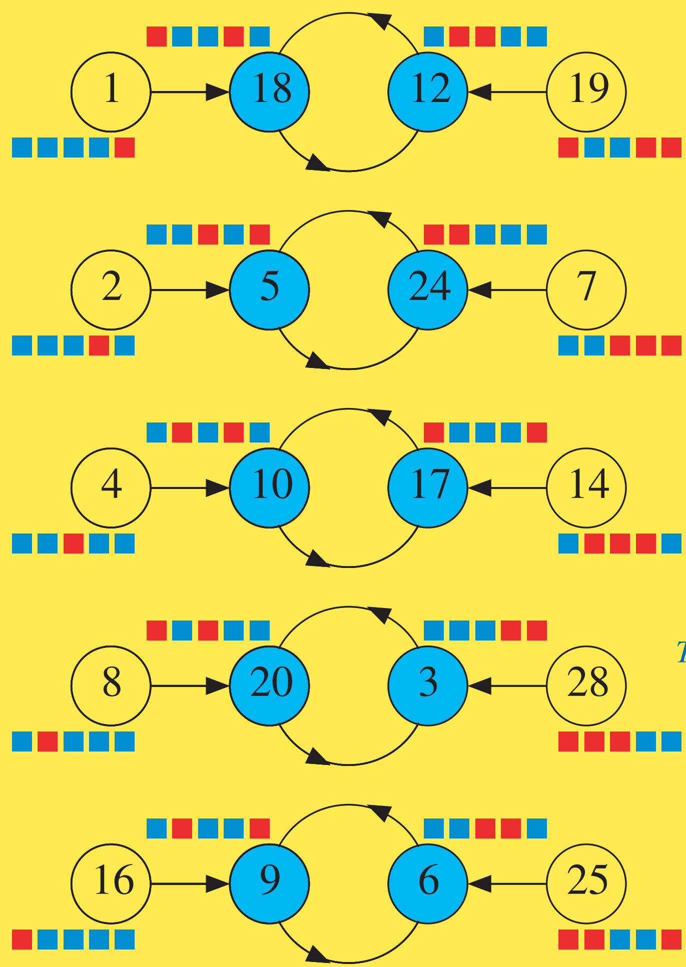

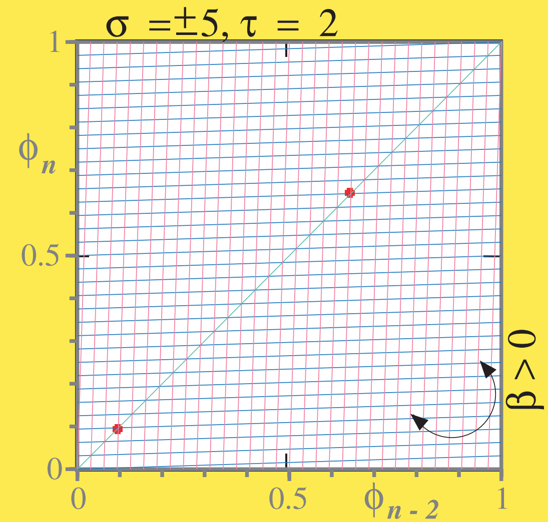

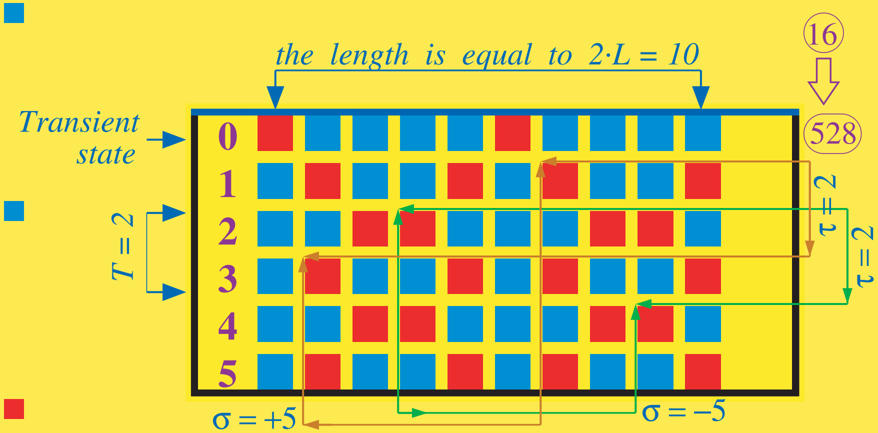

Gallery 18 - 4

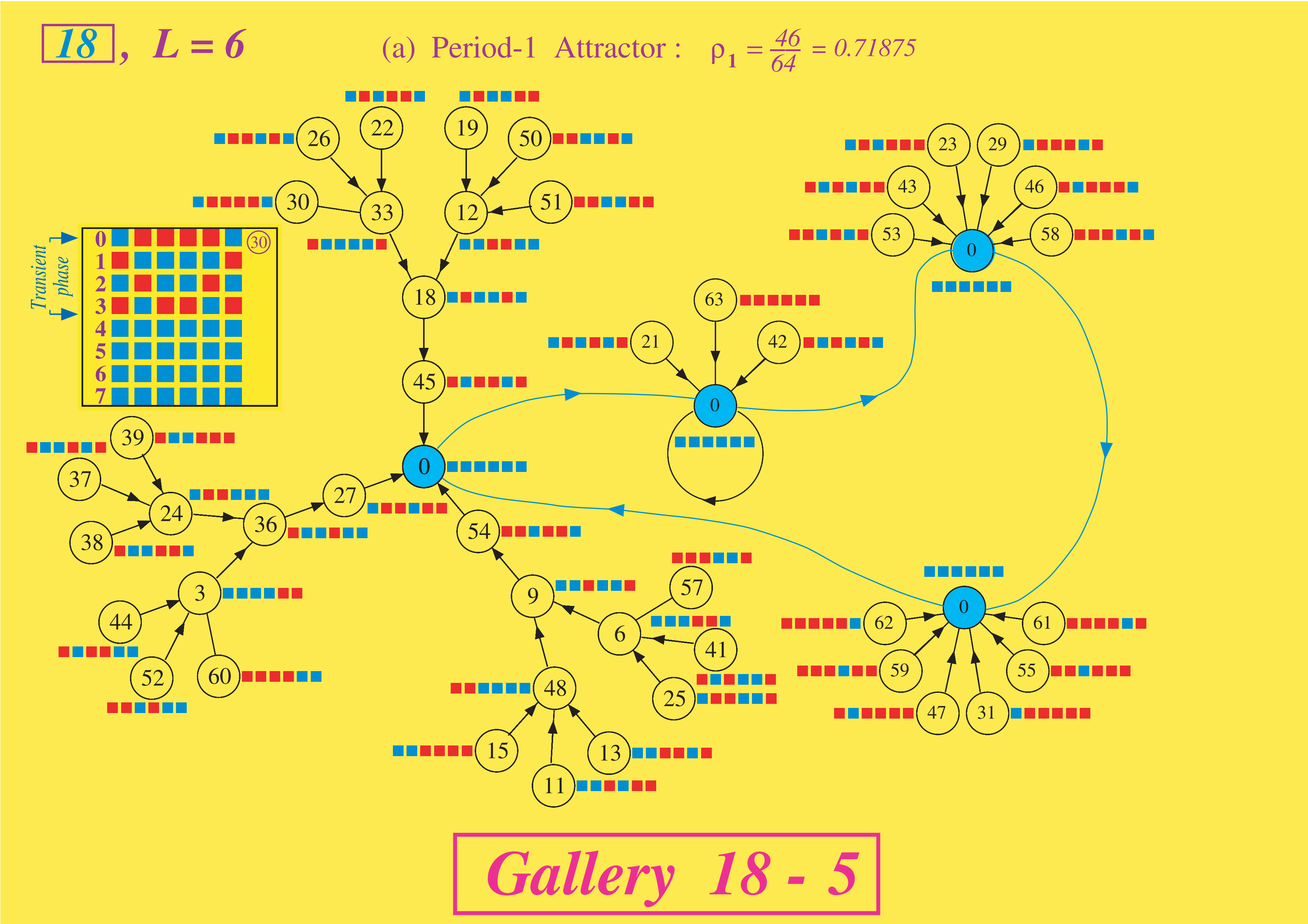
18, L = 6
(a) Period-1 Attractor : ρ1 = 46/64 = 0.71875
Transient phase
0 1 2 3 4 5 6 7
30
26 22 19 50 30 33 12 51 18 45 0 39 37 24 38 36 27 54 3 44 52 60 9 6 57 41 25 48 15 11 13
21 63 42 0
23 29 43 46 53 58 0
62 61 59 55 47 31 0
Gallery 18 - 5

18, $L = 6$ (b) Bernoulli ($\sigma = \pm 3, \tau = 1$) Period-2 Attractors : $\rho_2 = 3\frac{6}{64} = 0.28125$

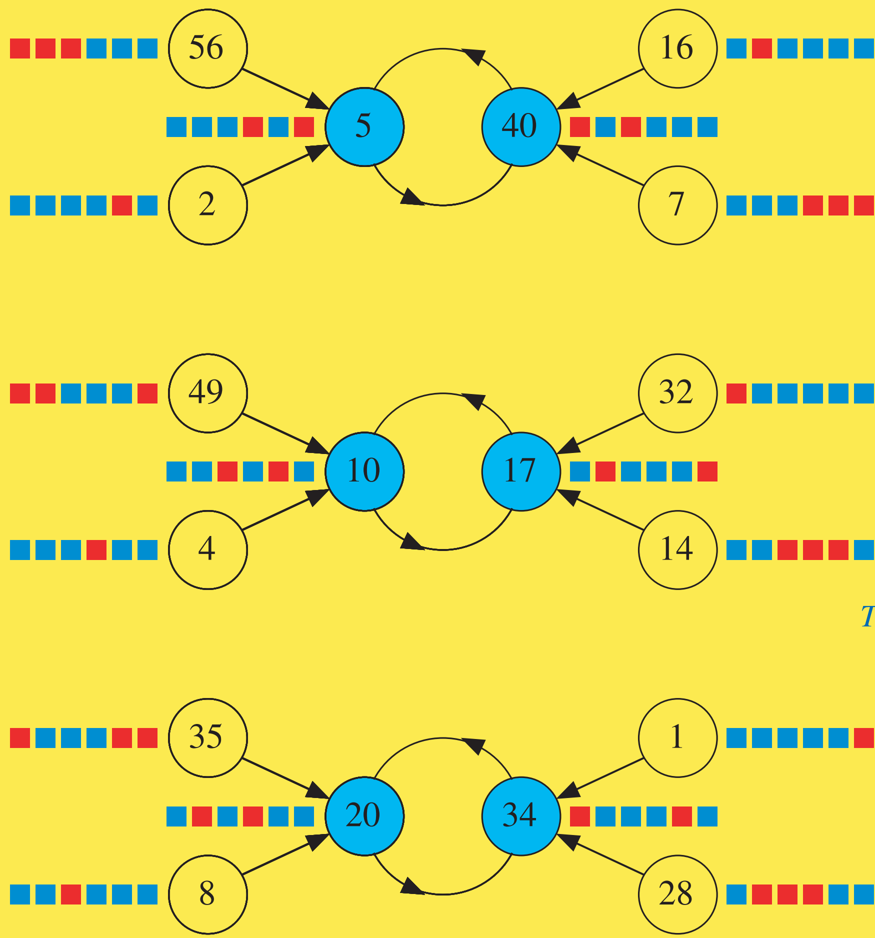

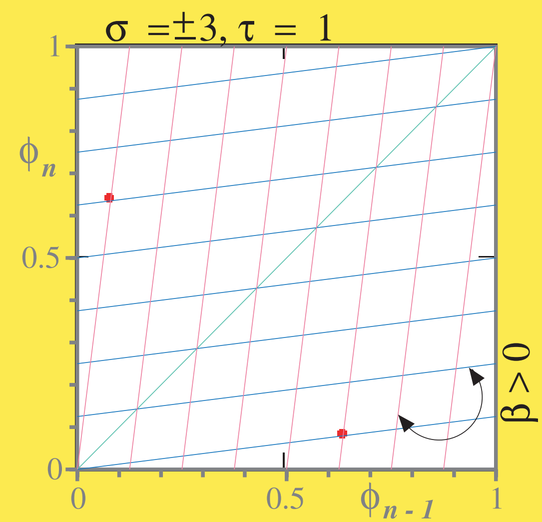

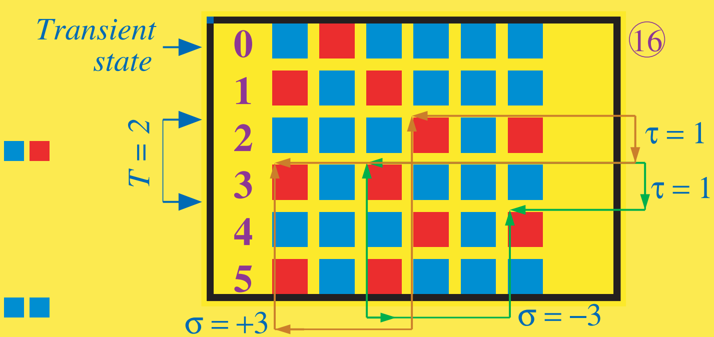

Gallery 18 - 6

18, ***L* = 7**

(a) Period-1 Attractor : $\rho_1 = \frac{128}{128} = 1$

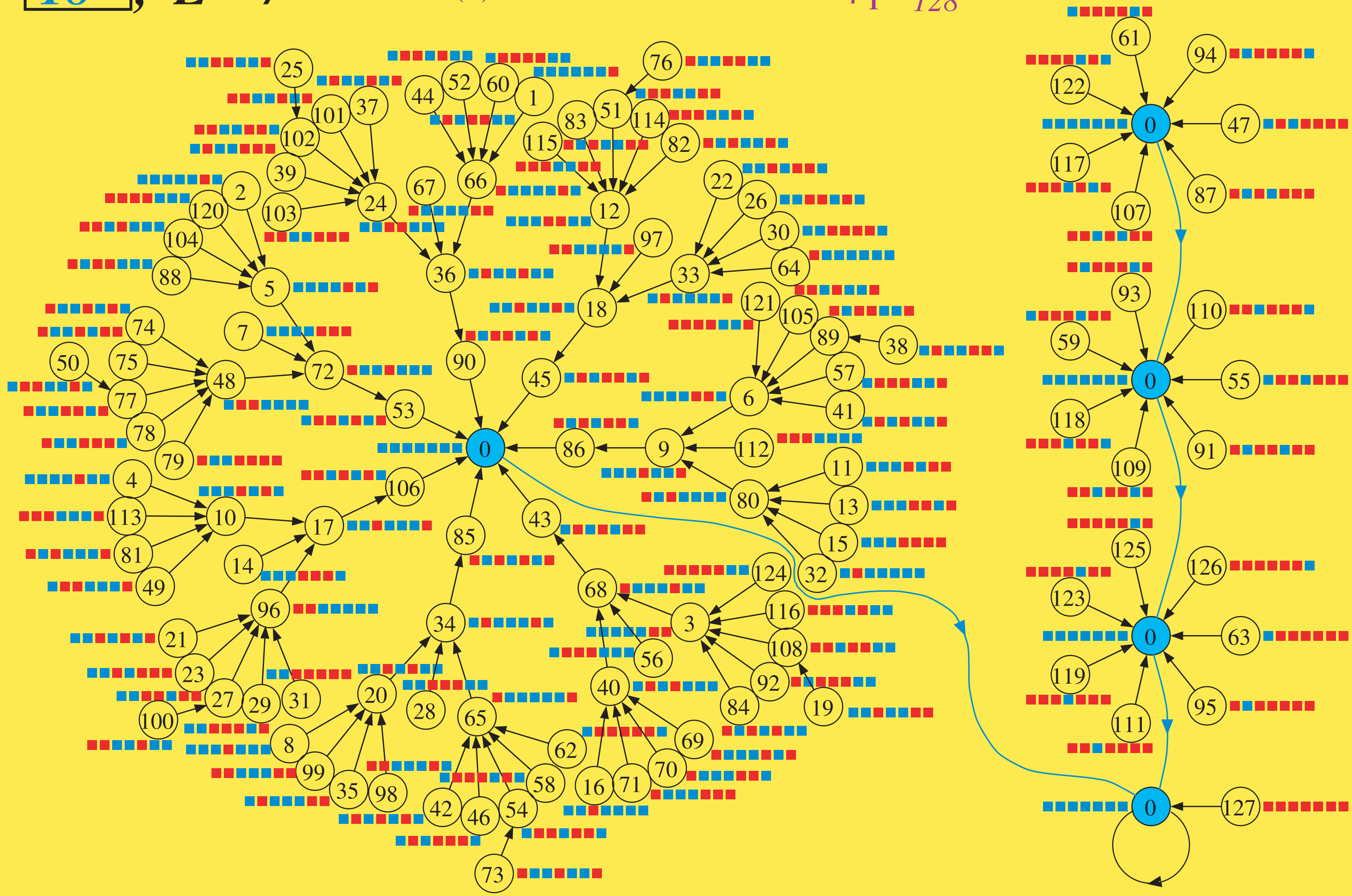

Gallery 18 - 7

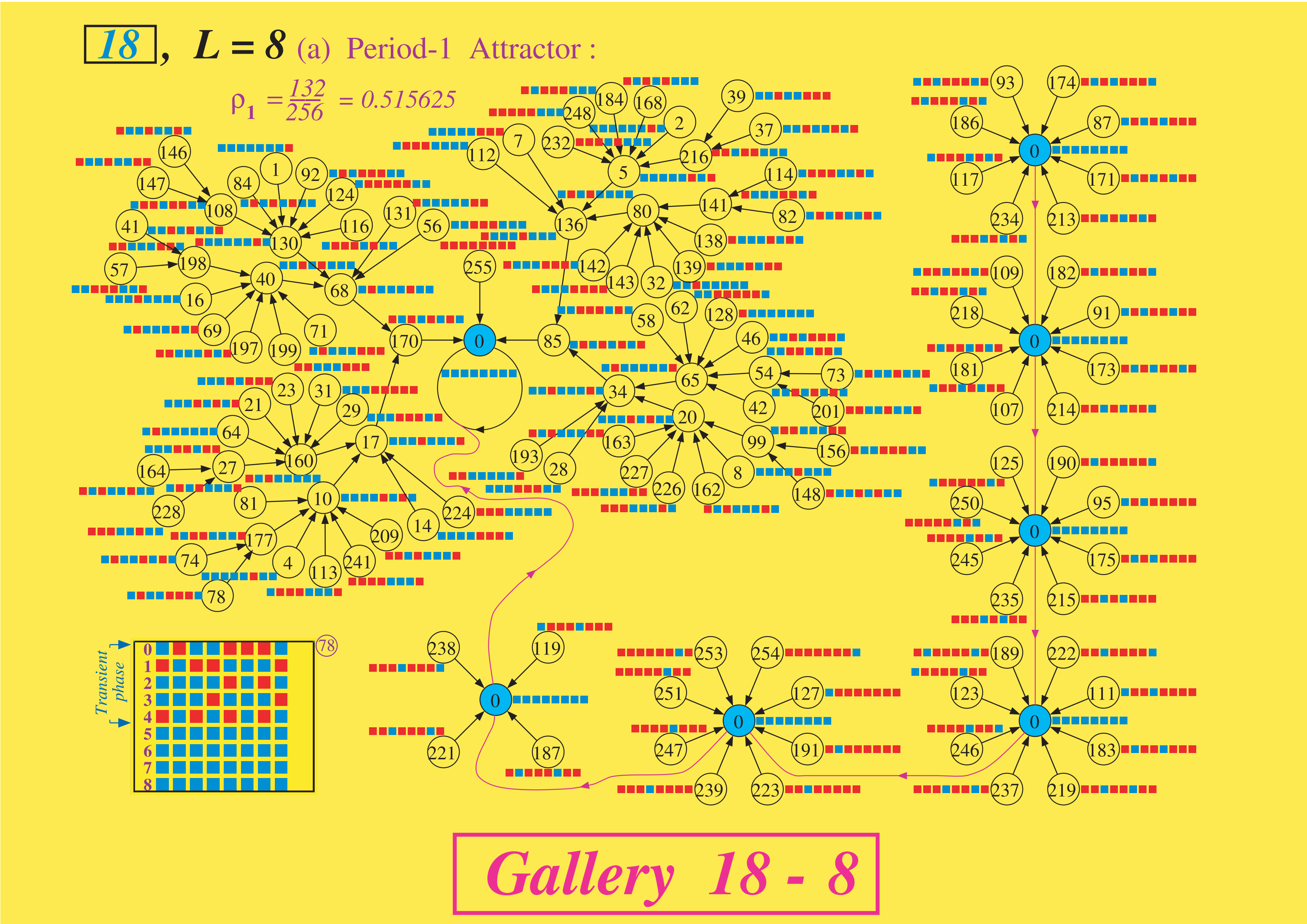
18, L = 8 (a) Period-1 Attractor :
$\rho_1 = \frac{132}{256} = 0.515625$
Transient phase
Gallery 18 - 8

18 , ***L* = 8** (b) Bernoulli ($\sigma = \pm 4, \tau = 3$) Period-6 Attractors : $\rho_2 = 4\frac{30}{256} = 0.46875$

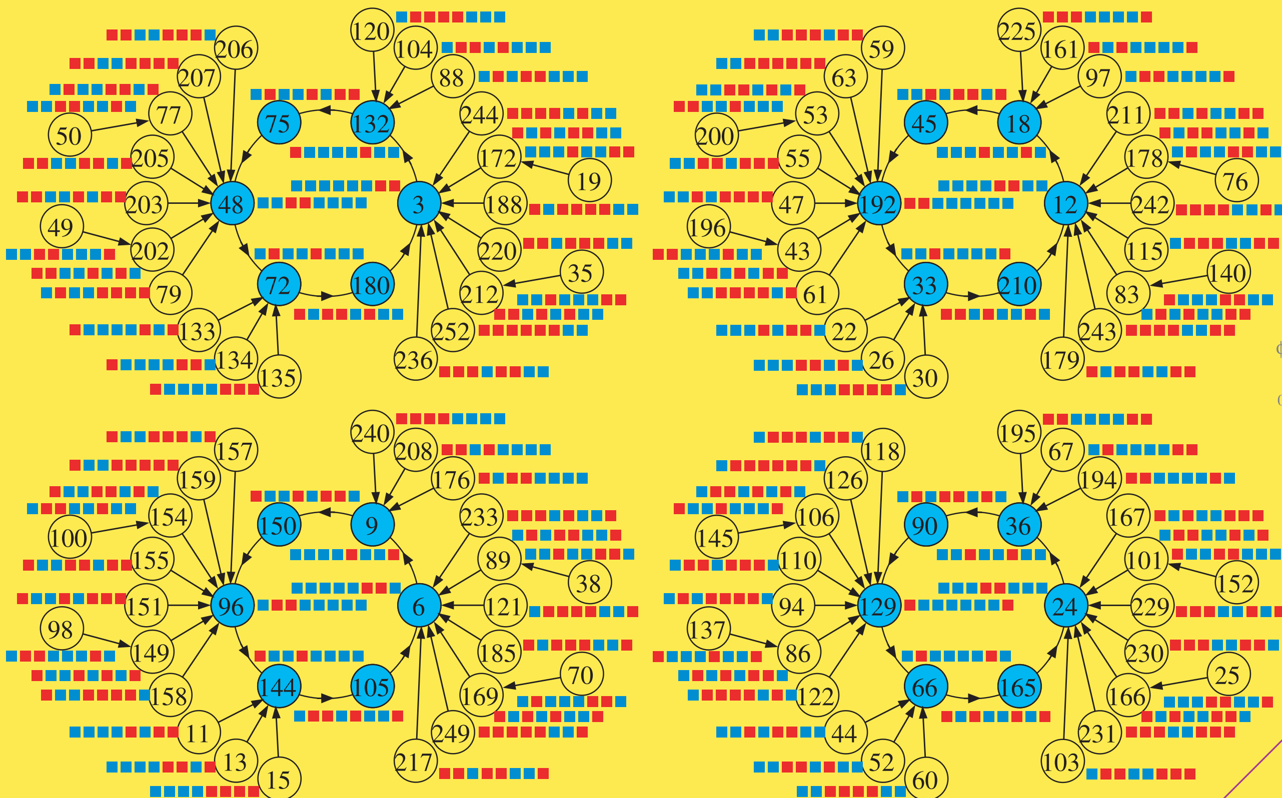

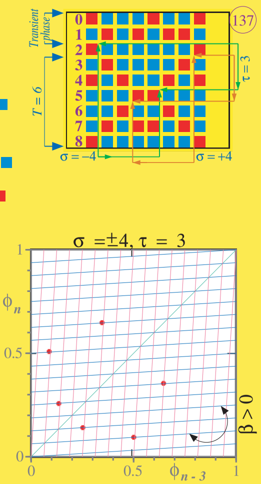

(c) Bernoulli ($\sigma = \pm 2, \tau = 1$) Period-2 Isles of Eden : $\rho_3 = 2\frac{2}{256} = 0.015625$

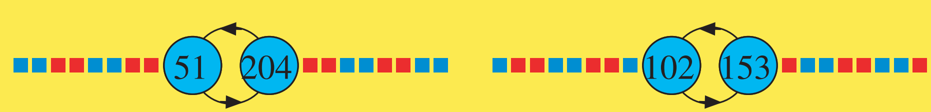

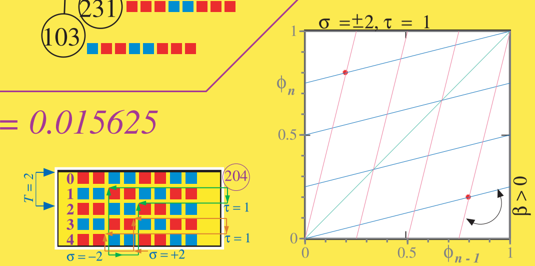

Gallery 18 - 9

and

$$1 \bullet 2^2 + 1 \bullet 2^1 + 0 \bullet 2^0 = 6$$

respectively. These numbers are enclosed by small circles, and are represented as *nodes* of a *digraph* where a *directed* edge pointing from node S_1 to node S_2 means that bit string S_1 maps to bit string S_2 after one iteration under rule $\boxed{N}$.

For example, Gallery 18-1 shows the basin trees $\Im(\Gamma_1(\boxed{18})) = \{7; 2\ 5; 4, 3; 1, 6\}$ converging to a period-1 (fixed point) orbit $\Gamma_1(\boxed{18}) = \{0\}$. The *self-loop* attached to node 0 means that bit string 0 maps into itself, *ad infinitum*, thereby implying 0 is a *period-1 orbit*.

Each sequence of nodes along each branch of the tree $\Im(\Gamma_1(\boxed{18}))$ depicts successive evolutions over time. For example, the sequence $2 \to 5 \to 0$ translates into the space-time pattern shown in the upper right-hand corner of Table 14-1. Similarly, the sequence $4 \to 3 \to 0$ translates into the space-time pattern shown in the lower right-hand corner.

Observe that the first two rows in both space-time patterns on the right of Gallery 18-1 represent the *transient phase* of the dynamic evolution; they correspond to nodes belonging to the basin tree[7] $\Im(\Gamma_1(\boxed{18}))$. The next four rows in these two space-time patterns correspond to the *steady state*, which is a period-1 orbit in this case.

Whenever a basin tree $\Im(\Gamma_1(\boxed{18}))$ is *not empty*, the associated periodic orbit 0 in steady state is called an *attractor* because the period-1 bit string 0 attracts all orbits belonging to the tree $\Im(\Gamma_1(\boxed{18}))$. We now extend this definition to period-n orbits.

Definition 5. Period-n attractor. A *period-n orbit* $\Gamma_n(\boxed{N})$ of a local rule $\boxed{N}$ is said to be *a period-n attractor iff* it has a nonempty basin tree, i.e.

$$\Im(\Gamma_n(\boxed{N})) \neq \emptyset \tag{15}$$

It follows from *Proposition 1* that *every period-n orbit* of a local rule $\boxed{N}$ is either an *attractor*, or an *isle of Eden*. Although a period-n orbit $\Gamma_n(\boxed{N})$ of $\boxed{N}$ contains n distinct bit strings $\boldsymbol{x}, \chi^1_{\boxed{N}}(\boldsymbol{x}), \chi^2_{\boxed{N}}(\boldsymbol{x}), \ldots\ \chi^{n-1}_{\boxed{N}}(\boldsymbol{x})$, we will usually refer to each bit string $\boldsymbol{x}$ or $\chi^k_{\boxed{N}}(\boldsymbol{x})$, $k = 1, 2, \ldots, n-1$, as a *period-n attractor*, or a *period-n isle of Eden*, respectively, to avoid clutter. In other words, a period-n attractor or isle of Eden can mean either any bit string in a "ring" orbit, or to the collection of all "n" bit strings in the "*ring*".

Also listed on top of each gallery is the *robustness coefficient*

$$\boxed{\rho_i = \frac{n_i}{n\left(\sum^L\right)} \triangleq \frac{n_i}{2^L}} \tag{16}$$

of the ith period-n orbit (n is a generic symbol denoting the actual period of each periodic orbit) where $n(\sum^L)$ denotes the total number of all bit strings in the *symbolic state space* $\sum^L$ composed of all binary bit strings of length L, and where n_i denotes the total number of nodes (i.e. bit strings) in the basin of attraction of the ith period-n orbit, where $i = 1, 2, \ldots, m$, and m is the total number of period-n orbits. In Gallery 18-1, $m = 1$ since there is only "one" attractor when $L = 3$. Hence, $i = 1$ in Gallery 18-1. In the basin tree $\Im(\Gamma_1(\boxed{18}))$ shown in Gallery 18-1, there are all together eight nodes and hence $n_i = 8$. Since $L = 3$, we have $\rho_1 = 8/2^3 = 1$.

The robustness coefficient ρ_i in Eq. (16) measures the percentage of initial bit strings which converge to the ith attractor in question. In this case $\rho_i = \rho_1 = 1$ because there is only one attractor in this example and hence *all* orbits must converge to 0. In general, $0 < \rho_i \leq 1$, where $\rho_i = 1$ correspond to maximum robustness.

2.4.1. *Highlights from Rule* $\boxed{18}$

$$\boxed{\text{Gallery 18-1} : L = 3, n\left(\sum^3\right) = 8}$$

There are seven basin-tree strings, all of which converge to the *global period-1 attractor* $\{0\}$. Hence the period-1 attractor 0 has maximum robustness with $\rho_1 = 1$.

$$\boxed{\text{Gallery 18-2} : L = 4, n\left(\sum^4\right) = 16}$$

(a) There is a *period-1 attractor* $\{0\}$ with robustness coefficient $\rho_1 = 0.75$.

(b) There are two *period-2 isles of Eden* $\{3, 12\}$, and $\{6, 9\}$ with a combined robustness coefficient $\rho_2 = 0.25$. The dynamics on each *isle of Eden* is a Bernoulli σ_τ-shift with $\sigma_1 = 2$, $\tau = 1$, or $\sigma_2 = -2$, $\tau = 1$, as depicted in the $\phi_n \mapsto \phi_{n-1}$ *time-1 map* in Gallery 18-2. Here, the red lines have

[7]Note that our definition of a basin tree $\Im(\Gamma_n(\boxed{N}))$ does *not* include bit strings belonging to the associated period-n orbit $\Gamma_n(\boxed{N})$.

slope equal to $2^{\sigma_1} = 4$, and the blue lines have slope equal to $2^{\sigma_2} = 1/4$. Both sets of parallel lines have a positive slope, implying that $\beta > 0$.

Observe that the two period-2 "red" dots correspond to the *decimal representation*

$$\boxed{\phi = \sum_{i=0}^{L-1} 2^{-(i+1)} x_i} \tag{17}$$

(defined in Eq. (2) of [Chua *et al.*, 2006]) of bit string 3 and 12 of the *isle of Eden* {3, 12} on the left; namely,

$$3 \mapsto 1 \bullet 2^{-3} + 1 \bullet 2^{-4} = 0.1875 \text{ (left red dot)}$$

$$12 \mapsto 1 \bullet 2^{-1} + 1 \bullet 2^{-2} = 0.75 \text{ (right red dot)}$$

Observe that the two red dots lie at the intersection of corresponding pairs of red and blue "Bernoulli" lines, thereby confirming that the dynamics on this isle of Eden can be described by a *left shift* of two bits ($\sigma = 2$) or, equivalently, by a *right shift* of two bits ($\sigma = -2$), per iteration ($\tau = 1$), as extensively illustrated in [Chua *et al.*, 2005a] and [Chua *et al.*, 2006].

$$\boxed{\text{Gallery 18-3, 18-4} : L = 5, n\left(\sum^5\right) = 32}$$

(a) There is a *period-1 attractor* {0} with robustness coefficient $\rho_1 = 0.375$.

(b) There are five *period-2 attractors* with a combined robustness coefficient $\rho_2 = 0.625$. The dynamics on each *attractor* is a Bernoulli σ_τ-shift with $\sigma_1 = 5$, $\tau = 2$, or $\sigma_2 = -5$, $\tau = 2$, as depicted in the $\phi_{n-2} \mapsto \phi_n$ *time-2 map.*

The time-2 map $\phi_{n-2} \mapsto \phi_n$ consists of $\beta = 2^{\sigma_1} = 32$ parallel red Bernoulli lines with slope $2^{\sigma_1} = 32$, or equivalently, to $\beta = 2^{|-\sigma_2|} = 32$ parallel blue Bernoulli lines with slope $2^{\sigma_2} = 1/32$. Observe that the two red dots now fall on the diagonal of the *time-2* map, as expected of *period-2* orbits. Again, $\beta > 0$ because the slope of each red (or blue) Bernoulli line is positive.

For ease of visualization, we have displayed the space-time pattern using bit strings with double the length, namely, $2L = 10$, which corresponds to shifting around the period-2 ring twice. Note that the decimal code of the 5-bit basin tree 16 translates into the corresponding 10-bit string 528 shown in Gallery 18-4.

Observe that all basin subtrees contain only one bit string, implying that all basin trees of rule $\boxed{18}$ are *gardens of Eden*, when $L = 5$.

$$\boxed{\text{Gallery 18-5, 18-6} : L = 6, n\left(\sum^6\right) = 64}$$

(a) There is a *period-1 attractor* {0} with robustness coefficient $\rho_1 = 0.71875$. Note that there are three blue lines joining bit string 0 at three locations in the basin tree diagram. This is done to avoid clutter. The reader should interpret all three nodes labeled 0 as representing the same node. Observe also from the basin tree diagram that the longest transient regime is four iterations, such as the one depicted in the space-time pattern originating from string 30 in Gallery 18-5. The shortest transient regime is one iteration; they correspond to the 15 gardens of Eden in the three "translated" subtrees joined by blue lines.

(b) There are three *period-2 attractors* with a combined robustness coefficient $\rho_2 = 0.28125$. The dynamics on each attractor is a Bernoulli σ_τ-shift with $\sigma_1 = 3$, $\tau = 1$, or $\sigma_2 = -3$, $\tau = 1$. In this case, all basin trees are gardens of Eden.

$$\boxed{\text{Gallery 18-7} : L = 7, n\left(\sum^7\right) = 128}$$

There are 127 basin tree strings, all of which converge to the *global period-1 attractor* {0}. It follows that we have maximum robustness with $\rho_1 = 1$, as in Gallery 18-1.

$$\boxed{\text{Gallery 18-8, 18-9} : L = 8, n\left(\sum^8\right) = 256}$$

(a) There is a *period-1 attractor* {0} with robustness coefficient $\rho_1 = 0.515625$. The transient regime ranges from one iteration (corresponding to subtrees composed of garden of Edens) to five iterations, as illustrated in a typical space-time diagram starting from bit string 78 in Gallery 18-8.

(b) There are four *period-6 attractors* with a combined robustness coefficient $\rho_2 = 0.46875$. The dynamics on each attractor is a Bernoulli σ_τ-shift with $\sigma_1 = 4$, $\tau = 3$, or $\sigma_2 = -4$, $\tau = 3$.

The time-3 map $\phi_{n-3} \mapsto \phi_n$ shows $\beta = 2^4 = 16$ parallel Bernoulli "red" lines with slope $2^{\sigma_1} = 16$, or equivalently, 16 parallel Bernoulli "blue" lines with slope $2^{\sigma_2} = 1/16$. Observe that there are six red dots in the time-3 map, implying a *period-6* attractor. Again, $\beta > 0$ because both red and blue lines have a positive slope.

(c) There are two *period-2 isles of Eden* with a combined robustness coefficient $\rho_3 = 0.015625$. The dynamics on each isle of Eden is a Bernoulli σ_τ-shift $\sigma_1 = 2$, $\tau = 1$, or $\sigma_2 = -2$, $\tau = 1$.

The qualitative properties of local rule $\boxed{18}$ extracted from the above basin-tree Galleries 18-1 to 18-9 are summarized below:

Summary of Qualitative properties of local rule $\boxed{18}$ extracted from Gallery 18 for Rule $\boxed{18}$

L	ID Number i	Number of Period-n attractors	Number of Period-n Isles of Eden	Period n	Bernoulli Parameters σ_1	τ_1	β_1	σ_2	τ_2	β_2	Robustness coefficient ρ
3	1	1		1	0	1	+				$\rho_1 = 1$
4	1	1		1	0	1	+				$\rho_1 = 0.75$
	2		2	2	2	1	+	-2	1	+	$\rho_2 = 0.25$
5	1	1		1	0	1	+				$\rho_1 = 0.375$
	2	5		2	5	2	+	-5	2	+	$\rho_2 = 0.625$
6	1	1		1	0	1	+				$\rho_1 = 0.71875$
	2	3		2	3	1	+	-3	1	+	$\rho_2 = 0.28125$
7	1	1		1	0	1	+				$\rho_1 = 1$
8	1	1		1	0	1	+				$\rho_1 = 0.515625$
	2	4		6	4	3	+	-4	3	+	$\rho_2 = 0.46875$
	3		2	2	2	1	+	-2	1	+	$\rho_3 = 0.015625$

Table 15. Basin tree diagrams for rule $\boxed{22}$.

Basin tree diagrams for Rule $\boxed{22}$

$\boxed{22}$, $L = 3$ (a) Period-1 Attractor : $\rho_1 = \frac{8}{8} = 1$

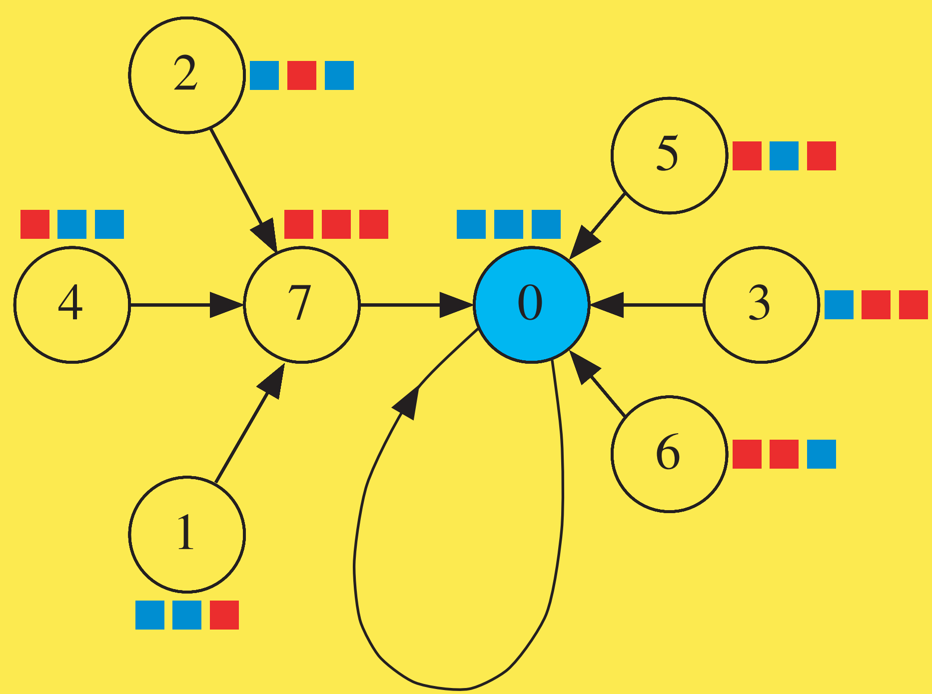

Gallery 22 - 1

Table 15. (*Continued*)

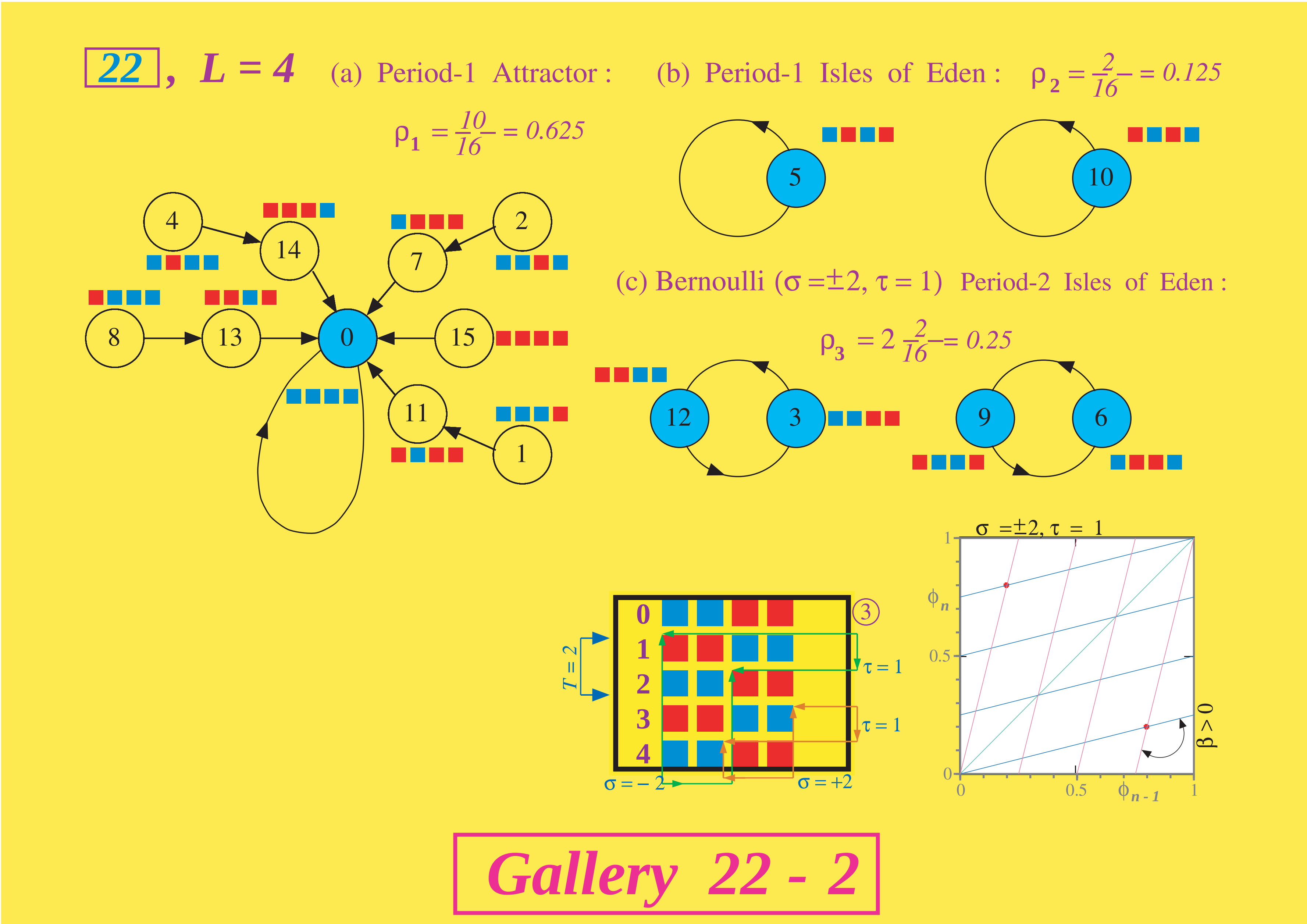

Table 15. (*Continued*)

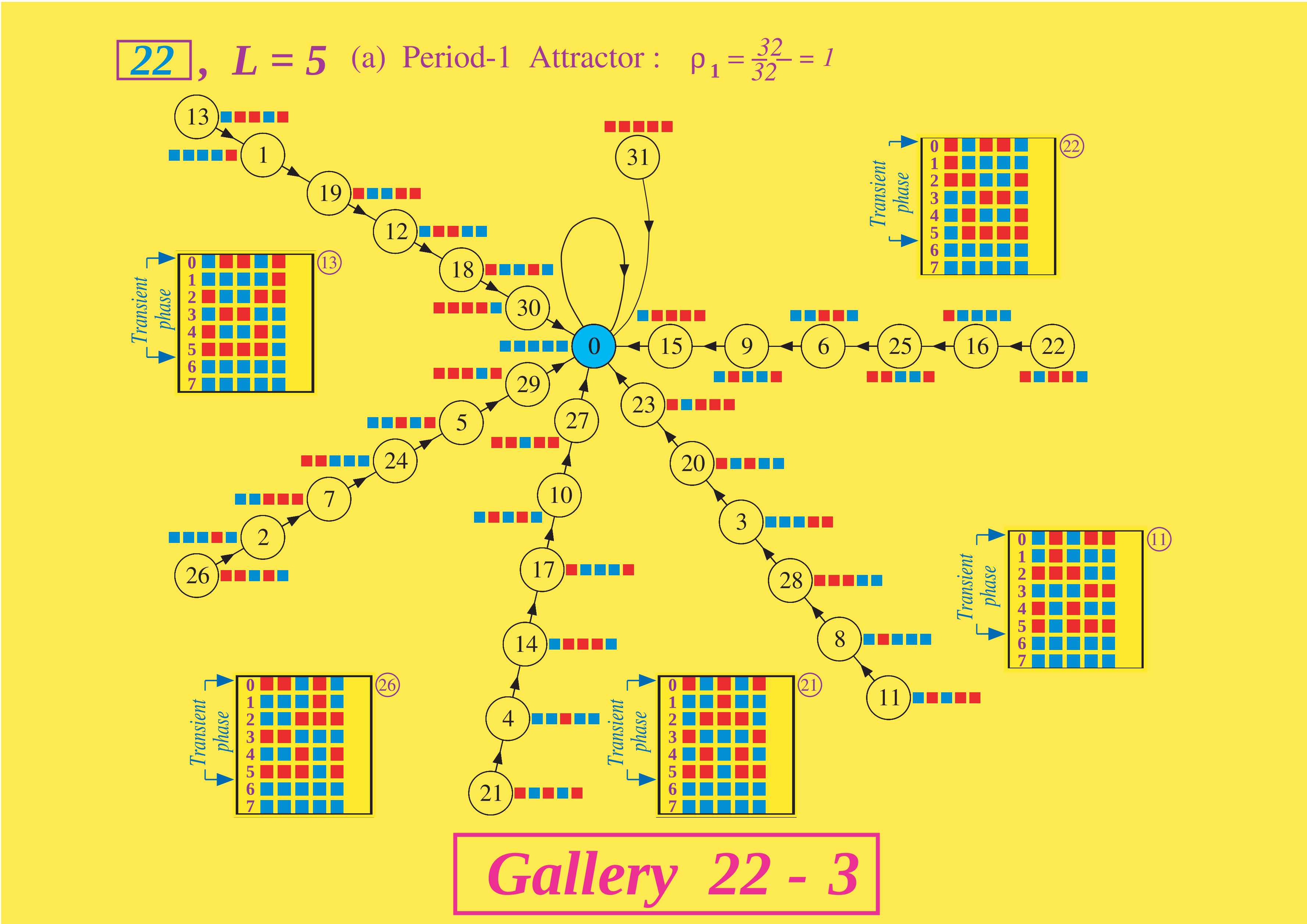

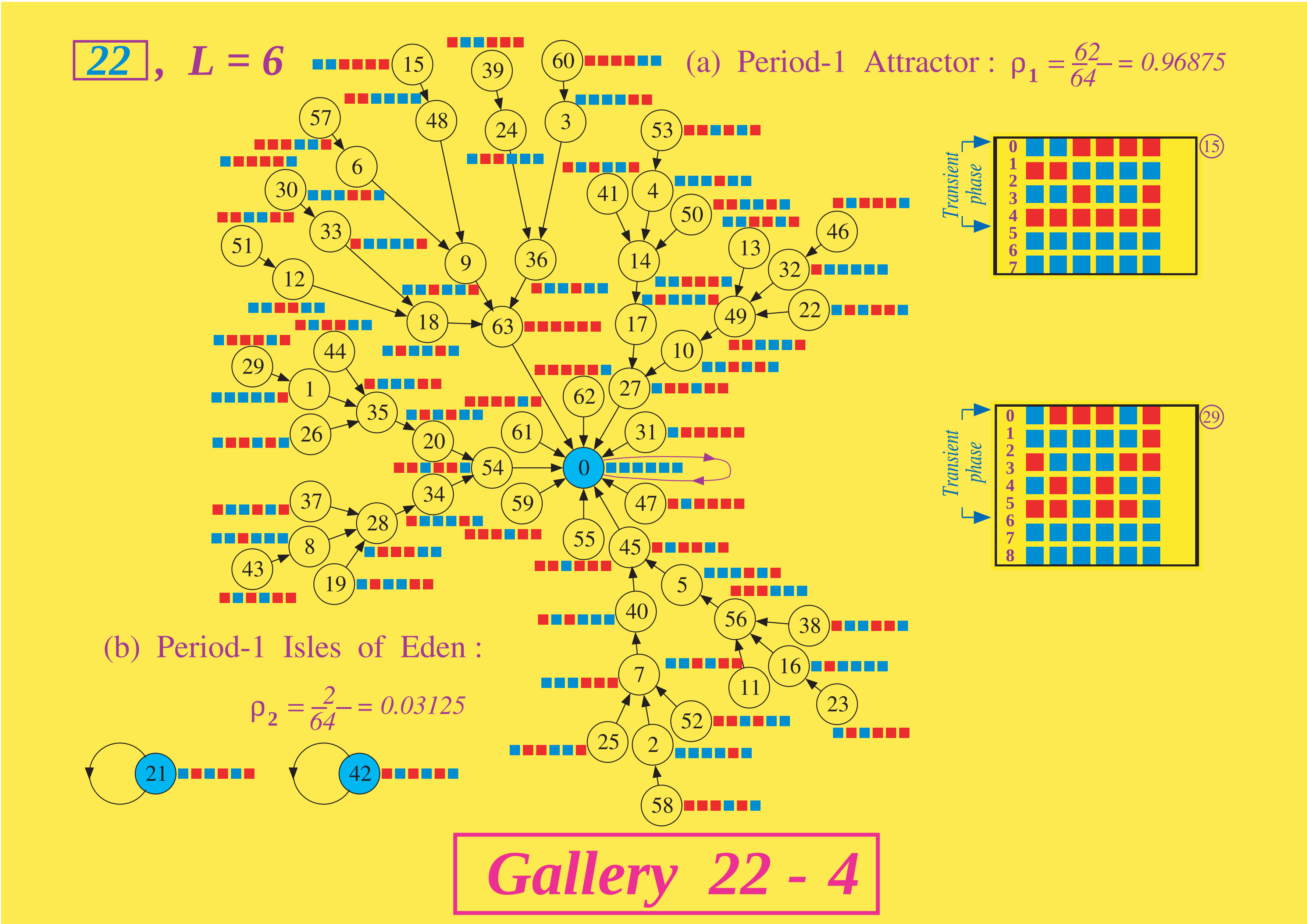
22, L = 6
(a) Period-1 Attractor : ρ1 = 62/64 = 0.96875
Transient phase
15
29
(b) Period-1 Isles of Eden :
ρ2 = 2/64 = 0.03125
Gallery 22 - 4

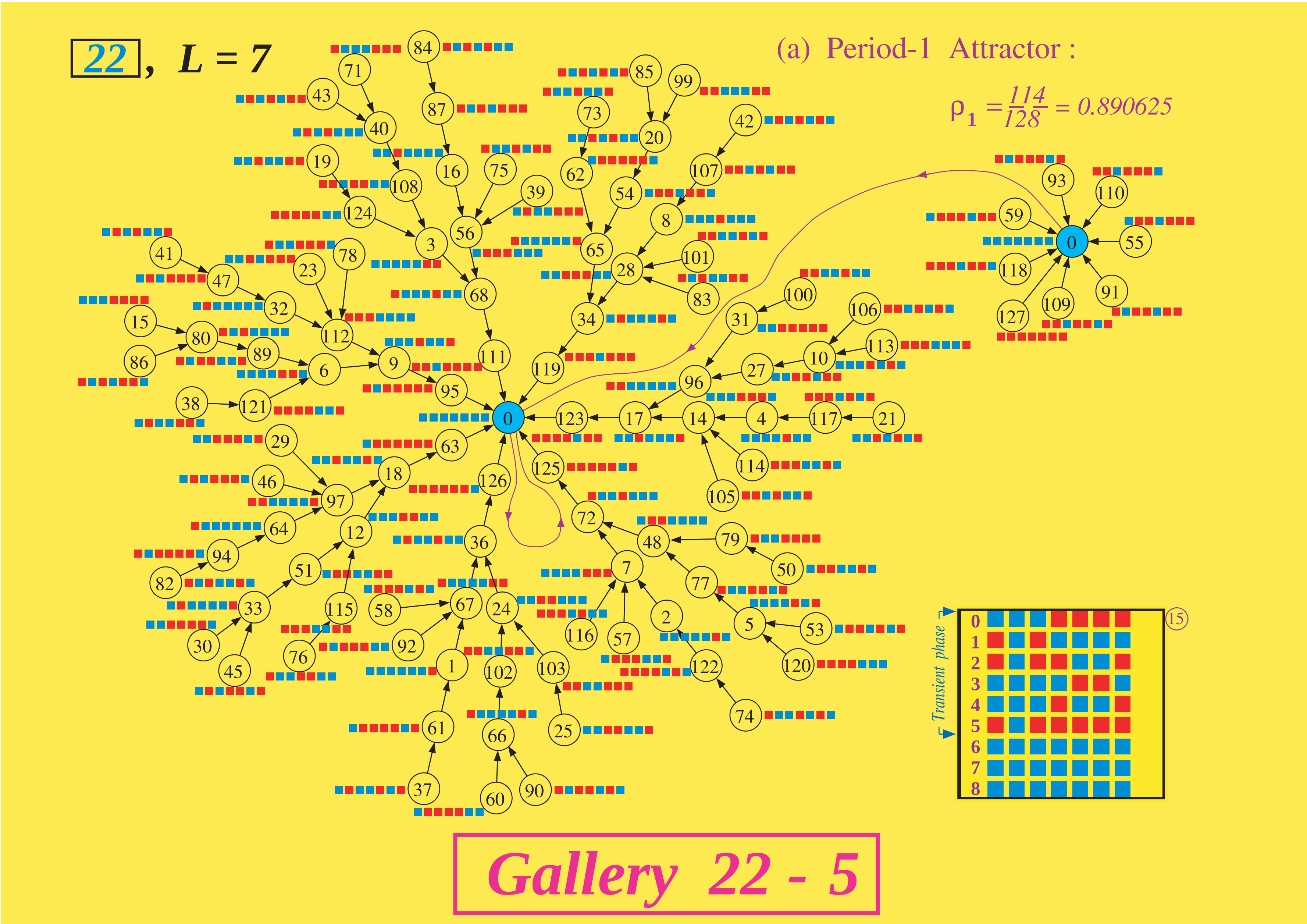
22, L = 7
(a) Period-1 Attractor :
$\rho_1 = \frac{114}{128} = 0.890625$
Transient phase
15
0
1
2
3
4
5
6
7
8
Gallery 22 - 5

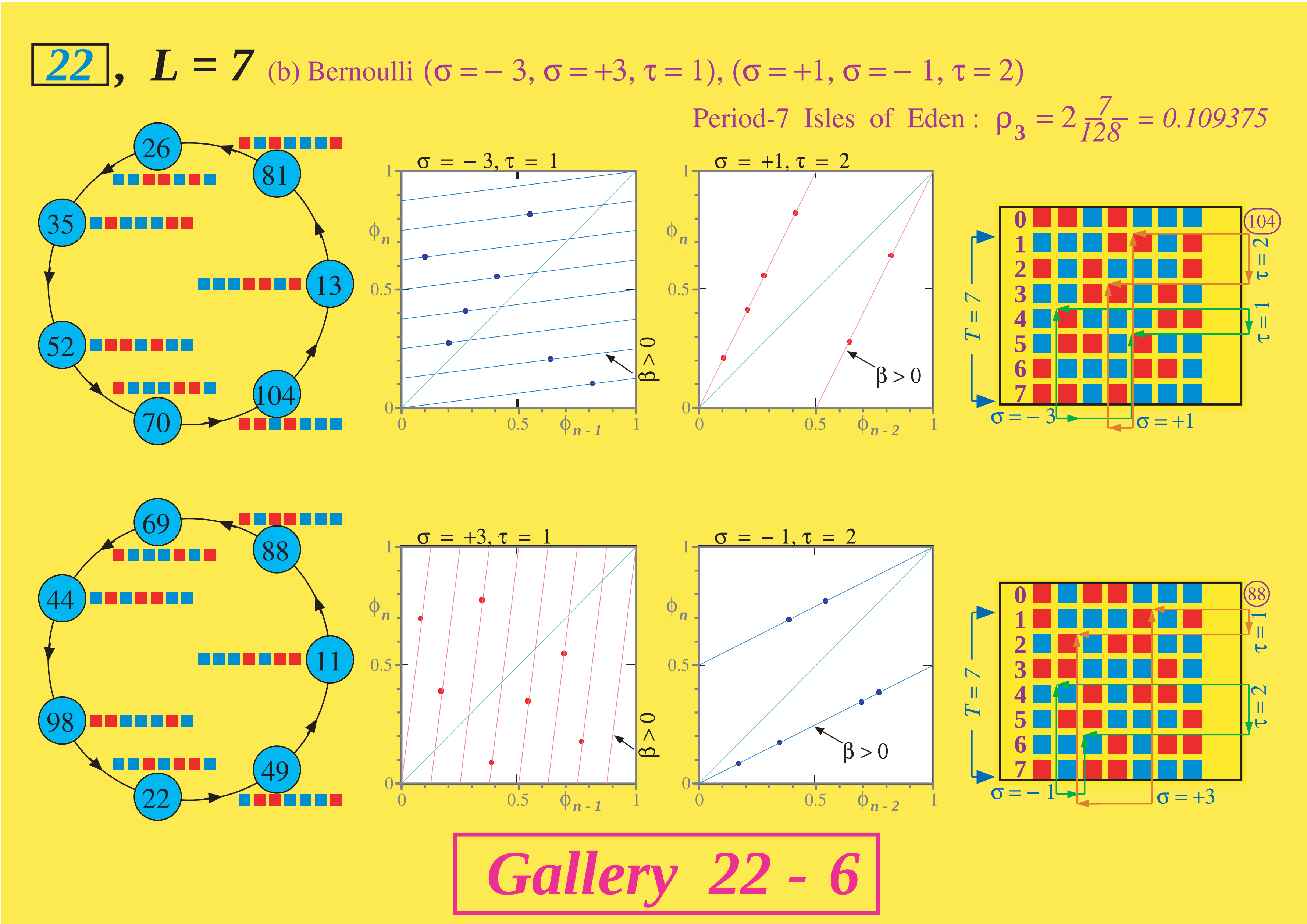
22, L = 7 (b) Bernoulli (σ = – 3, σ = +3, τ = 1), (σ = +1, σ = – 1, τ = 2)
Period-7 Isles of Eden : $\rho_3 = 2\frac{7}{128} = 0.109375$
σ = – 3, τ = 1
σ = +1, τ = 2
σ = +3, τ = 1
σ = – 1, τ = 2
β > 0
T = 7
Gallery 22 - 6

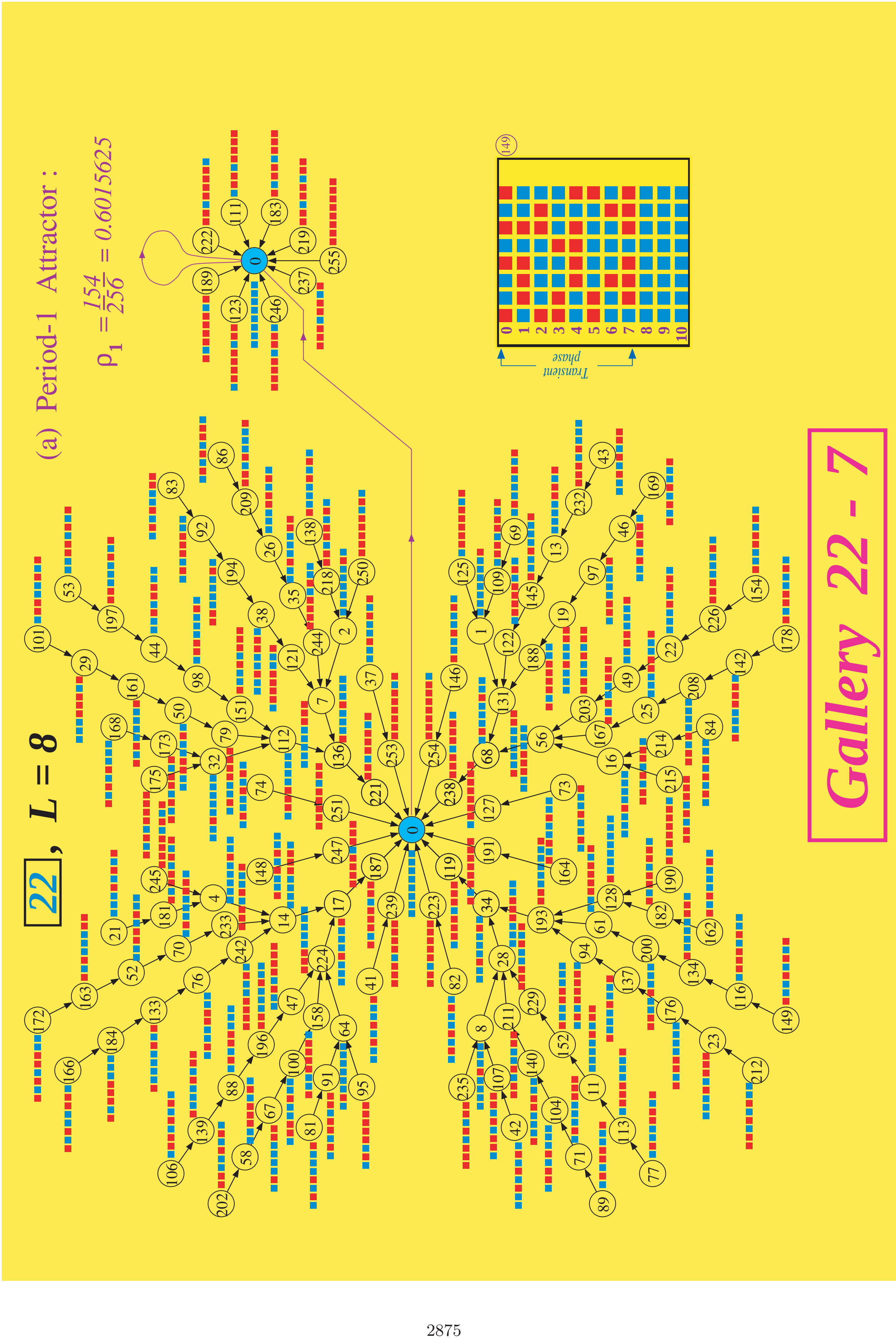
22, L = 8
(a) Period-1 Attractor :
ρ1 = 154/256 = 0.6015625
Transient phase
Gallery 22 - 7

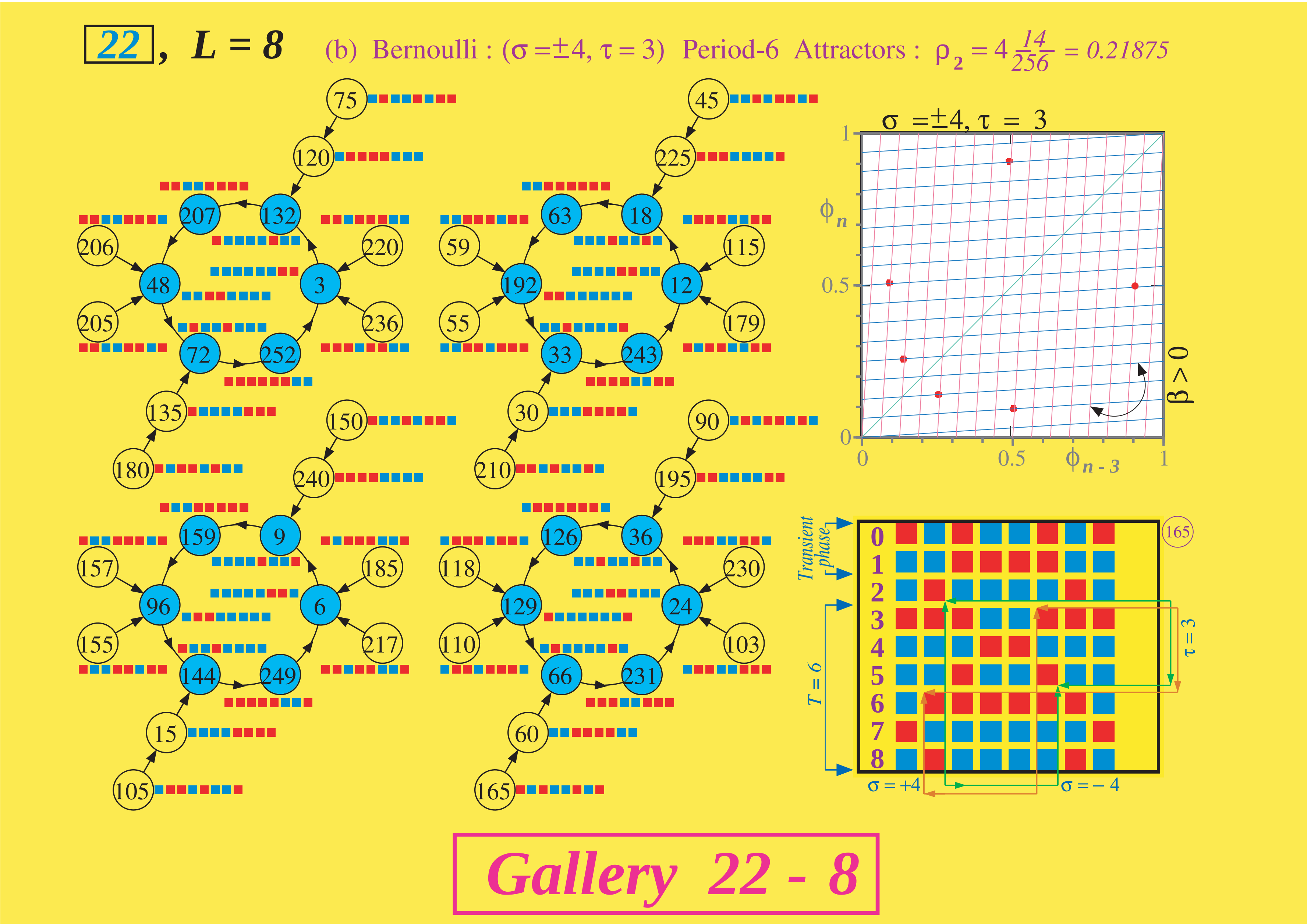

22, L = 8
(b) Bernoulli : (σ = ±4, τ = 3) Period-6 Attractors : $\rho_2 = 4\frac{14}{256} = 0.21875$
75
120
132
207
3
48
220
206
236
205
252
72
135
180
150
240
9
159
6
96
185
157
217
155
249
144
15
105
45
225
18
63
12
192
115
59
179
55
243
33
30
210
90
195
36
126
24
129
230
118
103
110
231
66
60
165
σ = ±4, τ = 3
ϕ_n
ϕ_{n-3}
0
0.5
1
β > 0
165
0
1
2
3
4
5
6
7
8
Transient phase
T = 6
σ = +4
σ = − 4
τ = 3
Gallery 22 - 8

22, ***L* = 8**

(c) Bernoulli : ($\sigma = \pm 4, \tau = 2$) Period-4 Attractors : $\rho_3 = 4\frac{10}{256} = 0.15625$

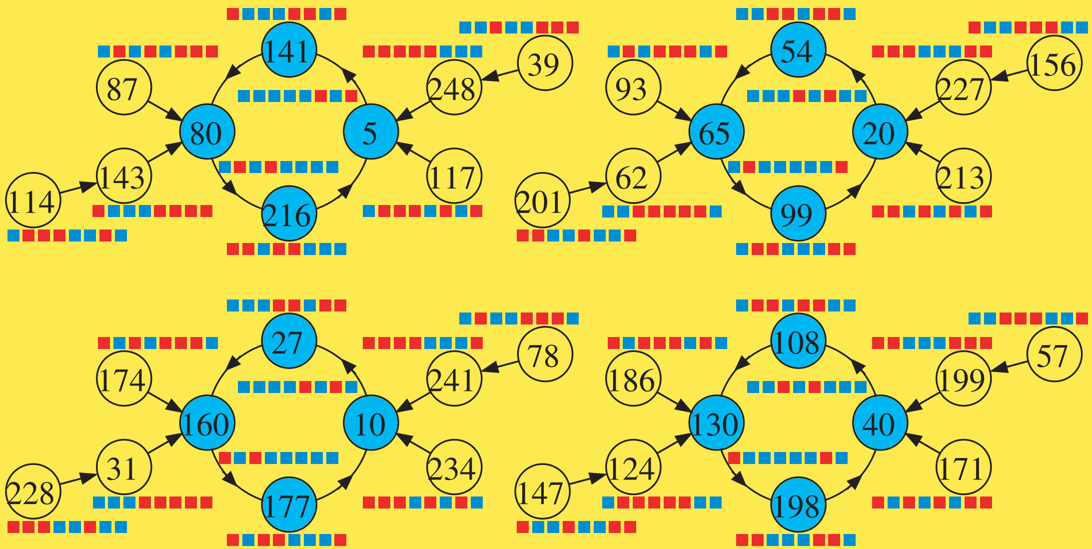

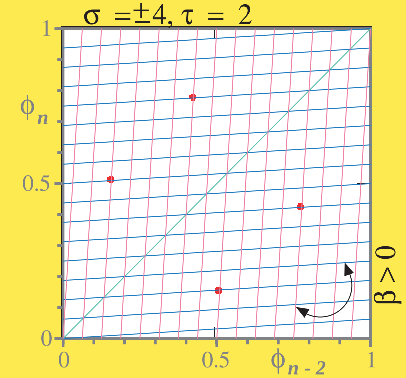

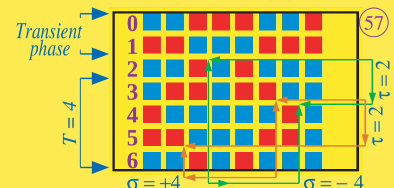

(d) Bernoulli : ($\sigma = \pm 2, \tau = 1$) Period-2 Isles of Eden : $\rho_4 = 2\frac{2}{256} = 0.015625$

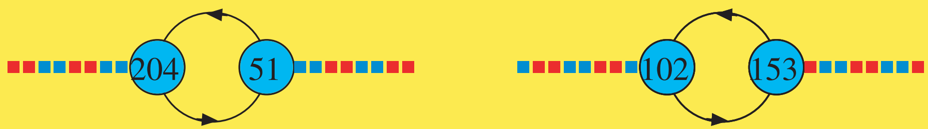

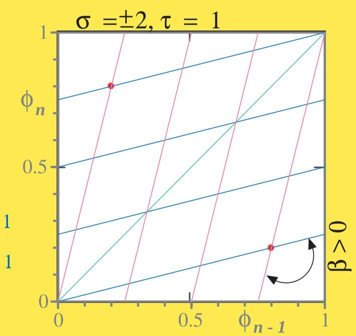

(e) Period-1 Isles of Eden : $\rho_5 = \frac{2}{256} = 0.0078125$

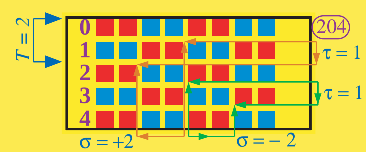

Gallery 22 - 9

2.4.2. *Highlights from Rule* 22

The basin tree diagrams of Rule 22 for $L = 3, 4, \ldots, 8$ are exhibited in Table 15. Following a detailed analysis of these diagrams, the qualitative properties of local rule 22 extracted from basin-tree Galleries 22-1 to 22-9 of Table 15 are summarized below:

Summary of Qualitative properties of local rule 22 extracted from Gallery 22 for Rule 22

L	ID Number i	Number of Period-n attractors	Number of Period-n Isles of Eden	Period n	Bernoulli σ_1	τ_1	β_1	Parameters σ_2	τ_2	β_2	Robustness coefficient ρ
3	1	1		1	0	1	+				$\rho_1 = 1$
4	1	1		1	0	1	+				$\rho_1 = 0.625$
	2		2	1	0	1	+				$\rho_2 = 0.125$
	3		2	2	2	1	+	-2	1	+	$\rho_3 = 0.25$
5	1	1		1	0	1	+				$\rho_1 = 1$
6	1	1		1	0	1	+				$\rho_1 = 0.96875$
	2		2	1	0	1	+				$\rho_2 = 0.03125$
7	1	1		1	0	1	+				$\rho_1 = 0.890625$
	2		2	7	∓ 3	1	+	± 1	2	+	$\rho_2 = 0.109375$
8	1	1		1	0	1	+				$\rho_1 = 0.6015625$
	2	4		6	4	3	+	-4	3	+	$\rho_2 = 0.21875$
	3	4		4	4	2	+	-4	2	+	$\rho_3 = 0.15625$
	4		2	2	2	1	+	-2	1	+	$\rho_4 = 0.015625$
	5		2	1	0	1	+				$\rho_5 = 0.0078125$

Table 16. Basin tree diagrams for rule $\boxed{54}$.

Basin tree diagrams for Rule $\boxed{54}$

$\boxed{54}$, $L = 3$ (a) Period-1 Attractor : $\rho_1 = \frac{8}{8} = 1$

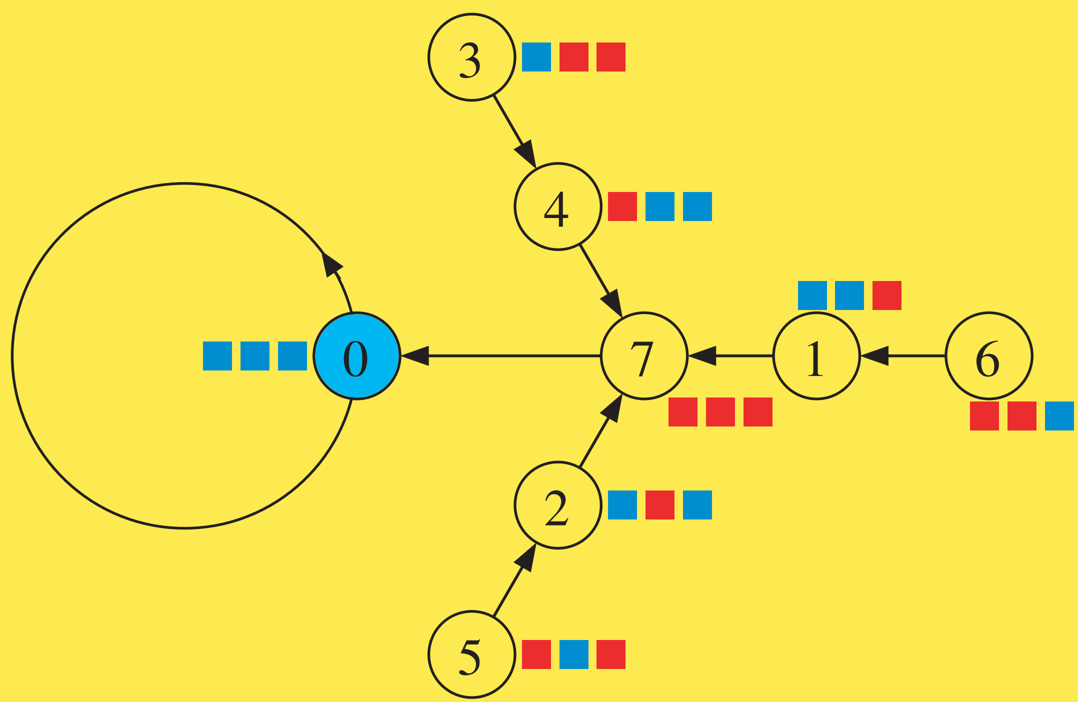

Gallery 54 - 1

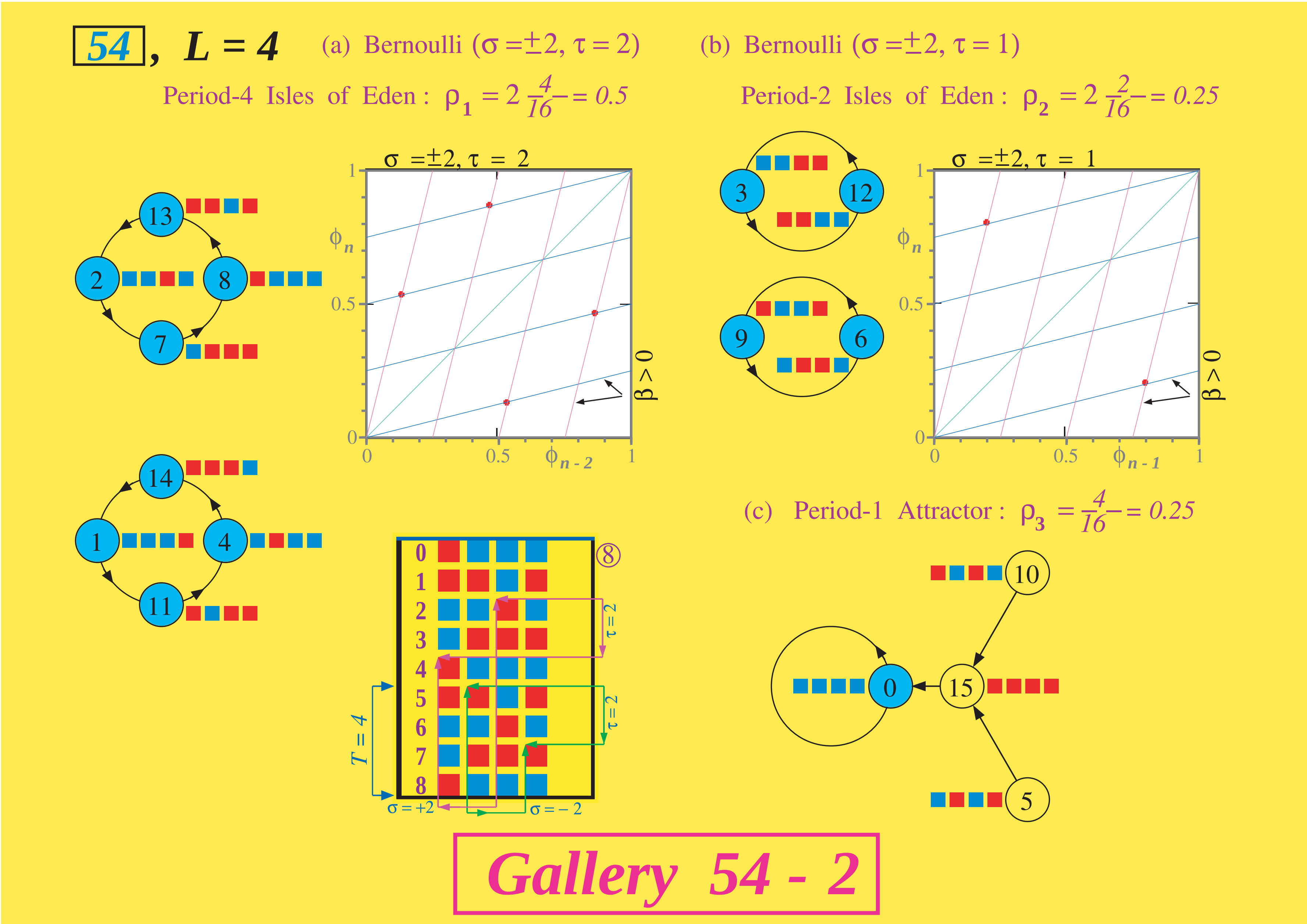
54, L = 4
(a) Bernoulli (σ = ±2, τ = 2)
Period-4 Isles of Eden : ρ1 = 2 4/16 = 0.5
(b) Bernoulli (σ = ±2, τ = 1)
Period-2 Isles of Eden : ρ2 = 2 2/16 = 0.25
σ = ±2, τ = 2
σ = ±2, τ = 1
φn
φn-2
φn-1
β > 0
(c) Period-1 Attractor : ρ3 = 4/16 = 0.25
T = 4
τ = 2
σ = +2
σ = − 2
Gallery 54 - 2

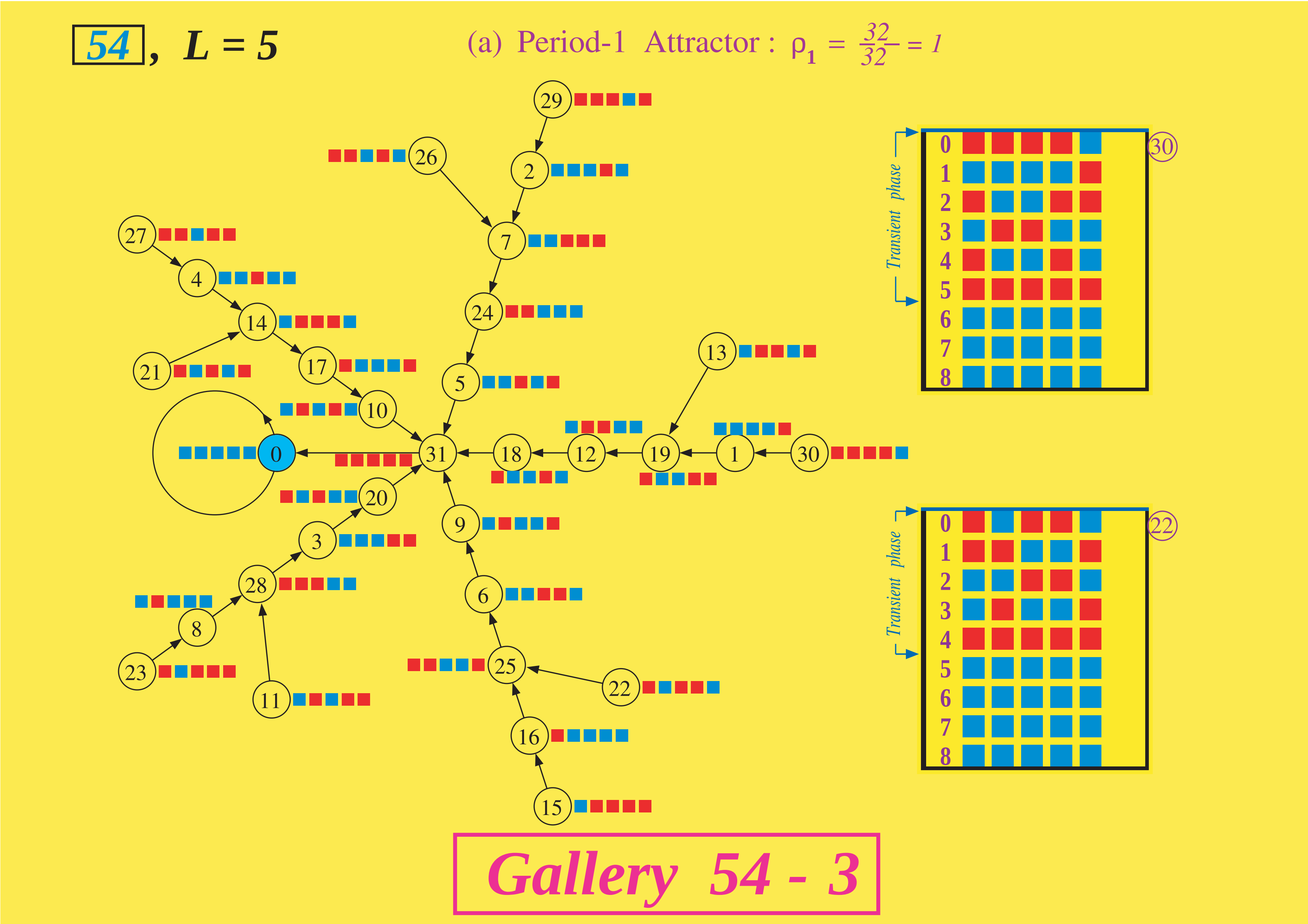

54, L = 5
(a) Period-1 Attractor : $\rho_1 = \frac{32}{32} = 1$
Transient phase
30
22
Gallery 54 - 3

$\boxed{54}$, $L = 6$ (a) Period-1 Attractor : $\rho_1 = \frac{34}{64} = 0.53125$

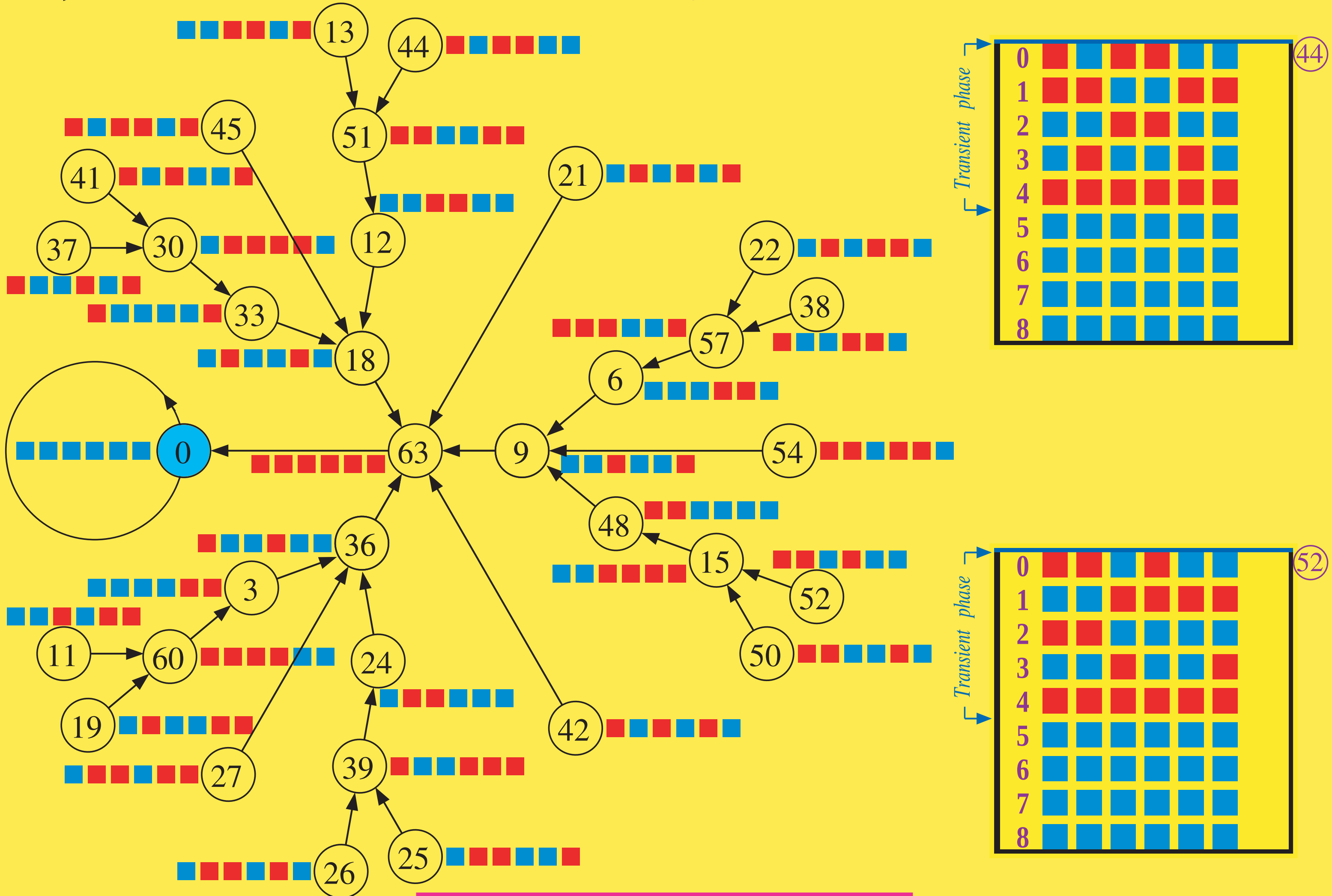

Gallery 54 - 4

Table 16. (*Continued*)

$\boxed{54}$, $L = 6$ (b) 6 Period-4 Attractors : $\rho_2 = 6\frac{5}{64} = 0.46875$

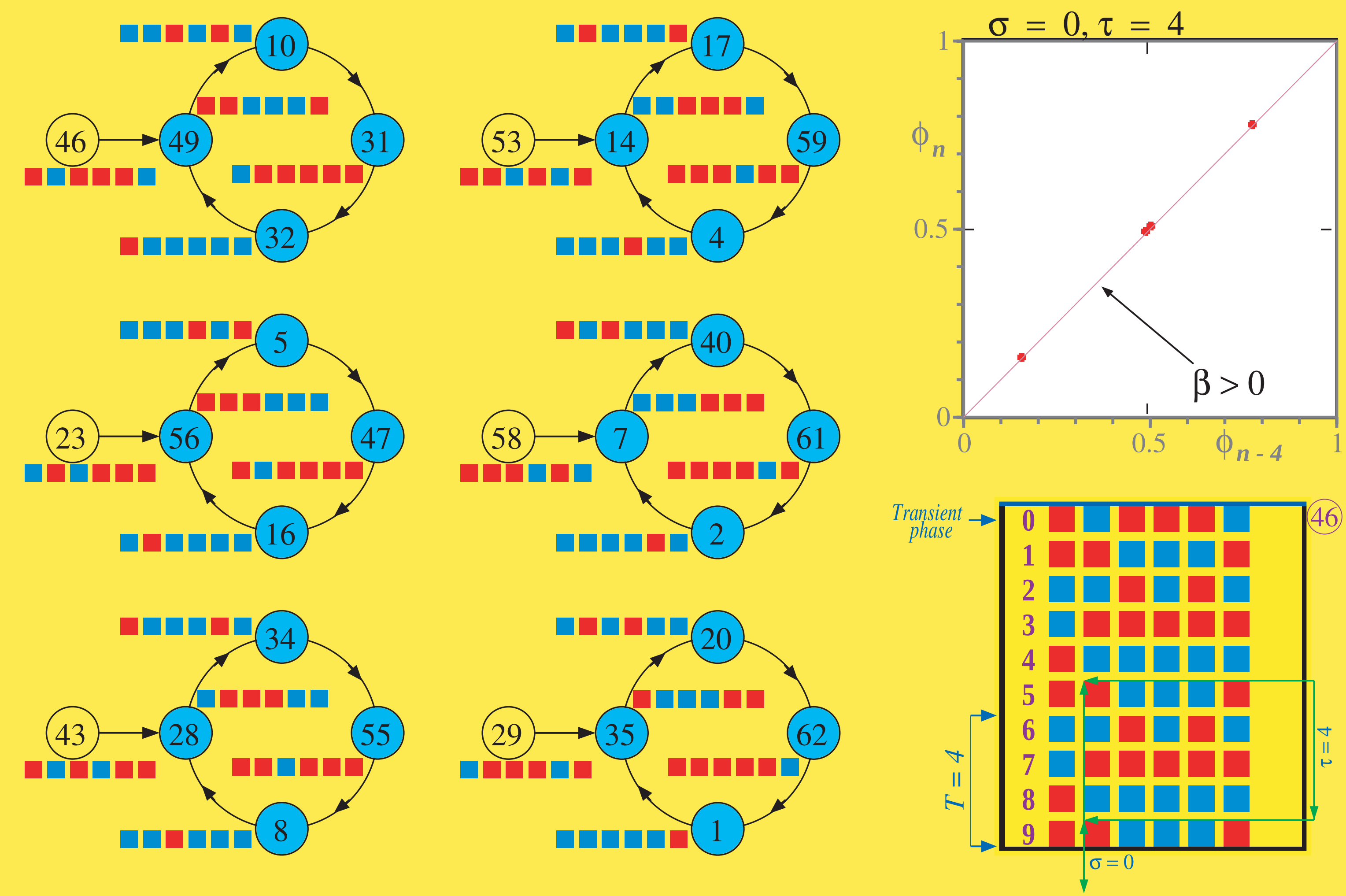

Gallery 54 - 5

54, ***L* = 7**

(a) Period-1 Attractor : $\rho_1 = \frac{9}{128} = 0.0703125$

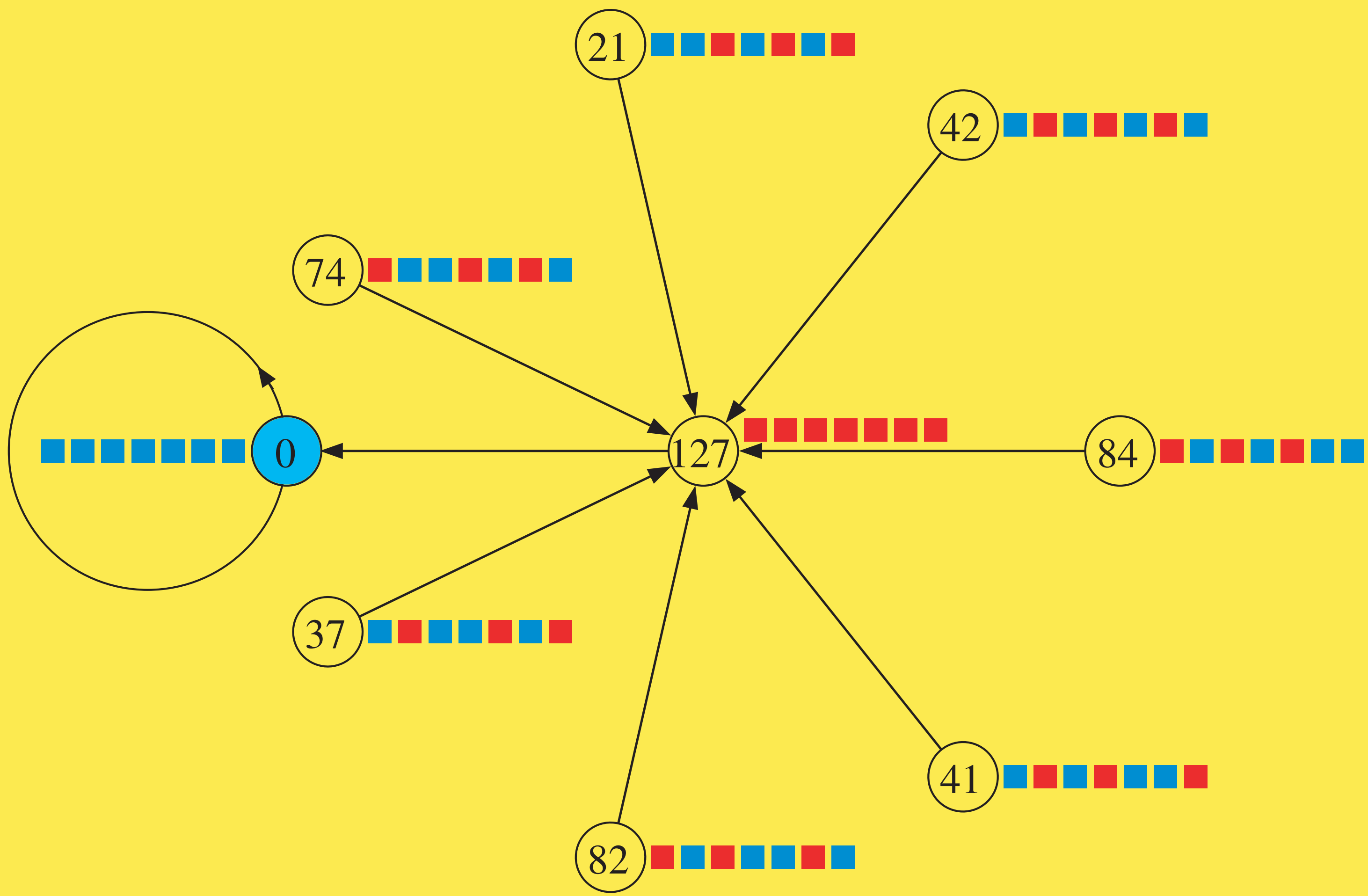

Gallery 54 - 6

Table 16. (*Continued*)

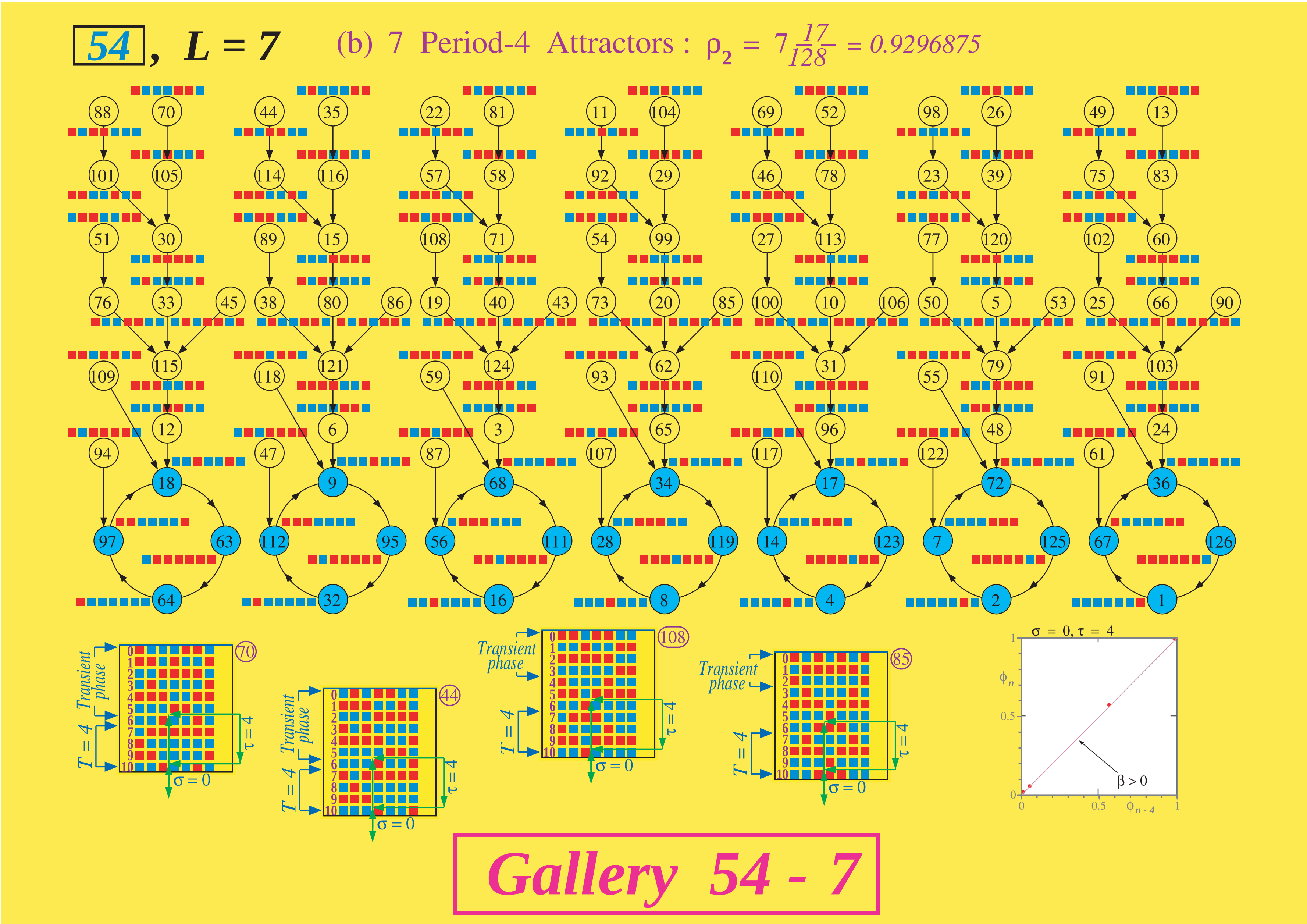

$\boxed{54}$, $L = 8$

(a) Period-1 Attractor : $\rho_1 = \frac{20}{256} = 0.078125$

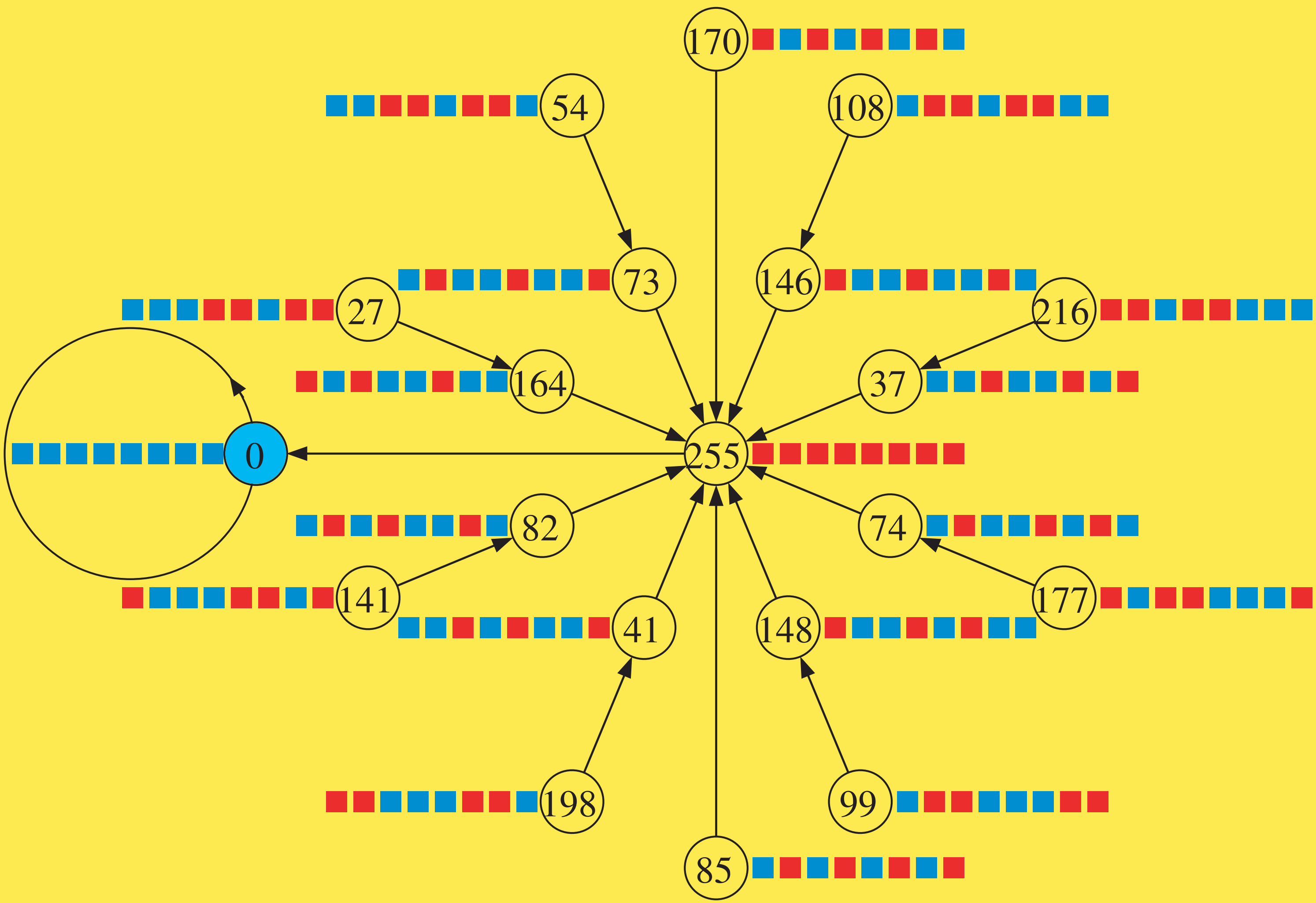

Gallery 54 - 8

54, ***L* = 8** (b) Bernoulli ($\sigma = \pm 2, \tau = 2$) 2 Period-4 Attractors : $\rho_2 = 2\frac{24}{256} = 0.1875$

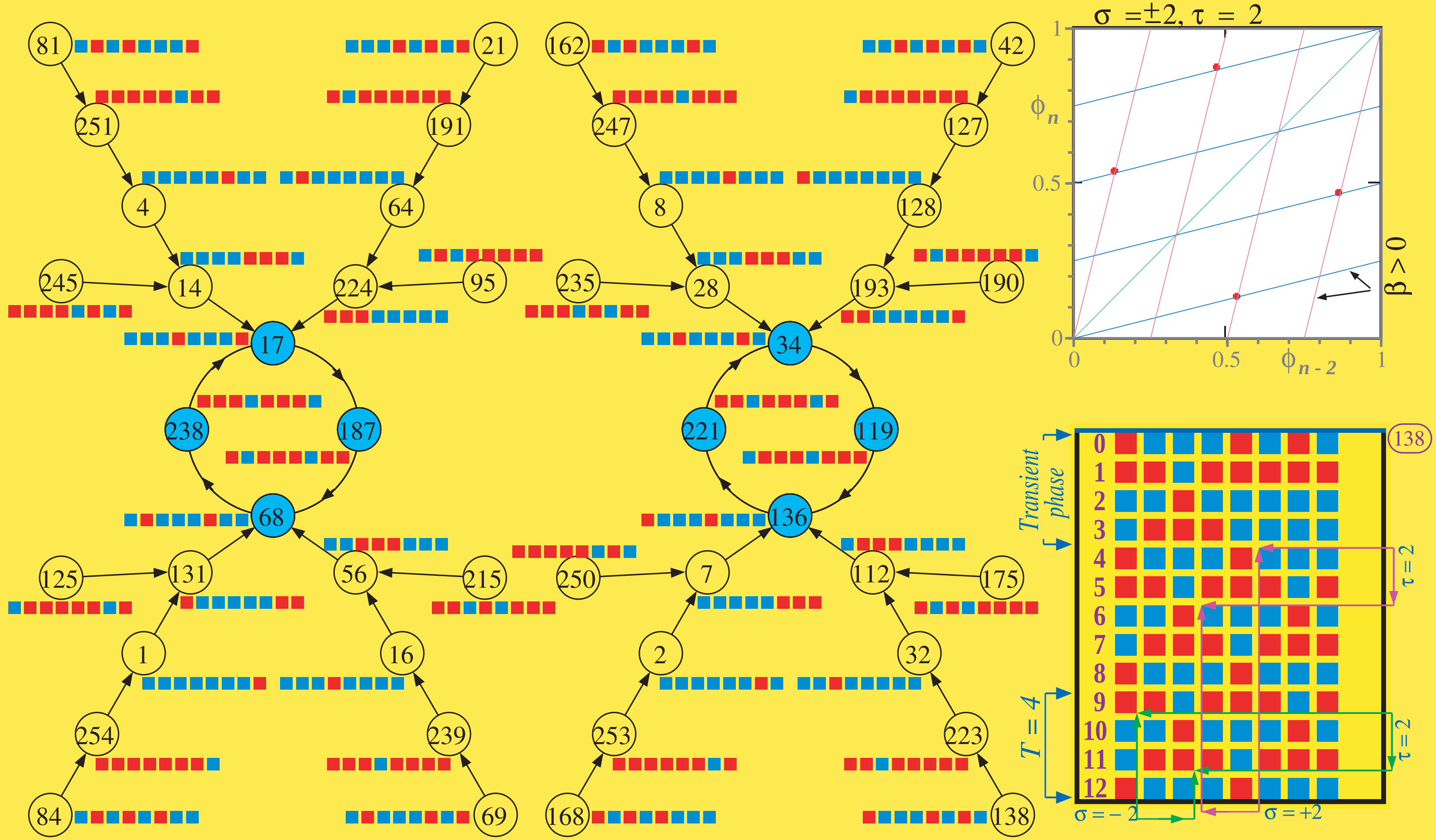

Gallery 54 - 9

Table 16. (*Continued*)

54, ***L* = 8** (c) Bernoulli ($\sigma = \pm 4, \tau = 2$) 4 Period-4 Attractors : $\rho_3 = 4\frac{14}{256} = 0.21875$

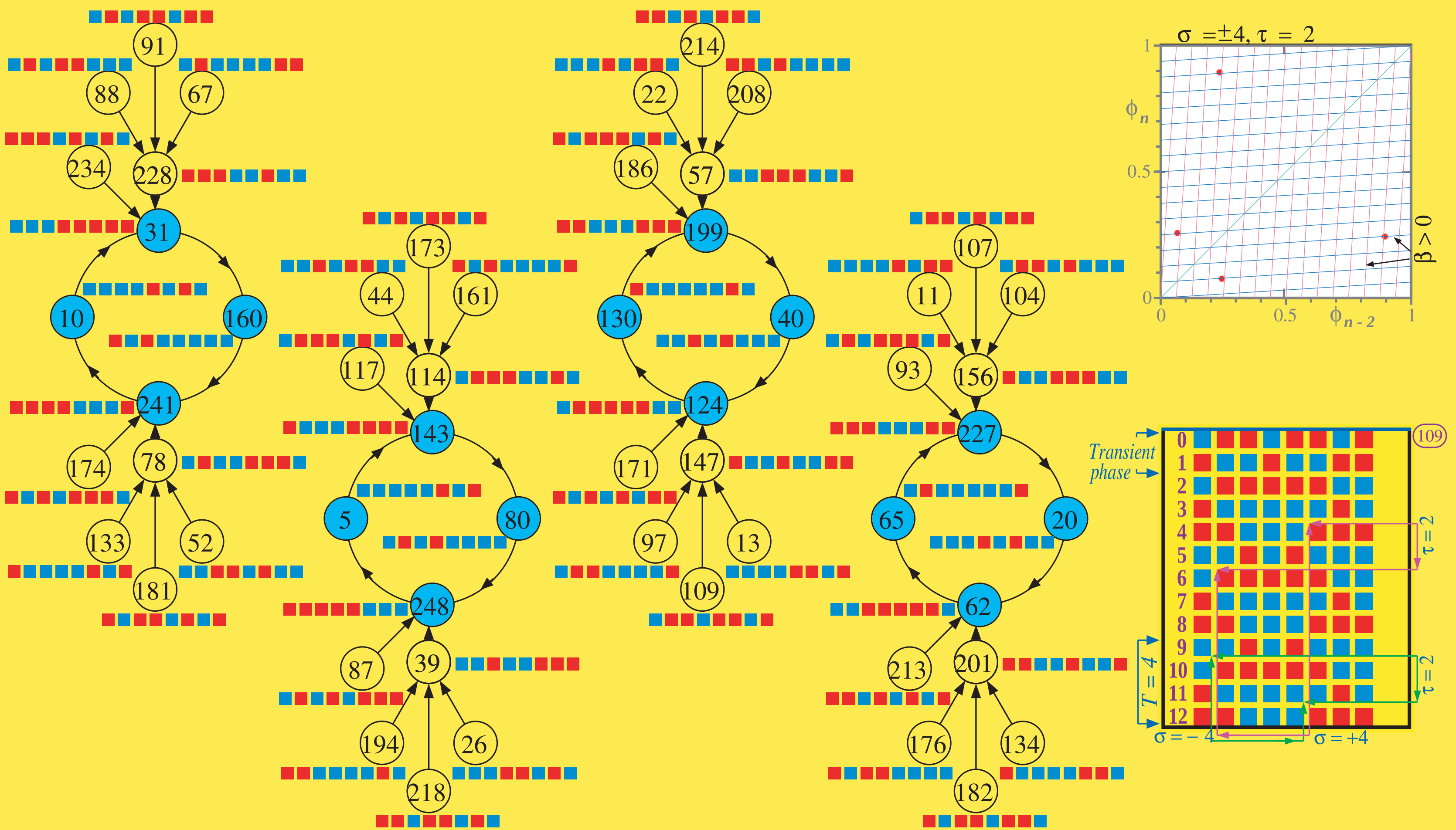

Gallery 54 - 10

$\boxed{54}$, $L = 8$

(d) Bernoulli ($\sigma = \pm 4, \tau = 3$) 4 Period-6 Attractors :

$\rho_4 = 4\frac{28}{256} = 0.4375$

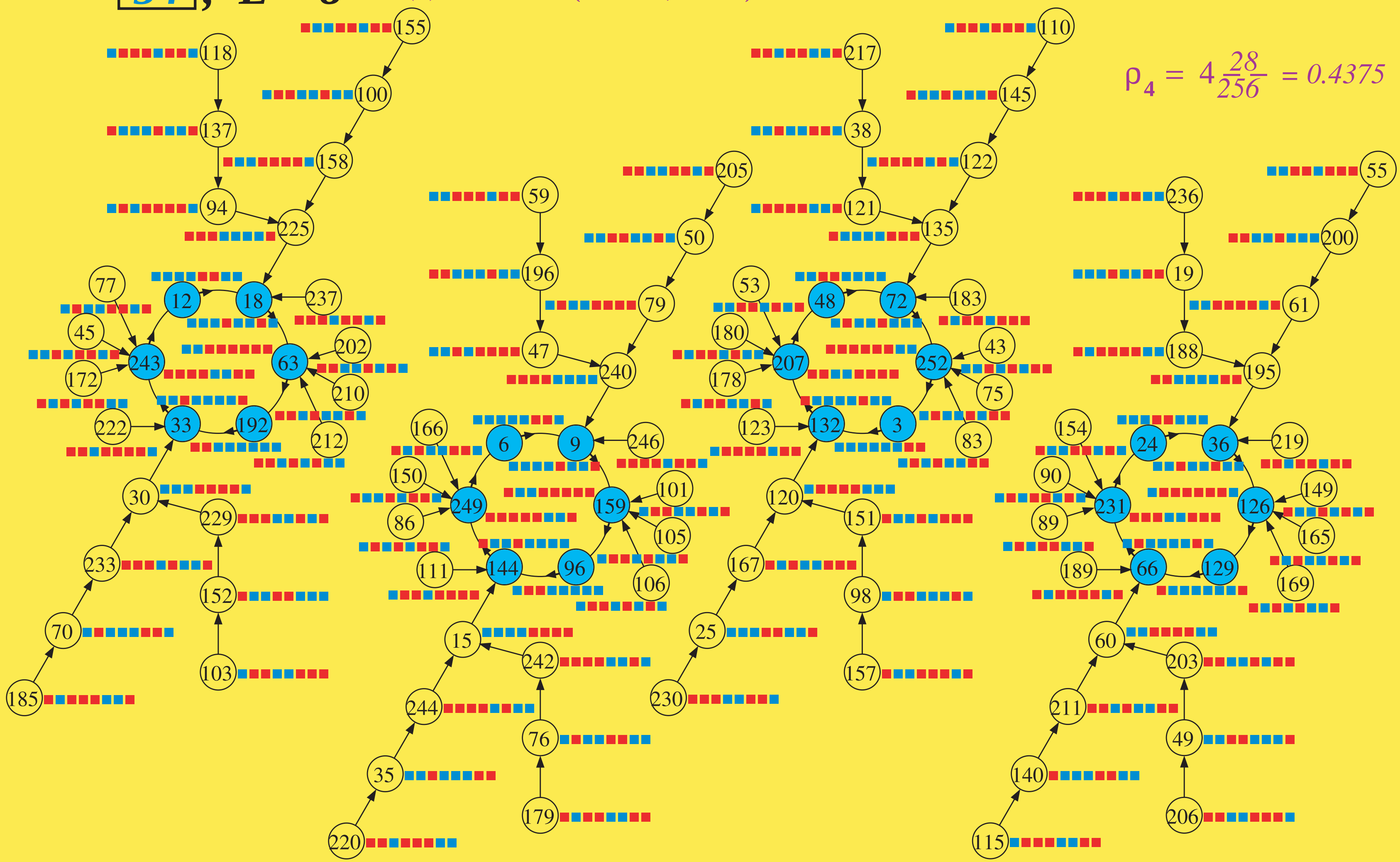

Gallery 54 - 11

$\boxed{54}$, $L = 8$

(d) Bernoulli ($\sigma = \pm 4$, $\tau = 3$)

4 Period-6 Attractors *(continued)* :

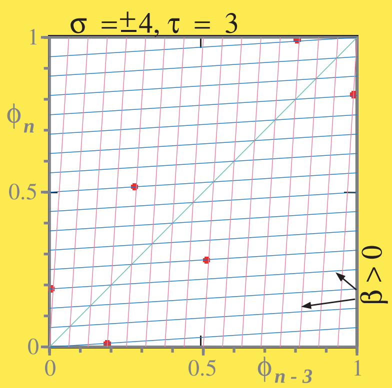

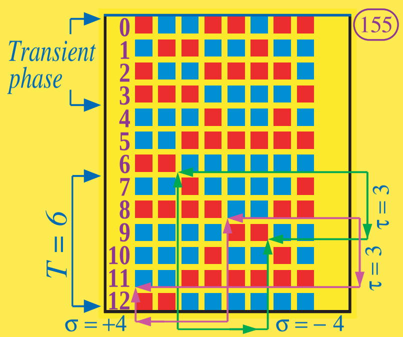

(e) Bernoulli ($\sigma = -3$, $\sigma = +3$, $\tau = 1$)

2 Period-8 Isles of Eden :

$\rho_5 = 2\frac{8}{256} = 0.0625$

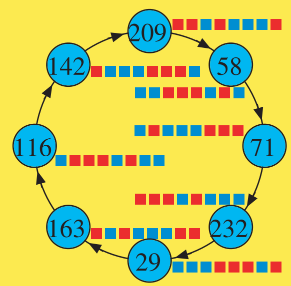

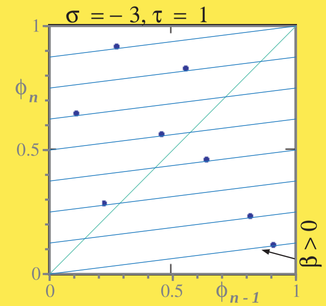

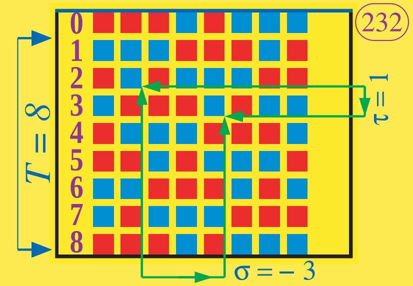

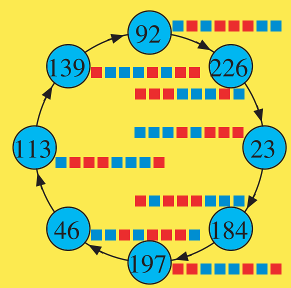

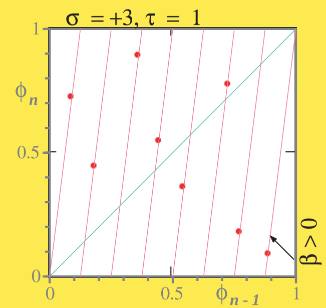

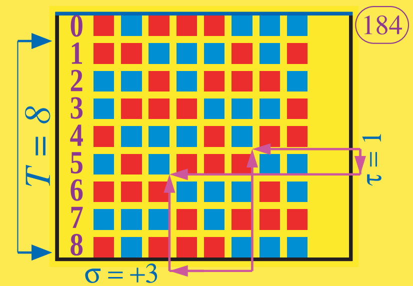

(f) Bernoulli ($\sigma = \pm 2$, $\tau = 1$)

2 Period-2 Isles of Eden :

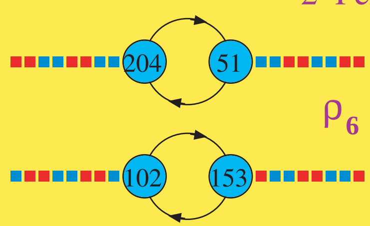

$\rho_6 = 2\frac{2}{256} = 0.015625$

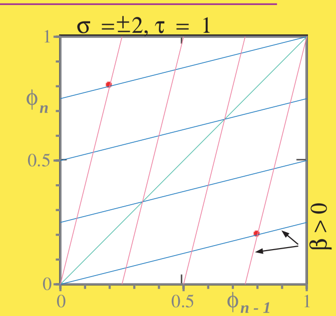

Gallery 54 - 12

2.4.3. *Highlights from Rule* $\boxed{54}$

The basin tree diagrams of Rule $\boxed{54}$ for $L = 3, 4, \ldots, 8$ are exhibited in Table 16. Following a detailed analysis of these diagrams, the qualitative properties of local rule $\boxed{54}$ extracted from basin-tree Galleries 54-1 to 54-12 of Table 16 are summarized below:

Summary of Qualitative properties of local rule $\boxed{54}$ extracted from Gallery 54 for Rule $\boxed{54}$

L	ID Number i	Number of Period-n attractors	Number of Period-n Isles of Eden	Period n	Bernoulli Parameters						Robustness coefficient ρ
					σ_1	τ_1	β_1	σ_2	τ_2	β_2	
3	1	1		1	0	1	+				$\rho_1 = 1$
4	1		2	4	2	2	+	-2	2	+	$\rho_1 = 0.5$
	2		2	2	2	1	+	-2	1	+	$\rho_2 = 0.25$
	3	1		1	0	1	+				$\rho_3 = 0.25$
5	1	1		1	0	1	+				$\rho_1 = 1$
6	1	1		1	0	1	+				$\rho_1 = 0.53125$
	2	6		4	0	4	+				$\rho_2 = 0.46875$
7	1	1		1	0	1	+				$\rho_1 = 0.0703125$
	2	7		4	0	4	+				$\rho_2 = 0.9296875$
8	1	1		1	0	1	+				$\rho_1 = 0.078125$
	2	2		4	2	2	+	-2	2	+	$\rho_2 = 0.1875$
	3	4		4	4	2	+	-4	2	+	$\rho_3 = 0.21875$
	4	4		6	4	3	+	-4	3	+	$\rho_4 = 0.4375$
	5		2	8	3	1	+	-3	1	+	$\rho_5 = 0.0625$
	6		2	2	2	1	+	-2	1	+	$\rho_6 = 0.015625$

Table 17. Basin tree diagrams for rule $\boxed{73}$.

Basin tree diagrams for Rule $\boxed{73}$

$\boxed{73}$, $L = 3$ (a) Period-2 Attractor : (b) Period-1 Isles of Eden :

$\rho_1 = \frac{5}{8} = 0.625$ $\rho_2 = \frac{3}{8} = 0.375$

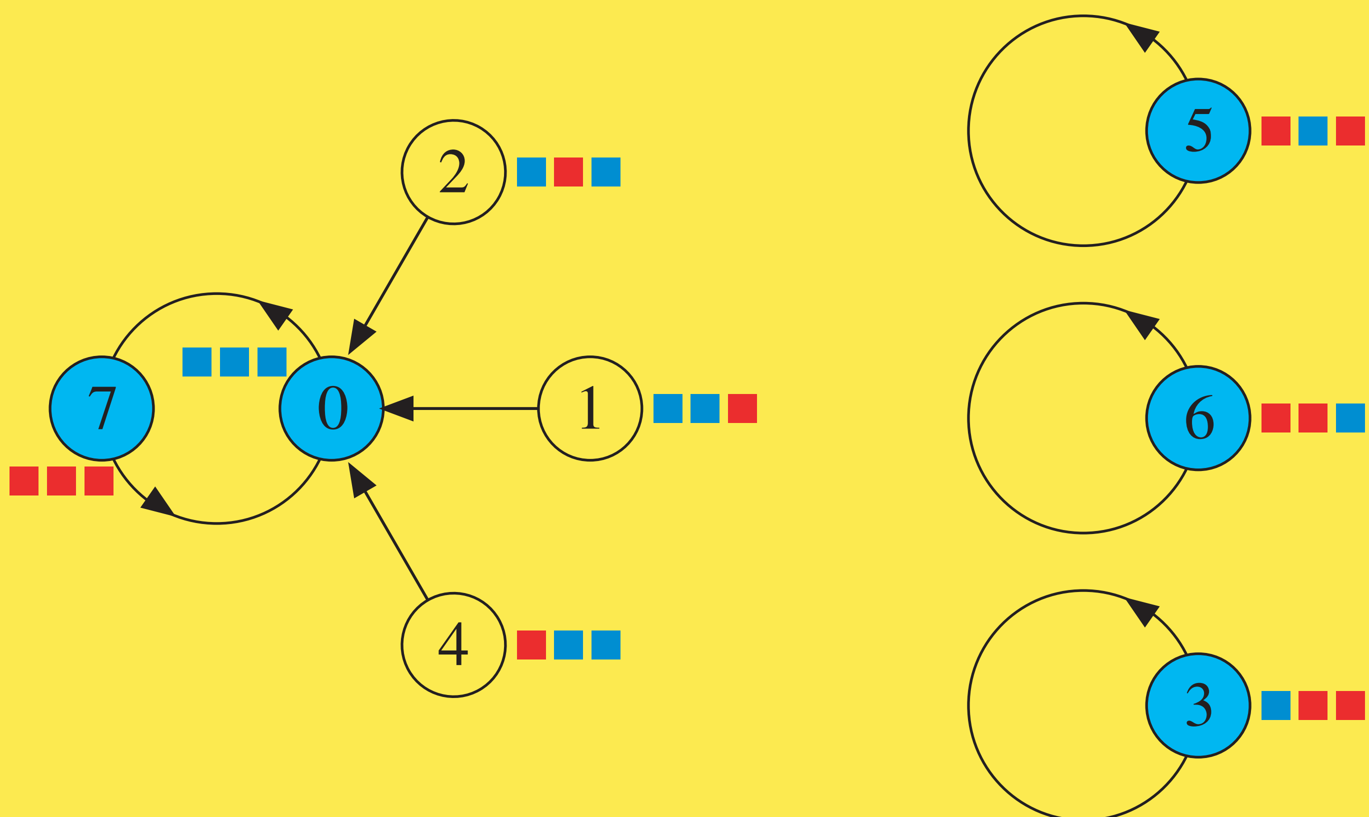

Gallery 73 - 1

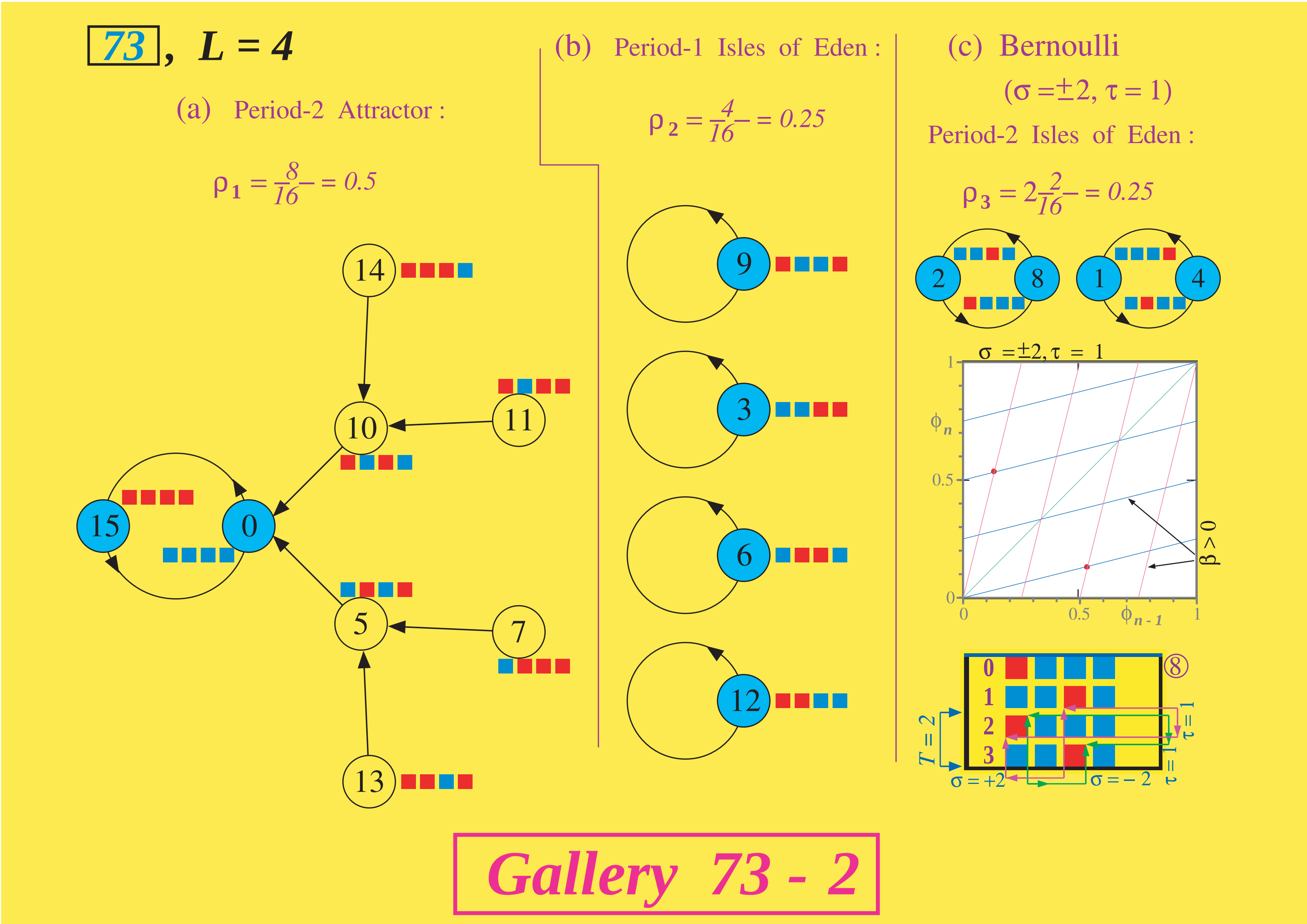
73, L = 4
(a) Period-2 Attractor :
$\rho_1 = \frac{8}{16} = 0.5$
15
0
14
10
11
5
7
13
(b) Period-1 Isles of Eden :
$\rho_2 = \frac{4}{16} = 0.25$
9
3
6
12
(c) Bernoulli
($\sigma = \pm 2, \tau = 1$)
Period-2 Isles of Eden :
$\rho_3 = 2\frac{2}{16} = 0.25$
2
8
1
4
$\sigma = \pm 2, \tau = 1$
ϕ_n
ϕ_{n-1}
$\beta > 0$
0
0.5
1
8
0
1
2
3
$T = 2$
$\sigma = +2$
$\sigma = -2$
$\tau = 1$
Gallery 73 - 2

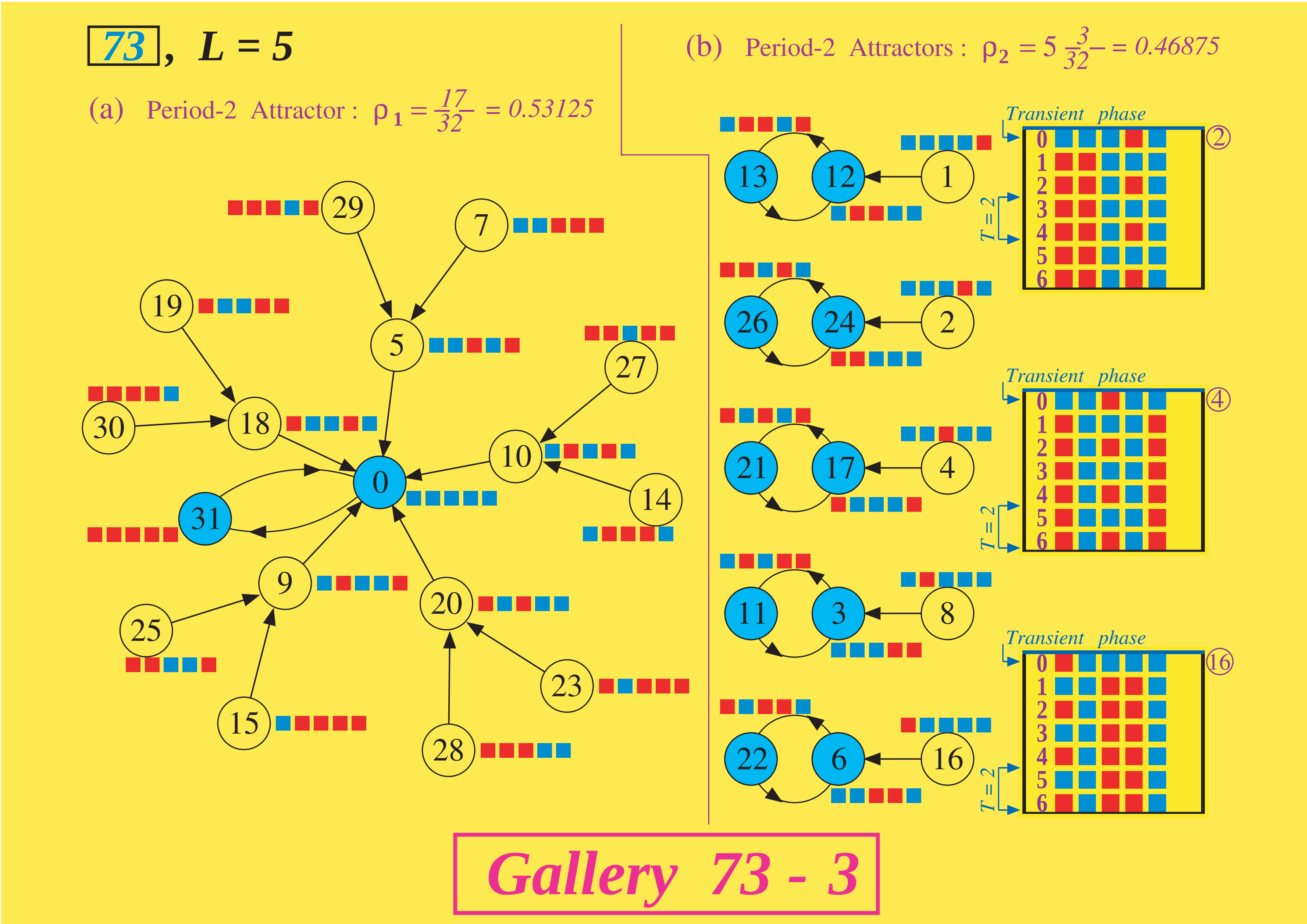
73, L = 5
(a) Period-2 Attractor : $\rho_1 = \frac{17}{32} = 0.53125$
(b) Period-2 Attractors : $\rho_2 = 5\ \frac{3}{32} = 0.46875$
Transient phase
T = 2
Gallery 73 - 3

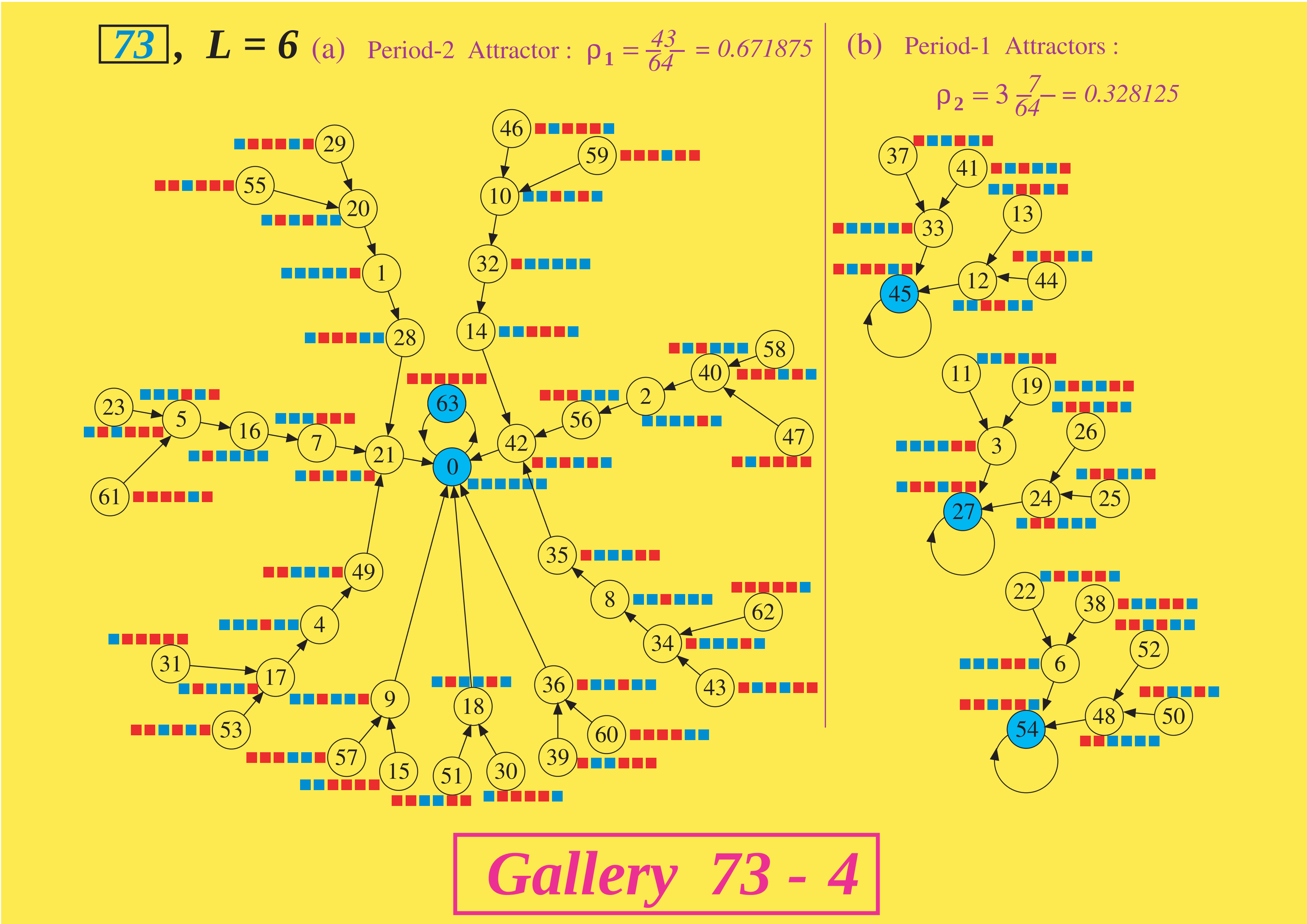
73, $L = 6$ (a) Period-2 Attractor : $\rho_1 = \frac{43}{64} = 0.671875$
(b) Period-1 Attractors :
$\rho_2 = 3\,\frac{7}{64} = 0.328125$
Gallery 73 - 4

$\boxed{73}$, $L = 7$ (a) Period-2 Attractor : $\rho_1 = \frac{44}{128} = 0.34375$

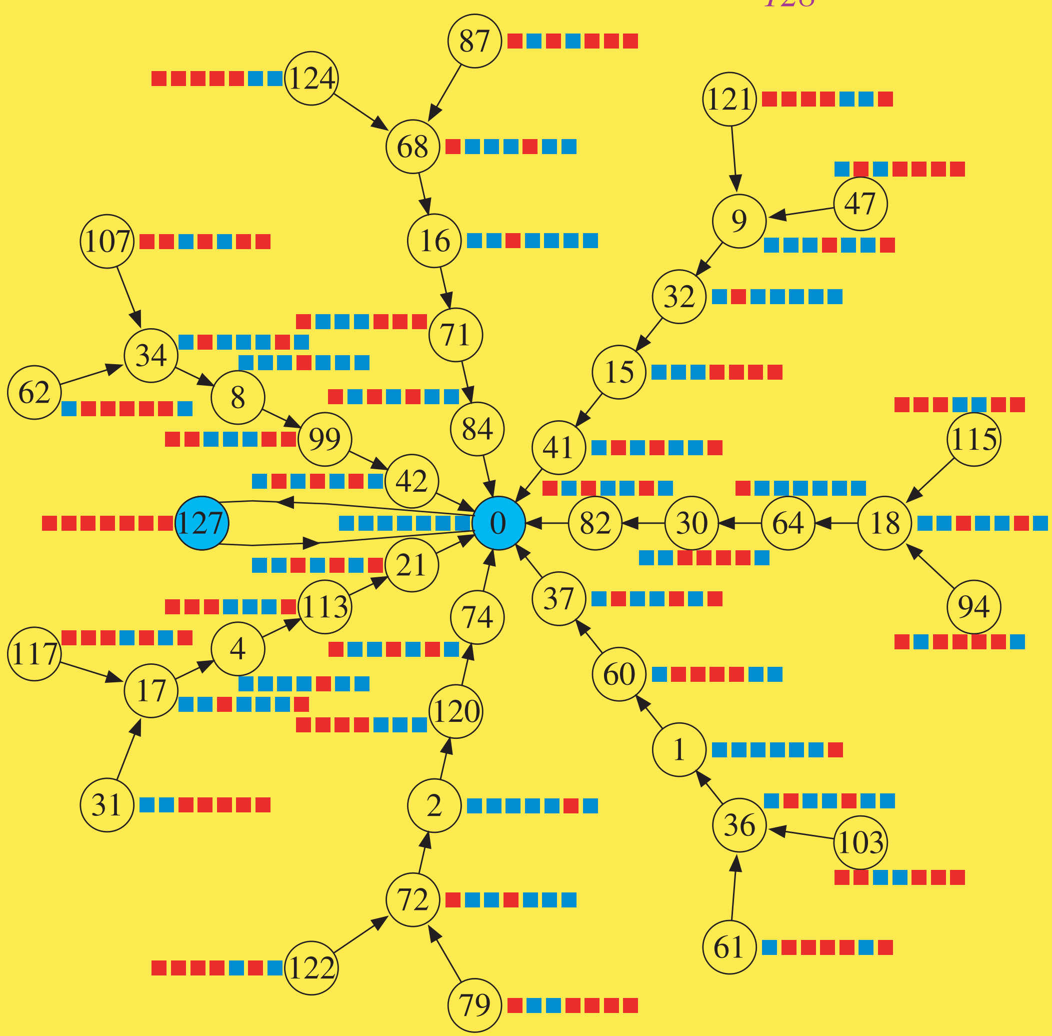

(b) Period-2 Isles of Eden :

$\rho_2 = 7\frac{2}{128} = 0.109375$

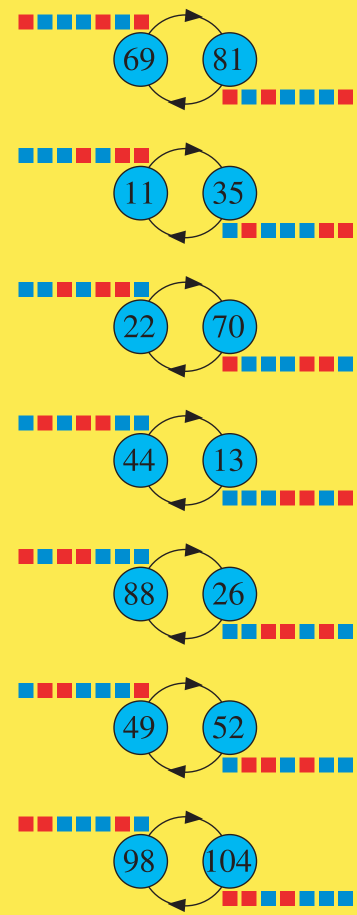

Gallery 73 - 5

Table 17. (*Continued*)

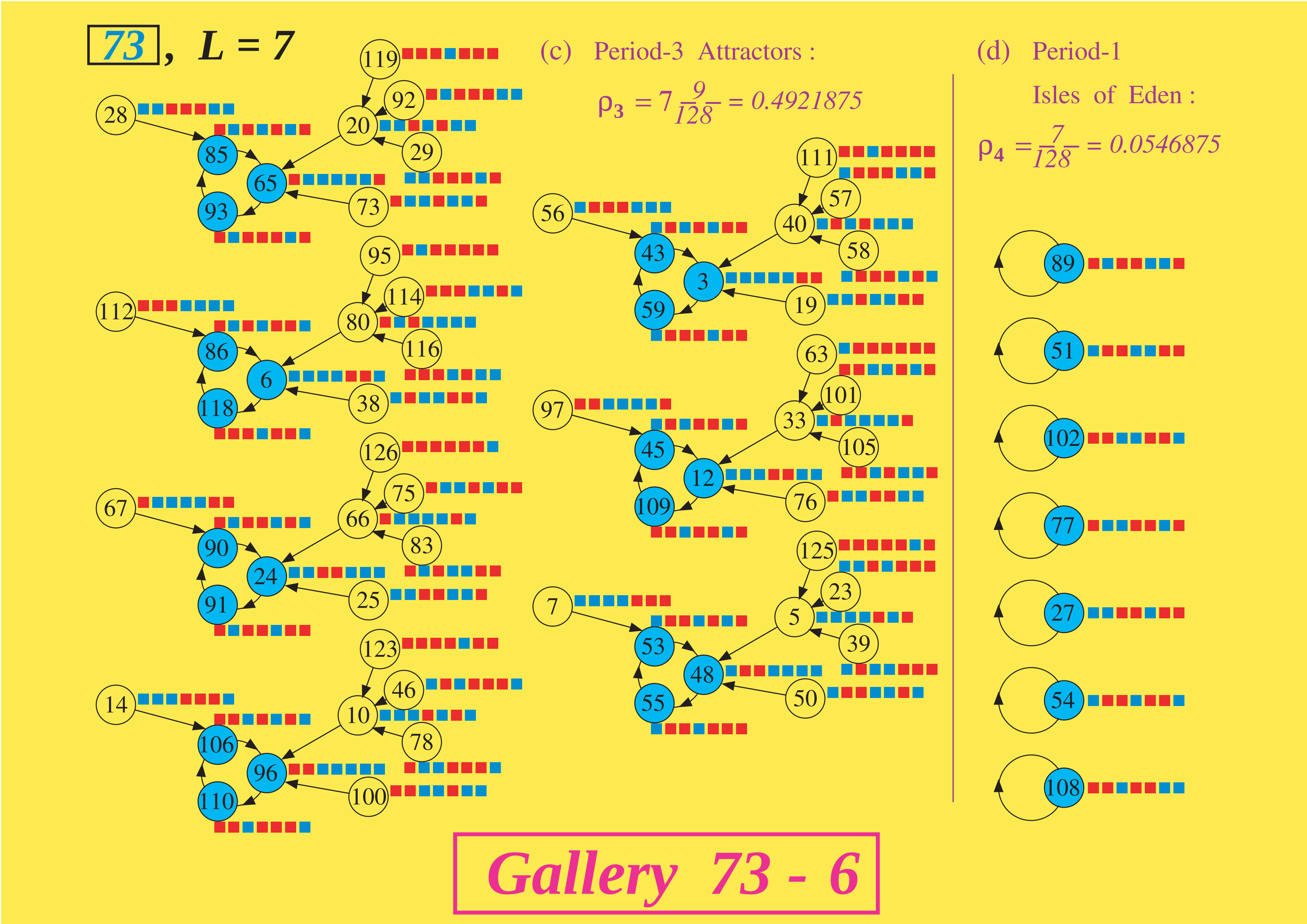

$\boxed{73}$, $L = 8$ (a) Bernoulli ($\sigma = \pm 4, \tau = 3$) Period-6 Attractors : $\rho_1 = 4\frac{10}{256} = 0.15625$

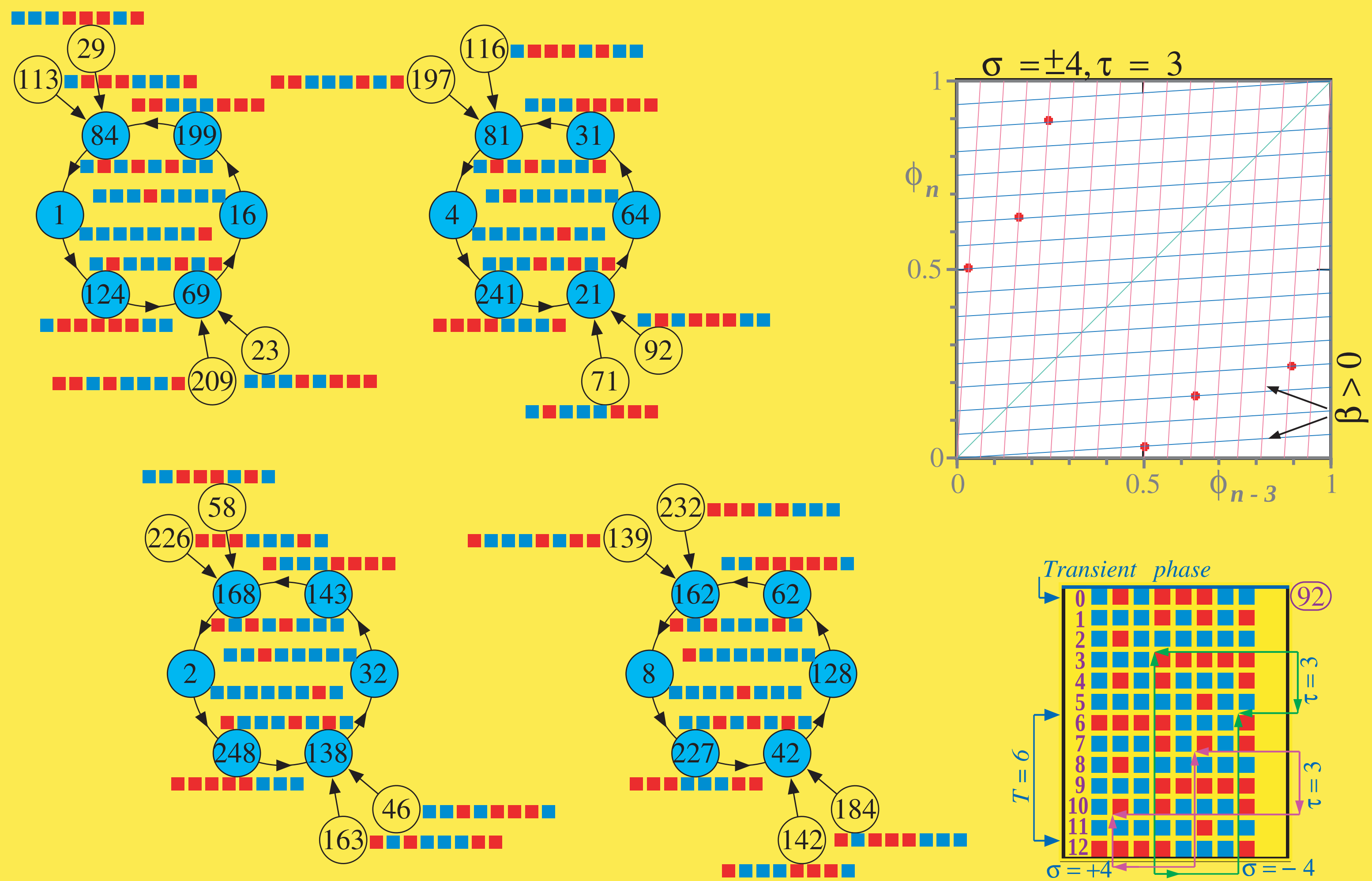

Gallery 73 - 7

73, $L = 8$ (b) Bernoulli ($\sigma = 0, \tau = 3$) Period-3 Attractors : $\rho_2 = 8\frac{5}{256} = 0.15625$

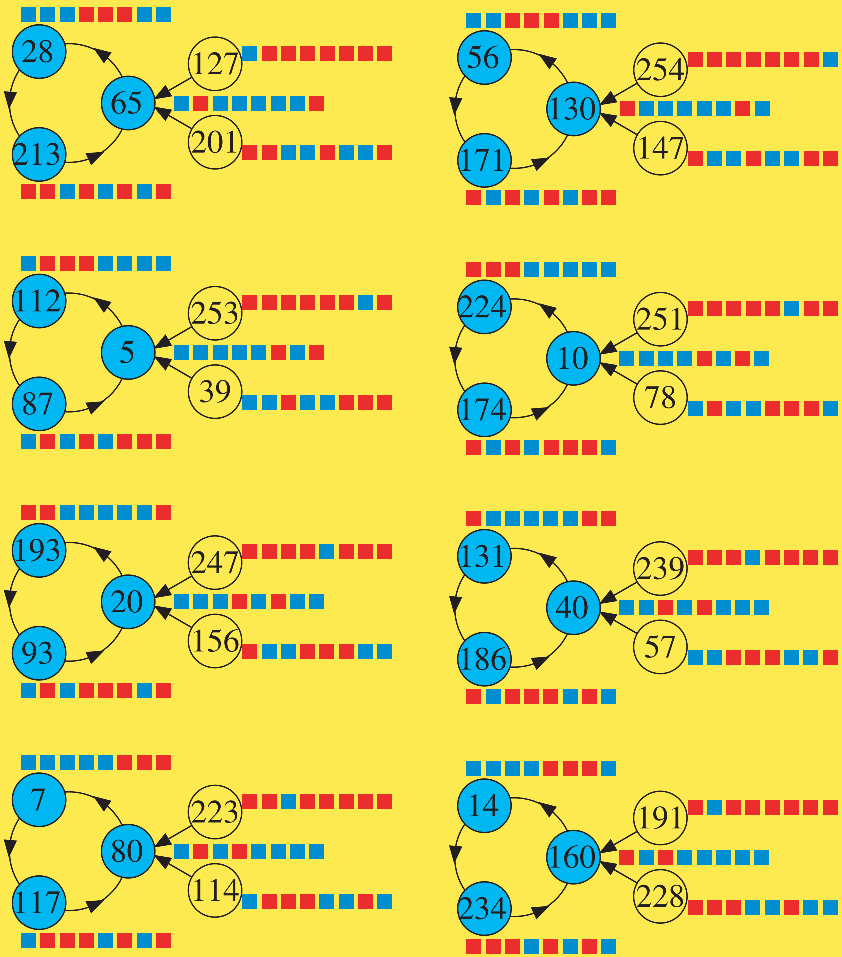

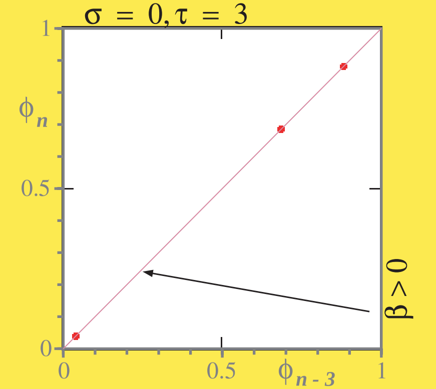

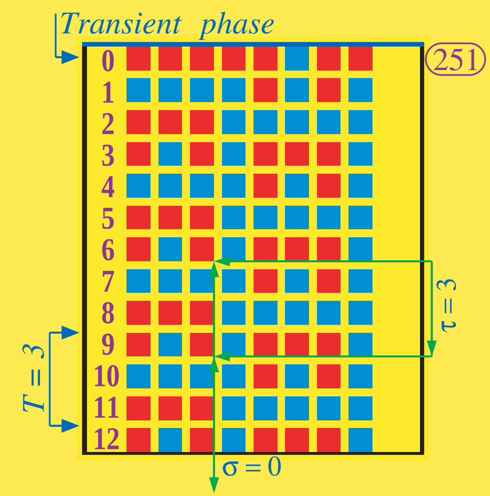

Gallery 73 - 8

73, ***L* = 8** (c) Period-3 Attractors : $\rho_3 = 8\,\frac{12}{256} = 0.375$

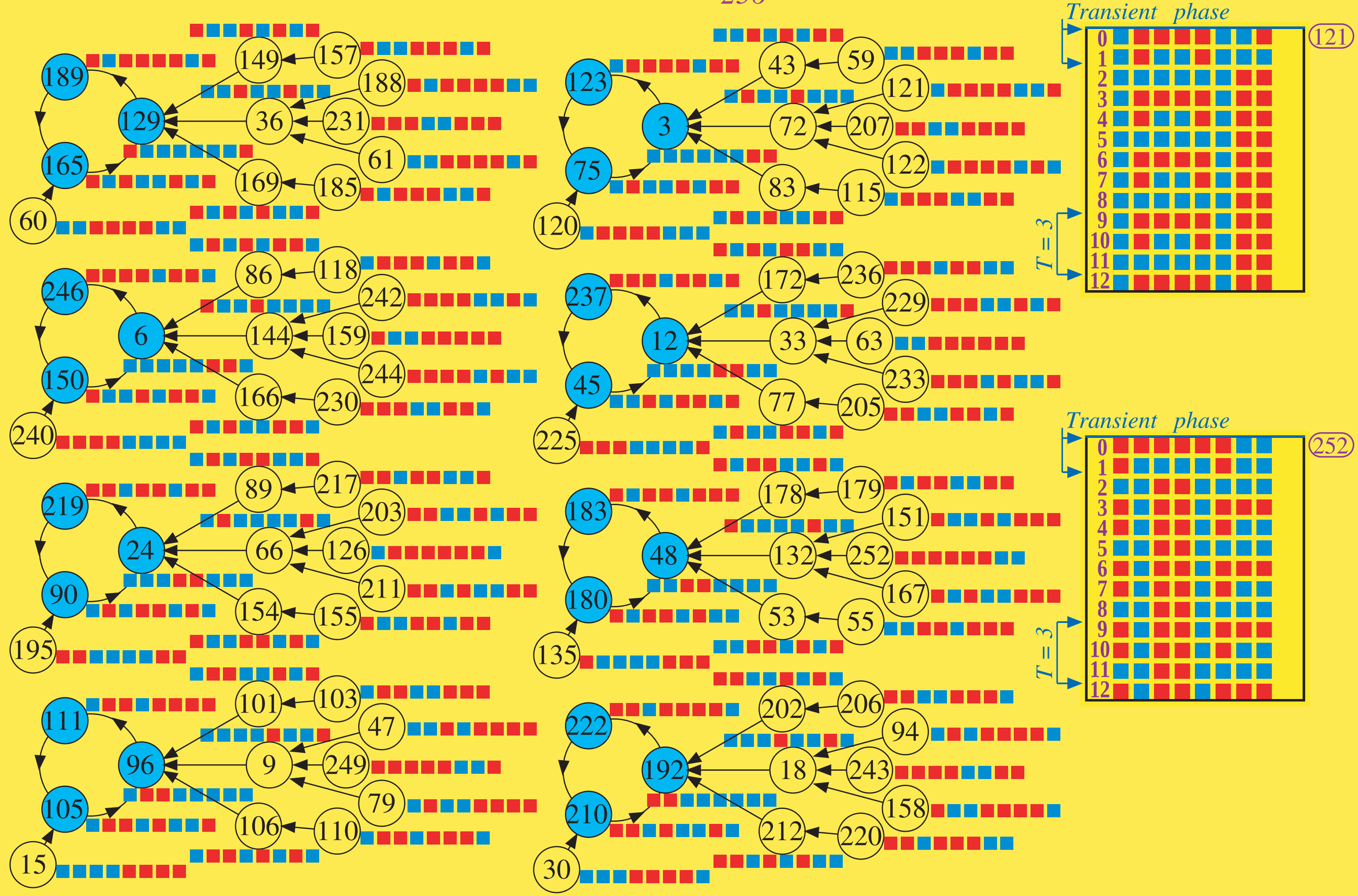

Gallery 73 - 9

$\boxed{73}$, $L = 8$

(d) Period-2 Attractors : $\rho_4 = 8\frac{6}{256} = 0.1875$

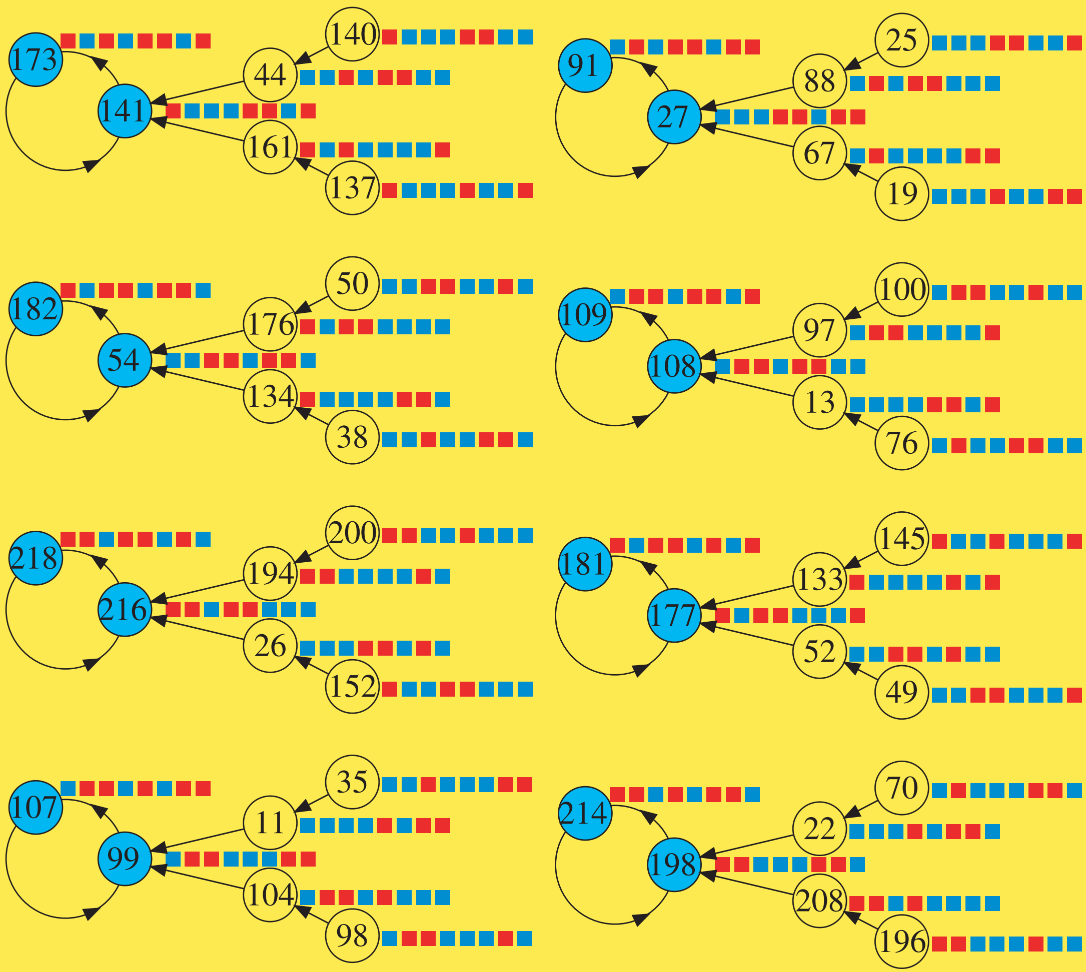

(e) Period-1 Isles of Eden :

$\rho_5 = \frac{4}{256} = 0.015625$

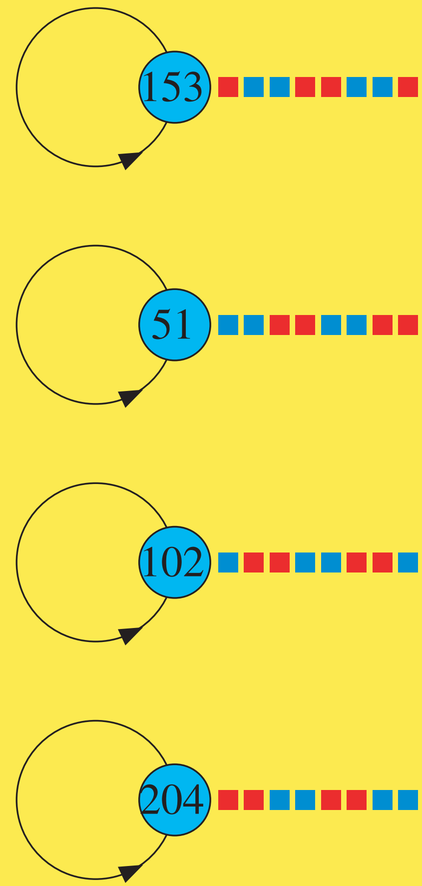

Gallery 73 - 10

$\boxed{73}$, ***L* = 8** (f) Period-2 Attractor :

$\rho_6 = \frac{16}{256} = 0.0625$

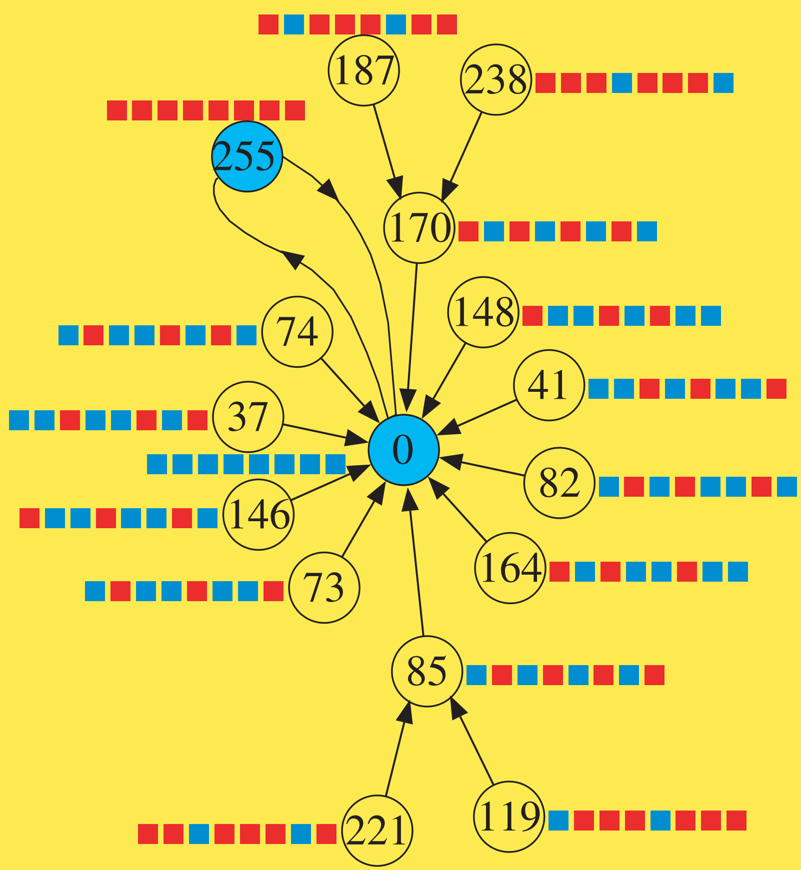

(g) Bernoulli ($\sigma = \pm 2, \tau = 1$)

Period-2 Attractors :

$\rho_7 = 2\frac{6}{256} = 0.046875$

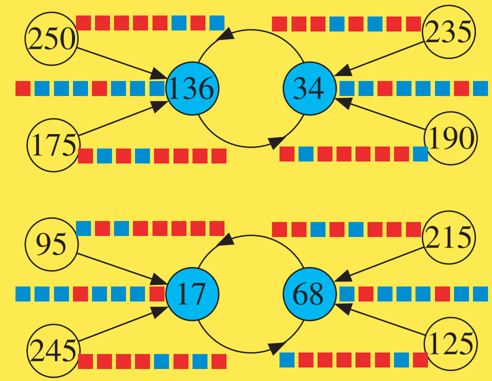

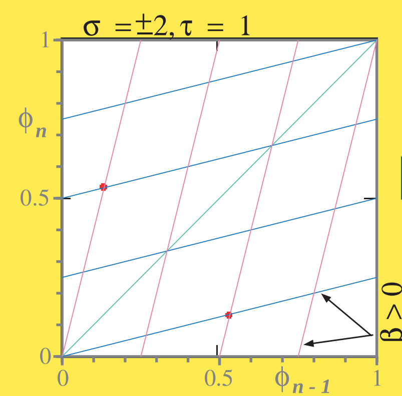

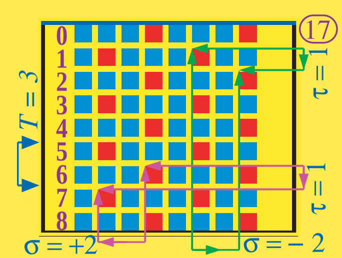

Gallery 73 - 11

2.4.4. *Highlights from Rule* $\boxed{73}$

The basin tree diagrams of Rule $\boxed{73}$ for $L = 3, 4, \ldots, 8$ are exhibited in Table 17. Following a detailed analysis of these diagrams, the qualitative properties of local rule $\boxed{73}$ extracted from basin-tree Galleries 73-1 to 73-11 of Table 17 are summarized below:

Summary of Qualitative properties of local rule $\boxed{73}$ extracted from Gallery 73 for Rule $\boxed{73}$

L	ID Number i	Number of Period-n attractors	Number of Period-n Isles of Eden	Period n	Bernoulli Parameters σ_1	τ_1	β_1	σ_2	τ_2	β_2	Robustness coefficient ρ
3	1	1		2	0	1	-				$\rho_1 = 0.625$
	2		3	1	0	1	+				$\rho_2 = 0.375$
4	1	1		2	0	1	-				$\rho_1 = 0.5$
	2		4	1	0	1	+				$\rho_2 = 0.25$
	3		2	2	2	1	+	-2	1	+	$\rho_3 = 0.25$
5	1	1		2	0	1	-				$\rho_1 = 0.53125$
	2	5		2	0	2	+				$\rho_2 = 0.46875$
6	1	1		2	0	1	-				$\rho_1 = 0.671875$
	2	3		1	0	1	+				$\rho_2 = 0.328115$
7	1	1		1	0	1	-				$\rho_1 = 0.34375$
	2		7	2	0	2	+				$\rho_2 = 0.109375$
	3	7		3	0	3	+				$\rho_3 = 0.4921875$
	4		7	1	0	1	+				$\rho_4 = 0.0546875$
8	1	4		6	4	3	+	-4	3	+	$\rho_1 = 0.15625$
	2	8		3	0	3	+				$\rho_2 = 0.15625$
	3	8		3	0	3	+				$\rho_3 = 0.375$
	4	8		2	0	2	+				$\rho_4 = 0.1875$
	5		4	1	0	1	+				$\rho_5 = 0.015625$
	6	1		2	0	1	-				$\rho_6 = 0.0625$
	7	2		2	2	1	+	-2	1	+	$\rho_7 = 0.046875$

Table 18. Basin tree diagrams for rule $\boxed{90}$.

Basin tree diagrams for Rule $\boxed{90}$

$\boxed{90}$, $L = 3$ (a) Period-1 Attractors : $\rho_1 = 4\,\frac{2}{8} = 1$

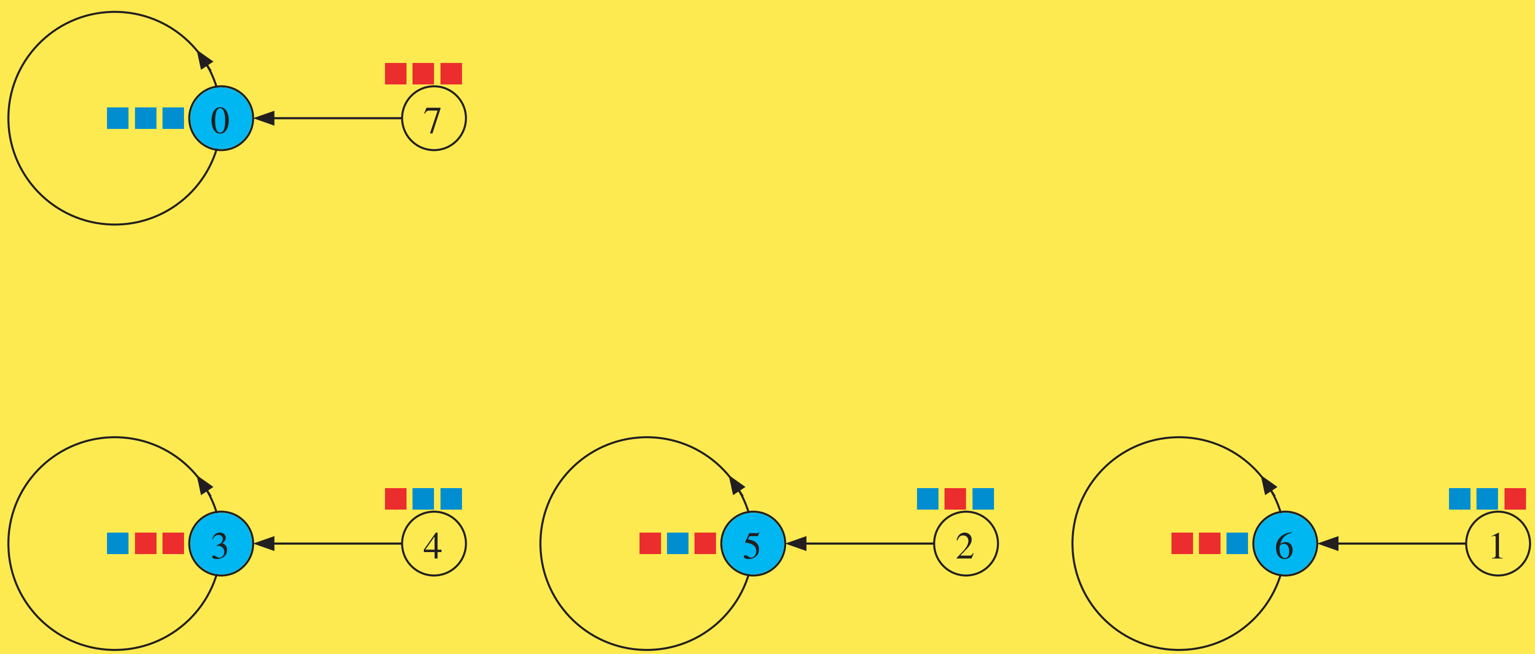

Gallery 90 - 1

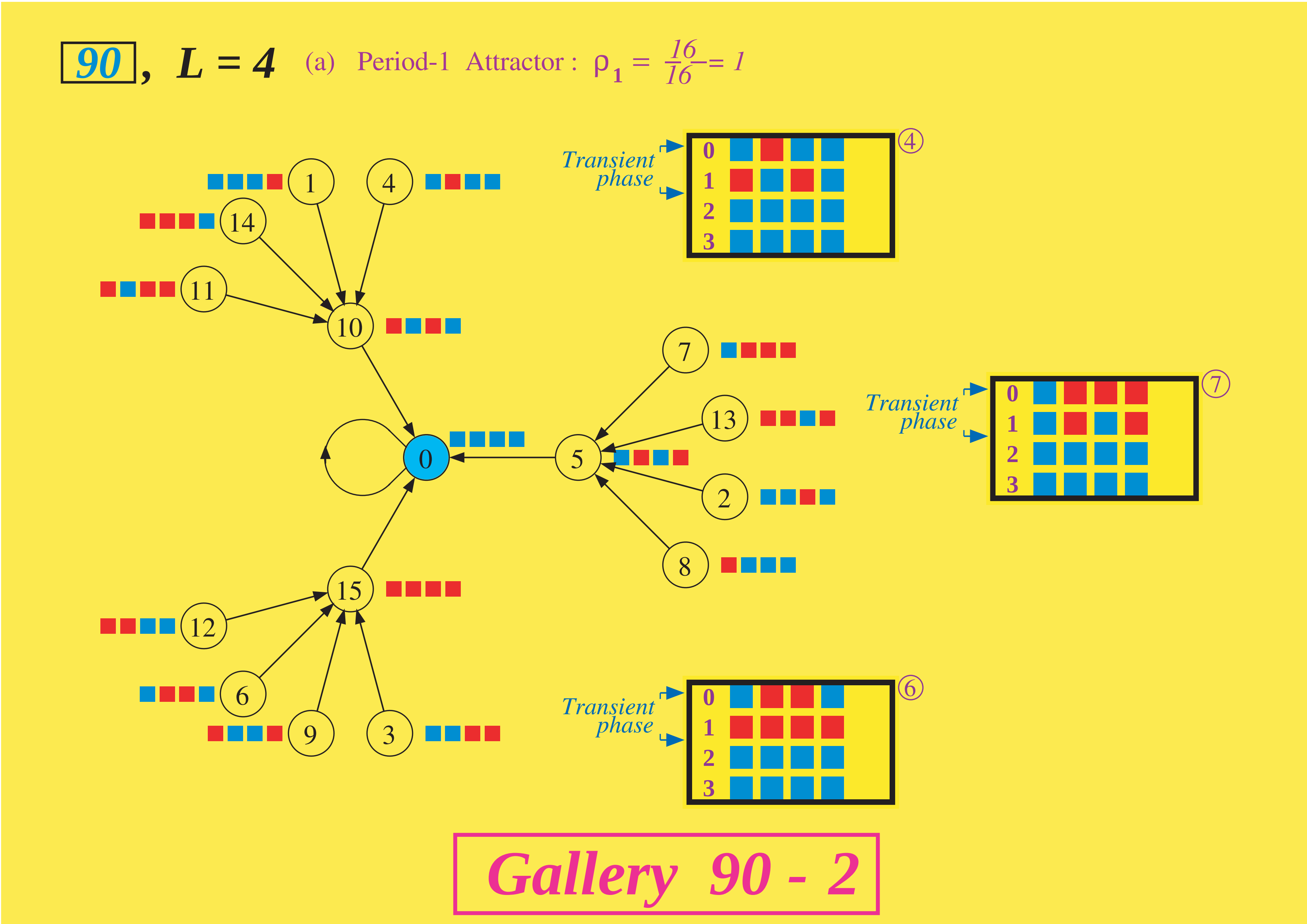

90, L = 4
(a) Period-1 Attractor : $\rho_1 = \frac{16}{16} = 1$
1
4
14
11
10
7
13
0
5
2
8
15
12
6
9
3
Transient phase
0
1
2
3
④
⑦
⑥
Gallery 90 - 2

$\boxed{90}$, $L = 5$ (a) Period-3 Attractors : $\rho_1 = 5\,\frac{6}{32} = 0.9375$

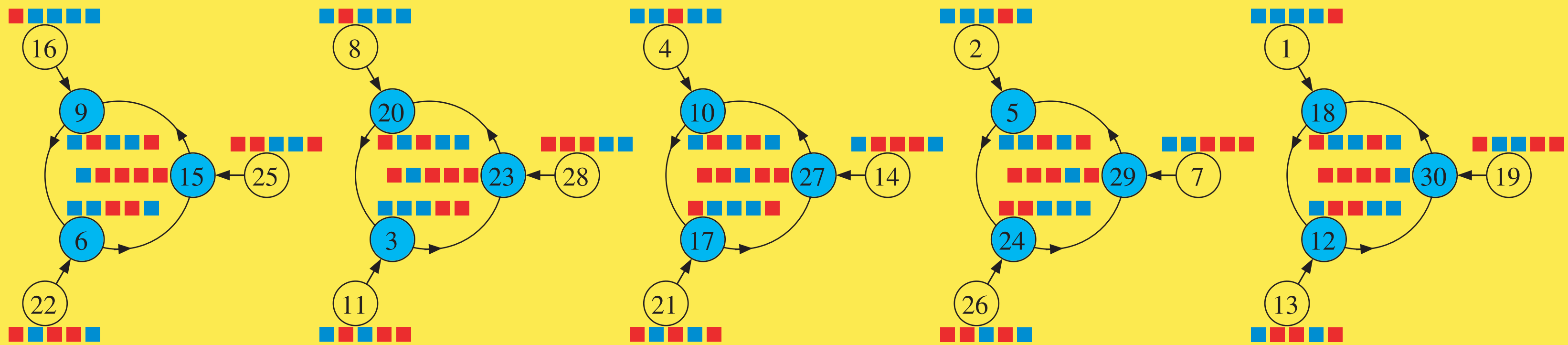

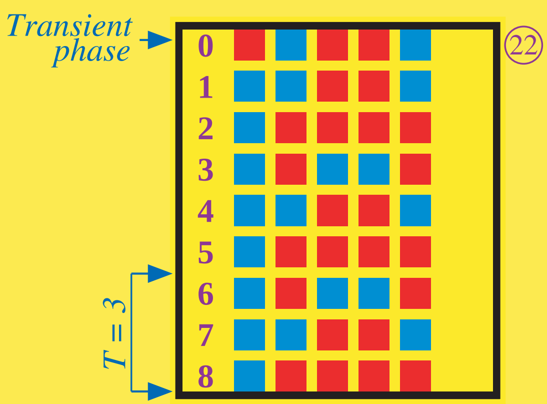

(b) Period-1 Attractor : $\rho_2 = \frac{2}{32} = 0.0625$

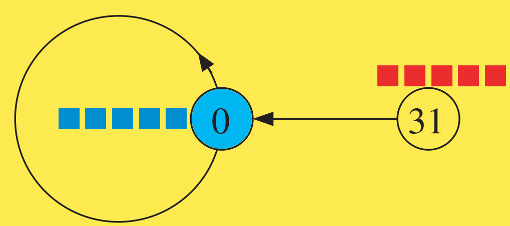

Gallery 90 - 3

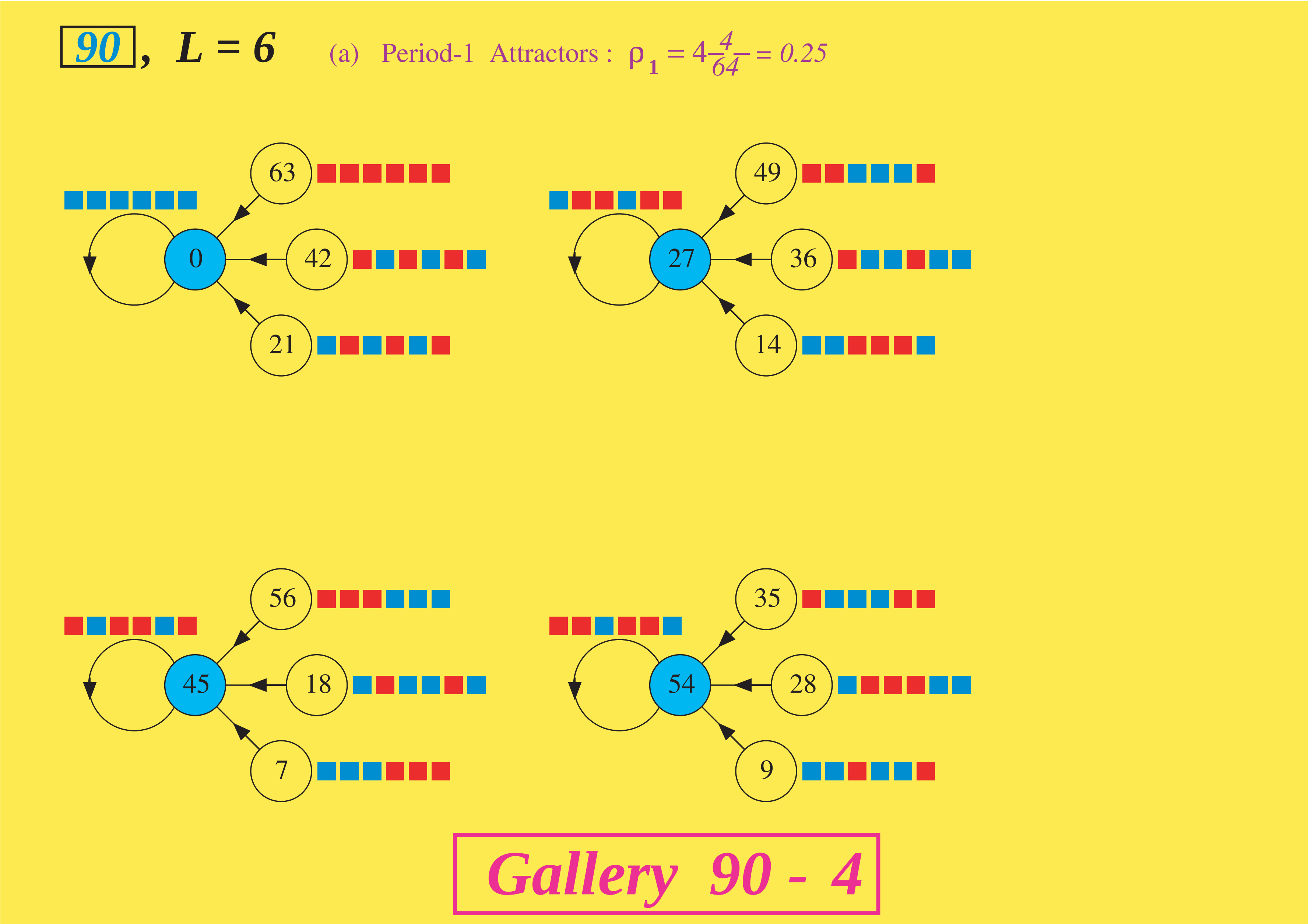
90 , L = 6
(a) Period-1 Attractors : $\rho_1 = 4\frac{4}{64} = 0.25$
63
0
42
21
49
27
36
14
56
45
18
7
35
54
28
9
Gallery 90 - 4

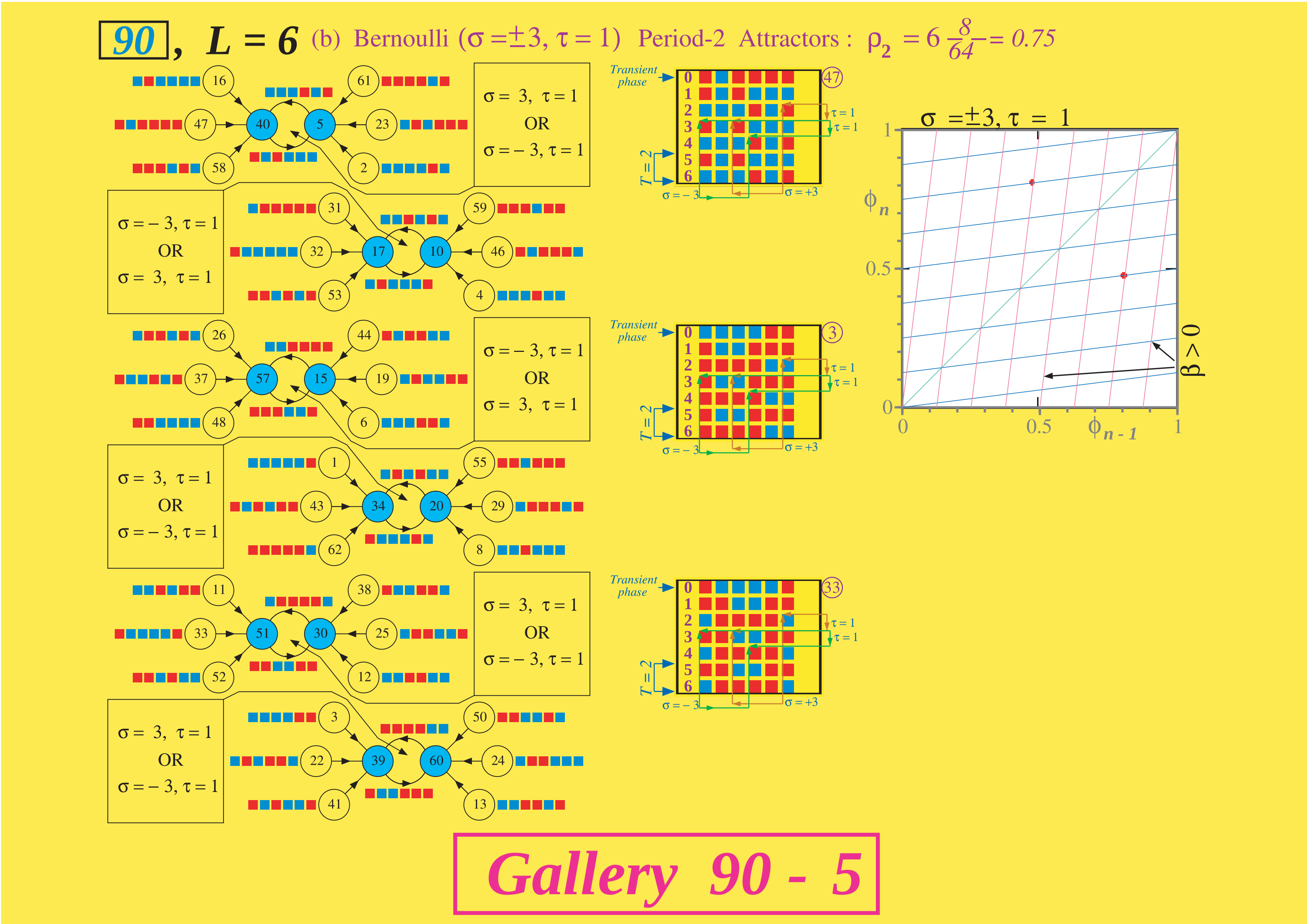
90, L = 6 (b) Bernoulli (σ = ±3, τ = 1) Period-2 Attractors : $\rho_2 = 6\frac{8}{64} = 0.75$
σ = 3, τ = 1
OR
σ = − 3, τ = 1
σ = − 3, τ = 1
OR
σ = 3, τ = 1
Transient phase
T = 2
τ = 1
σ = − 3
σ = +3
σ = ±3, τ = 1
ϕ_n
ϕ_{n-1}
β > 0
Gallery 90 - 5

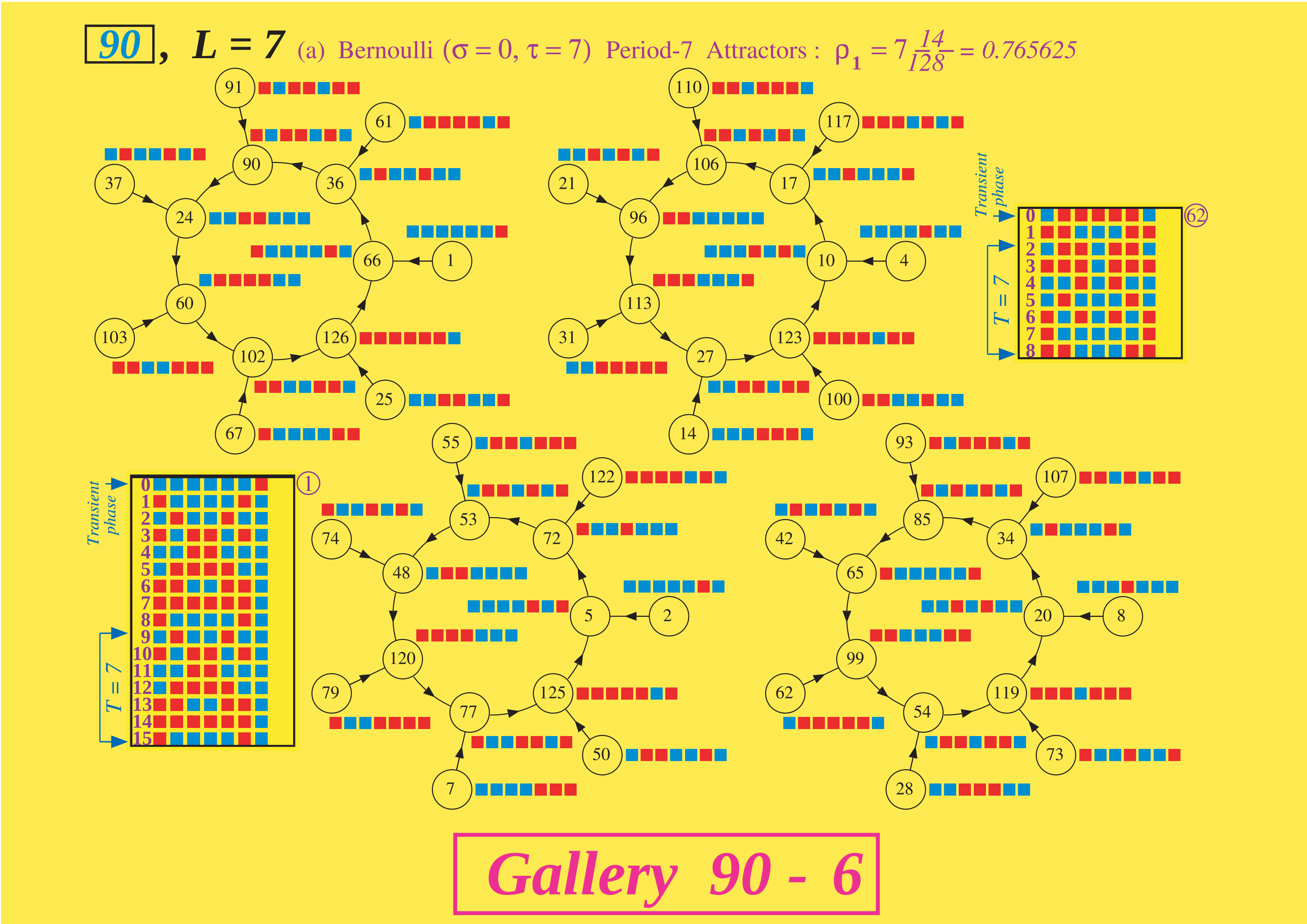
90, L = 7 (a) Bernoulli (σ = 0, τ = 7) Period-7 Attractors : $\rho_1 = 7\frac{14}{128} = 0.765625$
91 90 61 36 37 24 66 1 60 103 126 102 25 67
110 106 117 17 21 96 10 4 113 31 123 27 100 14
Transient phase
T = 7
62
1
55 53 122 72 74 48 5 2 120 79 125 77 50 7
93 85 107 34 42 65 20 8 99 62 119 54 73 28
Gallery 90 - 6

$\boxed{90}$, $L = 7$ (a) Bernoulli ($\sigma = 0, \tau = 7$) Period-7 Attractors *(continued)*

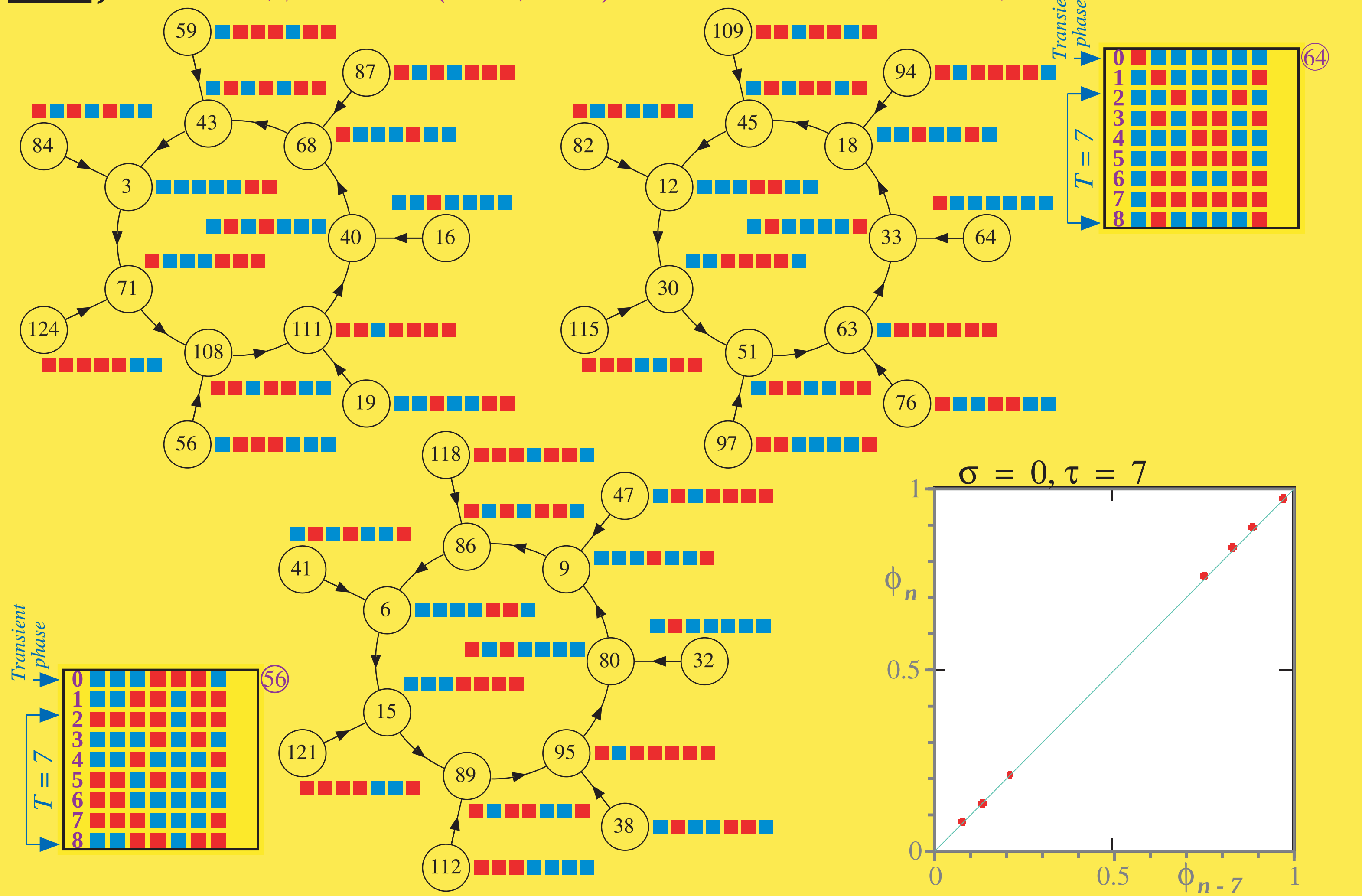

Gallery 90 - 7

Table 18. (*Continued*)

$\boxed{90}$, ***L* = 7** (b) Bernoulli ($\sigma = \pm 2$, $\sigma = \mp 5$, $\tau = 1$) Period-7 Attractors :

$$\rho_2 = 2\frac{14}{128} = 0.21875$$

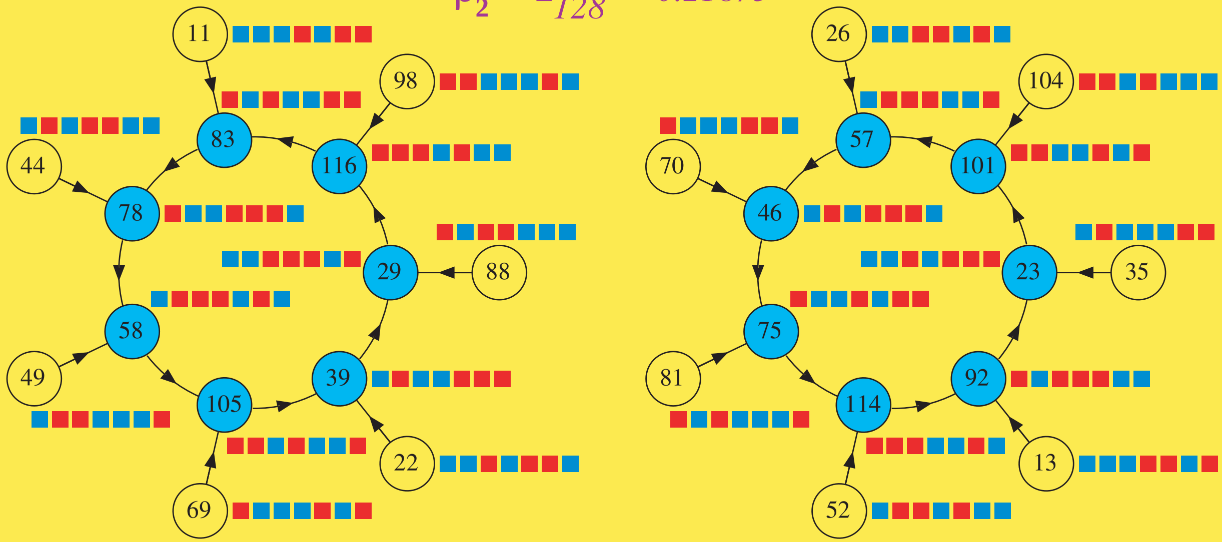

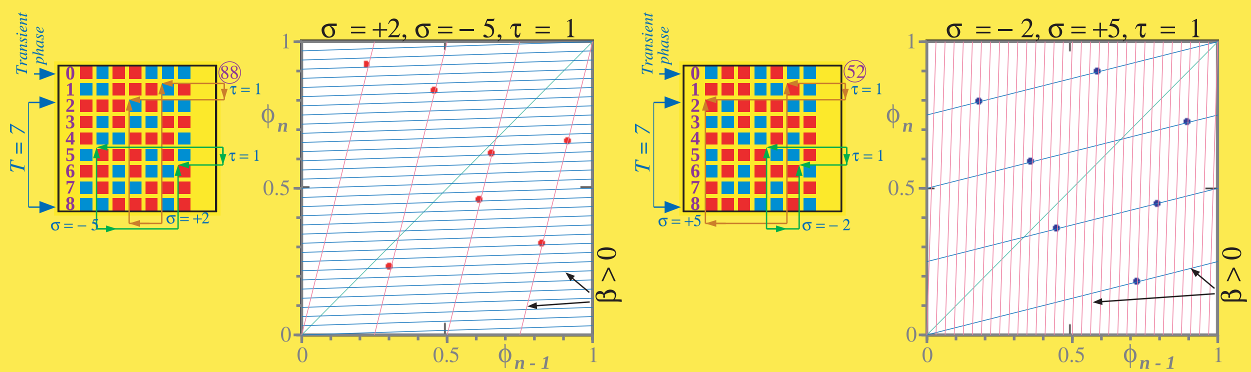

(c) Period-1 Attractor :

$$\rho_3 = \frac{2}{128} = 0.015625$$

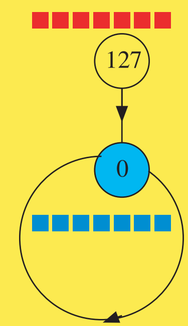

Gallery 90 - 8

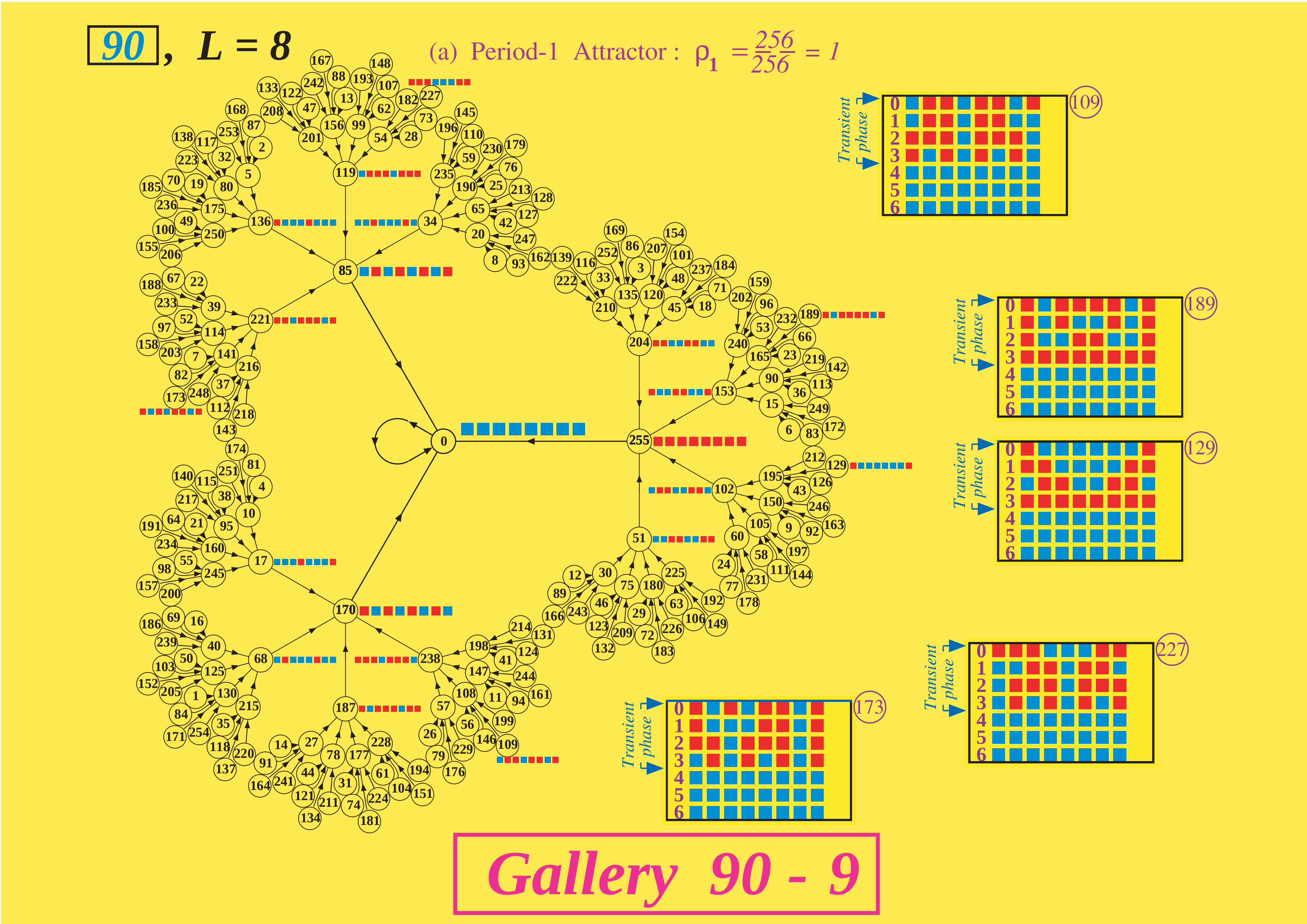
90, L = 8
(a) Period-1 Attractor : $\rho_1 = \frac{256}{256} = 1$
Transient phase
109
189
129
227
173
Gallery 90 - 9

2.4.5. *Highlights from Rule* $\boxed{90}$

The basin tree diagrams of Rule $\boxed{90}$ for $L = 3, 4, \ldots, 8$ are exhibited in Table 18. Following a detailed analysis of these diagrams, the qualitative properties of local rule $\boxed{90}$ extracted from basin-tree Galleries 90-1 to 90-9 of Table 18 are summarized below:

Summary of Qualitative properties of local rule $\boxed{90}$ extracted from Gallery 90 for Rule $\boxed{90}$

L	ID Number i	Number of Period-n attractors	Number of Period-n Isles of Eden	Period n	Bernoulli Parameters σ_1	τ_1	β_1	σ_2	τ_2	β_2	Robustness coefficient ρ
3	1	4		1	0	1	+				$\rho_1 = 1$
4	1	1		1	0	1	+				$\rho_1 = 1$
5	1	5		3	0	3	+				$\rho_1 = 0.9375$
	2	1		1	0	1	+				$\rho_2 = 0.0625$
6	1	4		1	0	1	+				$\rho_1 = 0.25$
	2	6		2	3	1	+	-3	1	+	$\rho_2 = 0.75$
7	1	7		7	0	1	+				$\rho_1 = 0.765625$
	2	2		7	± 2	1	+	∓ 5	1	+	$\rho_2 = 0.21875$
	3	1		1	0	1	+				$\rho_3 = 0.015625$
8	1	1		1	0	1	+				$\rho_1 = 1$

Table 19. Basin tree diagrams for rule $\boxed{105}$.

Basin tree diagrams for Rule $\boxed{105}$

$\boxed{105}$, $L = 3$ (a) Period-2 Attractor : $\rho_1 = \frac{8}{8} = 1$

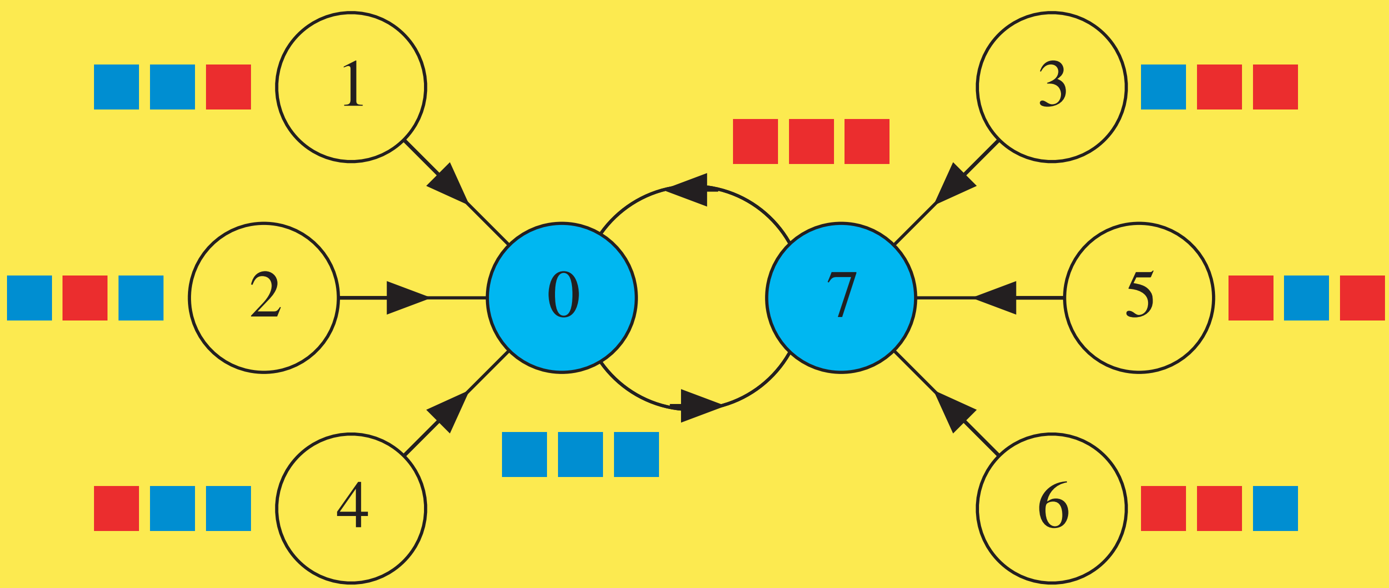

Gallery 105 - 1

105, ***L* = 4**

(a) Period-1 Isles of Eden : $\rho_1 = 4\,\frac{1}{16} = 0.25$

(b) Period-2 Isles of Eden :

$\rho_2 = 2\,\frac{2}{16} = 0.25$

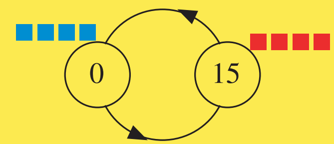

Bernoulli ($\sigma = \pm 1$, $\tau = 1$) shift :

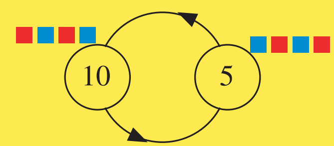

(c) Period-2 Isles of Eden: Bernoulli ($\sigma = \pm 2$, $\tau = 1$) shifts :

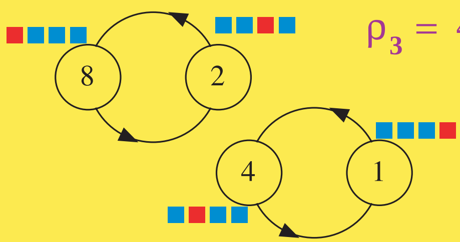

$\rho_3 = 4\,\frac{2}{16} = 0.5$

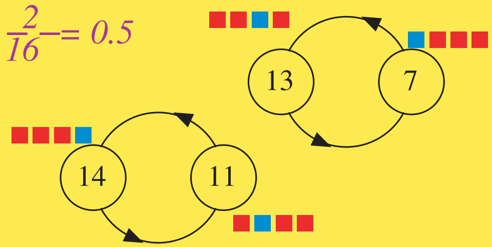

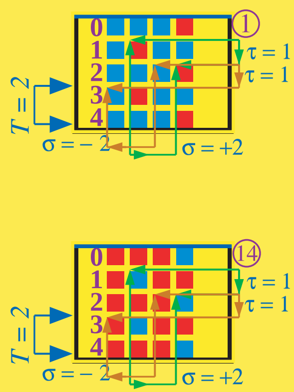

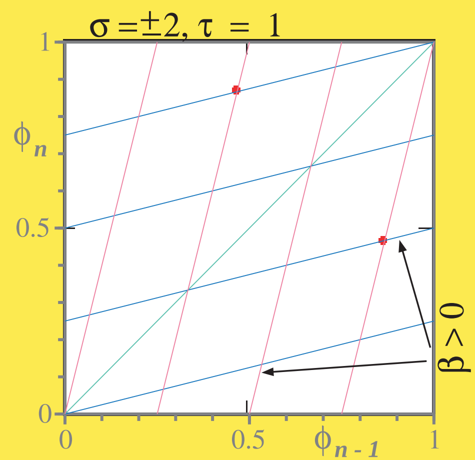

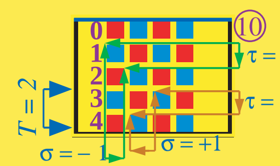

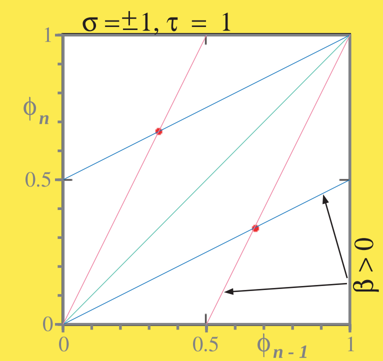

Gallery 105 - 2

105, $L = 5$ (a) Bernoulli ($\sigma = 0, \beta < 0, \tau = 3$) Period-6 Isles of Eden : $\rho_1 = 5\frac{6}{32} = 0.9375$

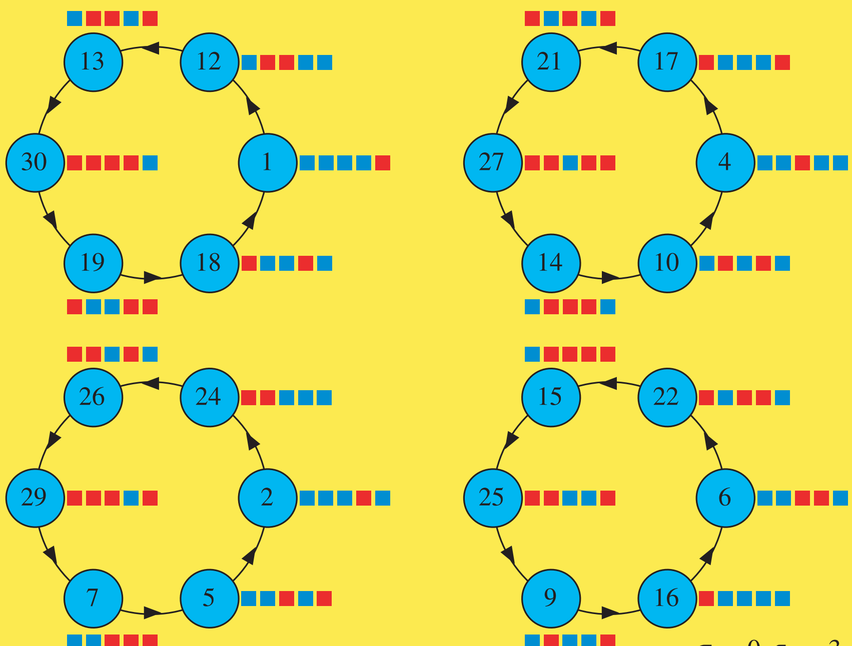

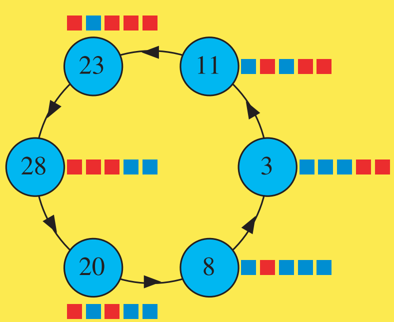

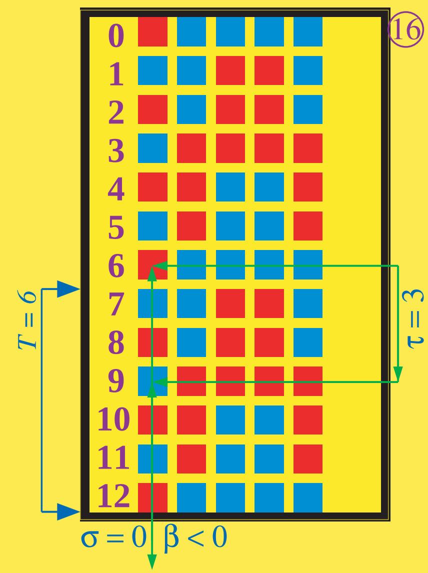

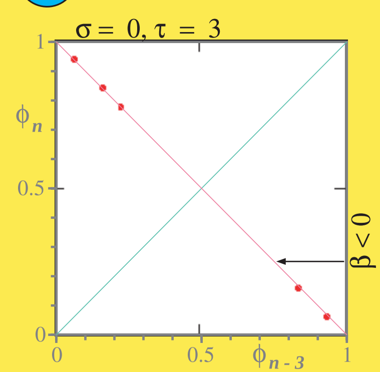

(b) Period-2 Isle of Eden :

$\rho_2 = \frac{2}{32} = 0.0625$

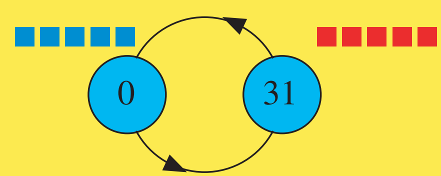

Gallery 105 - 3

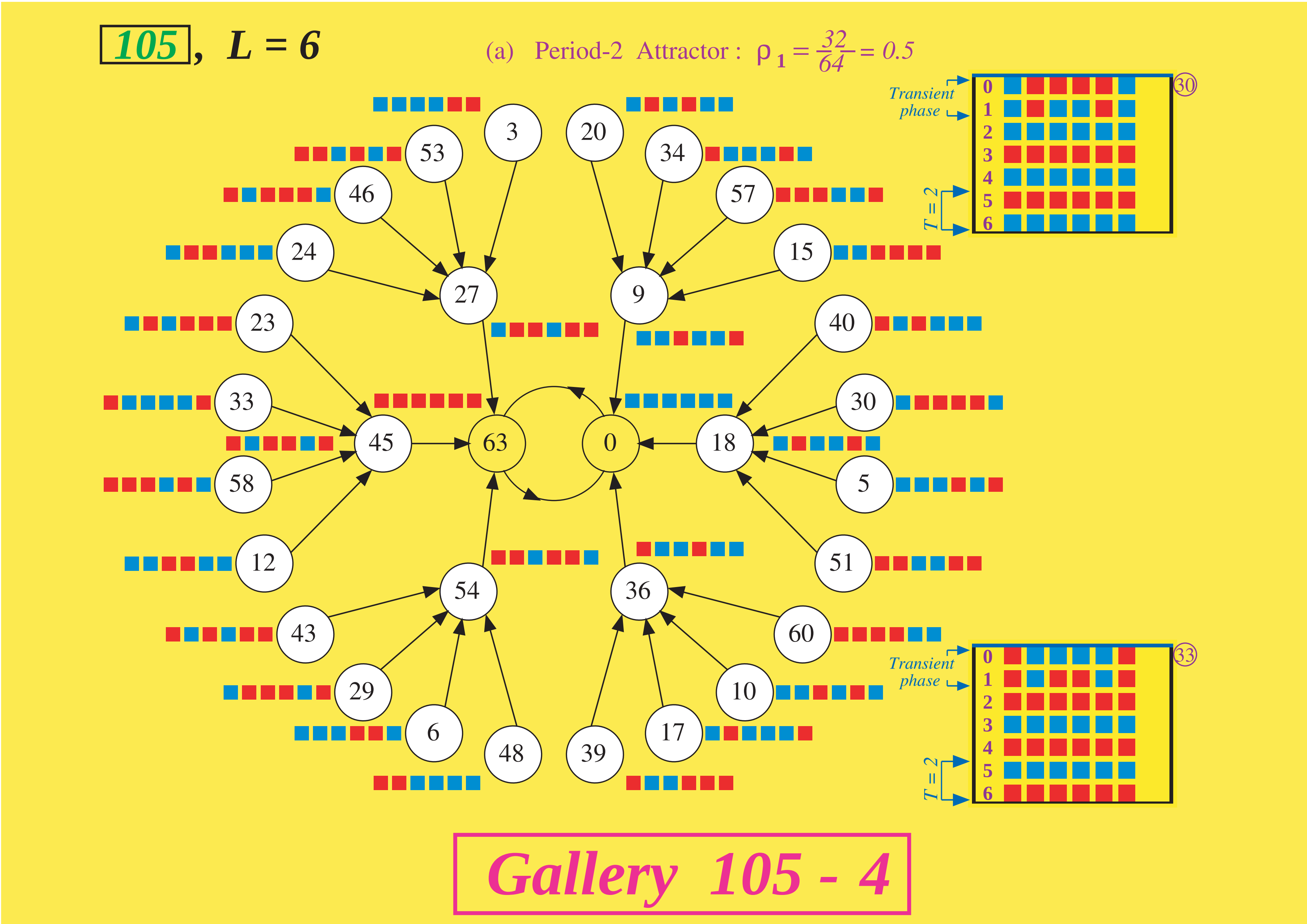

105, L = 6
(a) Period-2 Attractor : $\rho_1 = \frac{32}{64} = 0.5$
0
63
45
18
27
9
54
36
3
53
46
24
23
33
58
12
43
29
6
48
20
34
57
15
40
30
5
51
60
10
17
39
Transient phase
T = 2
0
1
2
3
4
5
6
(30)
(33)
Gallery 105 - 4

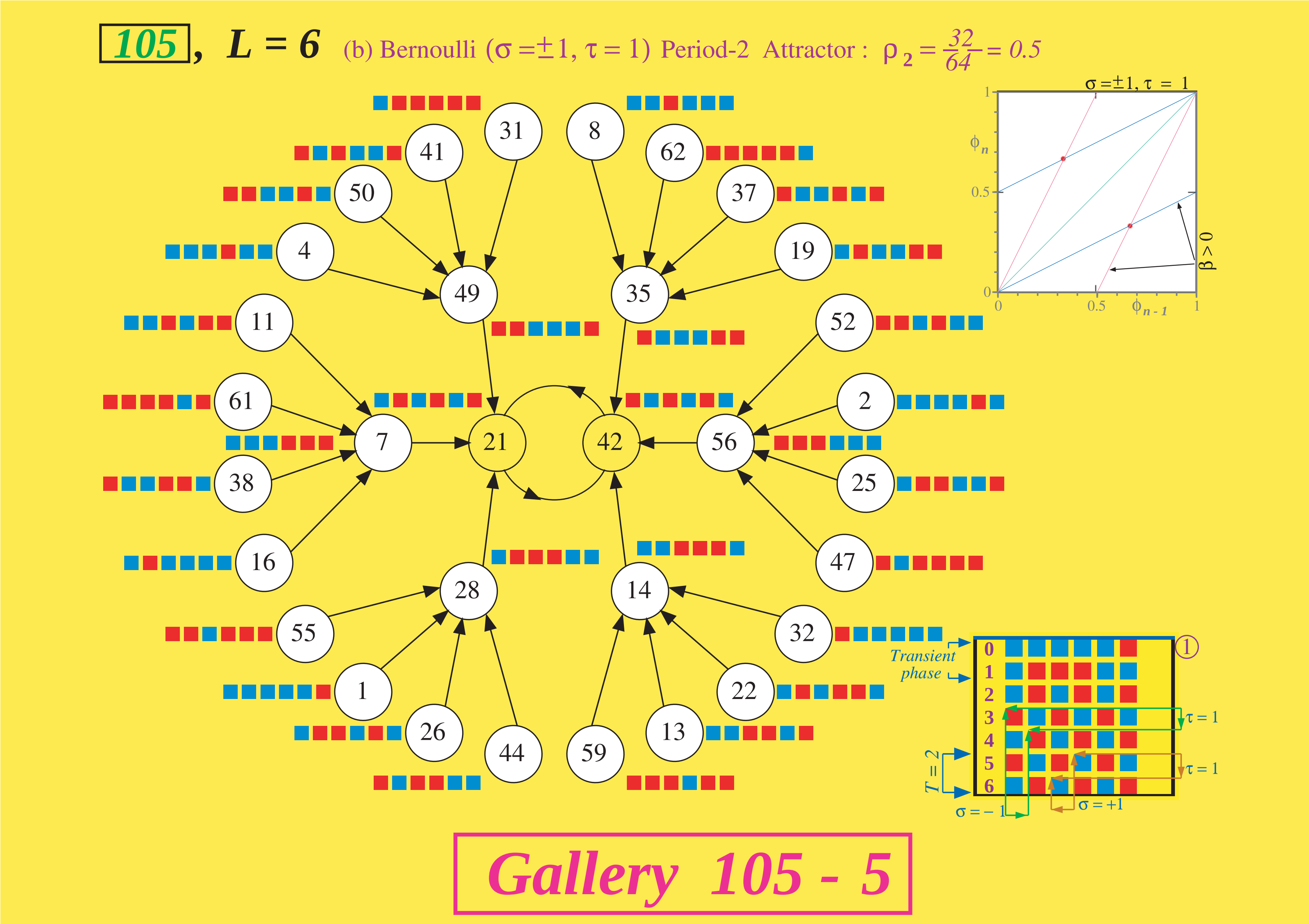
105, L = 6
(b) Bernoulli (σ = ±1, τ = 1) Period-2 Attractor : $\rho_2 = \frac{32}{64} = 0.5$
σ = ±1, τ = 1
ϕ_n
ϕ_{n-1}
β > 0
Transient phase
T = 2
τ = 1
σ = −1
σ = +1
Gallery 105 - 5

105, $L = 7$

(a) Period-2 Isle of Eden :

$\rho_1 = \frac{2}{128} = 0.015625$

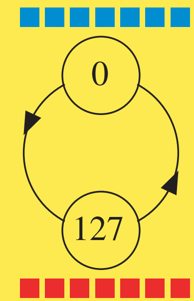

(b) 7 Bernoulli ($\sigma = 0, \tau = 7$) Period-14 Isles of Eden : $\rho_2 = 7\,\frac{14}{128} = 0.765625$

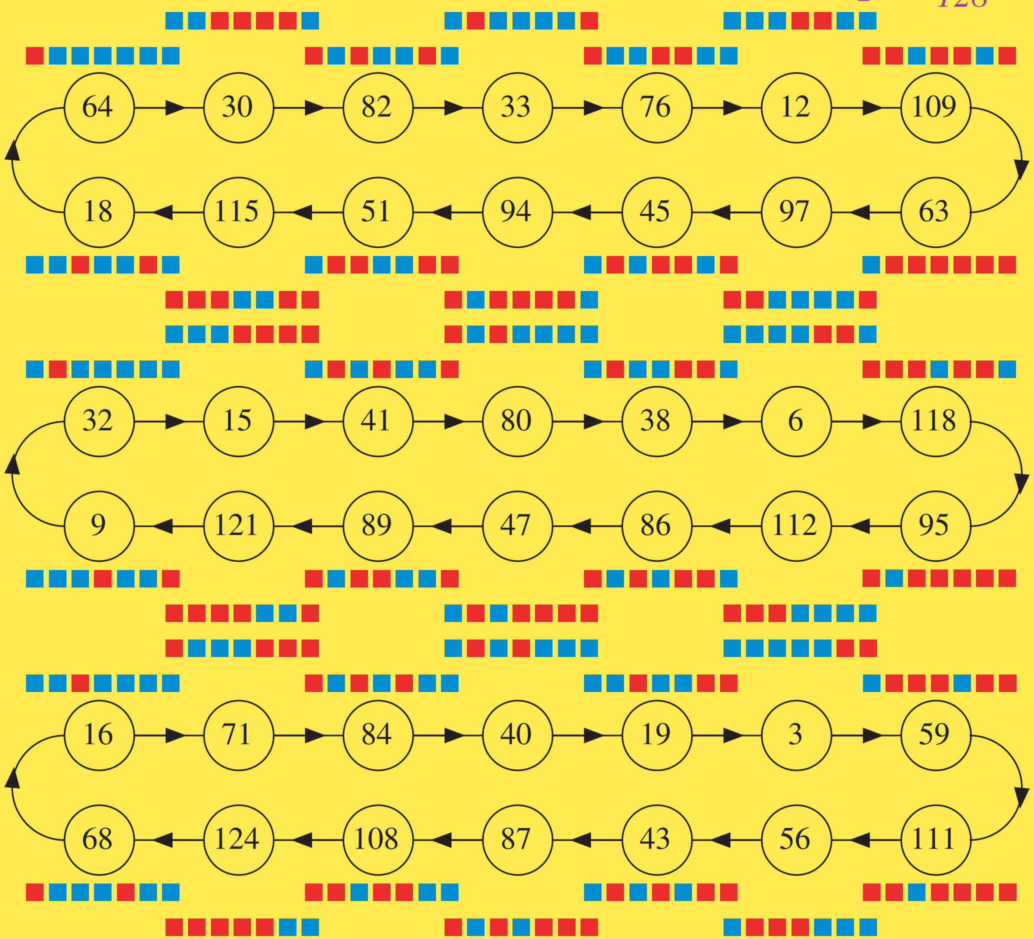

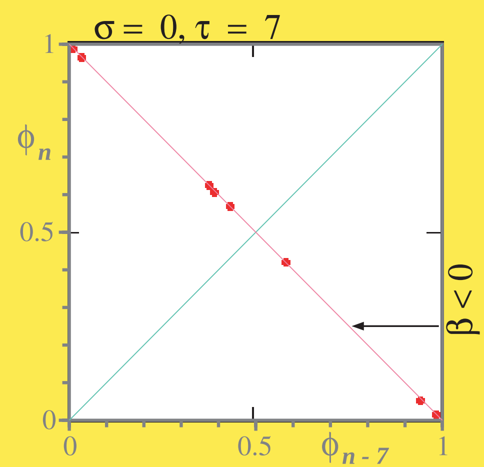

Gallery 105 - 6

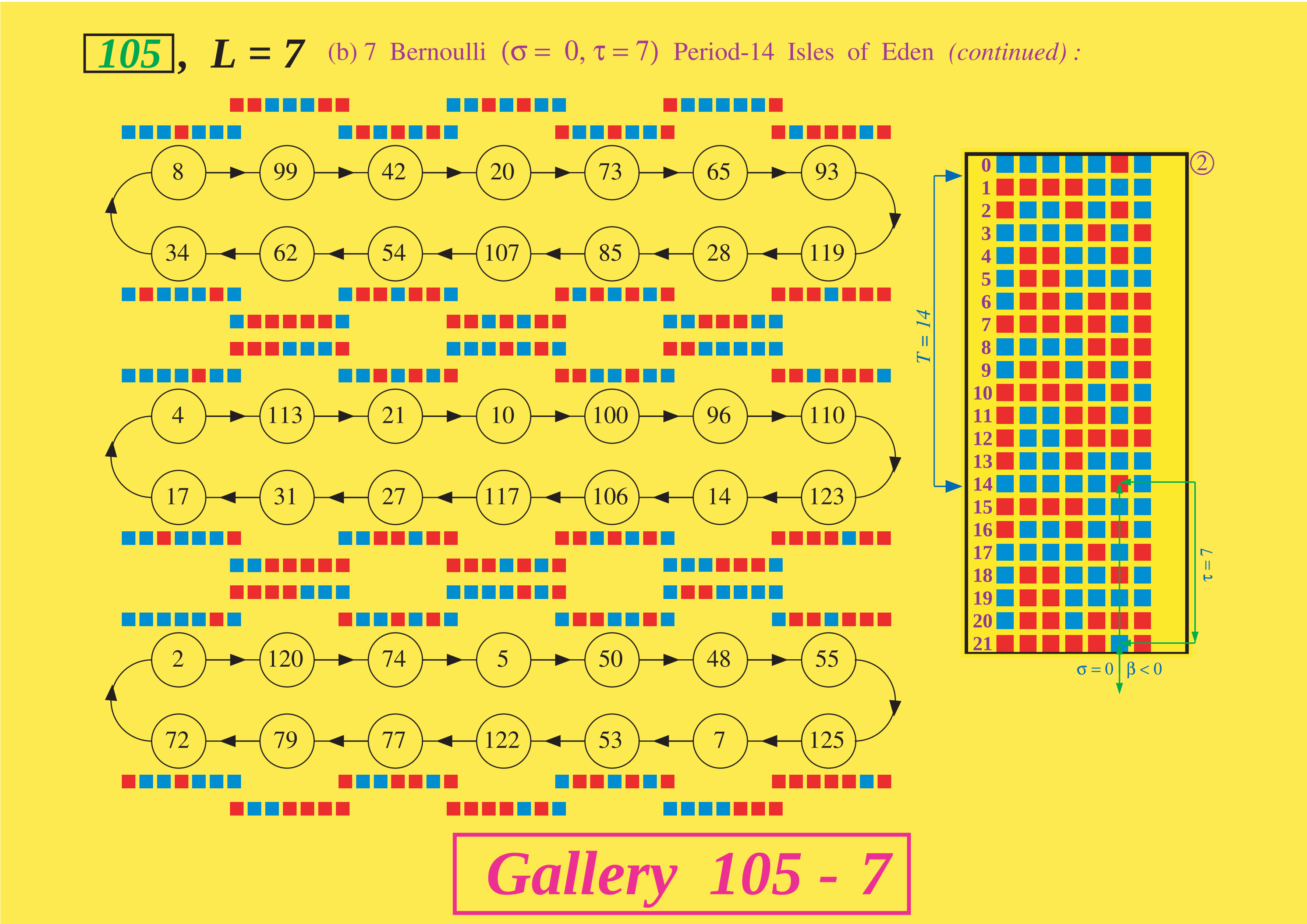
105, L = 7
(b) 7 Bernoulli (σ = 0, τ = 7) Period-14 Isles of Eden (continued) :
8
99
42
20
73
65
93
34
62
54
107
85
28
119
4
113
21
10
100
96
110
17
31
27
117
106
14
123
2
120
74
5
50
48
55
72
79
77
122
53
7
125
②
0
1
2
3
4
5
6
7
8
9
10
11
12
13
14
15
16
17
18
19
20
21
T = 14
τ = 7
σ = 0
β < 0
Gallery 105 - 7

105, $L = 7$ (b) 7 Bernoulli ($\sigma = 0, \tau = 7$)

Period-14 Isles of Eden *(continued)* :

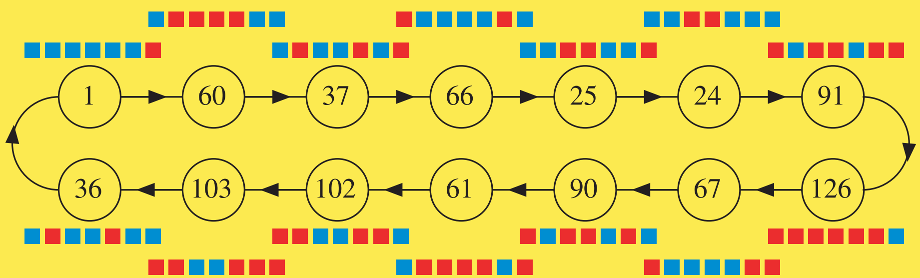

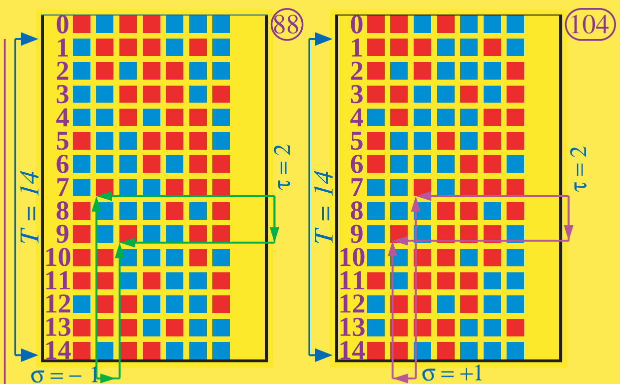

(c) 2 Bernoulli ($\sigma = +1, \sigma = -1, \tau = 2$) Period-14 Isles of Eden :

$$\rho_3 = 2\frac{14}{128}$$

$$= 0.21875$$

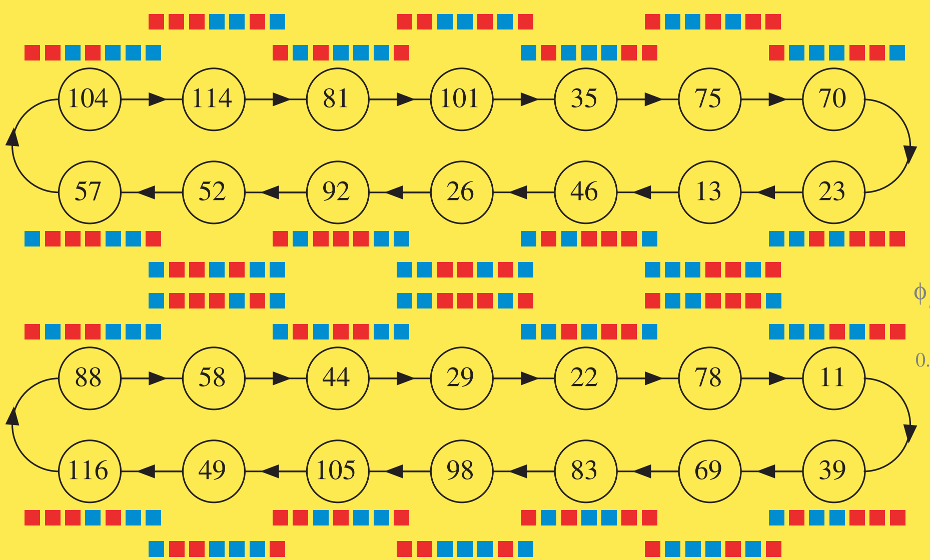

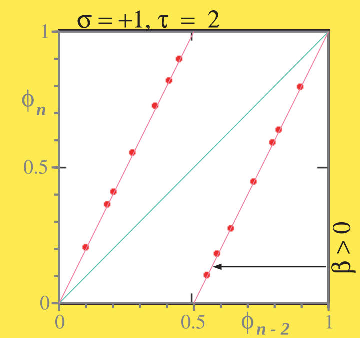

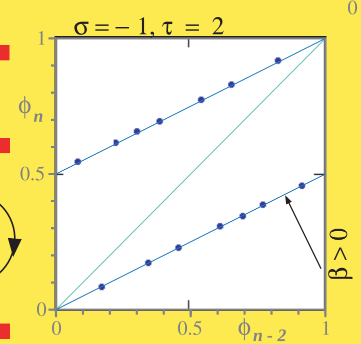

Gallery 105 - 8

$\boxed{105}$, $L = 8$

(a) 48 Period-4 Isles of Eden : $\rho_1 = 48\,\frac{4}{256} = 0.75$

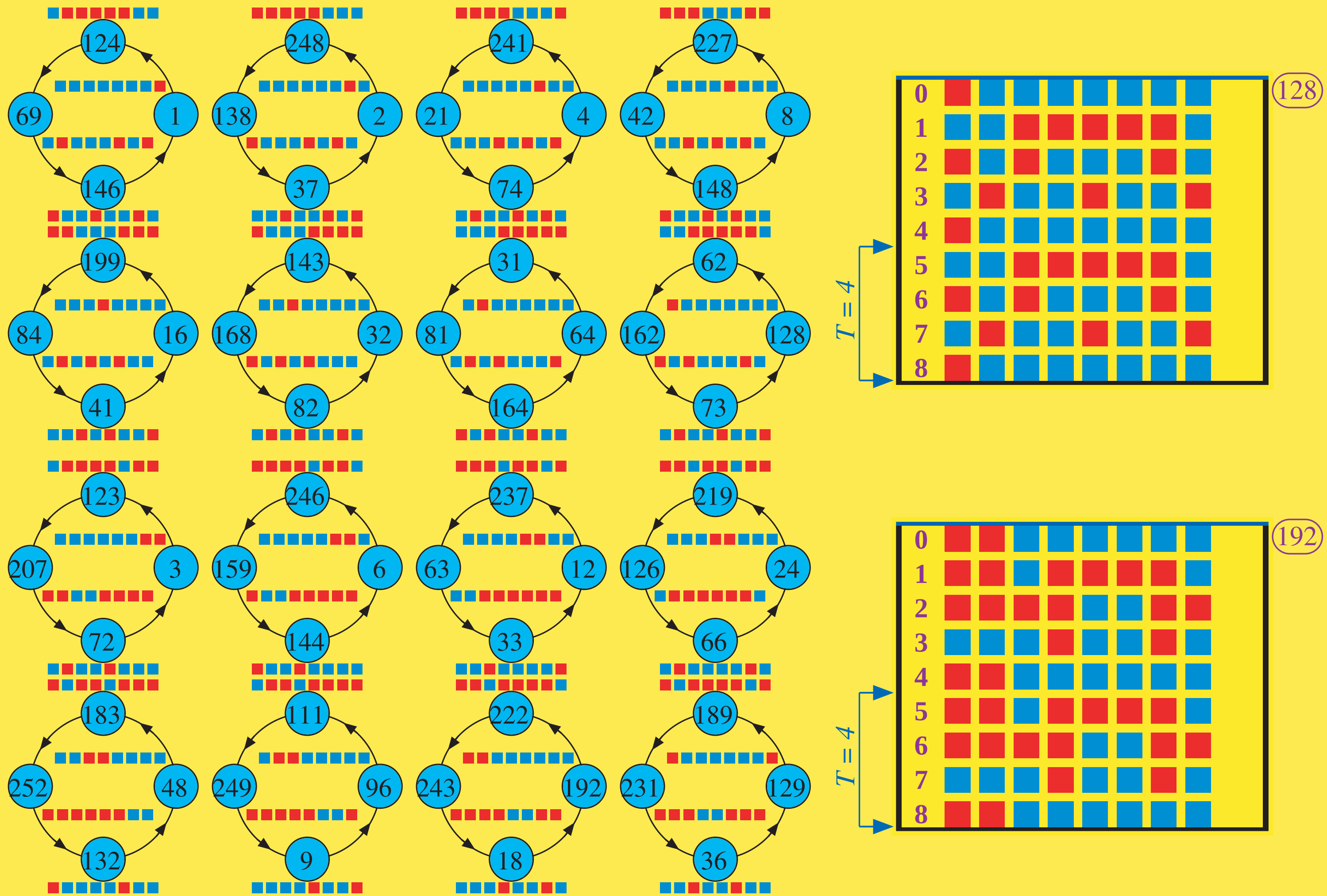

Gallery 105 - 9

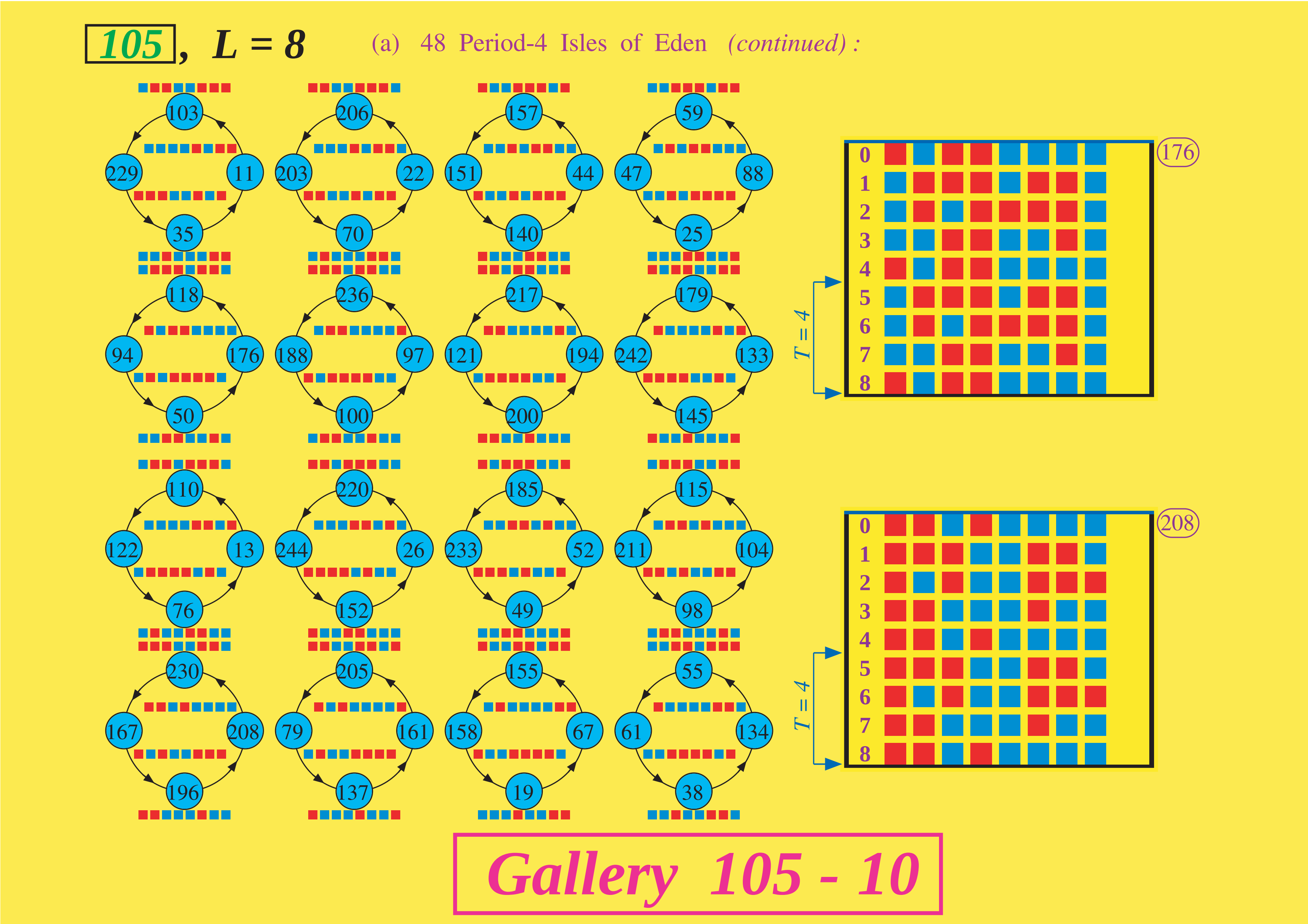
105, L = 8
(a) 48 Period-4 Isles of Eden (continued) :
103
229
11
35
206
203
22
70
157
151
44
140
59
47
88
25
118
94
176
50
236
188
97
100
217
121
194
200
179
242
133
145
110
122
13
76
220
244
26
152
185
233
52
49
115
211
104
98
230
167
208
196
205
79
161
137
155
158
67
19
55
61
134
38
176
208
T = 4
0
1
2
3
4
5
6
7
8
Gallery 105 - 10

105, ***L* = 8** (a) 48 Period-4 Isles of Eden *(continued)* :

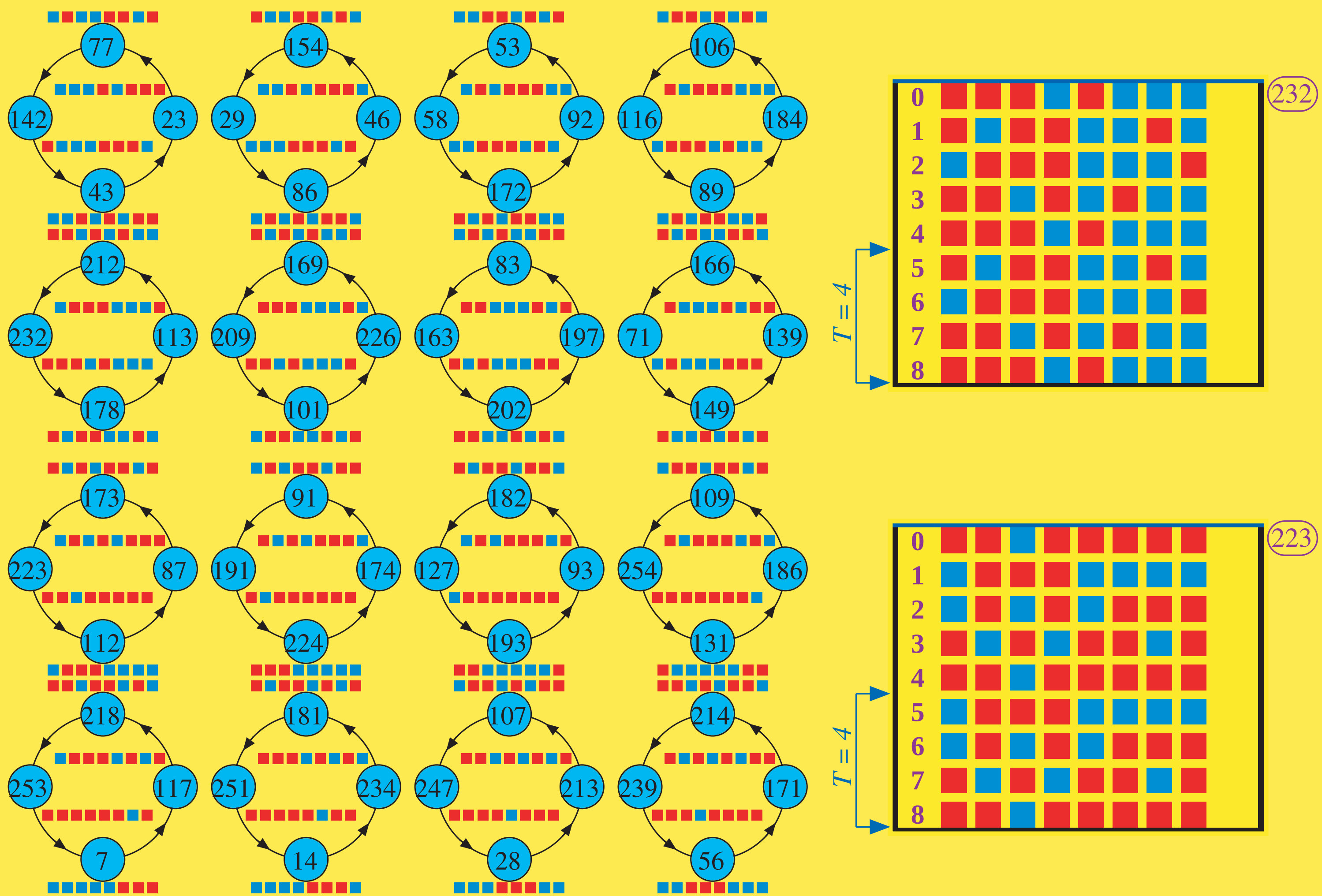

Gallery 105 - 11

$\boxed{105}$, $L = 8$ (b) 12 Bernoulli ($\sigma = \pm 4$, $\tau = 2$) Period-4

Isles of Eden $\rho_2 = 12\frac{4}{256} = 0.1875$

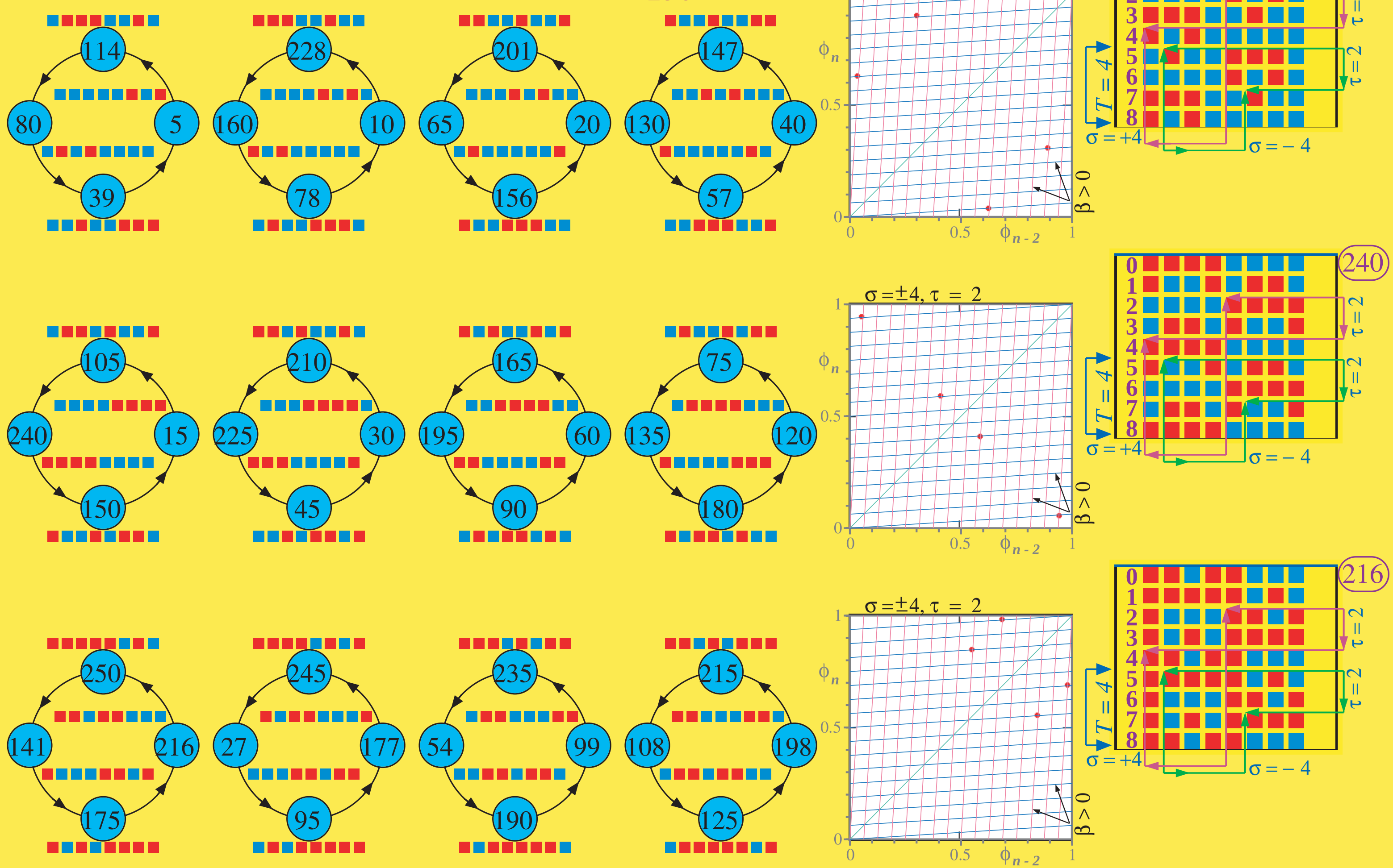

Gallery 105 - 12

105, $L = 8$ (c) Period-1 Isles of Eden $\rho_3 = \frac{4}{256} = 0.015625$

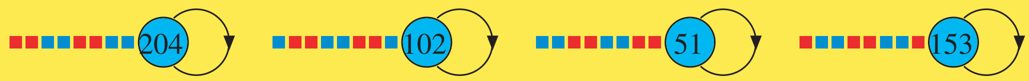

(d) 2 Bernoulli ($\sigma = \pm 2$, $\tau = 1$) Period-2 Isles of Eden

$\rho_4 = 4\frac{2}{256} = 0.03125$

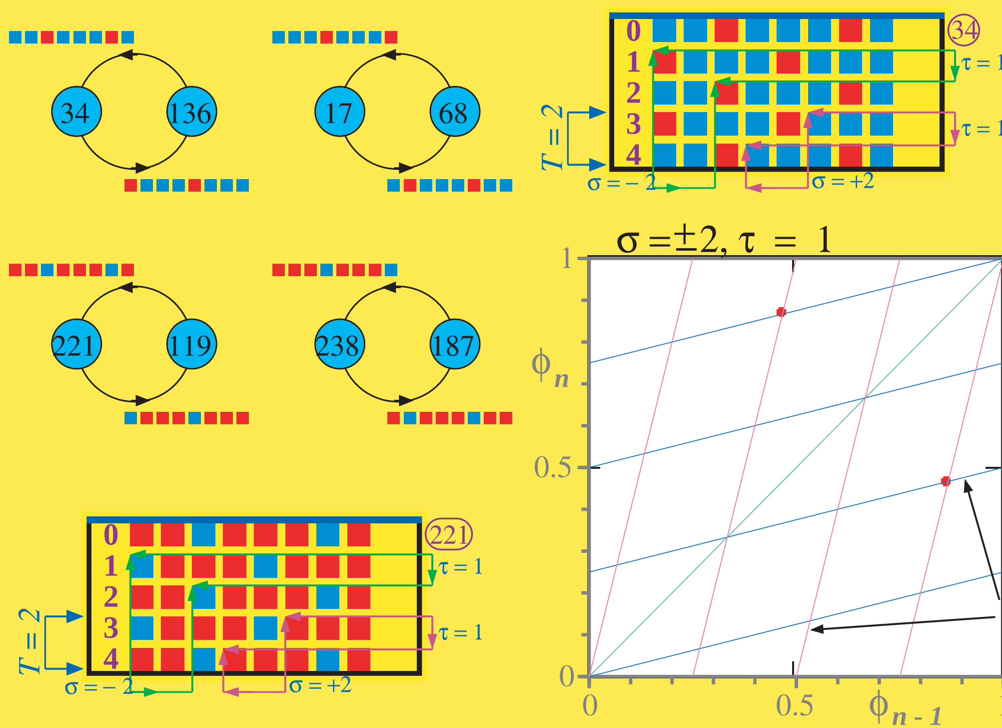

(e) Bernoulli ($\sigma = \pm 1$, $\tau = 1$)

Period-2 Isle of Eden

$\rho_5 = \frac{2}{256} = 0.0078125$

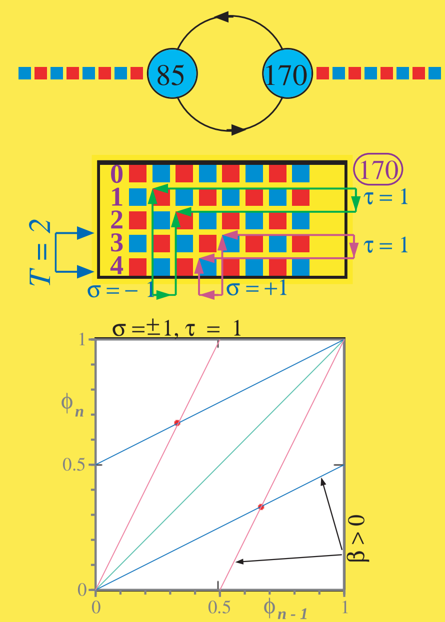

(f) Period-2 Isle of Eden

$\rho_6 = \frac{2}{256} = 0.0078125$

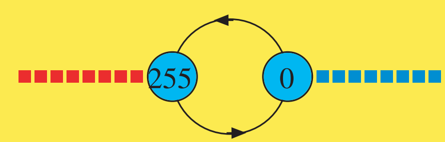

Gallery 105 - 13

2.4.6. *Highlights from Rule* $\boxed{105}$

The basin tree diagrams of Rule $\boxed{105}$ for $L = 3, 4, \ldots, 8$ are exhibited in Table 19. Following a detailed analysis of these diagrams, the qualitative properties of local rule $\boxed{105}$ extracted from basin-tree Galleries 105-1 to 105-13 of Table 19 are summarized below:

Summary of Qualitative properties of local rule $\boxed{105}$ extracted from Gallery 105 for Rule $\boxed{105}$

L	ID Number i	Number of Period-n attractors	Number of Period-n Isles of Eden	Period n	Bernoulli Parameters σ_1	τ_1	β_1	σ_2	τ_2	β_2	Robustness coefficient ρ
3	1	1		2	0	1	−				$\rho_1 = 1$
4	1		4	1	0	1	+				$\rho_1 = 0.25$
	2		2	2	1	1	+	-1	1	+	$\rho_2 = 0.25$
	3		4	2	2	1	+	-2	1	+	$\rho_3 = 0.5$
5	1		5	6	0	3	−				$\rho_1 = 0.9375$
	2		1	2	0	1	−				$\rho_2 = 0.0625$
6	1	1		2	0	1	−				$\rho_1 = 0.5$
	2	1		2	1	1	+	-1	1	+	$\rho_2 = 0.5$
7	1		1	2	0	1	−				$\rho_1 = 0.015625$
	2		7	14	0	7	+				$\rho_2 = 0.765625$
	3		2	14	1	2	+	-1	2	+	$\rho_3 = 0.21875$
8	1		48	4	0	1	+				$\rho_1 = 0.75$
	2		12	4	4	2	+	-4	2	+	$\rho_2 = 0.1875$
	3		4	1	0	1	+				$\rho_3 = 0.015625$
	4		4	2	2	1	+	-2	1	+	$\rho_4 = 0.03125$
	5		1	2	1	1	+	-1	1	+	$\rho_5 = 0.0078125$
	6		1	2	0	1	−				$\rho_6 = 0.0078125$

Table 20. Basin tree diagrams for rule $\boxed{122}$.

Basin tree diagrams for Rule $\boxed{122}$

$\boxed{122}$, $L = 3$ (a) Period-1 Attractor : $\rho_1 = \frac{8}{8} = 1$

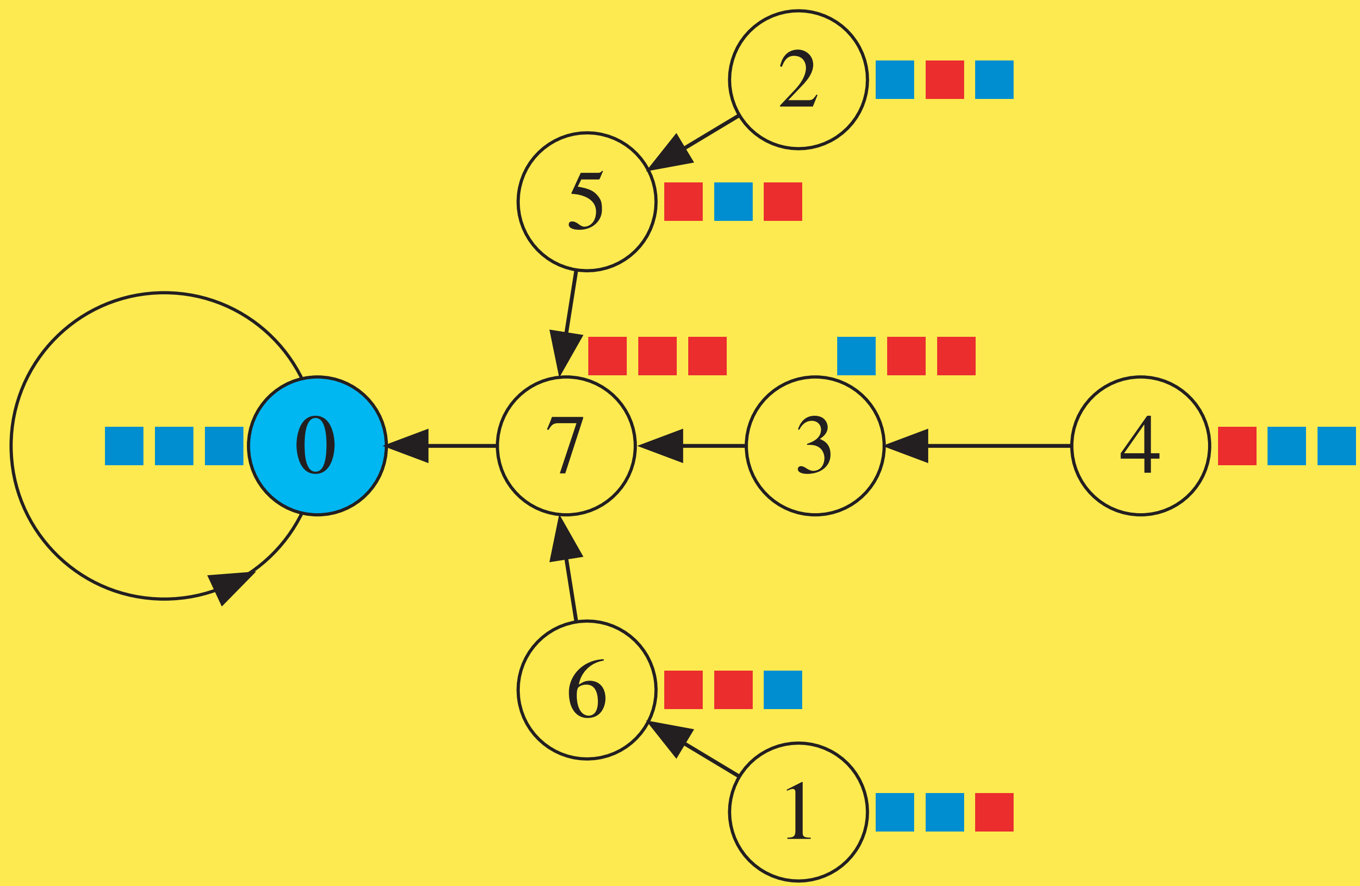

Gallery 122 - 1

$\boxed{122}$, $L = 4$

(a) Bernoulli ($\sigma = \pm 2$, $\tau = 1$)

Period-2 Isles of Eden :

$\rho_1 = 2\,\frac{2}{16} = 0.25$

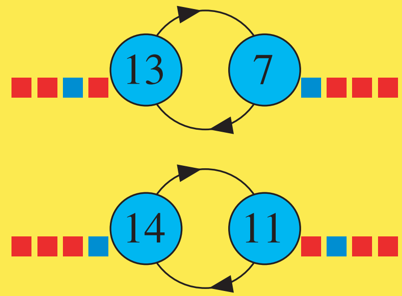

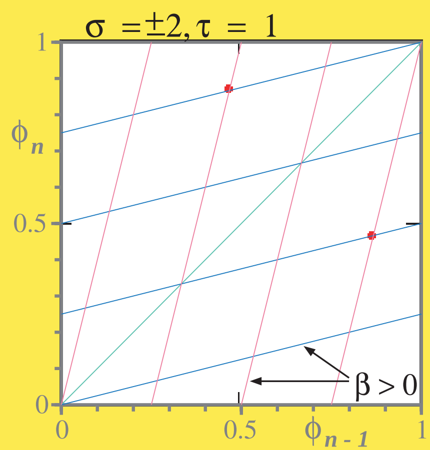

(b) Bernoulli ($\sigma = \pm 1$, $\tau = 1$)

Period-2 Attractor :

$\rho_2 = \frac{6}{16} = 0.375$

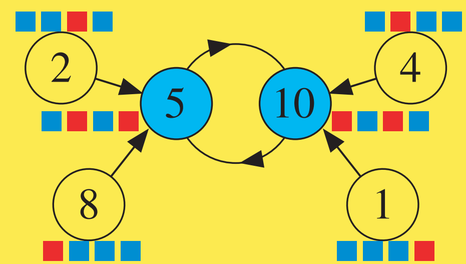

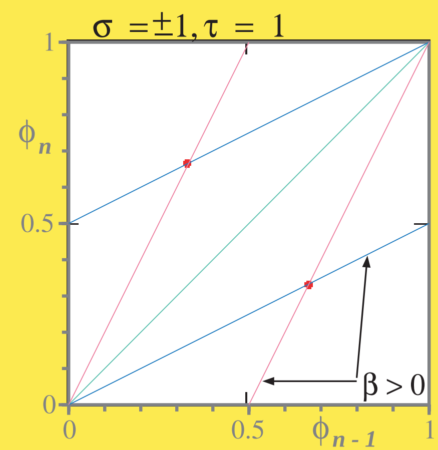

(c) Period-1 Attractor :

$\rho_3 = \frac{6}{16} = 0.375$

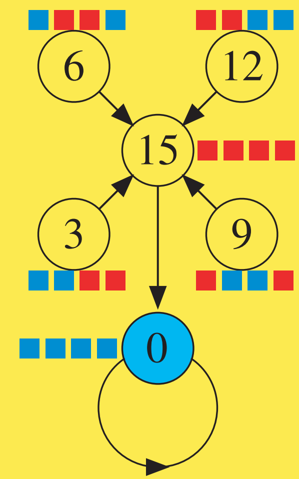

Gallery 122 - 2

$\boxed{122}$, *L* = 5

(a) Bernoulli ($\sigma = 0, \tau = 2$)

Period-2 Attractors : $\rho_1 = 5\,\frac{6}{32} = 0.9375$

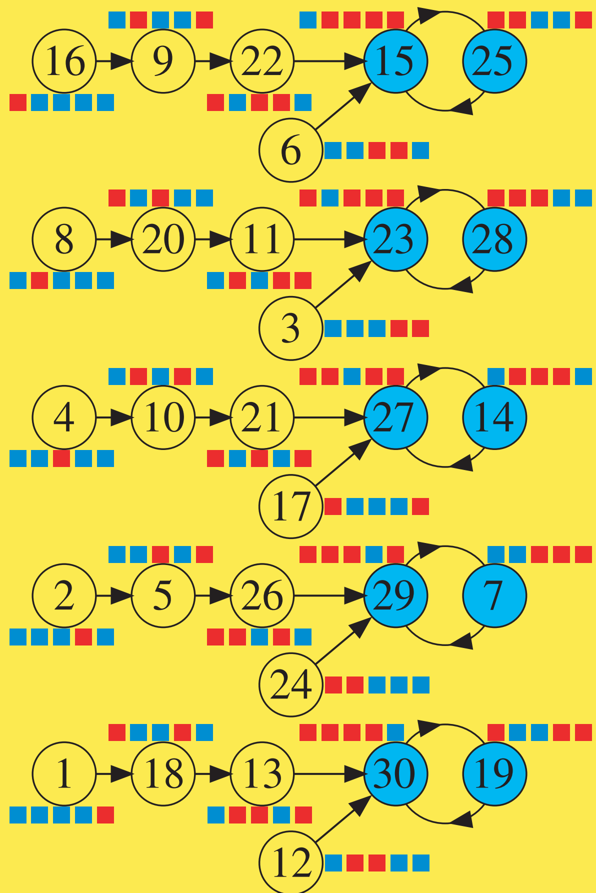

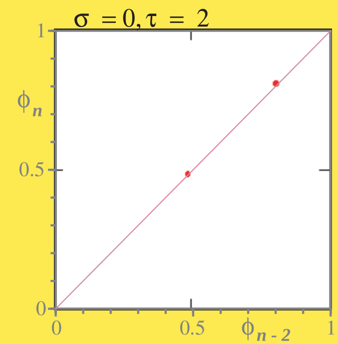

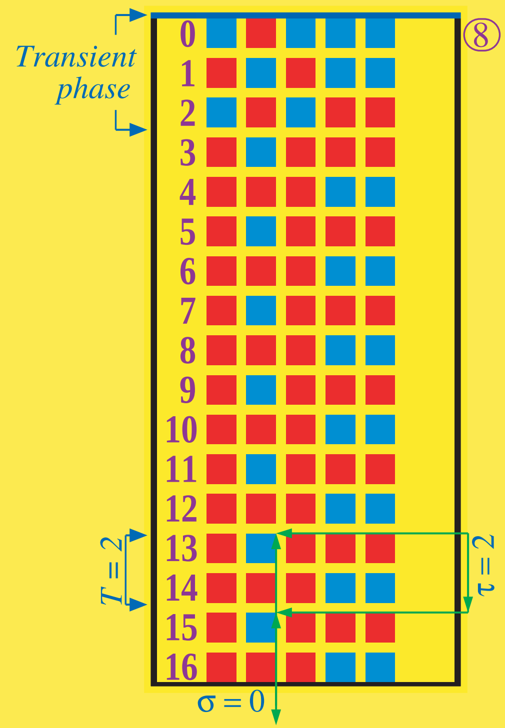

(b) Period-1 Attractor :

$\rho_2 = \frac{2}{32} = 0.0625$

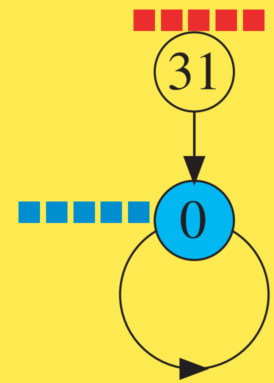

Gallery 122 - 3

$\boxed{122}$, $L = 6$

(a) Bernoulli ($\sigma = \pm 3$, $\tau = 1$)

Period-2 Attractors :

$$\rho_1 = 3\,\frac{4}{64} = 0.1875$$

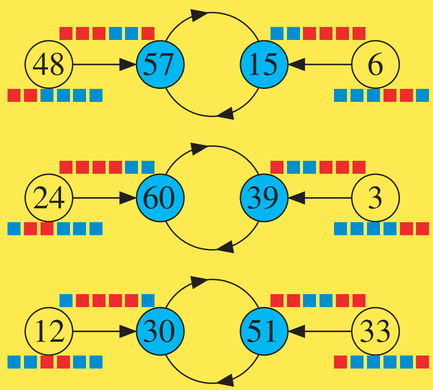

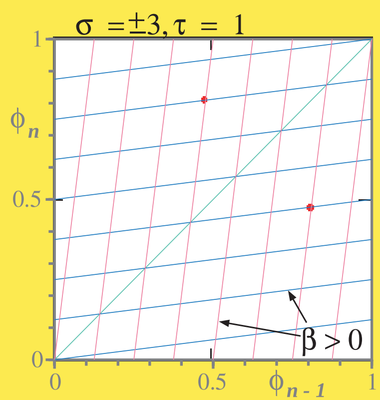

(b) Bernoulli ($\sigma = \pm 1$, $\tau = 1$)

Period-2 Attractor :

$$\rho_2 = \frac{14}{64} = 0.21875$$

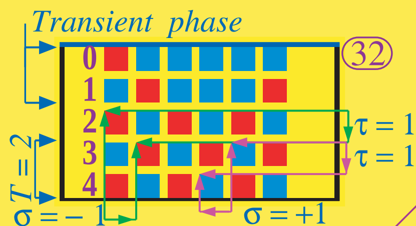

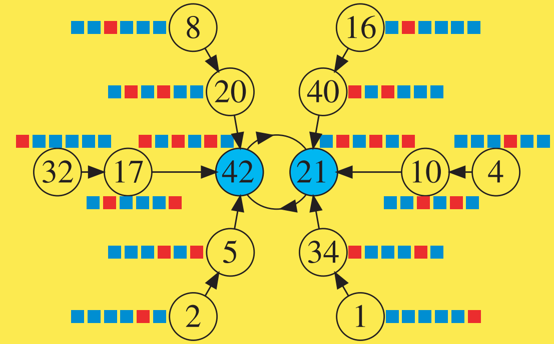

(c) Period-1

Attractor :

$$\rho_3 = \frac{38}{64} = 0.59375$$

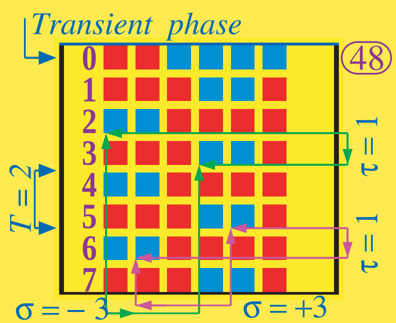

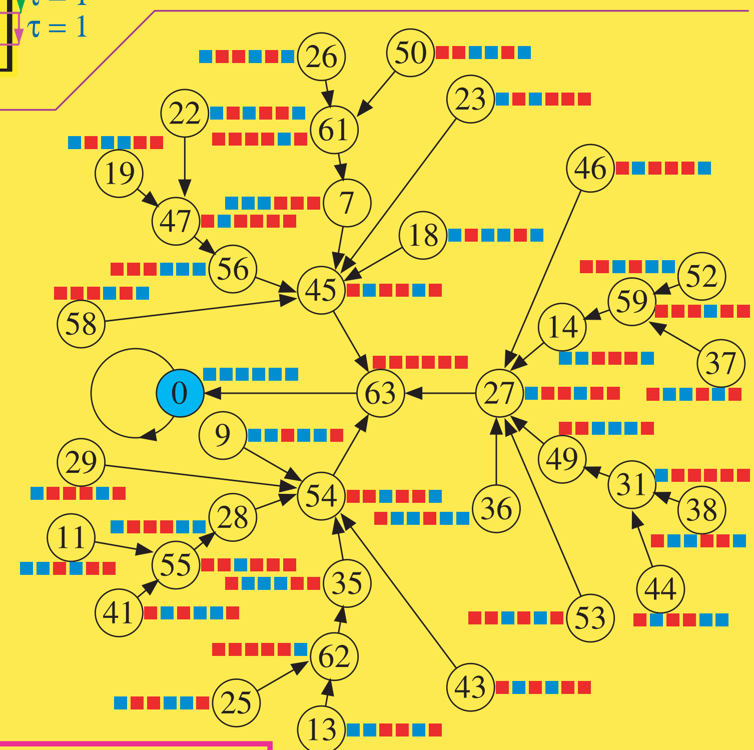

Gallery 122 - 4

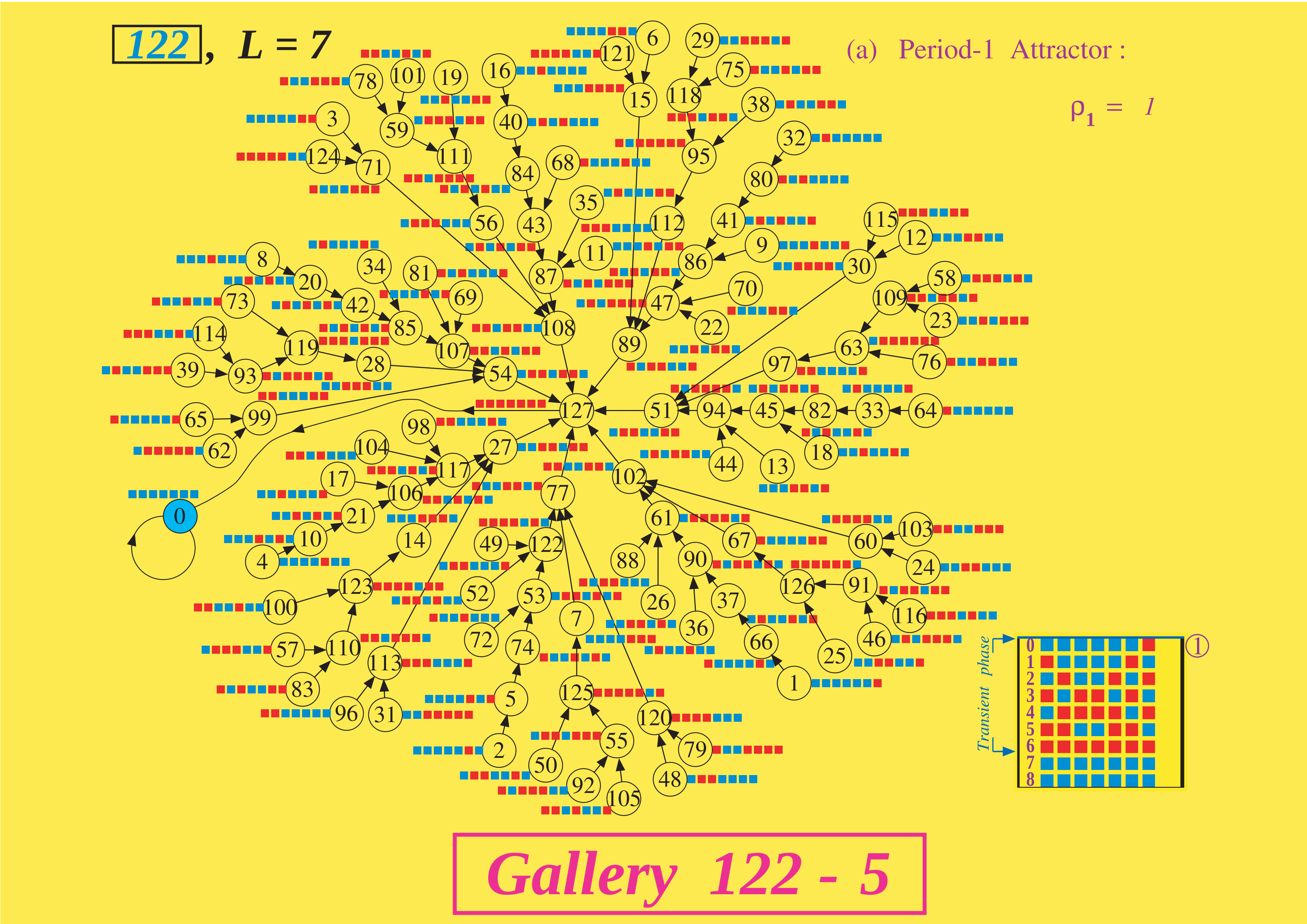
122, L = 7
(a) Period-1 Attractor :
ρ1 = 1
Transient phase
Gallery 122 - 5

122, ***L* = 8** (a) Bernoulli ($\sigma = \pm 4$, $\tau = 3$) Period-6 Attractors : $\rho_1 = 4\,\frac{40}{256} = 0.625$

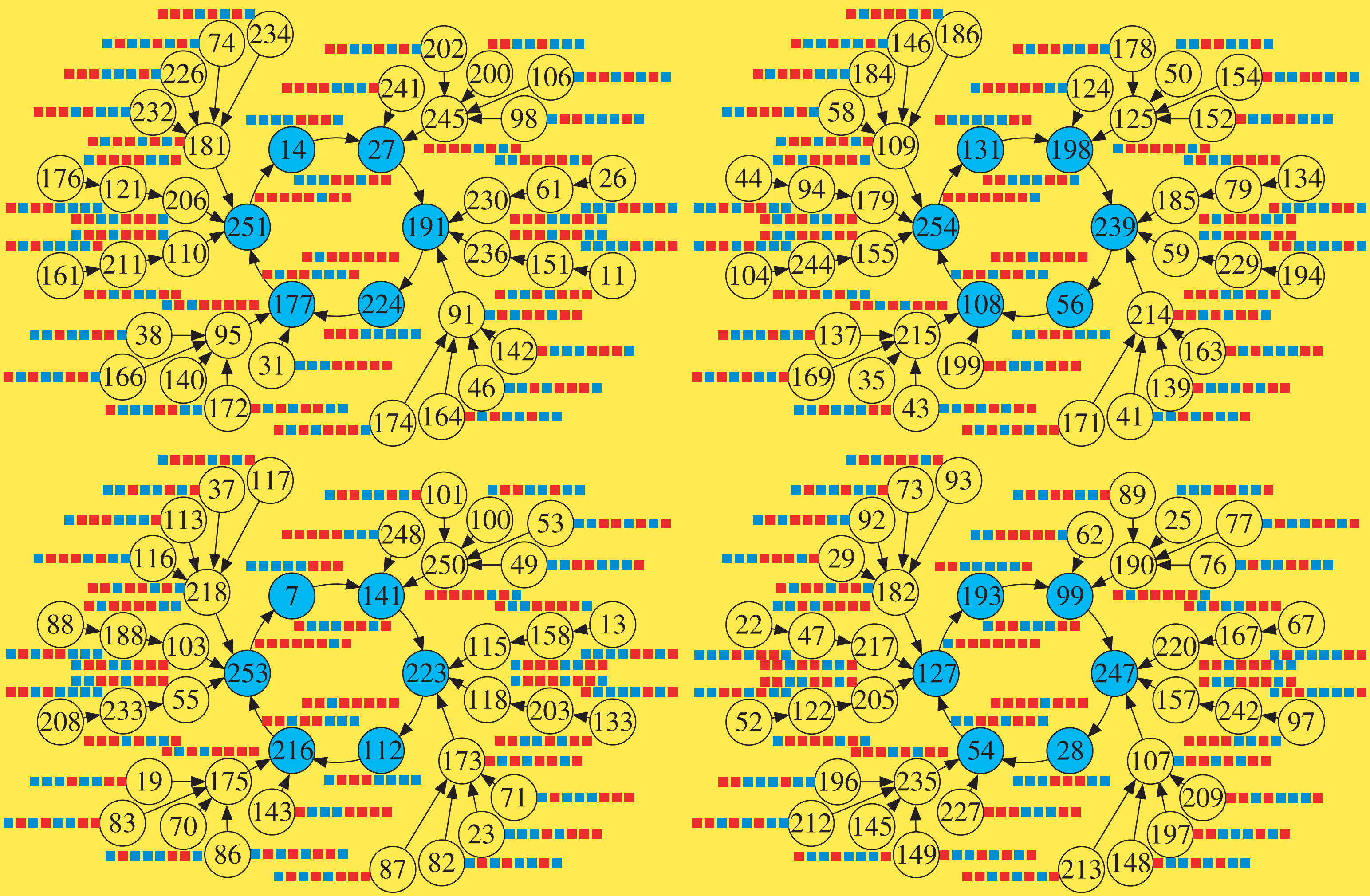

Gallery 122 - 6

$\boxed{122}$, $L = 8$

(a) Bernoulli ($\sigma = \pm 4$, $\tau = 3$)

Period-6 Attractors *(continued)* :

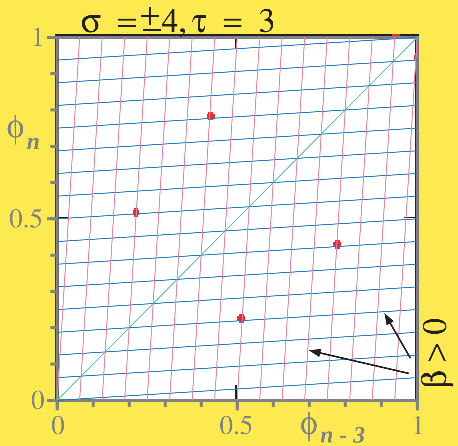

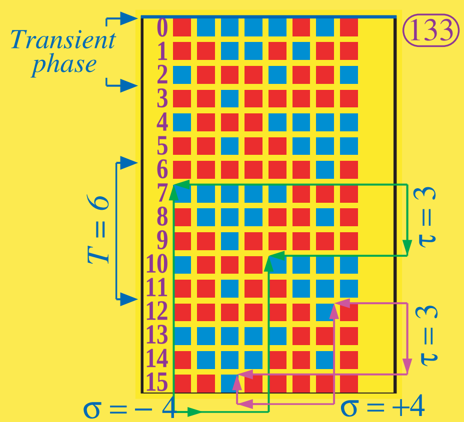

(b) Period-1 Attractor : $\rho_2 = \frac{54}{256} = 0.2109375$

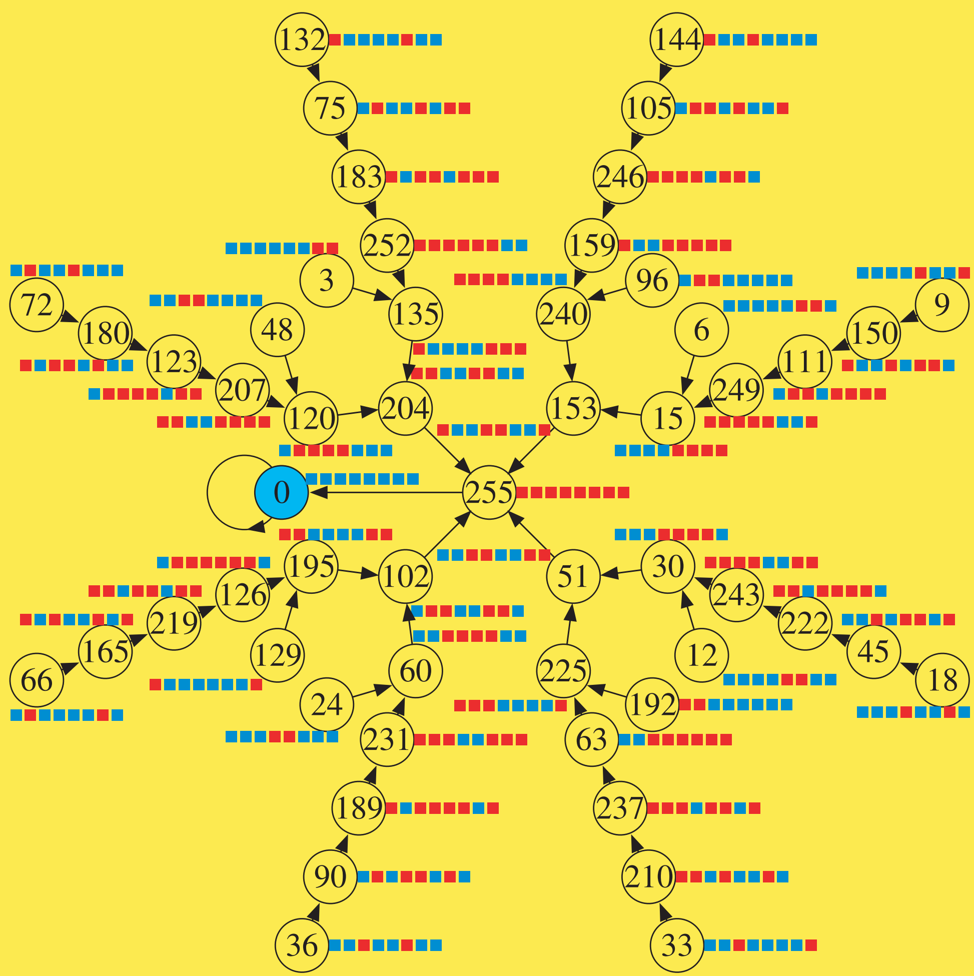

Gallery 122 - 7

$\boxed{122}$, $L = 8$

(c) Bernoulli ($\sigma = \pm 1, \tau = 1$)

Period-2 Attractor $\rho_3 = \frac{30}{256} = 0.1171875$

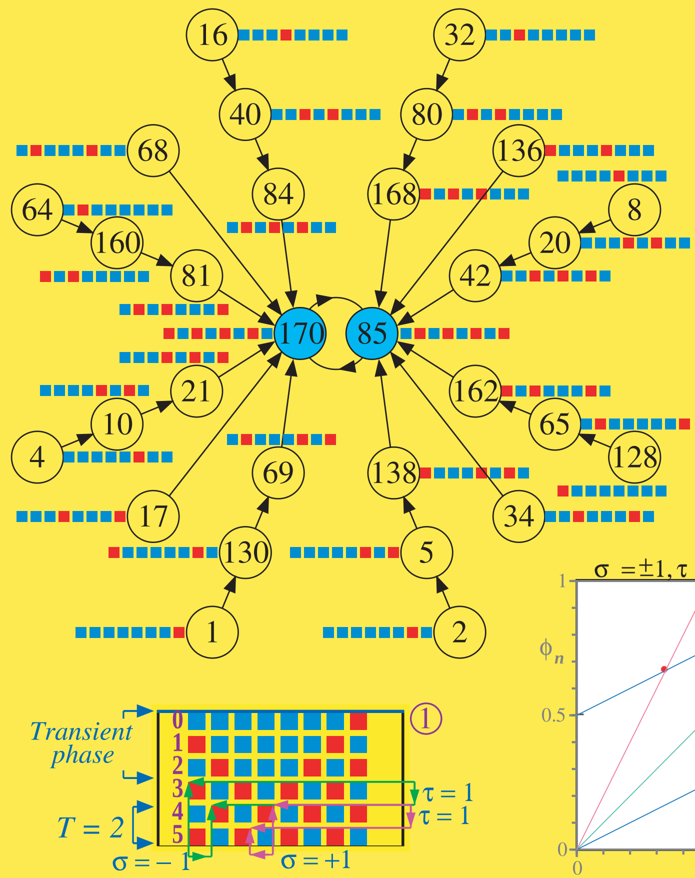

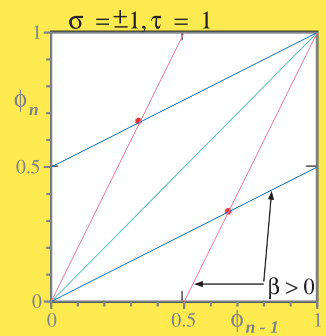

(d) Bernoulli ($\sigma = \pm 2, \tau = 1$)

Period-2 Attractors : $\rho_4 = 2\frac{6}{256} = 0.046875$

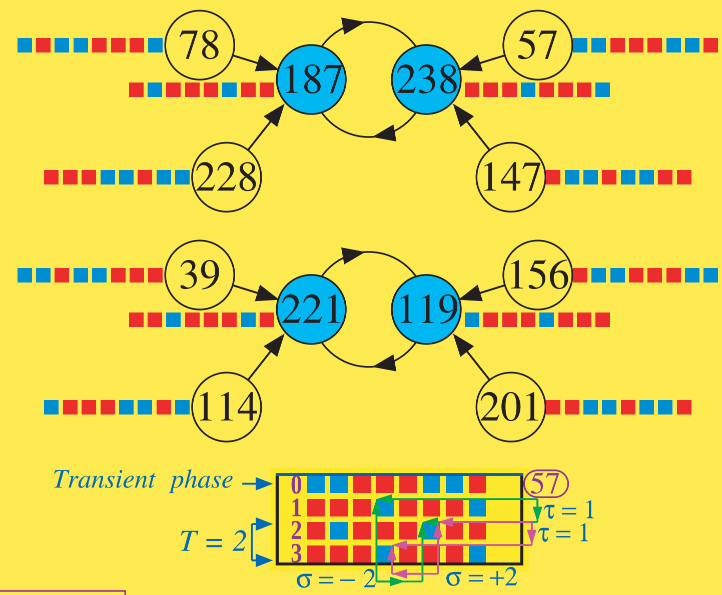

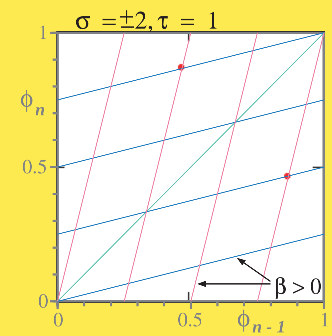

Gallery 122 - 8

2.4.7. *Highlights from Rule* $\boxed{122}$

The basin tree diagrams of Rule $\boxed{122}$ for $L = 3, 4, \ldots, 8$ are exhibited in Table 20. Following a detailed analysis of these diagrams, the qualitative properties of local rule $\boxed{122}$ extracted from basin-tree Galleries 122-1 to 122-8 of Table 20 are summarized below:

Summary of Qualitative properties of local rule $\boxed{122}$ extracted from Gallery 122 for Rule $\boxed{122}$

L	ID Number i	Number of Period-n attractors	Number of Period-n Isles of Eden	Period n	Bernoulli Parameters σ_1	τ_1	β_1	σ_2	τ_2	β_2	Robustness coefficient ρ
3	1	1		1	0	1	+				$\rho_1 = 1$
4	1		2	2	2	1	+	-2	1	+	$\rho_1 = 0.25$
	2	1		2	1	1	+	-1	1	+	$\rho_2 = 0.375$
	3	1		1	0	1	+				$\rho_3 = 0.375$
5	1	5		2	0	2	+				$\rho_1 = 0.9375$
	2	1		1	0	1	+				$\rho_2 = 0.0625$
6	1	3		2	3	1	+	-3	1	+	$\rho_1 = 0.1875$
	2	1		2	1	1	+	-1	1	+	$\rho_2 = 0.21875$
	3	1		1	0	1	+				$\rho_3 = 0.59375$
7	1	1		1	0	1	+				$\rho_1 = 1$
8	1	4		6	4	3	+	-4	3	+	$\rho_1 = 0.625$
	2	1		1	0	1	+				$\rho_2 = 0.2109375$
	3	1		2	1	1	+	-1	1	+	$\rho_3 = 0.1171875$
	4	2		2	2	1	+	-2	1	+	$\rho_4 = 0.046875$

Table 21. Basin tree diagrams for rule $\boxed{126}$.

Basin tree diagrams for Rule $\boxed{126}$

$\boxed{126}$, ***L* = 3** (a) Period-1 Attractor : $\rho_1 = \frac{8}{8} = 1$

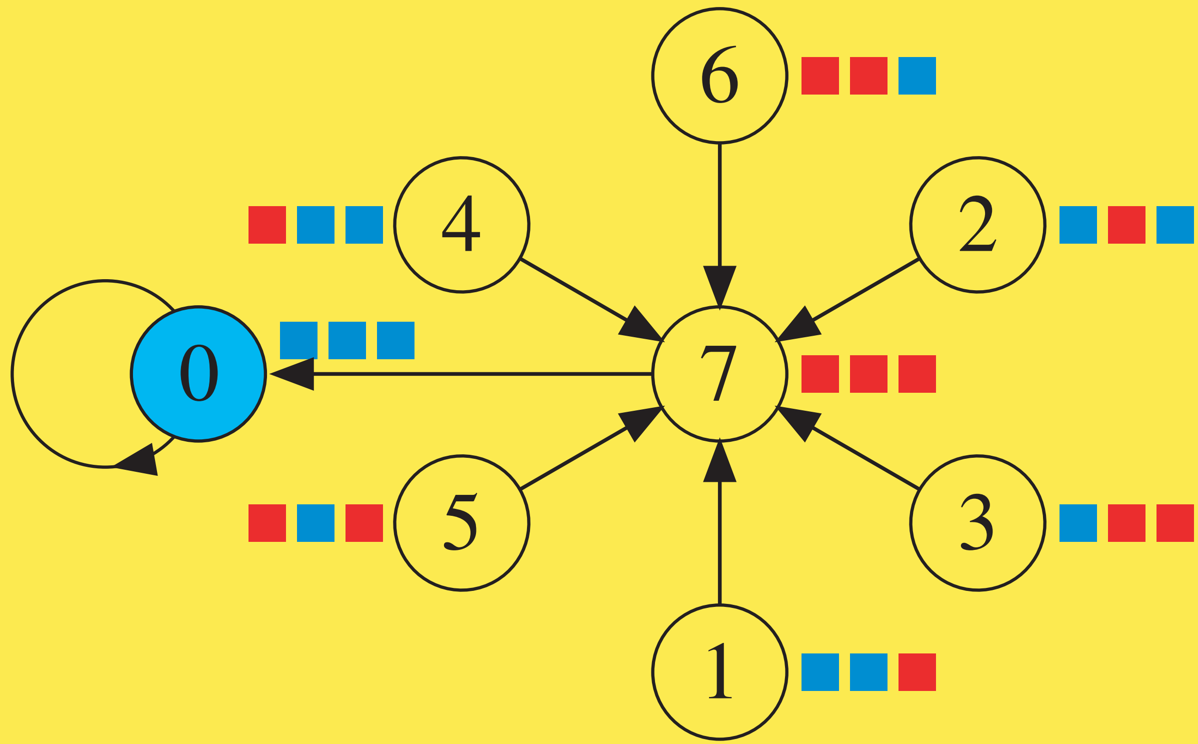

Gallery 126 - 1

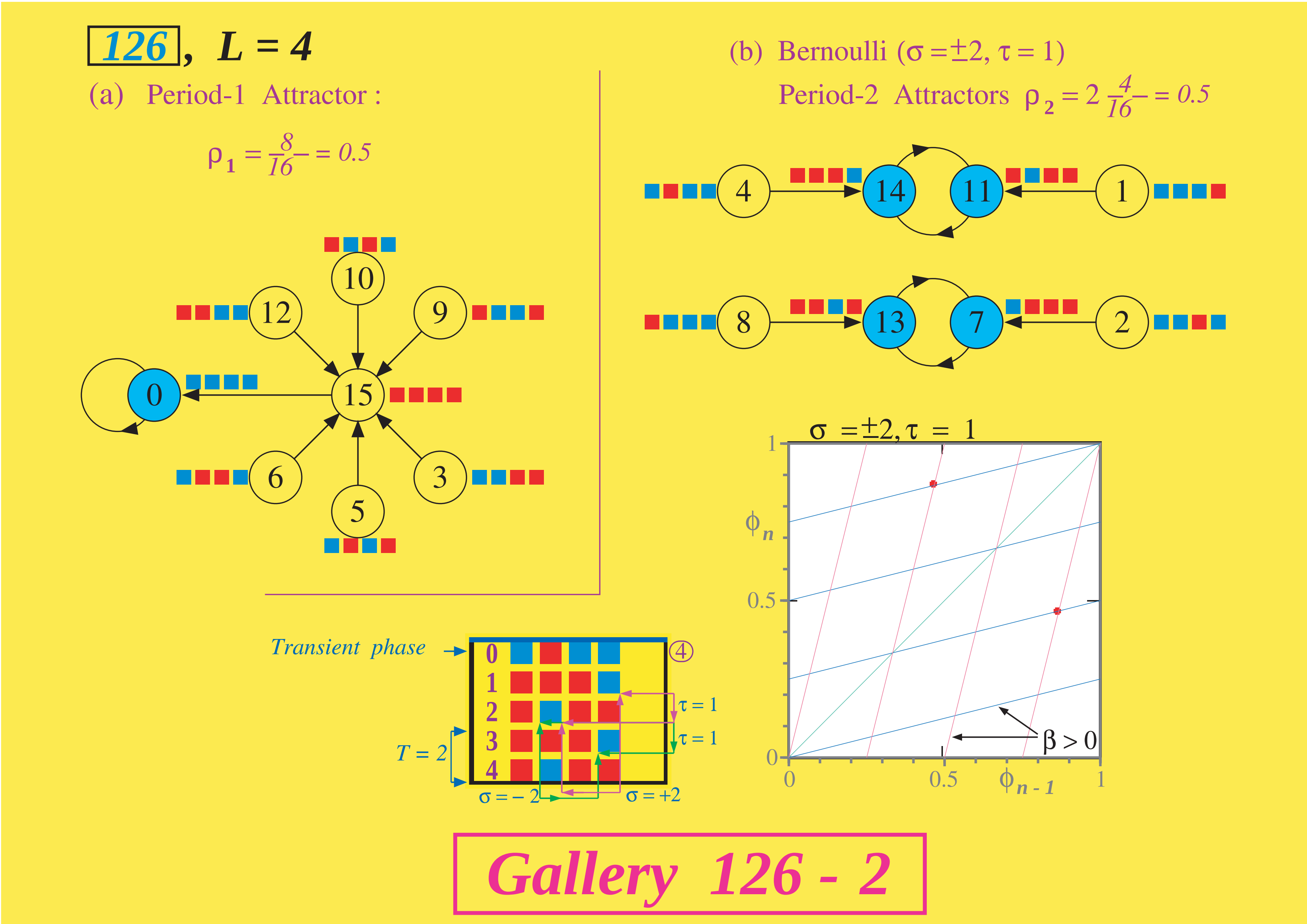
126, L = 4
(a) Period-1 Attractor :
$\rho_1 = \frac{8}{16} = 0.5$
0
15
12
10
9
6
5
3
(b) Bernoulli ($\sigma = \pm 2, \tau = 1$)
Period-2 Attractors $\rho_2 = 2\,\frac{4}{16} = 0.5$
4
14
11
1
8
13
7
2
$\sigma = \pm 2, \tau = 1$
ϕ_n
ϕ_{n-1}
0
0.5
1
$\beta > 0$
Transient phase
T = 2
0
1
2
3
4
4
$\tau = 1$
$\tau = 1$
$\sigma = -2$
$\sigma = +2$
Gallery 126 - 2

Table 21. (*Continued*)

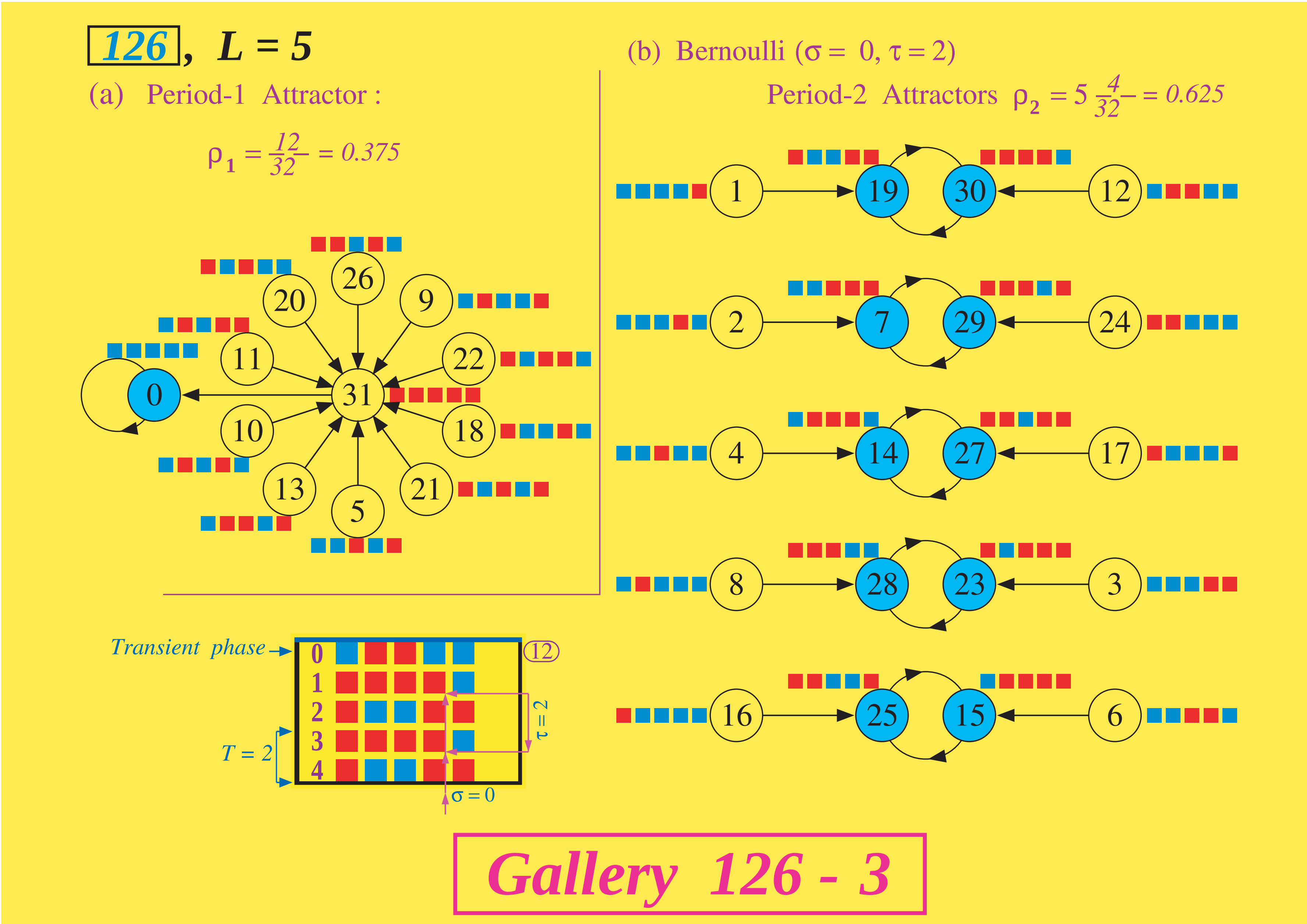

$\boxed{126}$, $L = 6$

(a) Bernoulli ($\sigma = \pm 3$, $\tau = 1$)

Period-2 Attractors :

$\rho_1 = 3\,\frac{4}{64} = 0.1875$

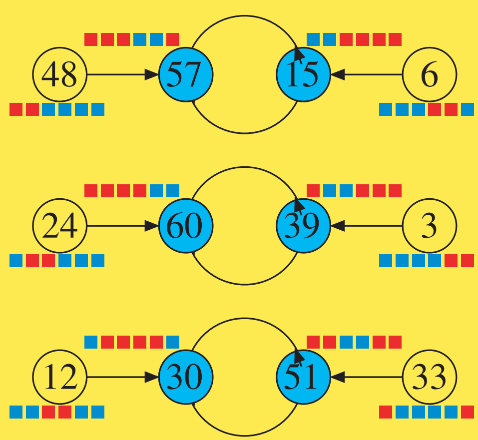

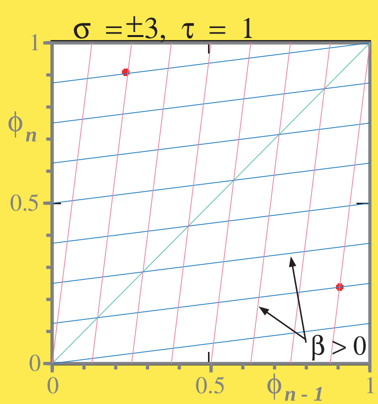

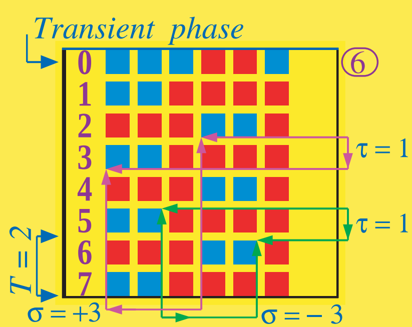

(b) Period-1 Attractor : $\rho_2 = \frac{52}{64} = 0.8125$

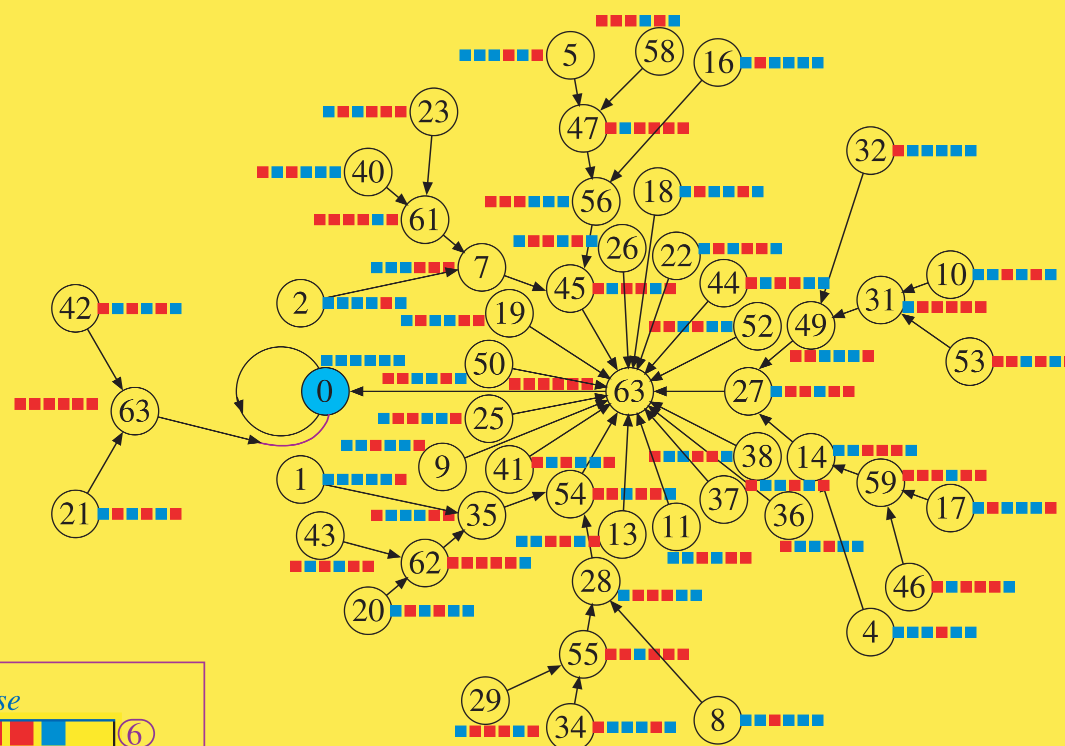

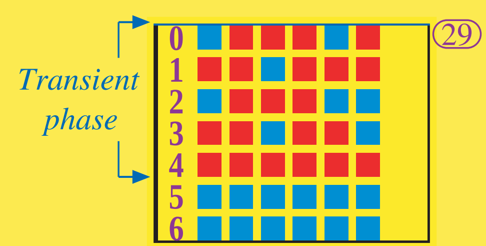

Gallery 126 - 4

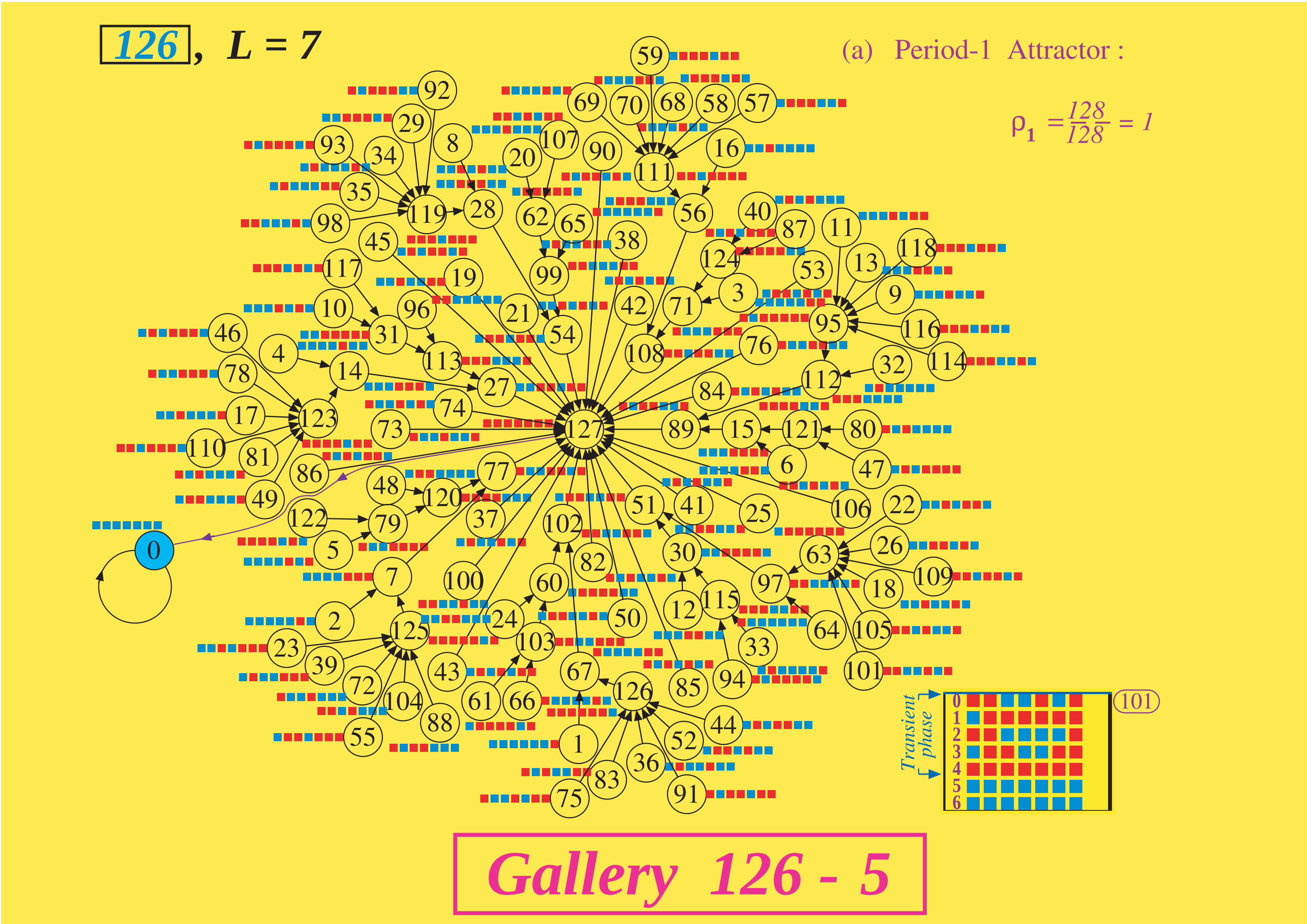
126, L = 7
(a) Period-1 Attractor :
$\rho_1 = \frac{128}{128} = 1$
Transient phase
101
0
1
2
3
4
5
6
Gallery 126 - 5

$\boxed{126}$, $L = 8$ (a) Bernoulli ($\sigma = \pm 4$, $\tau = 3$) Period-6 Attractors : $\rho_1 = 4\frac{28}{256} = 0.4375$

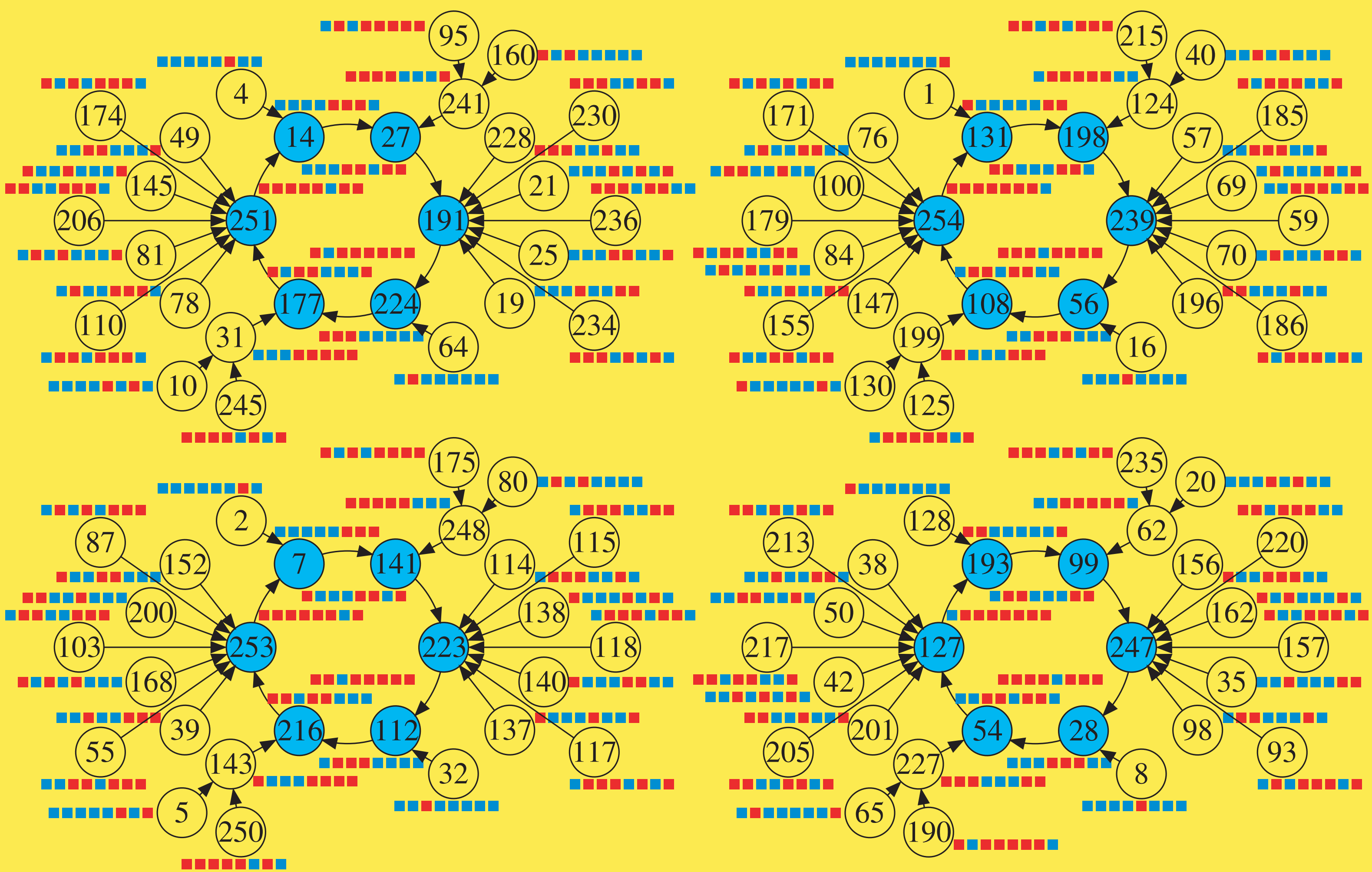

Gallery 126 - 6

$\boxed{126}$, $L = 8$

(a) Bernoulli ($\sigma = \pm 4$, $\tau = 3$)

Period-6 Attractors *(continued)* :

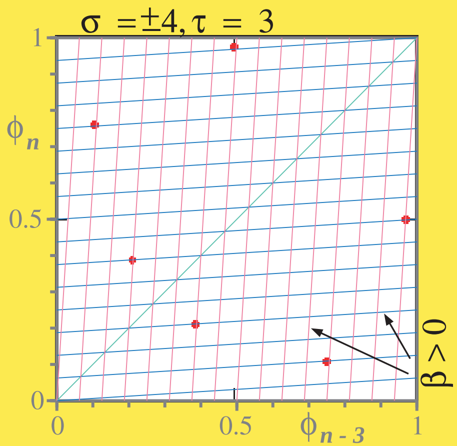

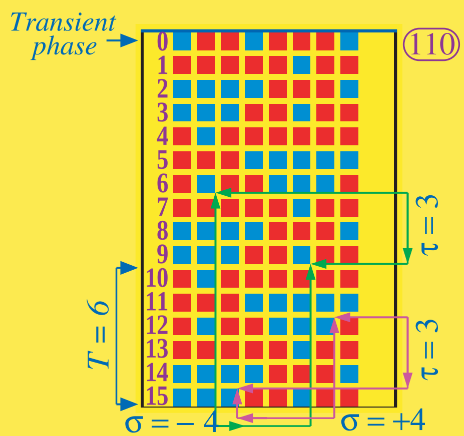

(b) Bernoulli ($\sigma = \pm 2$, $\tau = 1$) Period-2 Attractors :

$\rho_2 = 2\frac{4}{256} = 0.03125$

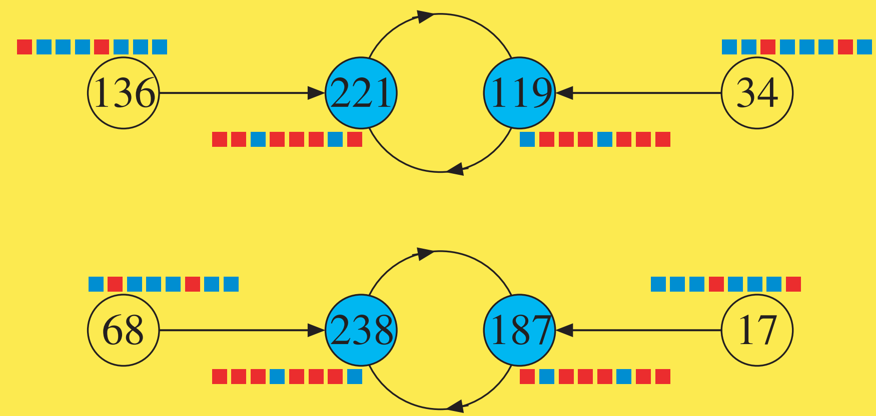

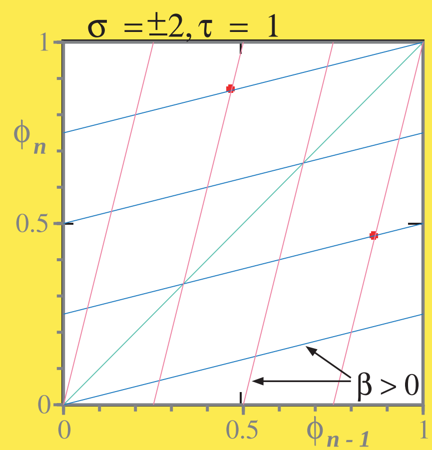

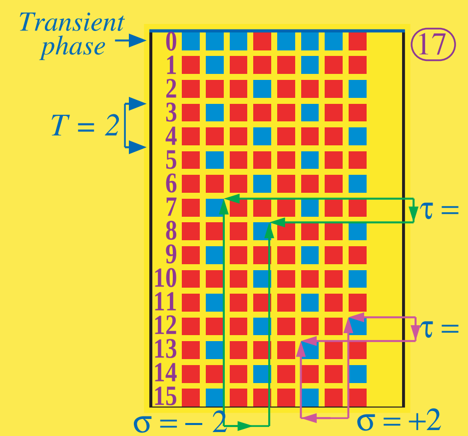

Gallery 126 - 7

$\boxed{126}$, $L = 8$

(c) Period-1 Attractor : $\rho_3 = \frac{136}{256} = 0.53125$

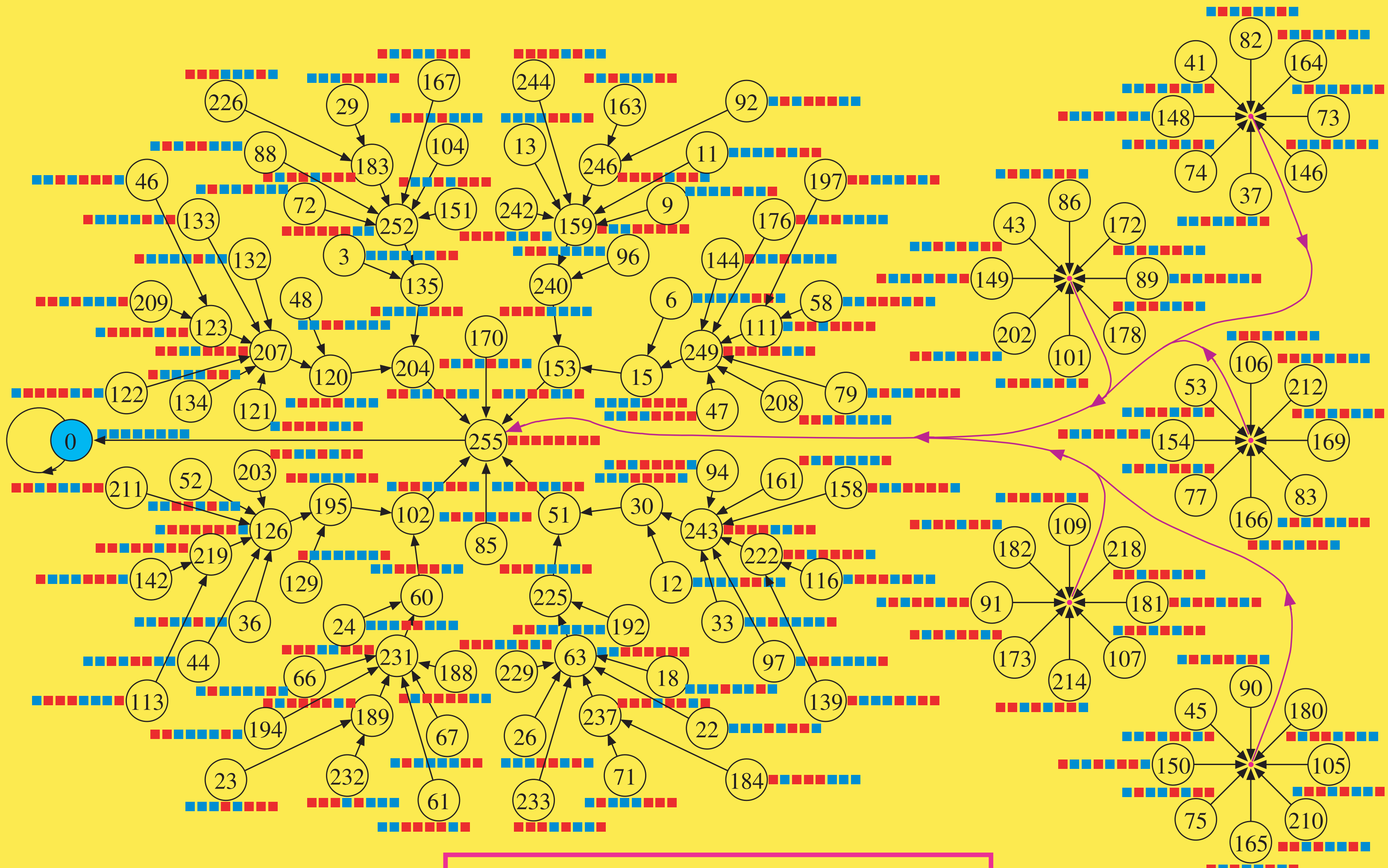

Gallery 126 - 8

2.4.8. *Highlights from Rule* $\boxed{126}$

The basin tree diagrams of Rule $\boxed{126}$ for $L = 3, 4, \ldots, 8$ are exhibited in Table 21. Following a detailed analysis of these diagrams, the qualitative properties of local rule $\boxed{126}$ extracted from basin-tree Galleries 126-1 to 126-8 of Table 21 are summarized below:

Summary of Qualitative properties of local rule $\boxed{126}$ extracted from Gallery 126 for Rule $\boxed{126}$

L	ID Number i	Number of Period-n attractors	Number of Period-n Isles of Eden	Period n	Bernoulli Parameters						Robustness coefficient ρ
					σ_1	τ_1	β_1	σ_2	τ_2	β_2	
3	1	1		1	0	1	+				$\rho_1 = 1$
4	1	1		1	0	1	+				$\rho_1 = 0.5$
	2	2		2	2	1	+	-2	1	+	$\rho_2 = 0.5$
5	1	1		1	0	1	+				$\rho_1 = 0.375$
	2	5		2	0	2	+				$\rho_2 = 0.625$
6	1	3		2	3	1	+	-3	1	+	$\rho_1 = 0.1875$
	2	1		1	0	1	+				$\rho_2 = 0.8125$
7	1	1		1	0	1	+				$\rho_1 = 1$
8	1	4		6	4	3	+	-4	3	+	$\rho_1 = 0.4375$
	2	2		2	2	1	+	-2	1	+	$\rho_2 = 0.03125$
	3	1		1	0	1	+				$\rho_3 = 0.53125$

Table 22. Basin tree diagrams for rule $\boxed{146}$.

Basin tree diagrams for Rule $\boxed{146}$

$\boxed{146}$, $L = 3$

(a) Period-1 Isle of Eden :

$\rho_1 = \frac{1}{8} = 0.125$

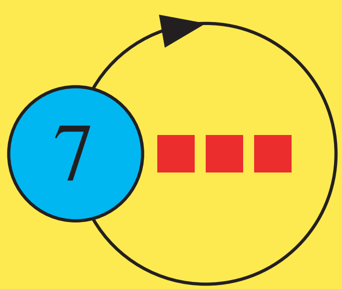

(b) Period-1 Attractor : $\rho_2 = \frac{7}{8} = 0.875$

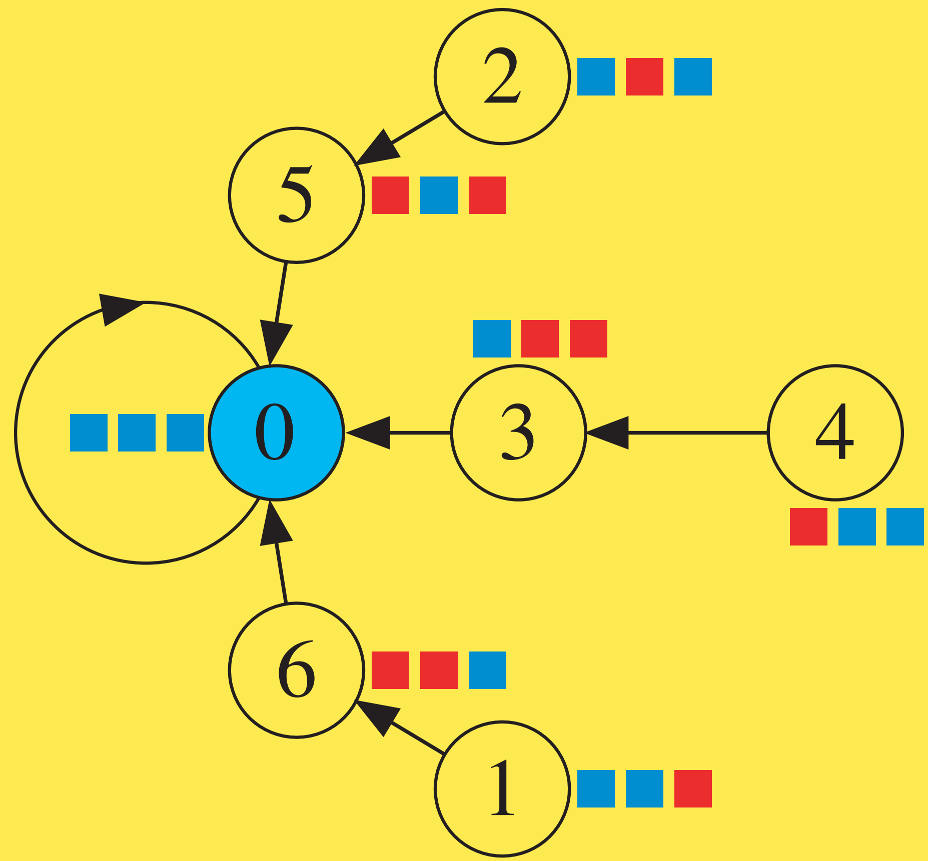

Gallery 146 - 1

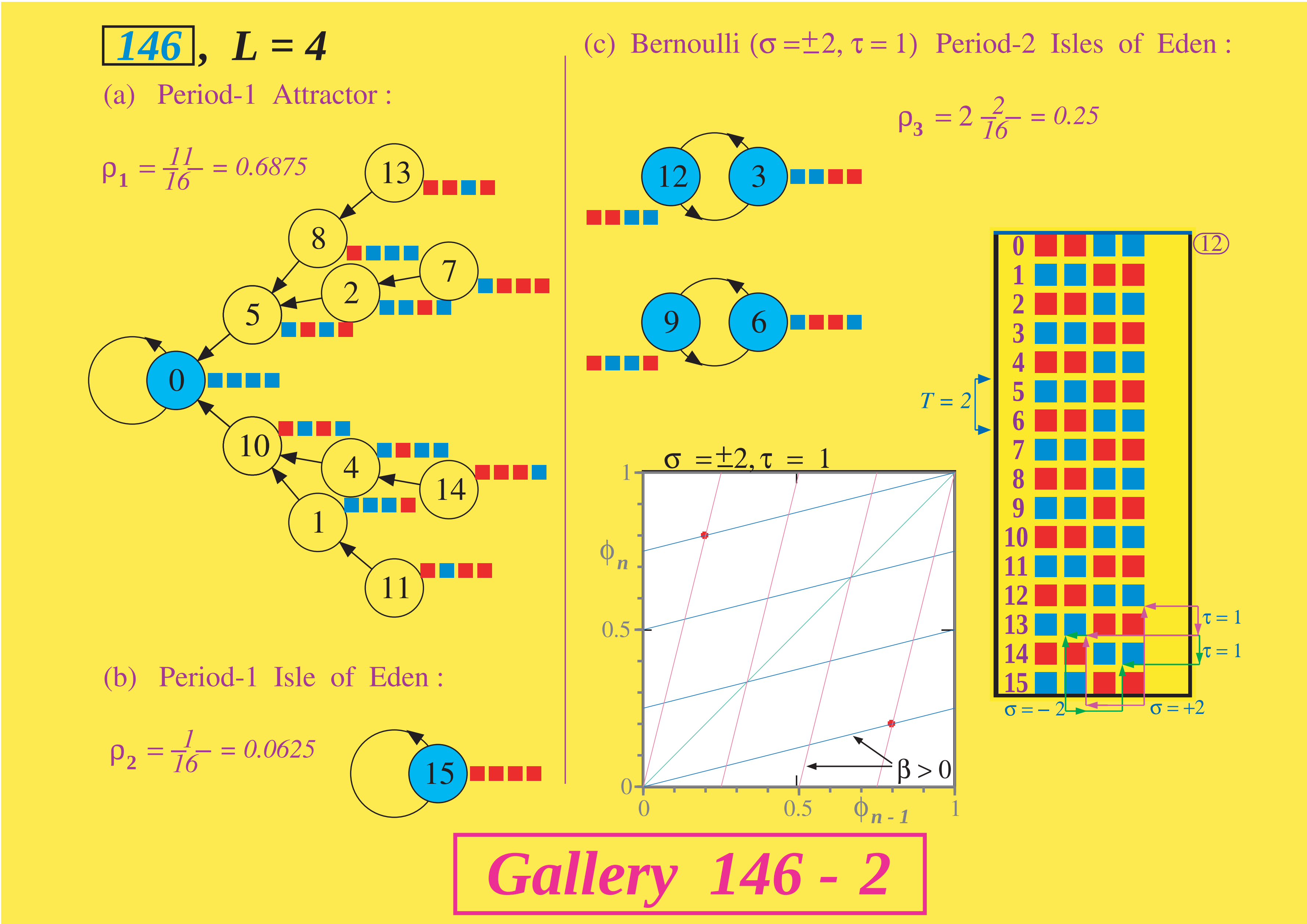
146, L = 4
(a) Period-1 Attractor :
ρ1 = 11/16 = 0.6875
0
5
10
8
2
4
1
13
7
14
11
(b) Period-1 Isle of Eden :
ρ2 = 1/16 = 0.0625
15
(c) Bernoulli (σ = ±2, τ = 1) Period-2 Isles of Eden :
ρ3 = 2 2/16 = 0.25
12
3
9
6
σ = ±2, τ = 1
ϕn
ϕn-1
0
0.5
1
β > 0
T = 2
τ = 1
σ = −2
σ = +2
0
1
2
3
4
5
6
7
8
9
10
11
12
13
14
15
Gallery 146 - 2

Table 22. (*Continued*)

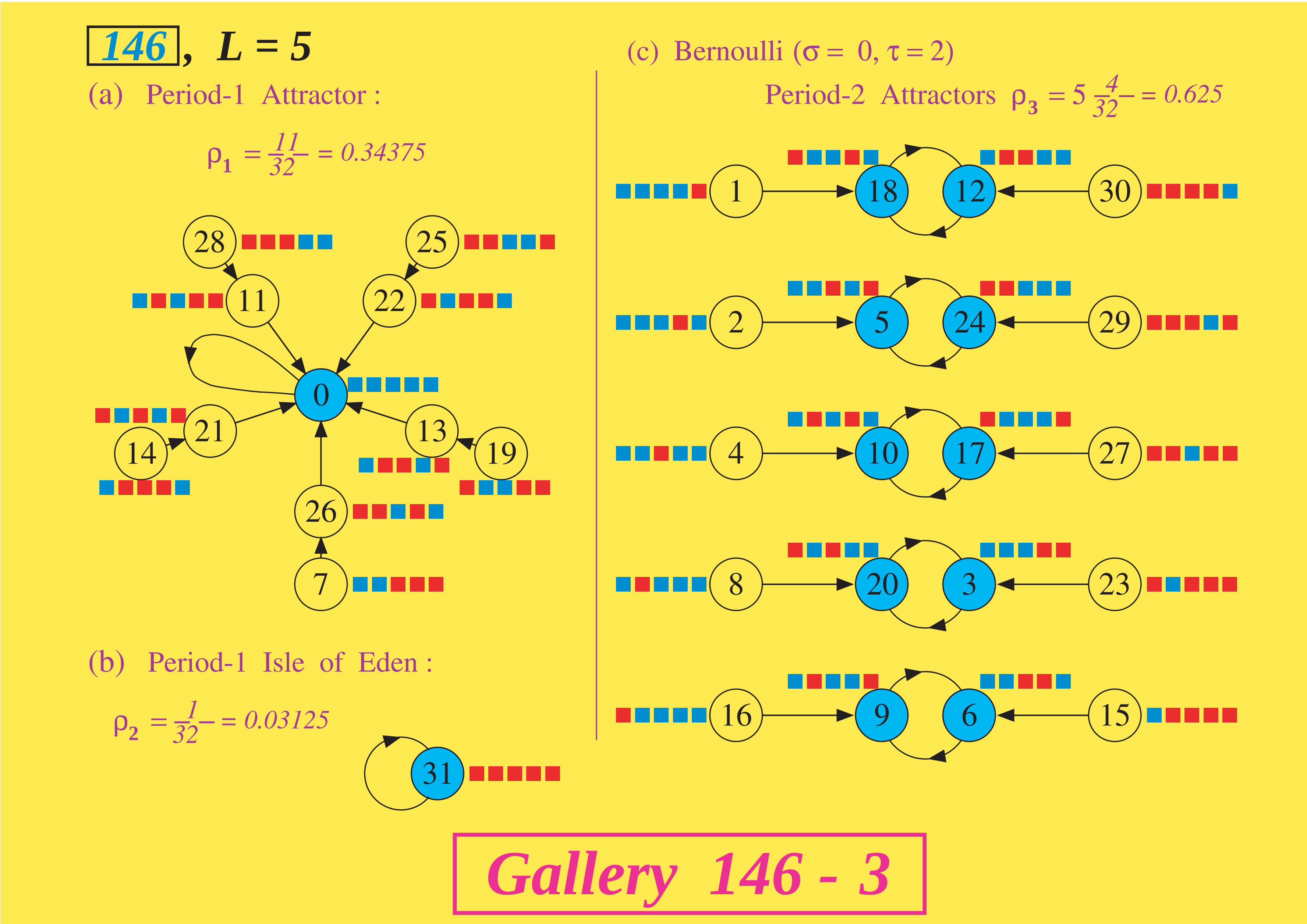

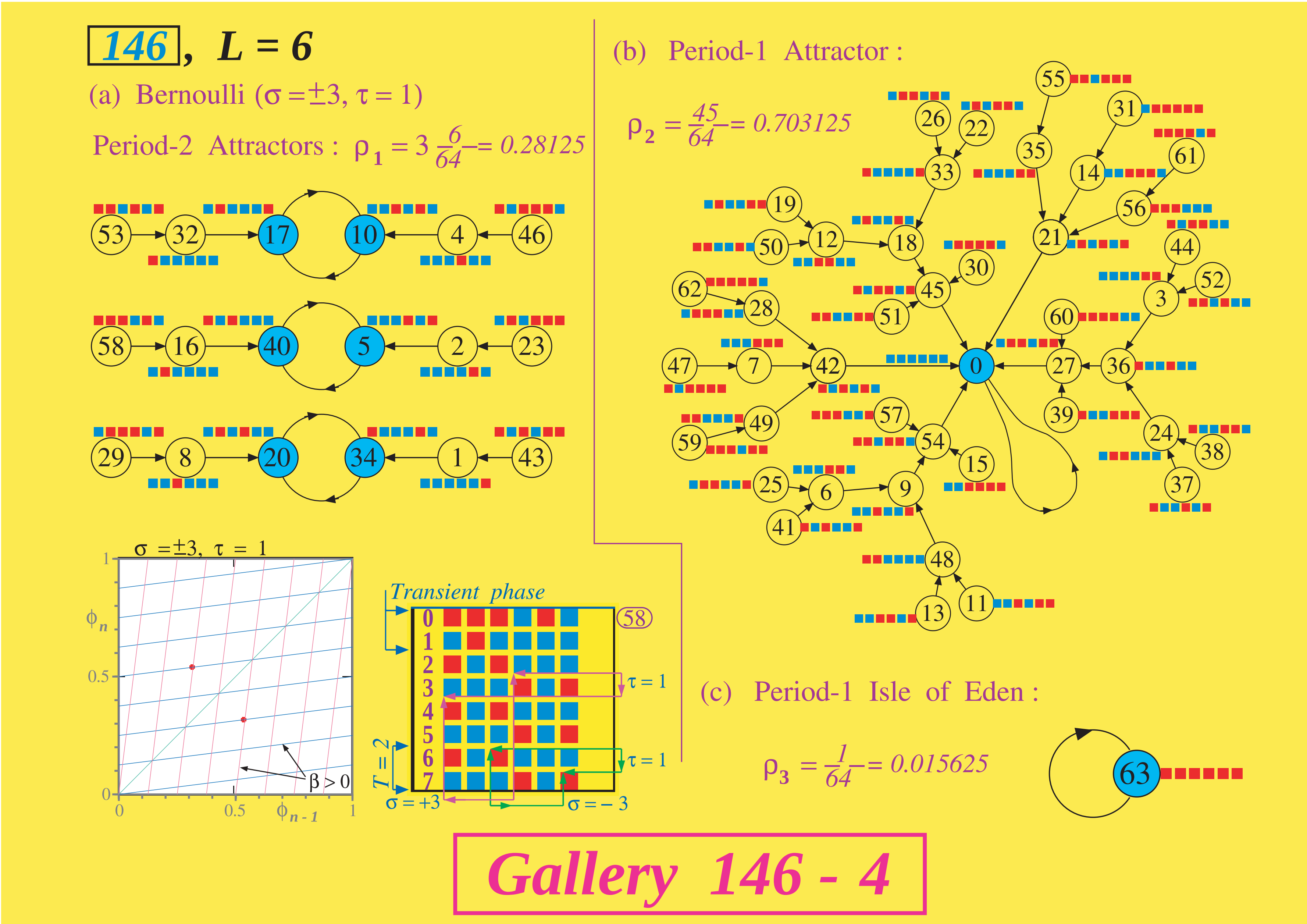
146, L = 6
(a) Bernoulli (σ = ±3, τ = 1)
Period-2 Attractors : ρ1 = 3 6/64 = 0.28125
σ = ±3, τ = 1
β > 0
Transient phase
58
τ = 1
τ = 1
T = 2
σ = +3
σ = − 3
(b) Period-1 Attractor :
ρ2 = 45/64 = 0.703125
(c) Period-1 Isle of Eden :
ρ3 = 1/64 = 0.015625
Gallery 146 - 4

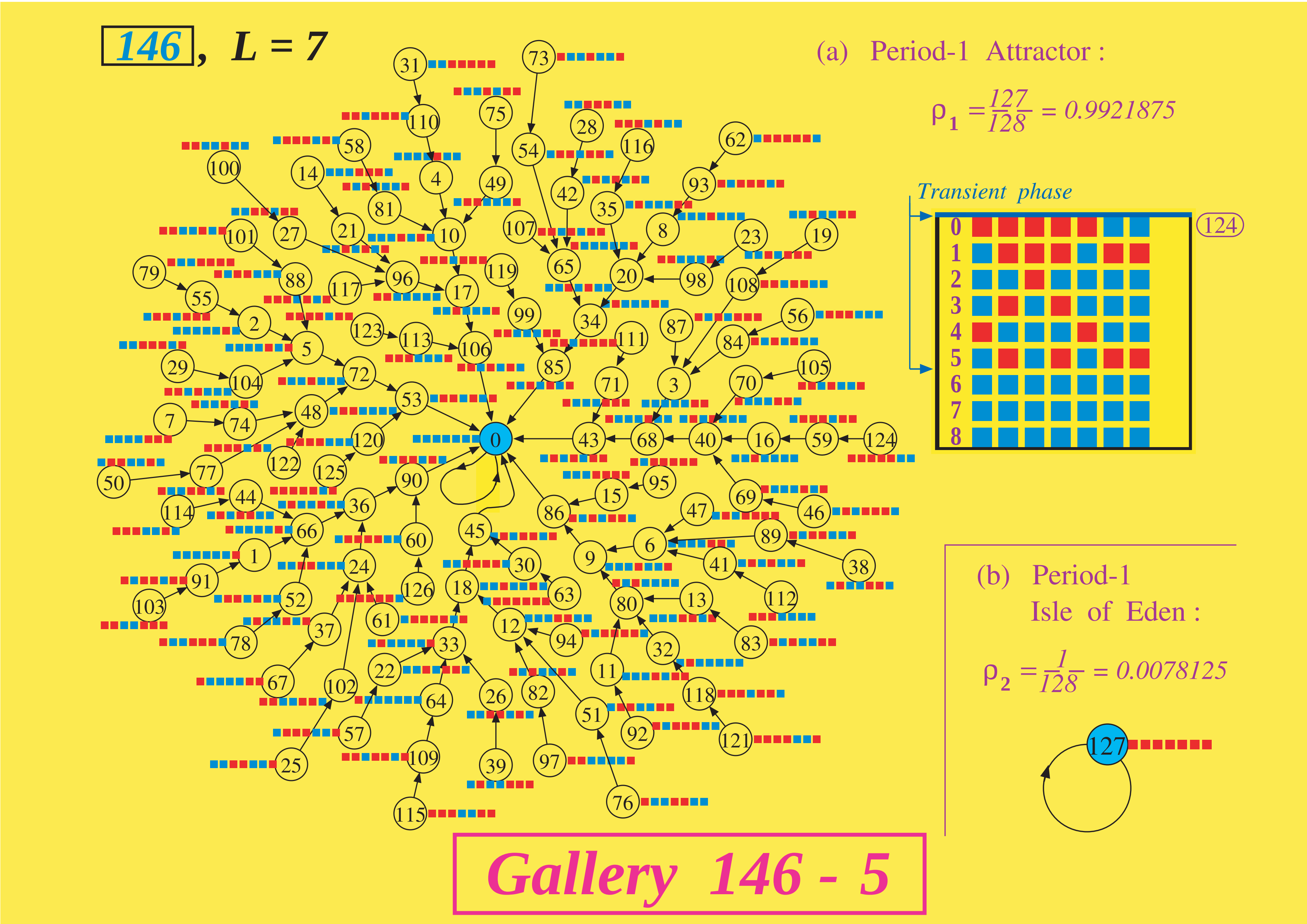
146, L = 7
(a) Period-1 Attractor :
$\rho_1 = \frac{127}{128} = 0.9921875$
Transient phase
0
1
2
3
4
5
6
7
8
124
(b) Period-1
Isle of Eden :
$\rho_2 = \frac{1}{128} = 0.0078125$
127
Gallery 146 - 5

146, ***L* = 8** (a) Bernoulli ($\sigma = \pm 4$, $\tau = 3$) Period-6 Attractors :

$$\rho_1 = 4\frac{28}{256} = 0.4375$$

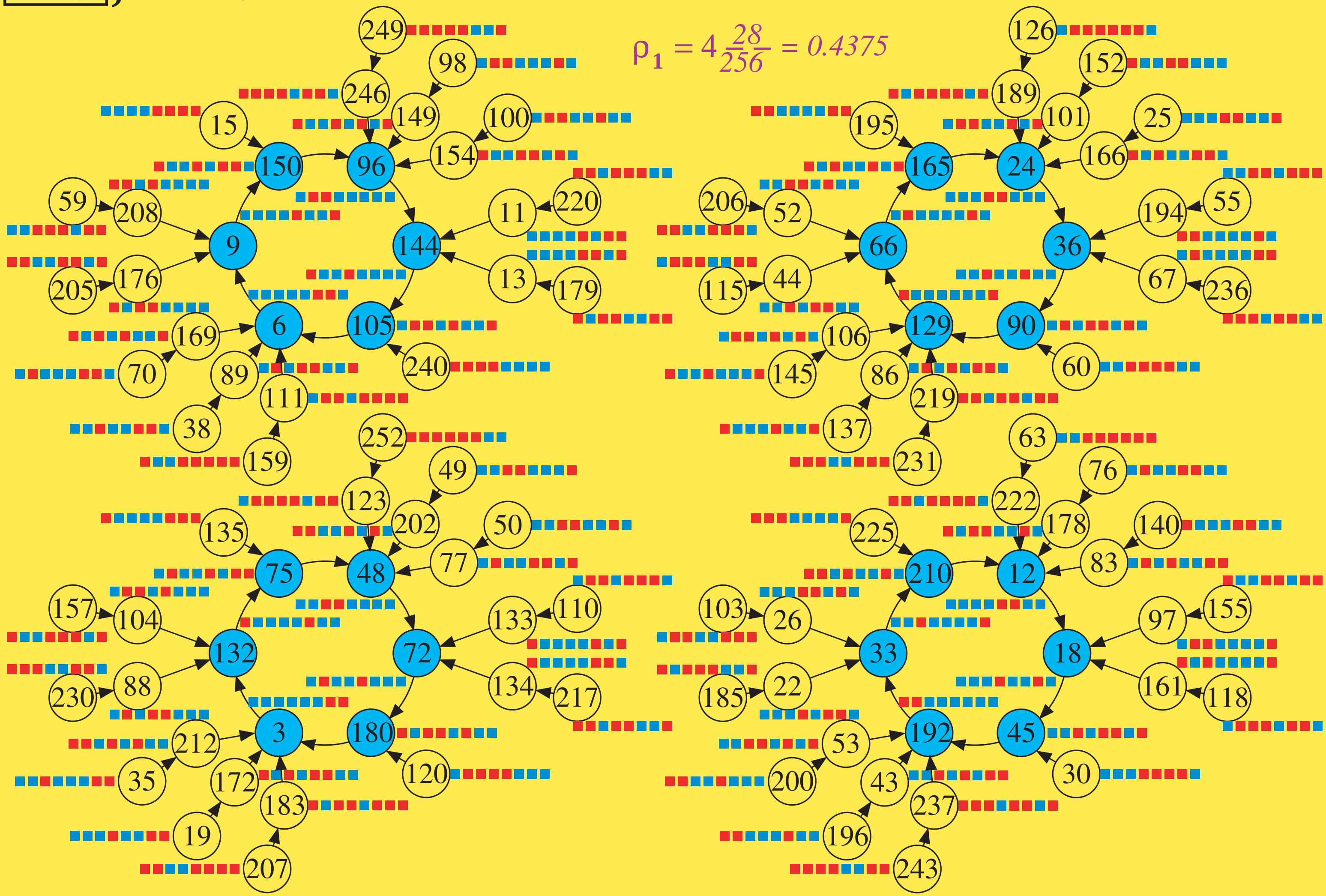

Gallery 146 - 6

$\boxed{146}$, $L = 8$

(a) Bernoulli ($\sigma = \pm 4$, $\tau = 3$)

Period-6 Attractors *(continued)* :

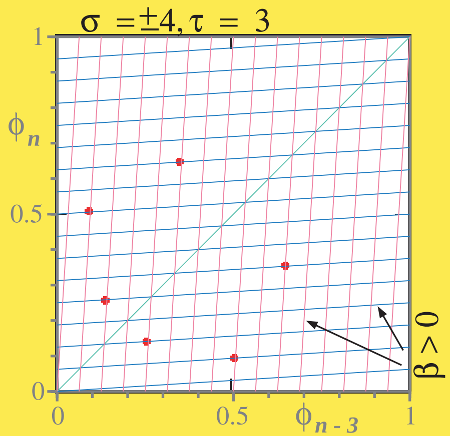

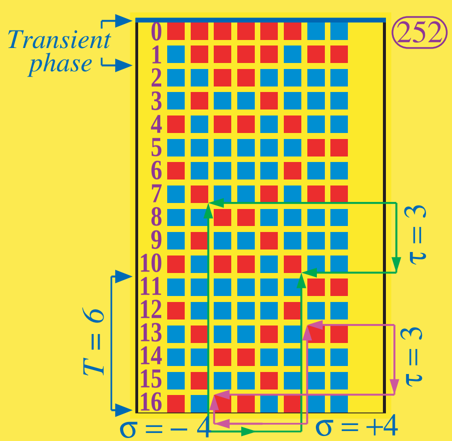

(b) Bernoulli ($\sigma = \pm 2$, $\tau = 1$)

Period-2 Isles of Eden :

$$\rho_2 = 2\frac{2}{256} = 0.015625$$

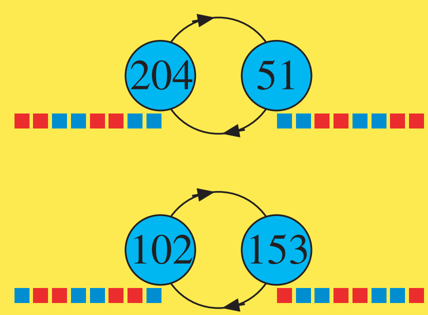

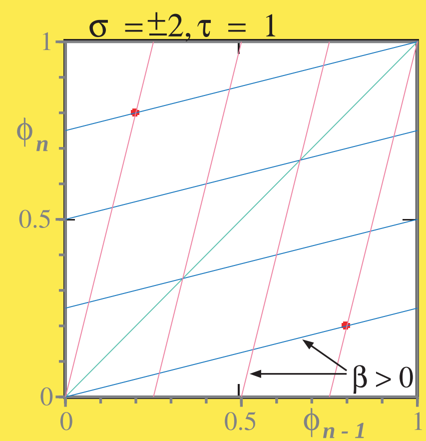

(c) Period-1 Isle of Eden :

$$\rho_3 = \frac{1}{256} = 0.00390625$$

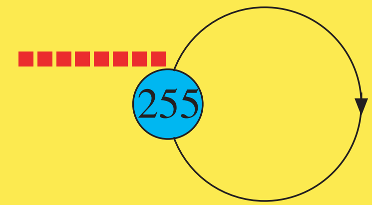

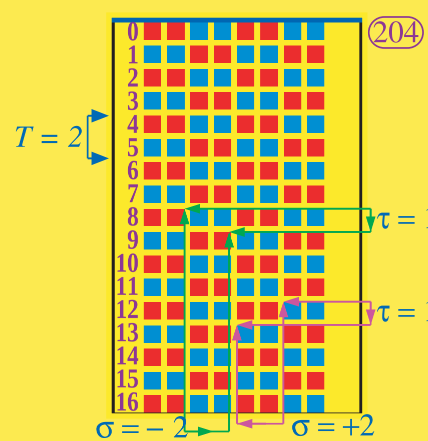

Gallery 146 - 7

146, ***L* = 8**

(d) Period-1 Attractor :

$\rho_4 = \frac{139}{256} = 0.54296875$

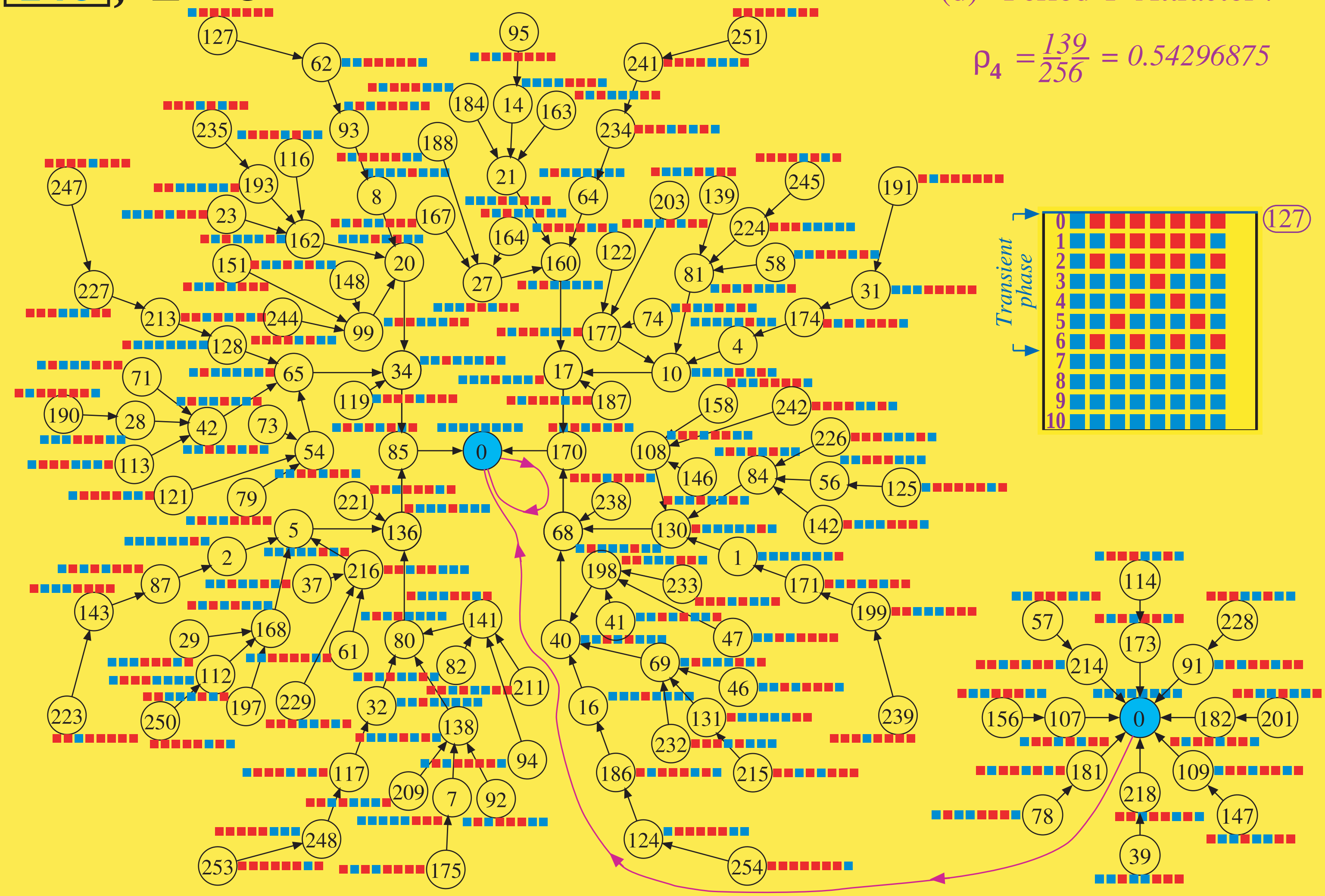

Gallery 146 - 8

2.4.9. *Highlights from Rule* $\boxed{146}$

The basin tree diagrams of Rule $\boxed{146}$ for $L = 3, 4, \ldots, 8$ are exhibited in Table 22. Following a detailed analysis of these diagrams, the qualitative properties of local rule $\boxed{146}$ extracted from basin-tree Galleries 146-1 to 146-8 of Table 22 are summarized below:

Summary of Qualitative properties of local rule $\boxed{146}$ extracted from Gallery 146 for Rule $\boxed{146}$

L	ID Number i	Number of Period-n attractors	Number of Period-n Isles of Eden	Period n	Bernoulli Parameters						Robustness coefficient ρ
					σ_1	τ_1	β_1	σ_2	τ_2	β_2	
3	1		1	1	0	1	+				ρ_1=0.125
	2	1		1	0	1	+				ρ_2=0.875
4	1	1		1	0	1	+				ρ_1=0.6875
	2		1	1	0	1	+				ρ_2=0.0625
	3		2	2	2	1	+	-2	1	+	ρ_3=0.25
5	1	1		1	0	1	+				ρ_1=0.34375
	2		1	1	0	1	+				ρ_2=0.03125
	3	5		2	0	2	+				ρ_3=0.625
6	1	3		2	3	1	+	-3	1	+	ρ_1=0.28125
	2	1		1	0	1	+				ρ_2=0.703125
	3		1	1	0	1	+				ρ_3=0.015625
7	1	1		1	0	1	+				ρ_1=0.9921875
	2		1	1	0	1	+				ρ_2=0.0078125
8	1	4		6	4	3	+	-4	3	+	ρ_1=0.4375
	2		2	2	2	1	+	-2	1	+	ρ_2=0.015625
	3		1	1	0	1	+				ρ_3=0.00390625
	4	1		1	0	1	+				ρ_4=0.54296875

Table 23. Basin tree diagrams for rule $\boxed{150}$.

Basin tree diagrams for Rule $\boxed{150}$

$\boxed{150}$, $L = 3$ (a) Period-1 Attractors : $\rho_1 = 2^{-\frac{4}{8}} = 1$

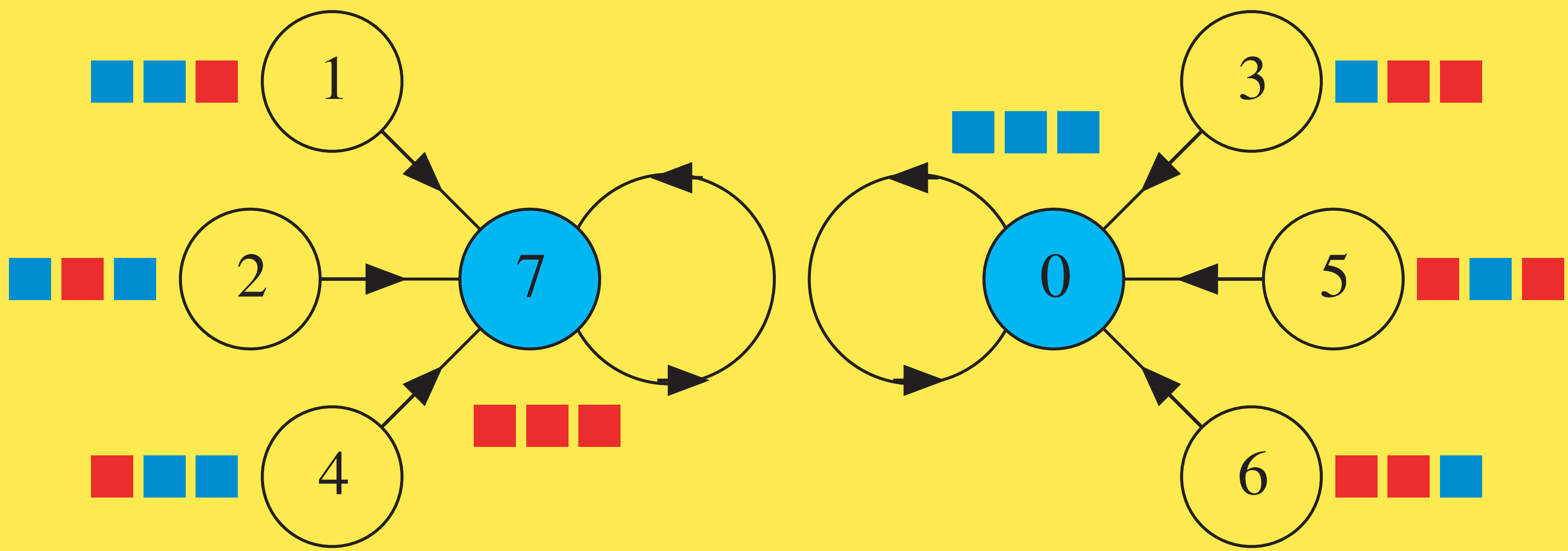

Gallery 150 - 1

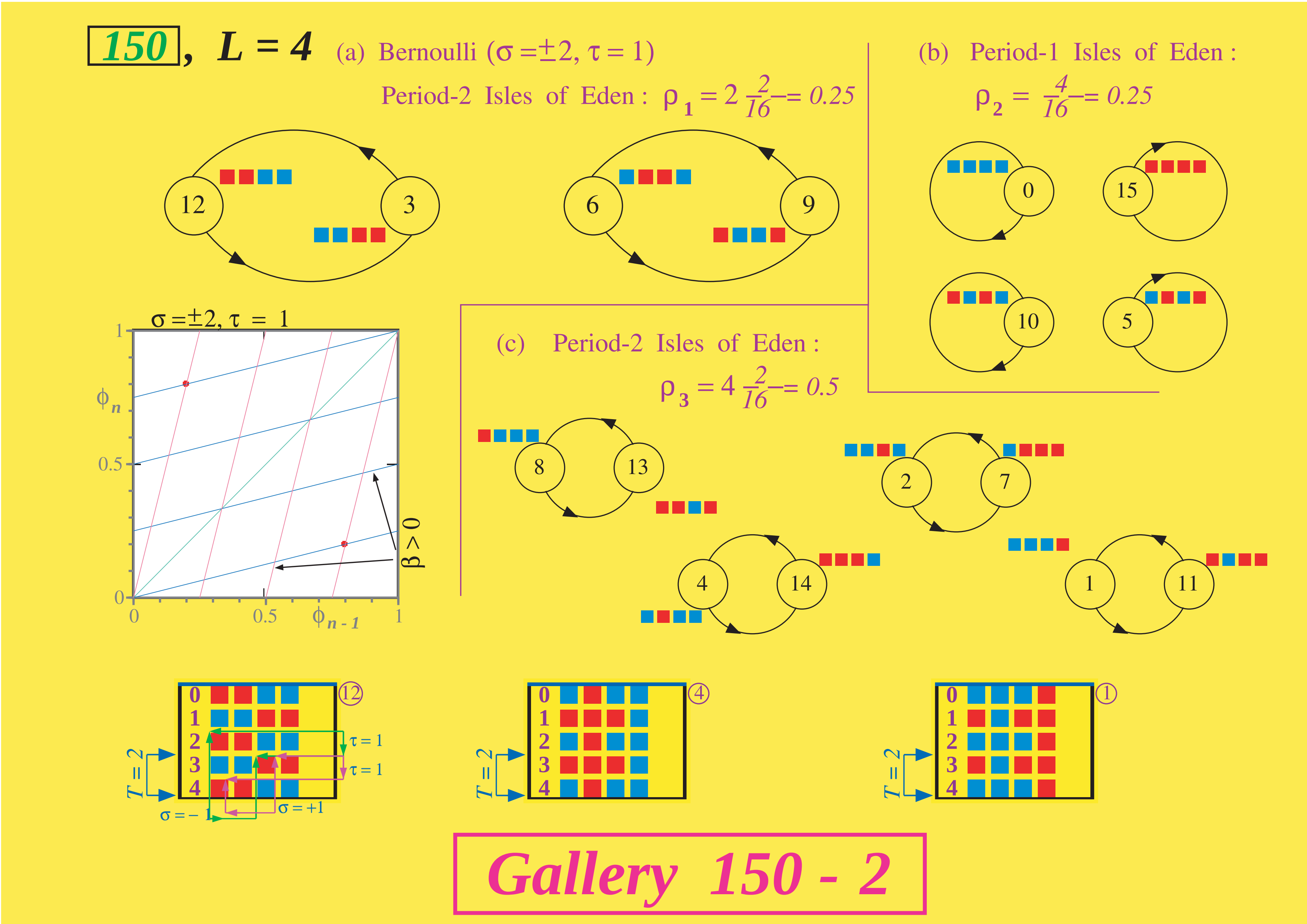
150, L = 4
(a) Bernoulli (σ = ±2, τ = 1)
Period-2 Isles of Eden : ρ1 = 2 2/16 = 0.25
(b) Period-1 Isles of Eden :
ρ2 = 4/16 = 0.25
(c) Period-2 Isles of Eden :
ρ3 = 4 2/16 = 0.5
12
3
6
9
0
15
10
5
8
13
2
7
4
14
1
11
σ = ±2, τ = 1
φn
φn-1
β > 0
0
0.5
1
T = 2
τ = 1
σ = −1
σ = +1
Gallery 150 - 2

Table 23. (*Continued*)

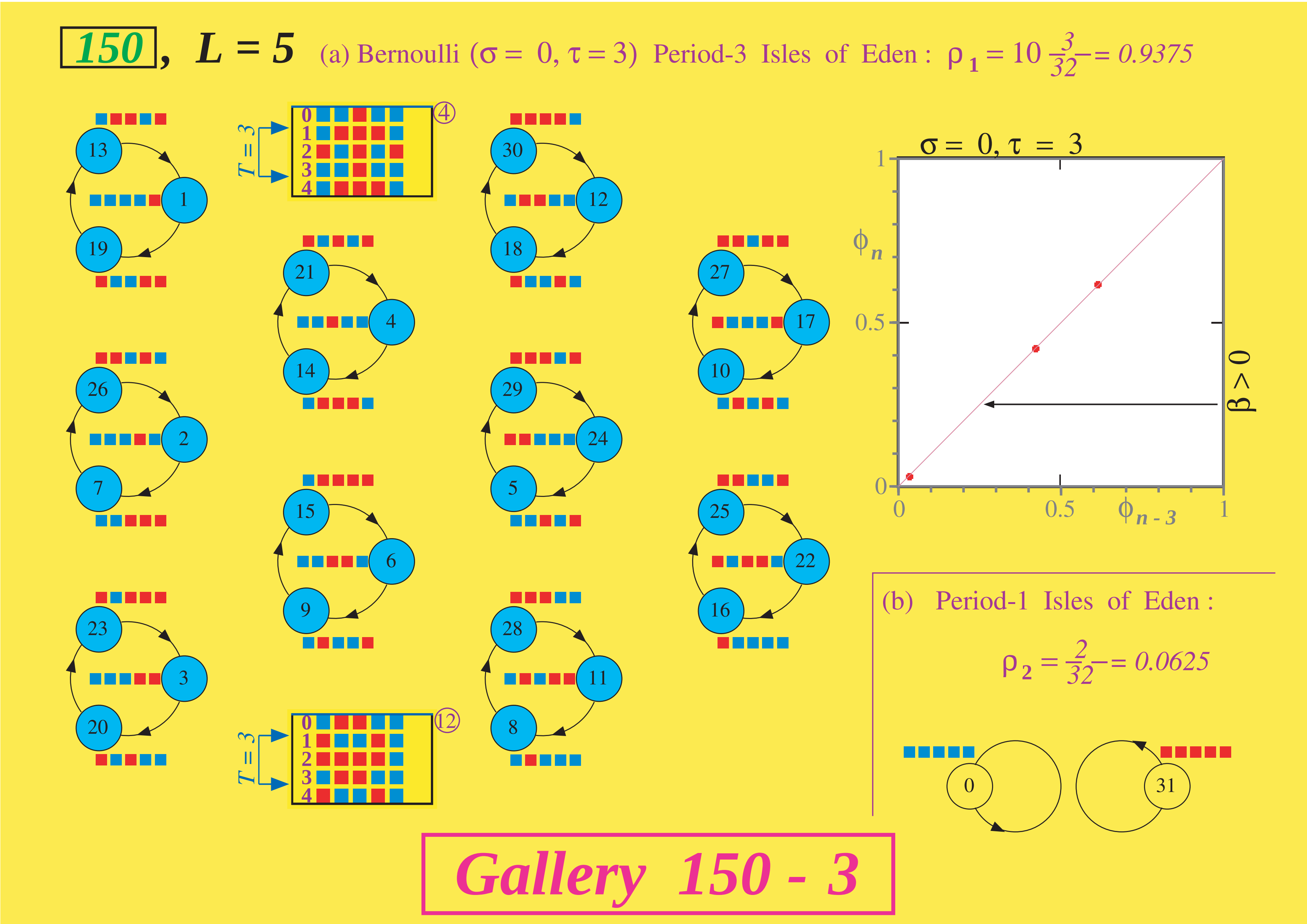

150, ***L* = 6**

(a) Period-1 Attractors : $\rho_1 = 2\,\frac{16}{64} = 0.5$

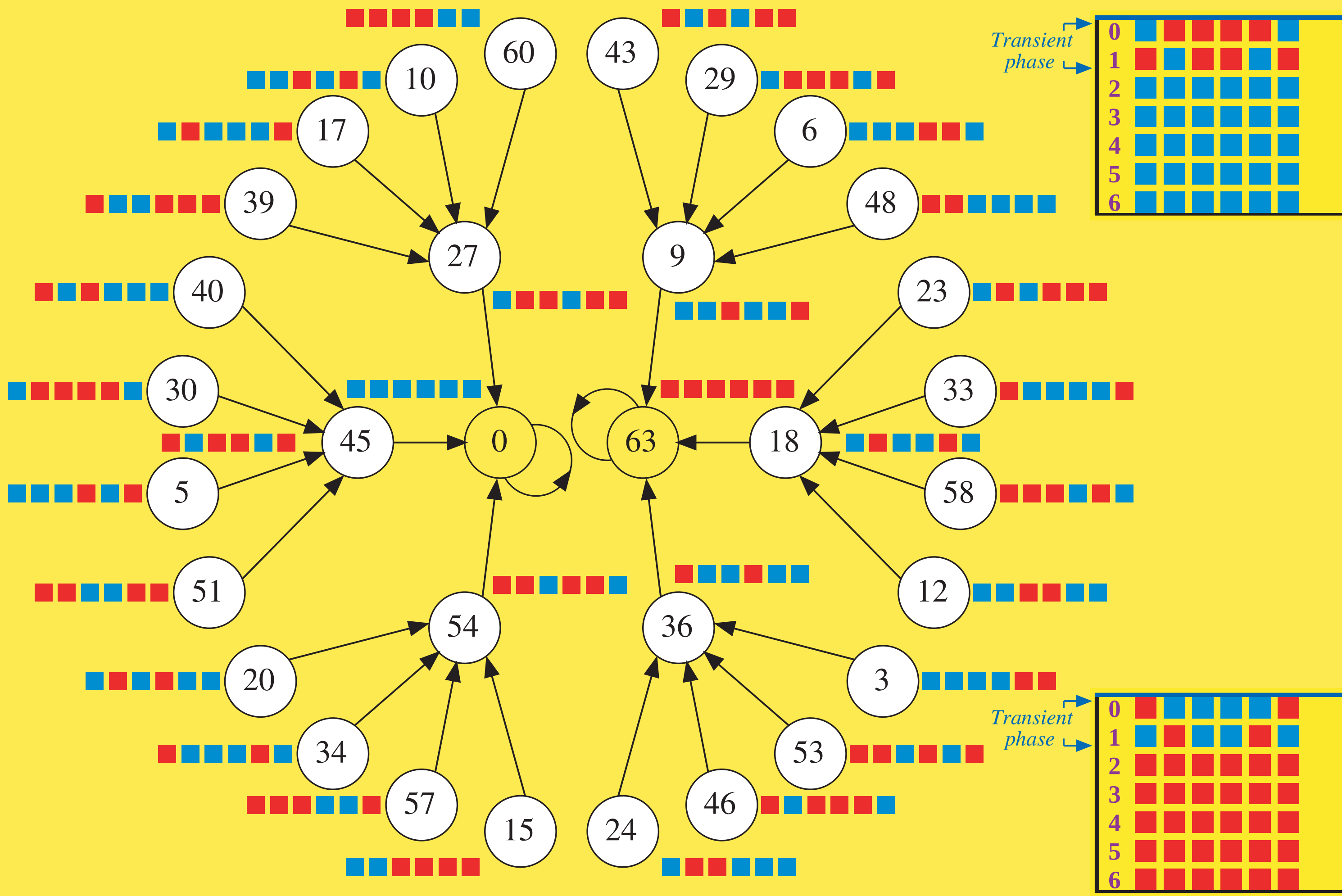

Gallery 150 - 4

$\boxed{150}$, $L = 6$

(b) Period-1 Attractors : $\rho_2 = 2\,\frac{16}{64} = 0.5$

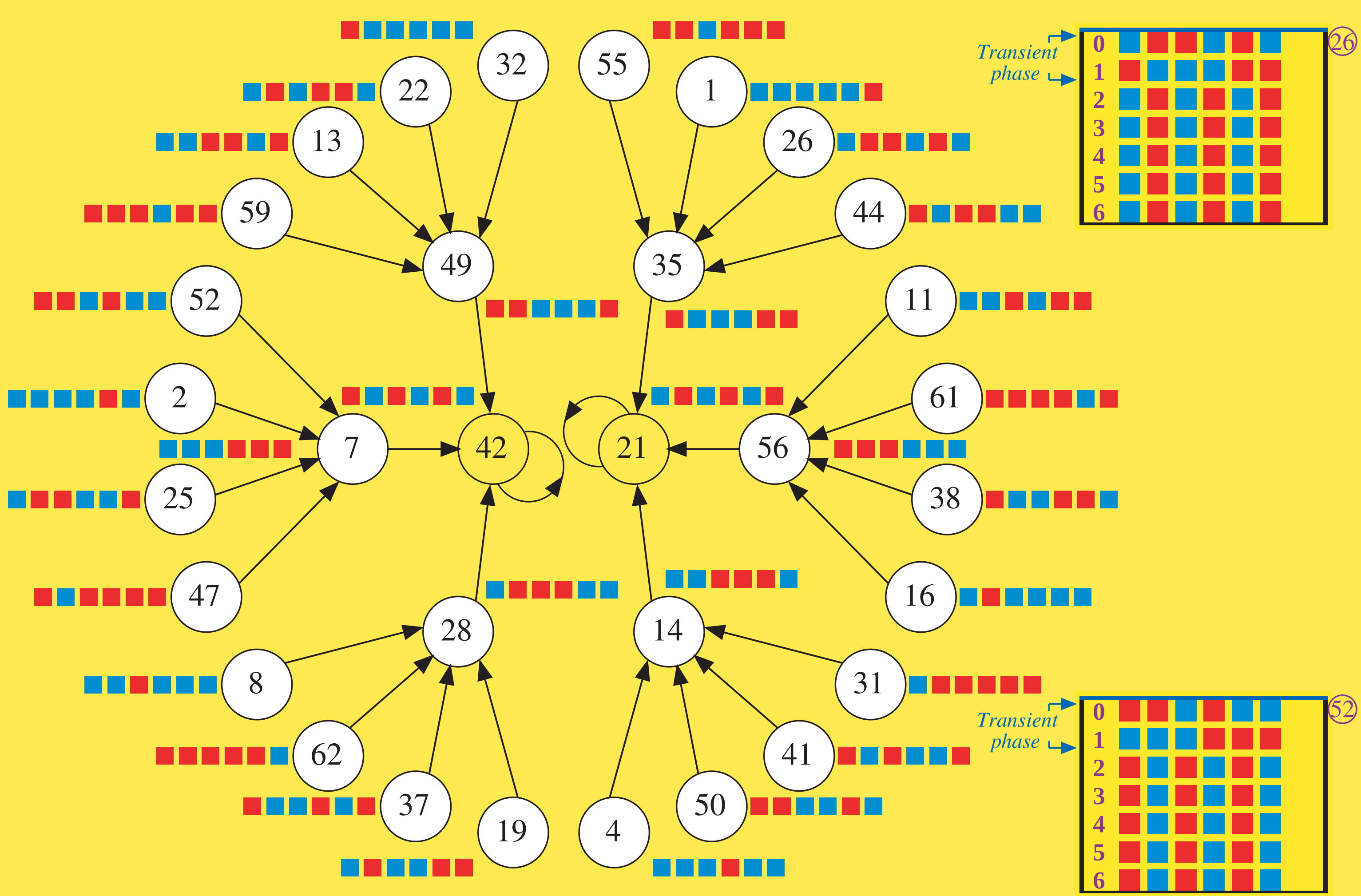

Gallery 150 - 5

Table 23. (*Continued*)

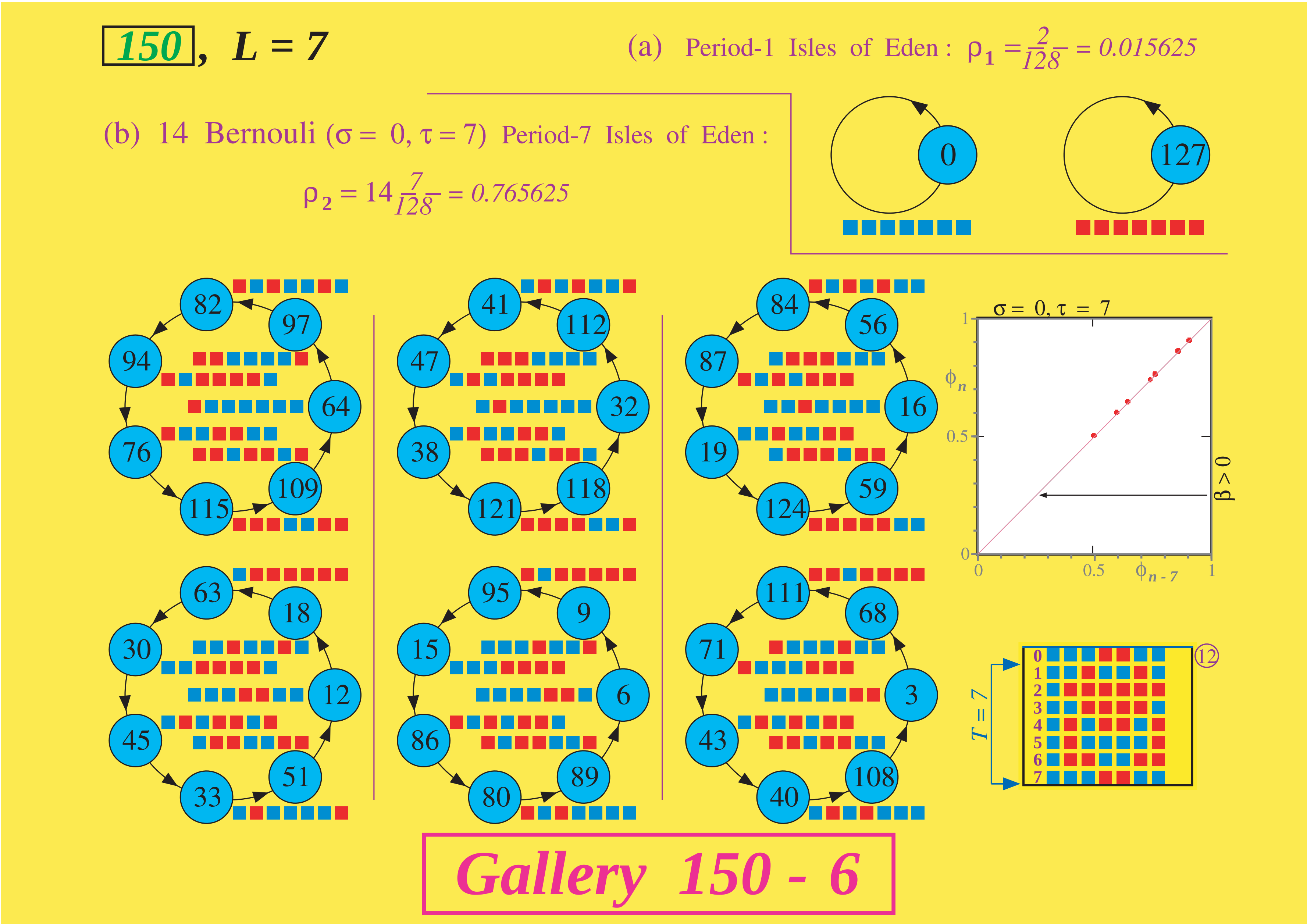

150, ***L* = 7**

(b) 14 Bernoulli ($\sigma = 0, \tau = 7$) Period-7 Isles of Eden *(continued)* :

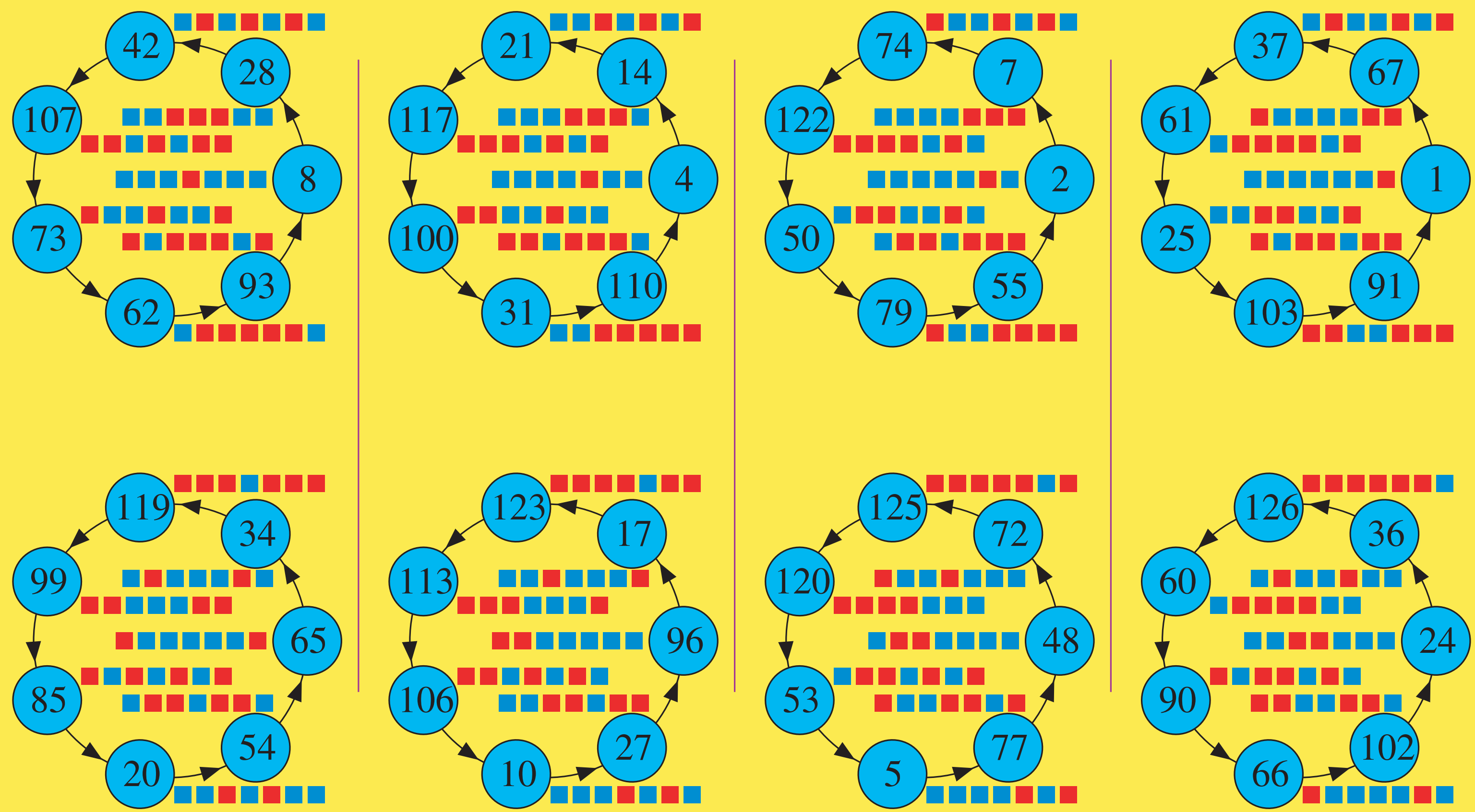

Gallery 150 - 7

150, $L = 7$ (c) 4 Bernoulli ($\sigma = +1, \sigma = -1, \tau = 2$) Period-7 Isles of Eden :

$$\rho_3 = 4\frac{7}{128} = 0.21875$$

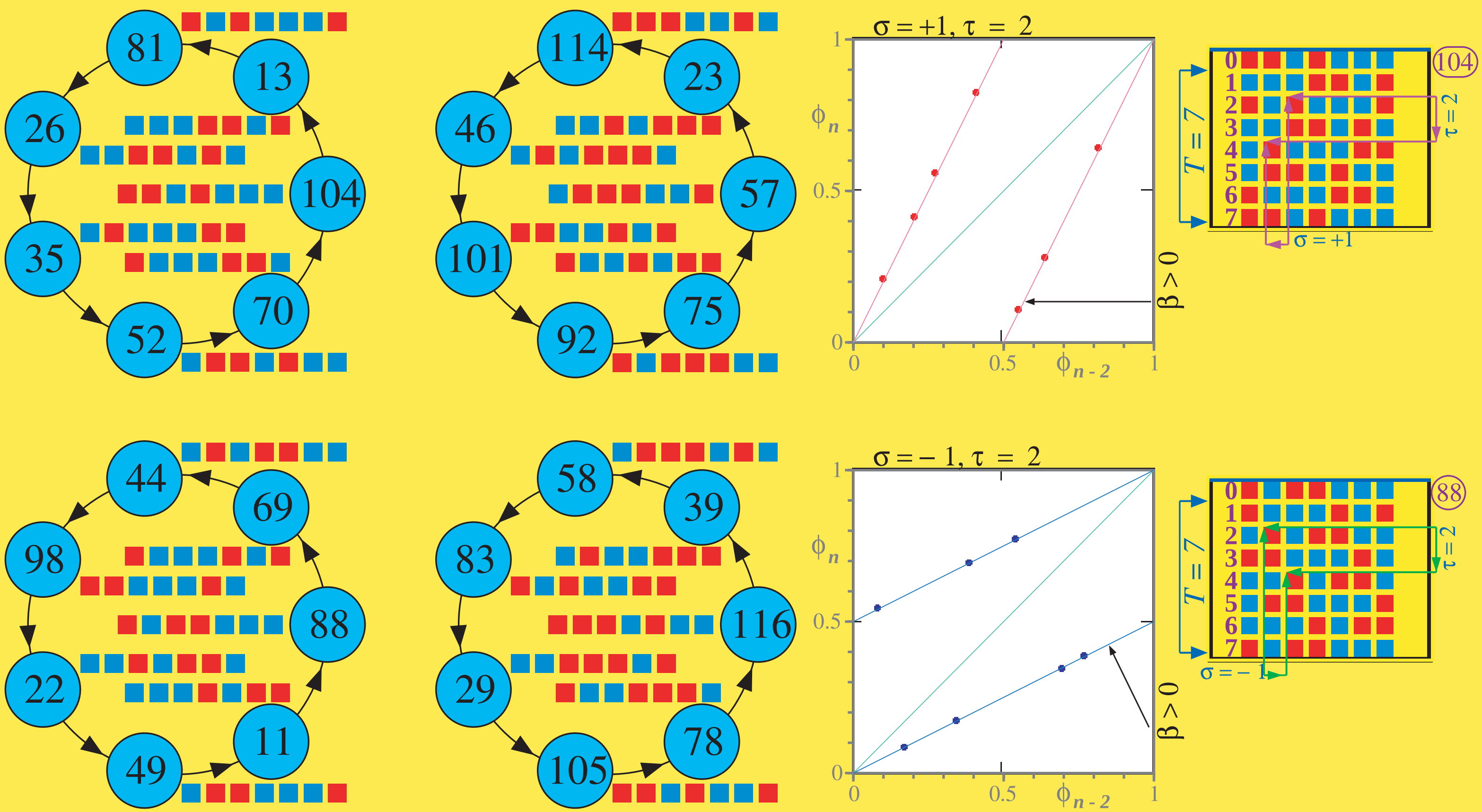

Gallery 150 - 8

Table 23. (*Continued*)

$\boxed{150}$, $L = 8$

(a) 48 Period-4 Isles of Eden : $\rho_1 = 48 \frac{4}{256} = 0.75$

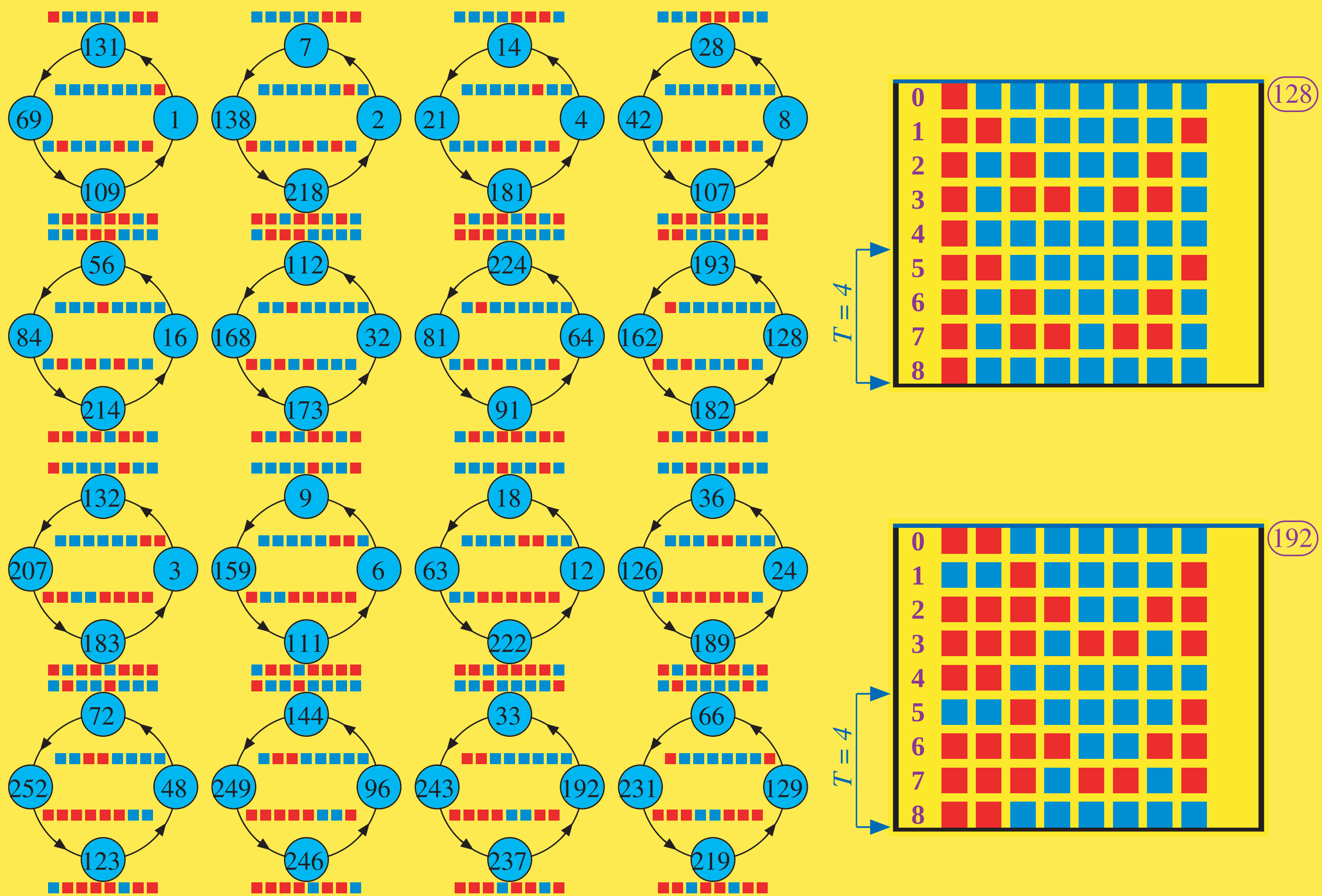

Gallery 150 - 9

150, ***L* = 8** (a) 48 Period-4 Isles of Eden *(continued)* :

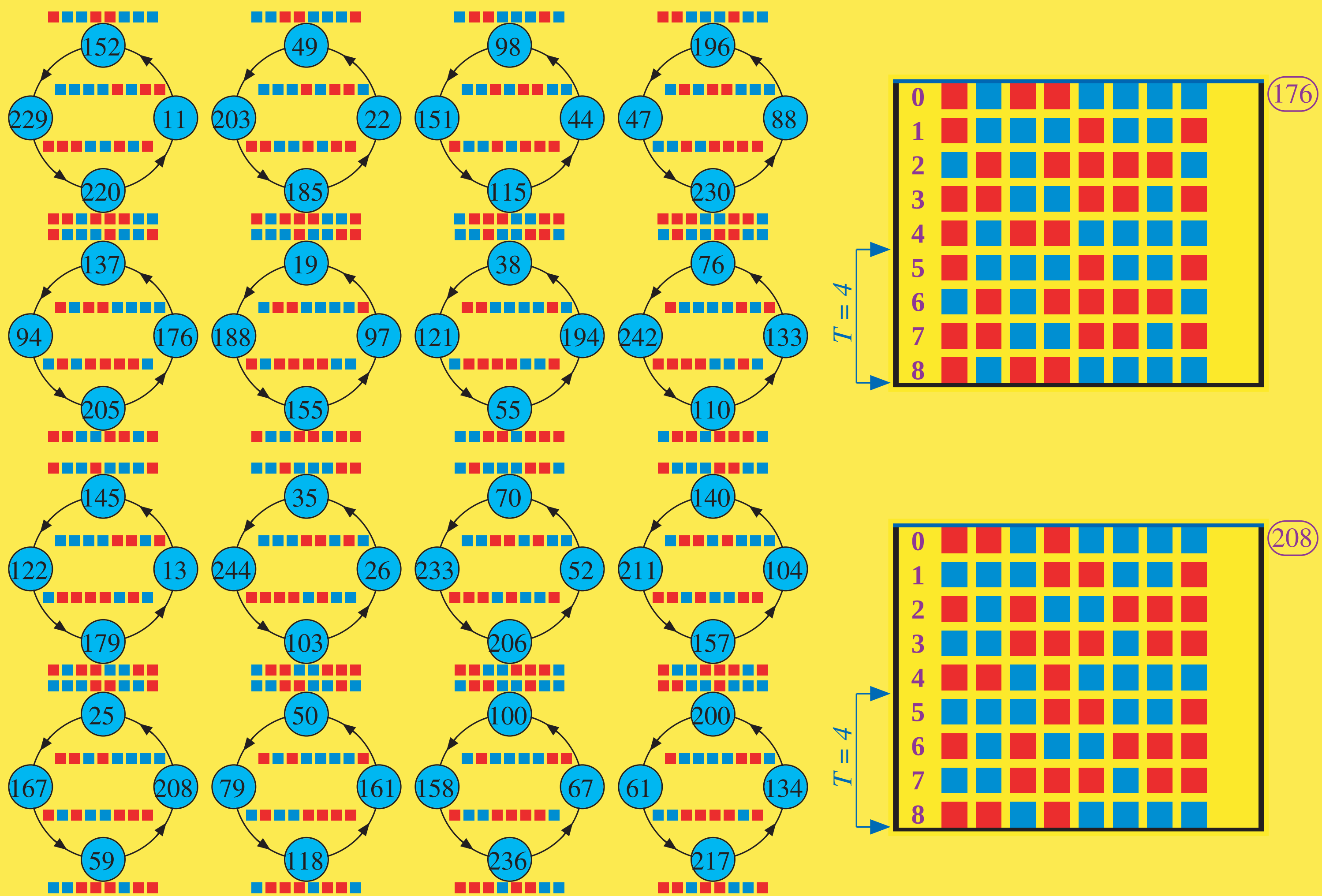

Gallery 150 - 10

150, ***L* = 8** (a) 48 Period-4 Isles of Eden *(continued)* :

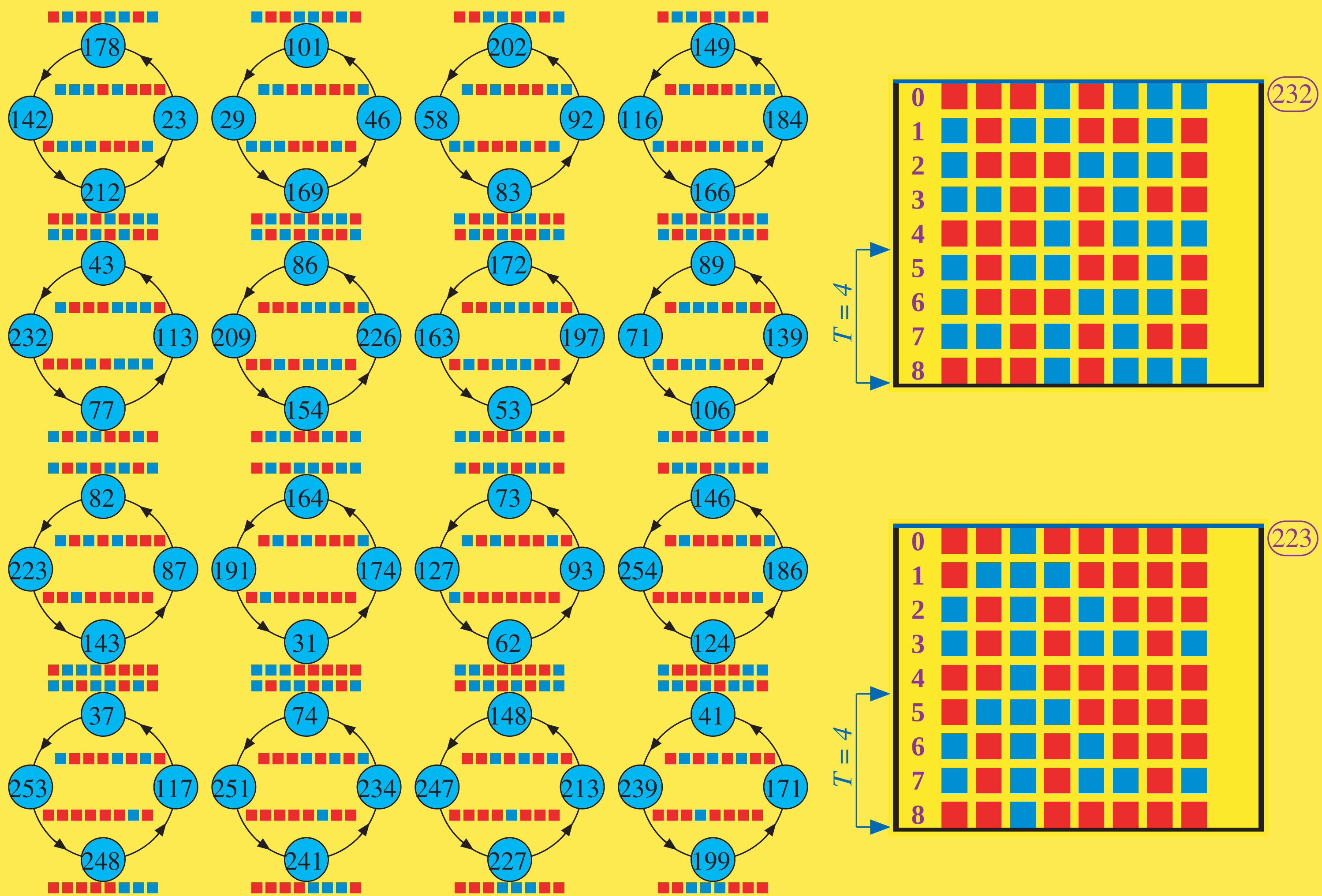

Gallery 150 - 11

150, ***L* = 8** (b) 12 Bernoulli ($\sigma = \pm 4, \tau = 2$) Period-4

Isles of Eden $\rho_2 = 12\frac{4}{256} = 0.1875$

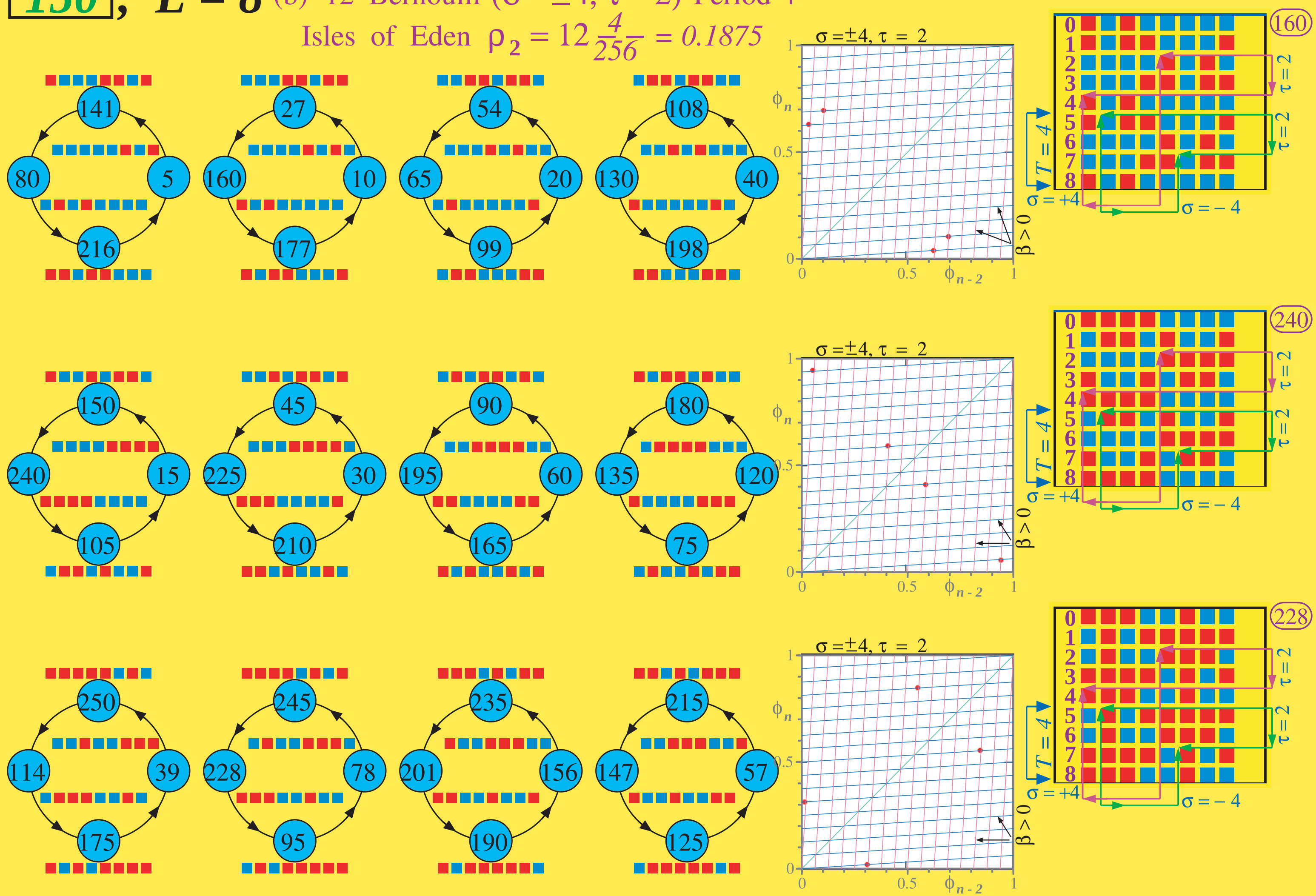

Gallery 150 - 12

150, ***L* = 8** (c) Period-1 Isles of Eden $\rho_3 = \frac{4}{256} = 0.015625$

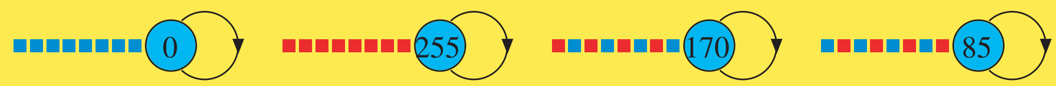

(d) 4 Bernoulli ($\sigma = \pm 2, \tau = 1, \beta < 0$) Period-2 Isles of Eden

$\rho_4 = 4\frac{2}{256} = 0.03125$

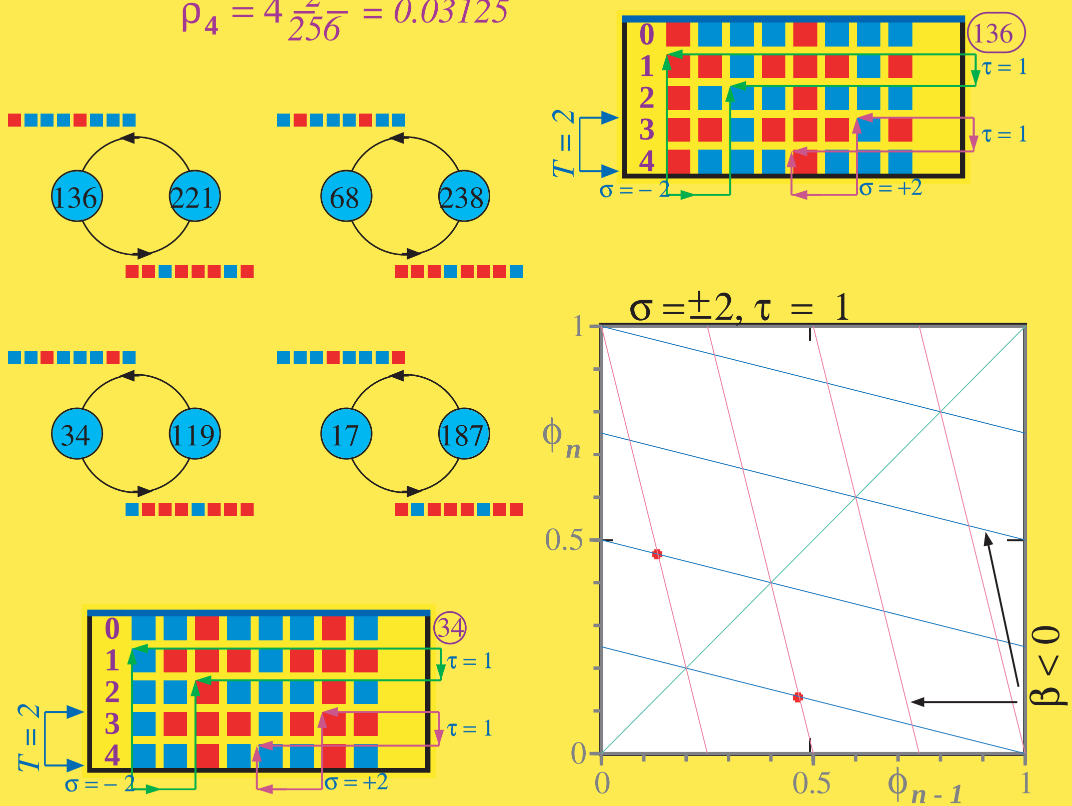

(e) Bernoulli ($\sigma = \pm 2, \tau = 1$)

Period-2 Isles of Eden

$\rho_5 = 2\frac{2}{256} = 0.015625$

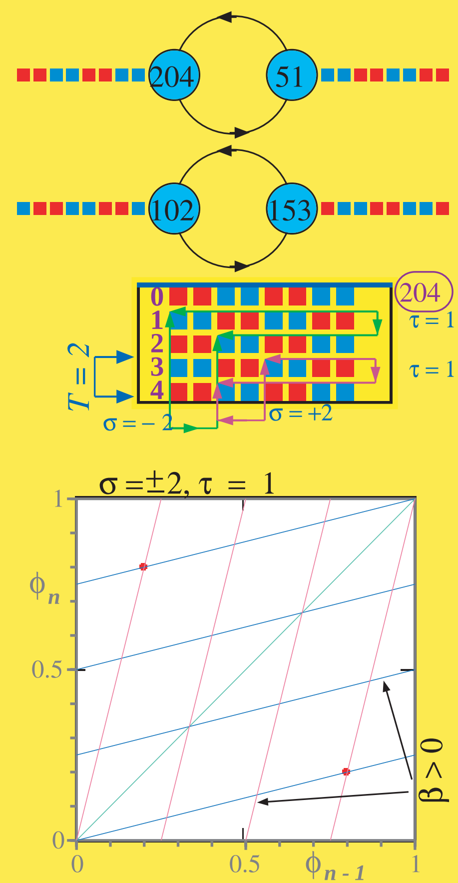

Gallery 150 - 13

2.4.10. *Highlights from Rule* $\boxed{150}$

The basin tree diagrams of Rule $\boxed{150}$ for $L = 3, 4, \ldots, 8$ are exhibited in Table 23. Following a detailed analysis of these diagrams, the qualitative properties of local rule $\boxed{150}$ extracted from basin-tree Galleries 150-1 to 150-13 of Table 23 are summarized below:

Summary of Qualitative properties of local rule $\boxed{150}$ extracted from Gallery 150 for Rule $\boxed{150}$

L	ID Number i	Number of Period-n attractors	Number of Period-n Isles of Eden	Period n	Bernoulli Parameters σ_1	τ_1	β_1	σ_2	τ_2	β_2	Robustness coefficient ρ
3	1	2		1	0	1	+				$\rho_1 = 1$
4	1		2	2	2	1	+	-2	1	+	$\rho_1 = 0.25$
	2		4	1	0	1	+				$\rho_2 = 0.25$
	3		4	2	2	1	−	-2	1	−	$\rho_3 = 0.5$
5	1		10	3	0	3	+				$\rho_1 = 0.9375$
	2		2	1	0	1	+				$\rho_2 = 0.0625$
6	1	2		1	0	1	+				$\rho_1 = 0.5$
	2	2		1	0	1	+				$\rho_2 = 0.5$
7	1		2	1	0	1	+				$\rho_1 = 0.015625$
	2		14	7	0	7	+				$\rho_2 = 0.765625$
	3		4	7	1	2	+	-1	2	+	$\rho_3 = 0.21875$
8	1		48	4	0	4	+				$\rho_1 = 0.75$
	2		12	4	4	2	+	-4	2	+	$\rho_2 = 0.1875$
	3		4	1	0	1	+				$\rho_3 = 0.015625$
	4		4	2	2	1	−	-2	1	−	$\rho_4 = 0.03125$
	5		2	2	2	1	+	-2	1	+	$\rho_5 = 0.015625$

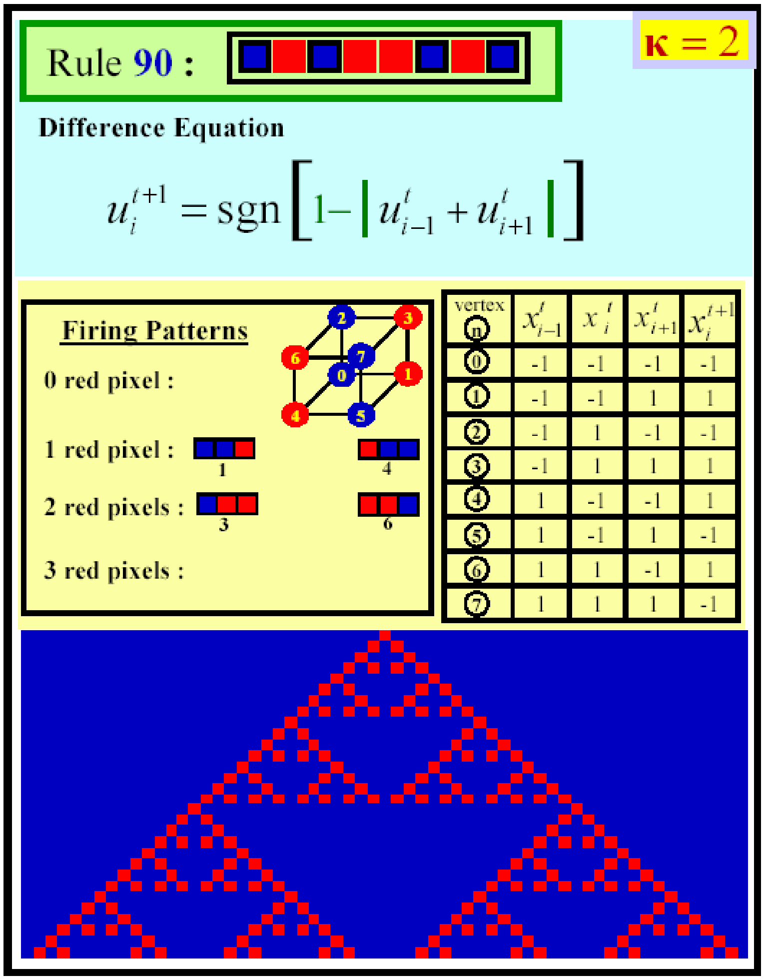

Fig. 2. Truth table, Boolean cube, Difference Equation, and space-time pattern of local rule $\boxed{90}$.

3. Global Analysis of Local Rule $\boxed{90}$

The *truth table*, *Boolean cube*, and "*Difference Equation*" defining the local rule $\boxed{90}$ along with a space-time pattern (with a single red-pixel initial state) exhibited in Table 5 of [Chua *et al.*, 2003] is reproduced in Fig. 2 for the reader's convenience. For this paper, it is more instructive to recast the Difference Equation defining $\boxed{90}$ into an *equivalent* difference equation involving only a *mod 2 addition* $\oplus$ (defined in Table 24).

Substituting $u_i = 2x_i - 1$ from Eq. (4) of [Chua *et al.*, 2005a] for u_i in the Difference Equation for $\boxed{90}$, we obtain

$$\begin{aligned} 2x_i^{t+1} - 1 &= \text{sgn}[1 - |2x_{i-1}^t + 2x_{i+1}^t - 2|] \\ &= \text{sgn}[1 - 2|x_{i-1}^t + x_{i+1}^t - 1|] \end{aligned} \quad (18)$$

Table 24. Table defining[8] $x_i \oplus x_j \triangleq x_i \, XOR \, x_j$.

$\oplus$	0	1
0	0	1
1	1	0

Simplifying Eq. (18) using Table 24, we obtain the following equivalent Difference Equation:

$$\text{Rule } \boxed{90} \quad \boxed{\begin{aligned} x_i^{t+1} &= (x_{i-1}^t + x_{i+1}^t) \bmod (2) \\ &= x_{i-1}^t \oplus x_{i+1}^t \end{aligned}} \quad (19)$$

[8]The *mod 2 operation* $x_i \oplus x_j$ between *two* binary variables is also called an *exclusive OR* operation in *mathematical logic*, and denoted by $x_i \oplus x_j \triangleq x_i \, XOR \, x_j$.

3.1. *Ru1e $\boxed{90}$ has no Isle of Eden*

A cursory glimpse at the basin-tree diagram of rule $\boxed{90}$ in Table 18 reveals that all bit strings converge to an *attractor* for $3 \leq L \leq 8$. We now prove this property is true for all L.

Theorem 1. *Rule $\boxed{90}$ does not have any* isle of Eden.

Proof. It follows from Eq. (19) that an arbitrary bit string

$$\boldsymbol{x}^t = (\boldsymbol{x}_0^t \quad \boldsymbol{x}_1^t \quad \boldsymbol{x}_2^t \quad \cdots \quad \boldsymbol{x}_{L-1}^t) \tag{20}$$

at time "t" is *linearly* related (mod 2) to its *image*

$$\boldsymbol{x}^{t+1} = (\boldsymbol{x}_0^{t+1} \quad \boldsymbol{x}_1^{t+1} \quad \boldsymbol{x}_2^{t+1} \quad \cdots \quad \boldsymbol{x}_{L-1}^{t+1}) \tag{21}$$

at time "$t+1$" via an $L \times L$ *circulant matrix* [Davis, 1979] $\boldsymbol{M}(\boxed{90})$, *henceforth called the local time-1 state transition matrix*:

$$\underbrace{\begin{bmatrix} x_0^{t+1} \\ x_1^{t+1} \\ x_2^{t+1} \\ x_3^{t+1} \\ \vdots \\ x_{L-2}^{t+1} \\ x_{L-1}^{t+1} \end{bmatrix}}_{\boldsymbol{x}^{t+1}} = \underbrace{\begin{bmatrix} 0 & 1 & 0 & 0 & 0 & \cdots & 1 \\ 1 & 0 & 1 & 0 & 0 & \cdots & 0 \\ 0 & 1 & 0 & 1 & 0 & \cdots & 0 \\ 0 & 0 & 1 & 0 & 1 & \cdots & 0 \\ \vdots & & & & \ddots & & \vdots \\ 0 & 0 & 0 & 0 & \cdots & 1 & 0 \\ 0 & 0 & 0 & 0 & \cdots & 0 & 1 \\ 1 & 0 & 0 & 0 & \cdots & 1 & 0 \end{bmatrix}}_{\boldsymbol{M}(\boxed{90})} \underbrace{\begin{bmatrix} x_0^t \\ x_1^t \\ x_2^t \\ x_3^t \\ \vdots \\ x_{L-2}^t \\ x_{L-1}^t \end{bmatrix}}_{\boldsymbol{x}^t} \tag{22}$$

where addition is mod (2) sum $\oplus$.

Note the *diagonal* elements of the circulant matrix $\boldsymbol{M}(\boxed{90})$ are all equal to *zero*. Observe also the elements directly below (resp. above) the diagonal of $\boldsymbol{M}(\boxed{90})$ are all equal to *one*. All other elements are zero, except for the top rightmost element, and the bottom leftmost elements, which are equal to *one*, respectively. It follows from this special structure that the *leftmost* column of $\boldsymbol{M}(\boxed{90})$ is equal to the *mod 2 sum* of the remaining L-1 columns. Since the columns of $\boldsymbol{M}(\boxed{90})$ are not *linearly independent*, mod 2, it follows that $\boldsymbol{M}$ does *not* have an inverse. Since the bit string $\boldsymbol{x}^{t+1}$ on the left side of Eq. (19) does not have a *unique preimage*, it follows that the bit string $\boldsymbol{x}^t$ is *not* an *isle of Eden* of $\boxed{90}$.

Since $\boldsymbol{x}^t$ is an arbitrary bit string, it follows that $\boxed{90}$ cannot possess an *isle of Eden* for any L. ■

3.2. *Period of Rule $\boxed{90}$ grows with L*

Since rule $\boxed{90}$ does *not* have isles of Eden, all bit strings of $\boxed{90}$ must converge to *period-T attractors* whose *period* "T" is bounded by

$$1 \leq T \leq T_{\max} \tag{23}$$

where $T_{\max} = 2^L$ as defined in Eq. (6). As an example, the period T of an attractor of $\boxed{90}$ is listed in Table 25 for $3 \leq L \leq 100$. Observe that the period T for *some* L (e.g. $L = 47, 49, 53$, etc.) is not listed in Table 25 because it is so large that it had exceeded the maximum simulation time allocated. A bit string belonging to one of the many period-T attractors for $3 \leq L \leq 25$ is given in Table 26. For example, the bit string listed for $L = 3$ corresponds to the third *period-1* attractor (out of 4) listed in Gallery 90-1 of Table 18. The bit string listed for $L = 5$ corresponds to node 6 of Gallery 90-3 of Table 18, out of five period-3 attractors. The bit string listed for $L = 6$ corresponds to node 30 in the fifth attractor shown on the left of Gallery 90-5. The bit string listed for $L = 7$ corresponds to node 68 in the top left attractor of $\boxed{90}$ shown on the top left of Gallery 90-7.

As examination of Table 25 shows that unlike the period-1 and period-2 local rules listed in Tables 7 and 8, and the period-3 local role $\boxed{62}$, which have a relatively small period, and independent of L, the period T of rule $\boxed{90}$ can increase at an *exponential* rate as a function of L, as depicted in Fig. 3. Such exponential growth of T as a function of L is a signature of all *complex Bernoulli* rules in Table 11, and *hyper-Bernoulli* rules in Table 12.

In spite of the very large values T of some period-T *attractors* of $\boxed{90}$, these periods are usually many orders of magnitude smaller than the upper bound $T_{\max}$ listed in Table 27 for $3 \leq L \leq 85$.[9] There exists, however, period T attractors whose period T approaches the upper bound $T_{\max}$. For example, Table 28 shows a period-504 bit string of an *isle of Eden* of rule $\boxed{45}$ for $L = 9$, which is almost as large as $T_{\max} = 2^9 = 512$! This example suggests that some of the empty slots in Tables 25 may never be filled.[10]

[9]It would take at least 105, 104, 783, 572 years for a 1 GHz PC to simulate all $T_{\max} = 2^L$ distinct bit strings!

[10]Rule $\boxed{45}$ will be studied in Part VIII where it is proved that *all* bit strings are *isles of Eden* if, and only if L is an *odd* number.

Table 25. Period "T" of attractors of local rule $\boxed{90}$ for $3 \le L \le 100$.

L	Attractor	L	Attractor	L	Attractor	L	Attractor	L	Attractor
1		21	*T* = *63*	41	*T* = *1023*	61		81	
2		22	*T* = *62*	42	*T* = *126*	62	*T* = *62*	82	*T* = *2046*
3	*T* = *1*	23	*T* = *2047*	43	*T* = *127*	63	*T* = *63*	83	
4	*T* = *1*	24	*T* = *8*	44	*T* = *124*	64	*T* = *1*	84	*T* = *252*
5	*T* = *3*	25	*T* = *1023*	45	*T* = *4095*	65	*T* = *63*	85	*T* = *255*
6	*T* = *2*	26	*T* = *126*	46	*T* = *4094*	66	*T* = *62*	86	*T* = *254*
7	*T* = *7*	27	*T* = *511*	47		67		87	
8	*T* = *1*	28	*T* = *28*	48	*T* = *16*	68	*T* = *60*	88	*T* = *248*
9	*T* = *7*	29	*T* = *16383*	49		69		89	*T* = *2047*
10	*T* = *6*	30	*T* = *30*	50	*T* = *2046*	70	*T* = *8190*	90	*T* = *8190*
11	*T* = *31*	31	*T* = *31*	51	*T* = *255*	71		91	*T* = *4095*
12	*T* = *4*	32	*T* = *1*	52	*T* = *252*	72	*T* = *56*	92	*T* = *8188*
13	*T* = *63*	33	*T* = *31*	53		73	*T* = *511*	93	*T* = *1023*
14	*T* = *14*	34	*T* = *30*	54	*T* = *1022*	74	*T* = *174762*	94	
15	*T* = *15*	35	*T* = *4095*	55		75		95	
16	*T* = *1*	36	*T* = *28*	56	*T* = *56*	76	*T* = *2044*	96	*T* = *32*
17	*T* = *15*	37	*T* = *87381*	57	*T* = *511*	77		97	
18	*T* = *14*	38	*T* = *1022*	58	*T* = *32766*	78	*T* = *8190*	98	
19	*T* = *511*	39	*T* = *4095*	59		79		99	*T* = *32767*
20	*T* = *12*	40	*T* = *24*	60	*T* = *60*	80	*T* = *48*	100	*T* = *4092*

3.3. *Global state-transition formula for rule* $\boxed{90}$

The state transition formula given in Fig. 2 and Eq. (19) for rule $\boxed{90}$ is *local in time* in the sense that it generates from a bit string $\boldsymbol{x}^t = (x_0^t \; x_1^t \; x_2^t \; \cdots \; x_{L-1}^t)$ at time "t" the next bit string $\boldsymbol{x}^{t+1} = (x_0^{t+1} \; x_1^{t+1} \; x_2^{t+1} \; \cdots \; x_{L-1}^{t+1})$ at time "$t+1$". Our next theorem gives an explicit formula which is *global in time* in the sense that it generates a bit string $\boldsymbol{x}_0^n = (x_0^n \; x_1^n \; x_2^n \; \cdots \; x_{L-1}^n)$ at any future time $n > t$.

Theorem 2. Global State-Transition Formula for $\boxed{90}$.

Each pixel x_i^n at time $n > t$ is determined from "$n+1$" initial pixels $x_{i-n}^0, x_{i-n+2}^0, \ldots, x_{i+n-2}^0, x_{i+n}^0$ at $t = 0$ via the binomial *formula.*

$$\boxed{x_i^n = \sum_{k=0}^{n} \frac{n!}{k!(n-k)!} \bullet x_{i-n+2k}^0 \quad \mathrm{mod}\ (2)} \tag{24}$$

Proof. Apply *mathematical induction* as follow:

(a) $n = 1$

Applying $n = 1$ in Eq. (24), we obtain[11]

$$x_i^1 = x_{i-1}^0 + x_{i+1}^0 \quad \mathrm{mod}\ (2) \tag{25}$$

which is Eq. (19) for $t = 0$.

[11]Recall the factorial notation $0! \triangleq 1$.

Table 26. Bit strings for generating a period-T attractor of Rule $\boxed{90}$.

L	T	A bit string on a Period-T attractor
3	1	
4	1	
5	3	
6	2	
7	7	
8	1	
9	7	
10	6	
11	31	
12	4	
13	63	
14	14	
15	15	
16	1	
17	15	
18	14	
19	511	
20	12	
21	63	
22	62	
23	2047	
24	8	
25	1023	

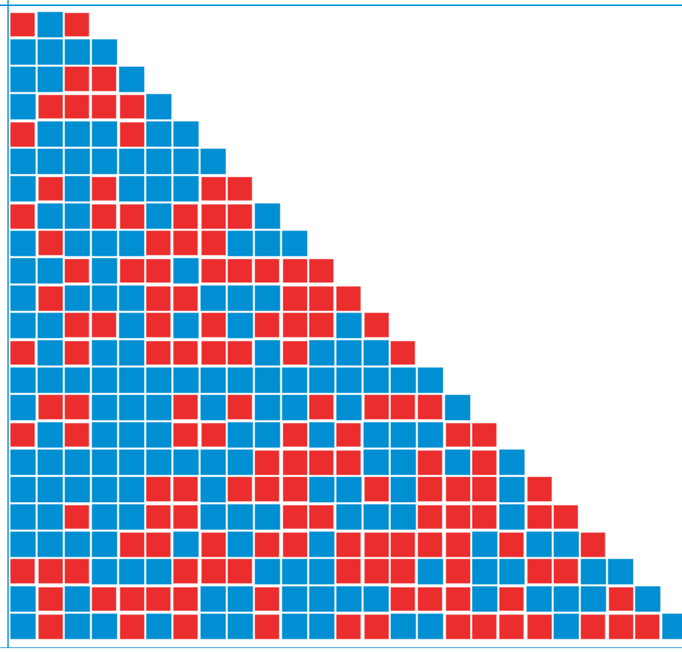

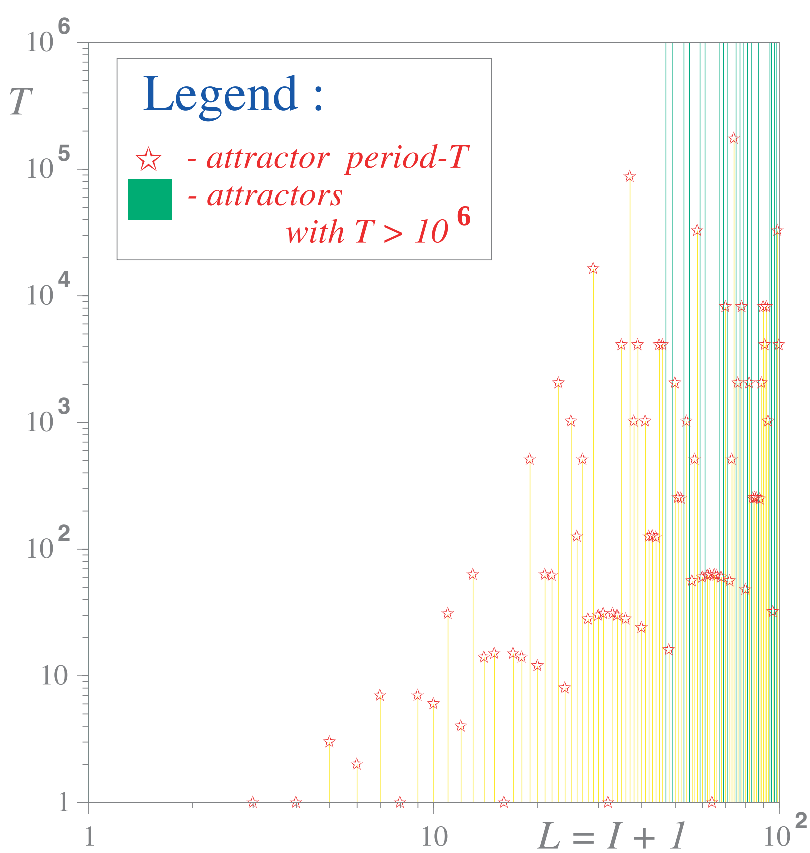

Fig. 3. Dependence of the period "T" of attractor of rule $\boxed{90}$ as a function of L (in logarithmic scale).

Table 27. The upper bound $T_{\max}$ of the period "T" as function of L for $3 \le L \le 85$.

L	$T_{max} = 2^L$
3	8
4	16
5	32
6	64
7	128
8	256
9	512
10	1024
11	2048
12	4096
13	8192
14	16384
15	32768
16	65536
⋮	⋮
85	38685626227668133590597632

(b) Assume Eq. (24) is true for $n = m$ (*induction hypothesis*); namely,

$$x_i^m = \sum_{k=0}^{m} \frac{m!}{k!(m-k)!} \bullet x^0_{i-m+2k} \quad \mathrm{mod}\ (2) \tag{26}$$

We must show that incrementing "m" to "$m+1$" in Eq. (26) gives Eq. (24) with $n = m+1$.

Substituting Eq. (26) to Eq. (19), we obtain

$$\begin{aligned} x_i^{m+1} &= x^m_{i-1} + x^m_{i+1} \quad \mathrm{mod}\ (2) \\ &= \sum_{k=0}^{m} \frac{m!}{k!(m-k)!} x^0_{(i-1)-m+2k} \\ &\quad + \sum_{k=0}^{m} \frac{m!}{k!(m-k)!} x^0_{(i+1)-m+2k} \quad \mathrm{mod}\ (2) \end{aligned} \tag{27}$$

Changing symbol "m" on the right-hand side of Eq. (27) to $m'-1$ gives

$$\begin{aligned} &\sum_{k=0}^{m'-1} \frac{(m'-1)!}{k!(m'-1-k)!} x^0_{i-m'+2k} \\ &\quad + \sum_{k=0}^{m'-1} \frac{(m'-1)!}{k!(m'-1-k)!} x^0_{i-m'+2k+2} \quad \mathrm{mod}\ (2) \end{aligned} \tag{28}$$

Changing symbol k in the second summation terms in Eq. (28) to $k'-1$ gives

$$\begin{aligned} &\sum_{k=0}^{m'-1} \frac{(m'-1)!}{k!(m'-1-k)!} x^0_{i-m'+2k} \\ &\quad + \sum_{k'=1}^{m'} \frac{(m'-1)!}{(k'-1)!(m'-k')!} x^0_{i-m'+2k'} \end{aligned} \tag{29}$$

Changing the dummy index k' in Eq. (29) back to k, we obtain

$$\left[\sum_{k=0}^{m'-1} \frac{(m'-1)!}{k!(m'-1-k)!} + \sum_{k=1}^{m'} \frac{(m'-1)!}{(k-1)!(m'-k)!}\right] \bullet x^0_{i-m'+2k} \tag{30}$$

The terms inside the bracket can be simplified by observing for $k = 1$ to $m'-1$, we have

$$\begin{aligned} &\frac{(m'-1)!}{k!(m'-1-k)!} + \frac{(m'-1)!}{(k-1)!(m'-k)!} \\ &\quad = \frac{(m'-1)!}{(k-1)!(m'-1-k)!}\left[\frac{1}{k} + \frac{1}{(m'-k)}\right] \\ &\quad = \frac{(m'-1)!}{(k-1)!(m'-1-k)!}\left[\frac{(m'-k)+k}{k(m'-k)}\right] \\ &\quad = \frac{m'!}{k!(m'-k)!} \end{aligned} \tag{31}$$

Moreover, when $k = 0$ and $k = m'$, Eq. (31) gives the same value as the first term on the left of Eq. (30), and the last term on the right of Eq. (30), respectively. Substituting back $m = m'-1$ in Eq. (31), and making use of Eqs. (27)–(31), we obtain

$$x_i^{m+1} = \sum_{k=0}^{m+1} \frac{(m+1)!}{k!(m+1-k)!} \bullet x^0_{i-(m+1)+2k} \quad \mathrm{mod}\ (2) \tag{32}$$

which is identical to incrementing m in the *induction hypothesis* (26) to $m+1$. ■

Table 29 gives the global state-transition formula (24) of rule $\boxed{90}$ for $n = 1, 2, 3, 4$ and 5. Observe that the coefficients $\binom{n}{k}$ for each time $n \ge 1$ is identical to the binomial coefficients in the expansion of $(x+y)^n$, as listed in Table 30 for $n = 1, 2, \ldots, 11$. These binomial coefficients are repackaged in Table 31 into the form of a Pascal's triangle where each coefficient under the pyramid is obtained by adding adjacent left and right coefficients above it.

Table 28. The period of the following isle of Eden for rule $\boxed{45}$ is $T = 504$, which is equal almost to $T_{\max} = 512$.

$\boxed{45}$, $L = 9$

(a) Bernoulli

$(\sigma = -2, \tau = 56)$

Period-504

Isle of Eden:

$\rho_1 = \frac{504}{512} = 0.984375$

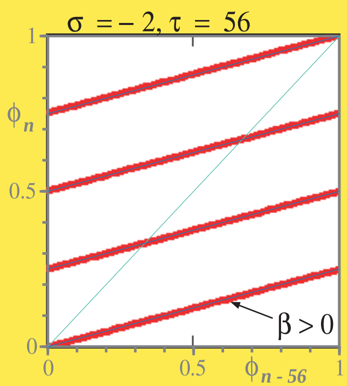

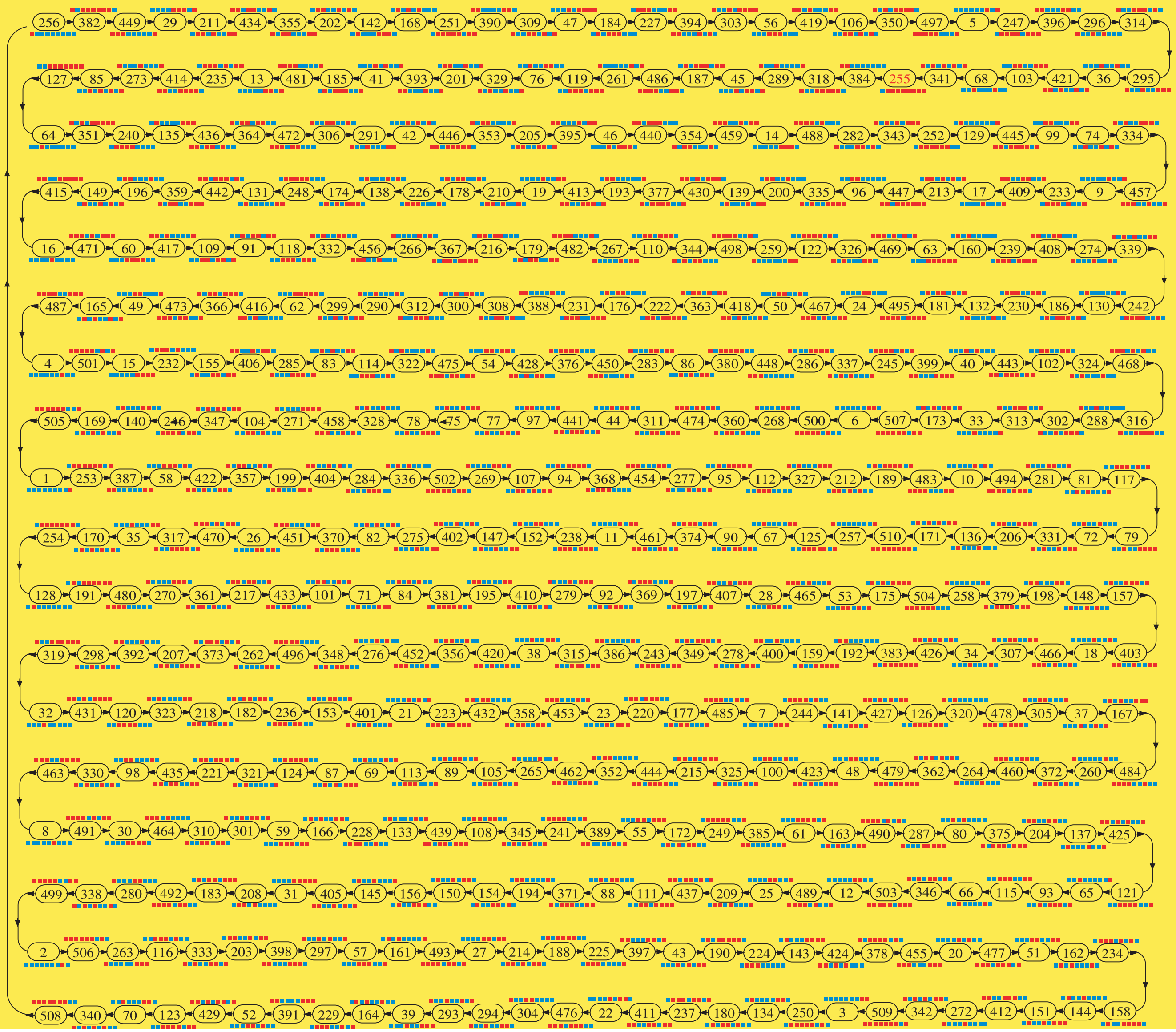

Table 29. Global state-transition formula for rule $\boxed{90}$ for $1 \le n \le 5$.

n	$x_i^n = \sum_{k=0}^{n} \frac{n!}{k!(n-k)!} \cdot x_{i-n+2k}^0 \quad \textbf{mod}(\,\mathbf{2}\,)$
1	$x_i^1 = x_{i-1}^0 + x_{i+1}^0 \quad \textbf{mod}(\,\mathbf{2}\,)$
2	$x_i^2 = x_{i-2}^0 + 2x_i^0 + x_{i+2}^0 \quad \textbf{mod}(\,\mathbf{2}\,)$
3	$x_i^3 = x_{i-3}^0 + 3x_{i-1}^0 + 3x_{i+1}^0 + x_{i+3}^0 \quad \textbf{mod}(\,\mathbf{2}\,)$
4	$x_i^4 = x_{i-4}^0 + 4x_{i-2}^0 + 6x_i^0 + 4x_{i+2}^0 + x_{i+4}^0 \quad \textbf{mod}(\,\mathbf{2}\,)$
5	$x_i^5 = x_{i-5}^0 + 5x_{i-3}^0 + 10x_{i-1}^0 + 10x_{i+1}^0 + 5x_{i+3}^0 + x_{i+5}^0 \quad \textbf{mod}(\,\mathbf{2}\,)$
$\cdots$	$\cdots$

Table 30. Table of $\binom{n}{k} \triangleq n!/k!\,(n-k)!$, $n = 1, 2, \ldots, 11$, $k = 0, 1, 2, \ldots, 11$.

n	k											
	0	1	2	3	4	5	6	7	8	9	10	11
1	1	1										
2	1	2	1									
3	1	3	3	1								
4	1	4	6	4	1							
5	1	5	10	10	5	1						
6	1	6	15	20	15	6	1					
7	1	7	21	35	35	21	7	1				
8	1	8	28	56	70	56	28	8	1			
9	1	9	36	84	126	126	84	36	9	1		
10	1	10	45	120	210	252	210	120	45	10	1	
11	1	11	55	165	330	462	462	330	165	55	11	1

Table 31. Binomial coefficients $\binom{n}{k}$ repackaged into a Pascal's triangle.

Pascal's Triangle

1
1 1
1 2 1
1 3 3 1
1 4 6 4 1
1 5 10 10 5 1
1 6 15 20 15 6 1
1 7 21 35 35 21 7 1
1 8 28 56 70 56 28 8 1
⋮

Taking the "*mod 2 equivalent*" of each coefficient in Table 29, we obtain the more compact but equivalent expansion in Table 32 where all nonzero terms correspond to those in Table 29 with "*odd number*" coefficients. The equivalent mod 2 coefficients are repackaged in Table 33. Observe that Table 33 can be obtained from Table 31 by replacing each odd (respectively, even) coefficient in Table 31 by a *one* (respectively, a *zero*). If we fill in the missing slot in each row of the mod 2 Pascal's triangle, we would obtain the pyramidal "fractal" space-time pattern of rule $\boxed{90}$ in Table 34, which is identical to that shown in the bottom of Fig. 2, where the initial configuration consists of a single red bit at the center, as in [Wolfram, 2002].

Example 1. Table 35 shows the *space-time pattern* obtained from the *global* state-transition formula of rule $\boxed{90}$ in (a) when the initial configuration consists of a single red bit at the center. The corresponding pattern obtained from the *local* state-transition formula is shown in (b). They are identical, as expected. The minor differences in the graphics and color are due to the differences in the softwares used to generate these patterns.

Example 2. Table 36 shows the corresponding results when the initial configuration consists of a string of *random* bits.

3.4. *Periodicity constraints of Rule* $\boxed{90}$

Theorem 1 implies that all bit strings of rule $\boxed{90}$ must converge to a period-T attractor, where $T \le T_{\max} \le 2^L$. We will prove in this subsection that for finite length $L \triangleq I+1$, the period T must satisfy certain constraints. Such *periodicity constraints* are useful on many occasions, such as verifying whether certain periodic orbit can exist, or to generate new periodic orbits, etc. The proof of many of these results depend on the following easily

Table 32. Compact global state-transition formula for rule $\boxed{90}$ for $1 \le n \le 5$.

n	$x_i^n = \sum_{k=0}^{n} \frac{n!}{k!(n-k)!} \cdot x_{i-n+2k}^0 \quad \mathbf{mod(2)}$
1	$x_i^1 = x_{i-1}^0 + x_{i+1}^0 \quad \mathbf{mod(2)}$
2	$x_i^2 = x_{i-2}^0 + x_{i+2}^0 \quad \mathbf{mod(2)}$
3	$x_i^3 = x_{i-3}^0 + x_{i-1}^0 + x_{i+1}^0 + x_{i+3}^0 \quad \mathbf{mod(2)}$
4	$x_i^4 = x_{i-4}^0 + x_{i+4}^0 \quad \mathbf{mod(2)}$
5	$x_i^5 = x_{i-5}^0 + x_{i-3}^0 + x_{i+3}^0 + x_{i+5}^0 \quad \mathbf{mod(2)}$
...	...

Table 33. Mod 2 binomial coefficients $\binom{n}{k}$ repackaged into a mod 2 Pascal's triangle.

Mod 2 Pascal's Triangle

1
1 1
1 0 1
1 1 1 1
1 0 0 0 1
1 1 0 0 1 1
1 0 1 0 1 0 1
1 1 1 1 1 1 1 1
1 0 0 0 0 0 0 0 1
⋮

verifiable identities:

Binomial Coefficient Lemma. *If* $n = 2^m$, *where* $m \geq 2$, *then the following identities hold*:

(i) $\binom{n-1}{k} = 1 \mod (2), \quad \text{for } k = 0, 1, 2, \ldots, n-1$ (33)

(ii) $\binom{n}{k} = \begin{cases} 0 \mod (2), & \text{for } k = 1, 2, \ldots, n-1 \\ 1 \mod (2), & \text{for } k = 0, n \end{cases}$ (34)

(iii) $\binom{n+1}{k} = \begin{cases} 0 \mod (2), & \text{for } k = 2, 3, \ldots, n-1 \\ 1 \mod (2), & \text{for } k = 0, 1, n, n+1 \end{cases}$ (35)

where

$$\binom{n}{k} \triangleq \frac{n!}{k!(n-k)!} \tag{36}$$

Theorem 3. Periodicity Condition: $L = 2^m$.
For $L = 2^m$, $m = 2, 3, 4, \ldots$, *rule* $\boxed{90}$ *has a* global period-1 attractor Γ; *namely*,

$$\boldsymbol{x}(\Gamma) = \underbrace{(0 \quad 0 \quad 0 \quad \cdots \quad 0)}_{L=2^m} \tag{37}$$

All bit strings not belonging to the attractor Γ converge to Γ in at most 2^{m-1} iterations.

Proof. Let $n = 2^{m-1}$ in the global state-transition formula (24). It follows from Eqs. (33) and (36) that

$$\frac{n!}{k!(n-k)!} \mod (2) = \begin{cases} 0, & \text{for } k = 1, 2, \ldots, n-1 \\ 1, & \text{for } k = 0, n = 2^{m-1} \end{cases} \tag{38}$$

It follows from Eq. (38) and the global state-transition formula (24) that x_i^n contains only two nonzero terms; namely, the leftmost and the

Table 34. Space-time pattern of the Pascal triangle fractal generated by rule $\boxed{90}$.

n	-8	-7	-6	-5	-4	-3	-2	-1	0	1	2	3	4	5	6	7	8
1	0	0	0	0	0	0	0	1	0	1	0	0	0	0	0	0	0
2	0	0	0	0	0	0	1	0	0	0	1	0	0	0	0	0	0
3	0	0	0	0	0	1	0	1	0	1	0	1	0	0	0	0	0
4	0	0	0	0	1	0	0	0	0	0	0	0	1	0	0	0	0
5	0	0	0	1	0	1	0	0	0	0	0	1	0	1	0	0	0
6	0	0	1	0	0	0	1	0	0	0	1	0	0	0	1	0	0
7	0	1	0	1	0	1	0	1	0	1	0	1	0	1	0	1	0
8	1	0	0	0	0	0	0	0	0	0	0	0	0	0	0	0	1

Table 35. Space-time pattern of the rule $\boxed{90}$ with red central bit initial configuration: (a) from global state-transition formula; (b) from local state-transition formula.

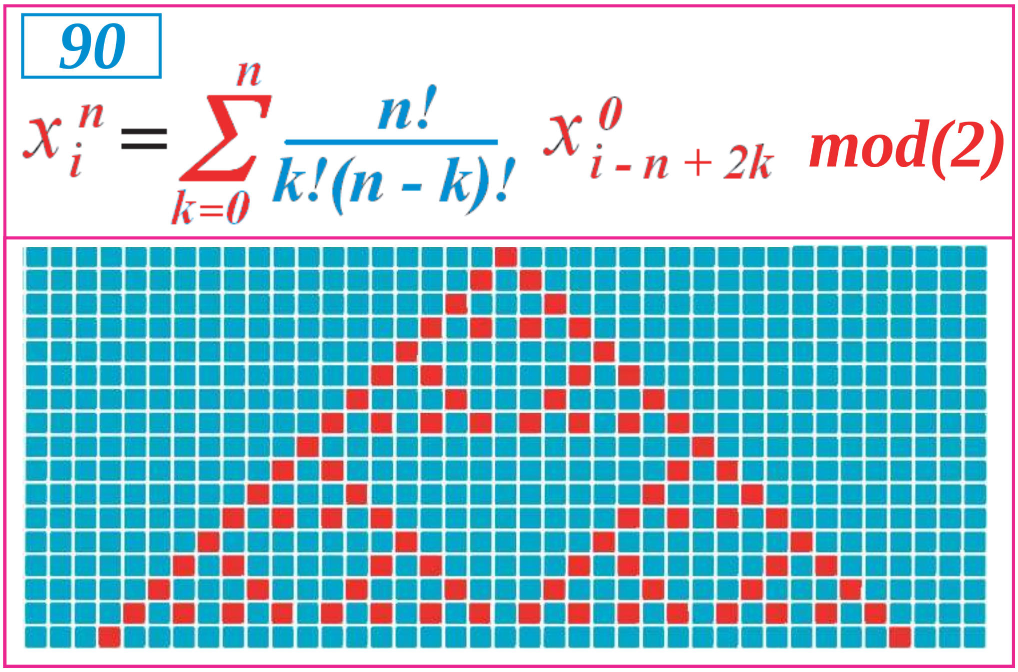

(a)

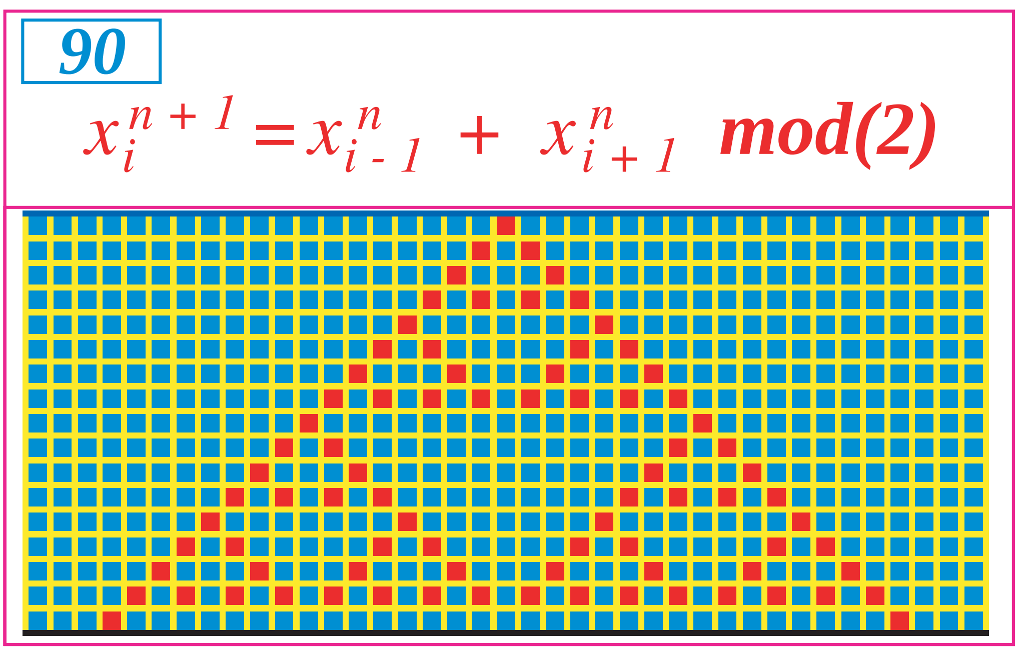

(b)

Table 36. Space-time pattern of the rule $\boxed{90}$ obtained from random initial state generated by: (a) global state-transition formula; (b) local state-transition formula.

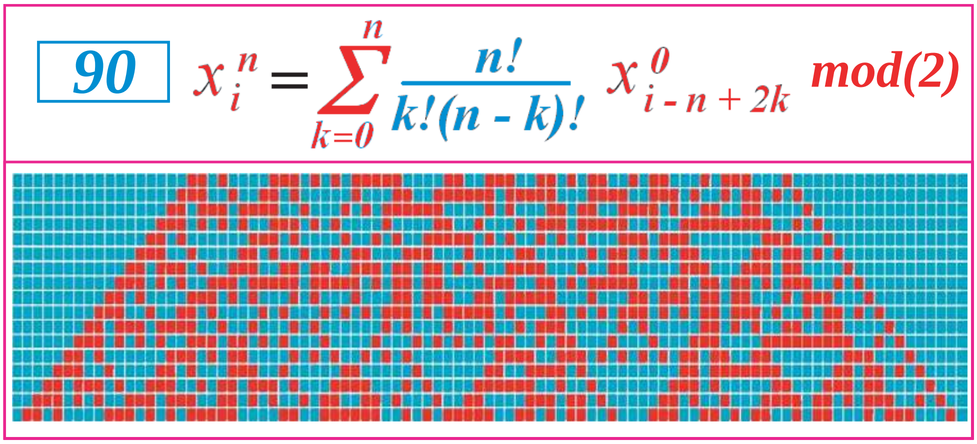

(a)

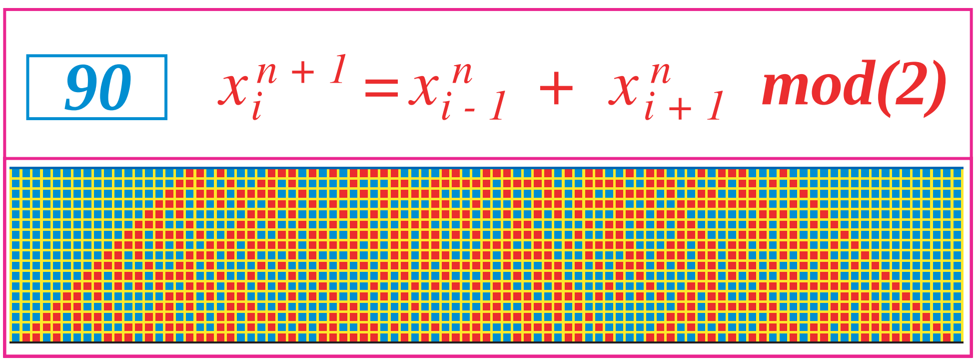

(b)

rightmost terms. Hence,

$$x_i^n = x_{i-n}^0 + x_{i+n}^0 \mod (2) \tag{39}$$

where $n = 2^{m-1}$. Substituting $i = n = 2^{m-1}$ in Eq. (39), we obtain

$$\begin{aligned} x_i^n &= x_{n-n}^0 + x_{n+n}^0 \mod (2) \\ &= x_0^0 + x_{2n}^0 \mod (2) \\ &= x_0^0 + x_{2m}^0 \mod (2) \\ &= x_0^0 + x_L^0 \mod (2) \\ &= 2x_0 \mod (2) \\ &= 0 \end{aligned} \tag{40}$$

because $x_0^0 = x_L$.

Since x_i^0 is arbitrary, it follows that all bit strings must converge to Eq. (7) in at most 2^{m-1} iterations. ■

Corollary to Theorem 2.
A bit string

$$\boldsymbol{x}^{\mathbf{0}} = (x_0^0 \quad x_1^0 \quad x_2^0 \quad \cdots \quad x_{L-1}^0) \tag{41}$$

of length $L = I + 1$ (*under* periodic boundary condition) *is a* period-n attractor *of local rule* $\boxed{90}$ if, and only *if*, *the* periodicity condition

$$\boxed{\begin{aligned} x^n_{i \bmod (L)} &= x_i^0 \\ &= \sum_{k=0}^{n} \frac{n!}{k!(n-k)!} \\ &\quad \bullet\, x^0_{((i-n+2k) \bmod (L))} \qquad \mod (2) \end{aligned}} \tag{42}$$

is satisfied *for all* i.

Proof. Follows directly from *Theorem 2* and the periodic boundary condition. ■

The *periodicity constraint* equation (42) is applicable to *any* period-n attractor of rule $\boxed{90}$.

The "**mod** ($\boldsymbol{L}$)" operation attached to the subscript index of x^0 is just a mathematically precise algorithm for implementing the *periodic boundary conditions*. It is also mathematically equivalent to *concatenating* replicas of the L-bit string $x_0\ x_1\ x_2\ \cdots\ x_I$ *ad infinitum*; namely,

$$\cdots \underbrace{x_0\quad x_1\quad x_2\quad \cdots\quad x_I}_{L \text{ bits}}\ \underbrace{x_0\quad x_1\quad x_2\quad \cdots\quad x_I}_{L \text{ bits}}\ \underbrace{x_0\quad x_1\quad x_2\quad \cdots\quad x_I}_{L \text{ bits}} \cdots \tag{43}$$

where $L = I + 1$.

In the special case where

$$n = 2^m - 1 \tag{44}$$

all binomial coefficients in Eq. (42) are equal to *unity*, in view of the Binomial Coefficient Lemma; namely,

$$\boxed{\frac{n!}{k!(n-k)!} \bmod (2) = 1, \quad k = 0, 1, 2, \ldots, n} \tag{45}$$

Equation (45) is obtained by substituting $n + 1 = 2^m$ from Eq. (44) in place of n in Eq. (33):

$$\binom{(n+1)-1}{k} = 1 \bmod (2), \quad k = 0, 1, 2, \ldots, n \tag{46}$$

Substituting Eq. (46) into Eq. (42), we obtain the following simplified periodicity constraint:

$$\begin{array}{c}\text{Valid if} \\ n = 2^m - 1\end{array} \boxed{\begin{aligned} & x^n_{i \bmod (L)} \\ & = x_i^0 \\ & = \sum_{k=0}^{2^m-1} x^0_{((i-n+2k) \bmod (L))} \quad \bmod (2) \\ & \qquad\qquad\qquad\qquad \text{for all } i \end{aligned}} \tag{47}$$

If we impose the additional constraint $L = n = 2^m - 1$, then we obtain the following simple method for finding period-$(2^m - 1)$ attractors:

Theorem 4. Periodicity Condition: $L = 2^m - 1$. *Rule* $\boxed{90}$ *has a* period-n attractor *where* $n = 2^m - 1$ and $L = 2^m - 1$ if, and only if,

$$\begin{array}{c}\text{Valid for} \\ n = 2^m - 1 \\ L = 2^m - 1\end{array} \boxed{\sum_{i=0}^{L-1} x_i^0 \bmod (2) = 0} \tag{48}$$

Proof. Let us list all terms from Eq. (47) as follows:

$$\begin{aligned} x^0_{i \bmod (L)} = x^0_{((i-n) \bmod (L))} + x^0_{((i-n+2) \bmod (L))} \\ + \cdots + x^0_{((i+n-2) \bmod (L))} \\ + x^0_{((i+n) \bmod (L))} \quad \bmod (2) \end{aligned} \tag{49}$$

Since "i" is an arbitrary index in Eq. (49), let it be "n". Substituting $i = n$ in Eq. (49), we obtain

$$\begin{aligned} x_0^0 = x_0^0 + x_2^0 + \cdots + \underbrace{x^0_{n-1}}_{n-1=2^m-2<L} + x^0_{((n+1) \bmod (L))} \\ + \cdots + x^0_{((2n-2) \bmod (L))} + x^0_{((2n) \bmod (L))} \\ \bmod (2) \end{aligned} \tag{50}$$

Observe next that for $n = L = 2^m - 1$, we have

$$(2n) \bmod (L) = 0, \quad ((2n-2) \bmod (L)) = L - 2,$$
$$((n+1) \bmod (L)) = 1.$$

Observe also that $L = 2^m - 1$ implies that $L - 2$, $L - 4$, etc. are *odd* numbers. Substituting these mod (L) equivalent indices into Eq. (50), we obtain

$$\begin{aligned} x_0^0 = x_0^0 + x_2^0 + \cdots + x^0_{L-1} + x_1^0 + x_3^0 \\ + \cdots + x^0_{L-2} + x_0^0 \quad \bmod (2) \end{aligned} \tag{51}$$

Observe that whereas the first x_0^0 on the right-hand side of Eq. (51) comes from the corresponding first term of Eq. (50), the last x_0^0 of Eq. (51) comes from the last bit $x^0_{((2n) \bmod (L))} = x_0^0$ of Eq. (50). Rearranging the terms in increasing subscript order in Eq. (51), we obtain

$$\begin{aligned} x_0^0 = x_0^0 + x_0^0 + x_1^0 + x_2^0 + \cdots + x^0_{L-2} \\ + x^0_{L-1} \bmod (2) \end{aligned} \tag{52}$$

Substituting $(x_0^0 + x_0^0) \bmod (2) = 0$ in Eq. (52), we obtain

$$\begin{aligned} x_0^0 = x_1^0 + x_2^0 + x_3^0 + \cdots + x^0_{L-2} \\ + x^0_{L-1} \bmod (2) \end{aligned} \tag{53}$$

By adding the bit x_0^0 to both sides of Eq. (53), we obtain

$$\begin{aligned} \underbrace{x_0^0 + x_0^0}_{0 \bmod (2)} = x_0^0 + x_1^0 + x_2^0 + \cdots + x^0_{L-2} \\ + x^0_{L-1} \bmod (2) \end{aligned} \tag{54}$$

It follows from Eq. (54) that

$$\sum_{i=0}^{L-1} x_i^0 \bmod (2) = 0 \tag{55}$$

■

Our next theorem shows that *the same* periodicity condition in Eq. (45) of Theorem 4 also holds for a *different* $L = 2^m + 1$ but for the same $n = 2^m - 1$.

Theorem 5. Periodicity Condition: $L = 2^m + 1$. *Rule* $\boxed{90}$ *has a* period-n attractor where $n = 2^m - 1$ and $L = 2^m + 1$ if, and only if,

$$\begin{array}{c} \text{Valid for} \\ n = 2^m - 1 \\ L = 2^m + 1 \end{array} \quad \boxed{\sum_{i=0}^{L-1} x_i^0 \bmod (2) = 0} \tag{56}$$

Proof. Since $n = 2^m - 1$ remains the same as in Theorem 4, Eqs. (47) and (49) remain unchanged. Substituting $i = n$ in Eq. (49), we obtain[12]

$$\begin{aligned} x_0^0 = x_0^0 + x_2^0 + \cdots + x_{n-1}^0 + \underbrace{x_{n+1}^0}_{n+1=2^m<L} \\ + x^0_{((n+3)\bmod(L))} + \cdots \\ + x^0_{((2n-2)\bmod(L))} \\ + x^0_{((2n)\bmod(L))} \quad \bmod (2) \end{aligned} \tag{57}$$

Observe next that for $L = 2^m+1$, we have $L = n+2$. Hence, unlike in Eq. (51) we must now replace L in mod (L) by $n + 2$ to obtain $(2n \bmod (n + 2)) = n - 2$, $((2n - 2) \bmod (n + 2)) = n - 4, \ldots, ((n + 3) \bmod (n + 2)) = 1$. Equation (57) now reduces to

$$\begin{aligned} x_0^0 &= x_0^0 + x_2^0 + \cdots + x_{n-1}^0 + x_{n+1}^0 + x_1^0 + x_3^0 \\ &\quad + \cdots + x_{n-4}^0 + x_{n-2}^0 \bmod (2) \\ &= x_0^0 + x_1^0 + x_2^0 + x_3^0 + \cdots + x_{n-2}^0 + x_{n-1}^0 \\ &\quad + x_{n+1}^0 \bmod (2) \end{aligned} \tag{58}$$

Observe that the term x_n^0 is missing from Eq. (58). Replacing n by $n = L - 2$ in Eq. (58) and by choosing $i = L - 2$ in Eq. (47), we obtain

$$\begin{aligned} x_{L-2}^0 = x_0^0 + x_1^0 + x_2^0 + \cdots + x_{L-4}^0 \\ + x_{L-3}^0 + x_{L-1}^0 \bmod (2) \end{aligned} \tag{59}$$

Adding the term $x_{L-2}^0 = x_{I-1}^0$ to both sides of Eq. (59), we obtain

$$\begin{aligned} \underbrace{x_{L-2}^0 + x_{L-2}^0}_{0 \bmod(2)} = x_0^0 + x_1^0 + x_2^0 + \cdots + x_{L-4}^0 + x_{L-3}^0 \\ + x_{L-2}^0 + x_{L-1}^0 \bmod (2) \end{aligned} \tag{60}$$

Hence, we have

$$\sum_{i=0}^{L-1} x_i^0 \bmod (2) = 0 \qquad \blacksquare$$

Corollary 1 to Theorems 4 and 5. *The total number of* red *pixels in the period* $2^m - 1$ *attractors of Theorems 4 and 5, must be an* even *number.*

Corollary 2 to Theorem 3, 4, 5. *Theorems 3–5 hold also for* infinite *bit strings* ($L \to \infty$).

Recap. Theorems 3–5 give necessary and sufficient conditions for rule $\boxed{90}$ to have the following *period-n attractors*:

Theorem 3			
	$n = 1$	and	$L = 2^m$
Theorem 4			
	$n = 2^m - 1$	and	$L = 2^m - 1$
Theorem 5			
	$n = 2^m - 1$	and	$L = 2^m + 1$

As illustrations of the applications of these *analytically* derived results, let us examine the basin tree diagrams exhibited in Tables 14–23.

Applications of Theorem 3

1. $m = 2$, $L = 2^m = 4$

Gallery 90-2 shows all bit strings converge to the unique global attractor ⓪, as predicted by Theorem 3.

2. $m = 3$, $L = 2^m = 8$

Gallery 90-9 shows all bit strings converge to the global attractor ⓪, as predicted by Theorem 3.

Applications of Theorem 4

$$m = 3, \quad n = 2^m - 1 = 7, \quad L = 2^m - 1 = 7$$

Galleries 90-6, 90-7 and 90-8 show nine period-7 attractors as predicted. Observe the number of red pixels in all attractors is an even number, as predicted. The only other attractor is a *period-1 attractor*, ⓪, which qualifies also as a period-7 attractor, with "0" red pixels, an even number, as predicted.

Applications of Theorem 5

$$m = 2, \quad n = 2^m - 1 = 3, \quad L = 2^m + 1 = 5$$

Gallery 90-3 shows five period-3 attractors, all have only orbits with an even number of red pixels. The only other attractor is a *period-1 attractor*, ⓪, which qualifies also as a period-3 attractor. In this case, there are no red bits, which is an *even* number, as predicted.

[12]Observe that unlike Eq. (50) where $n - 1 = 2^m - 2 < L$, we now have $n + 1 = 2^m < 1$.

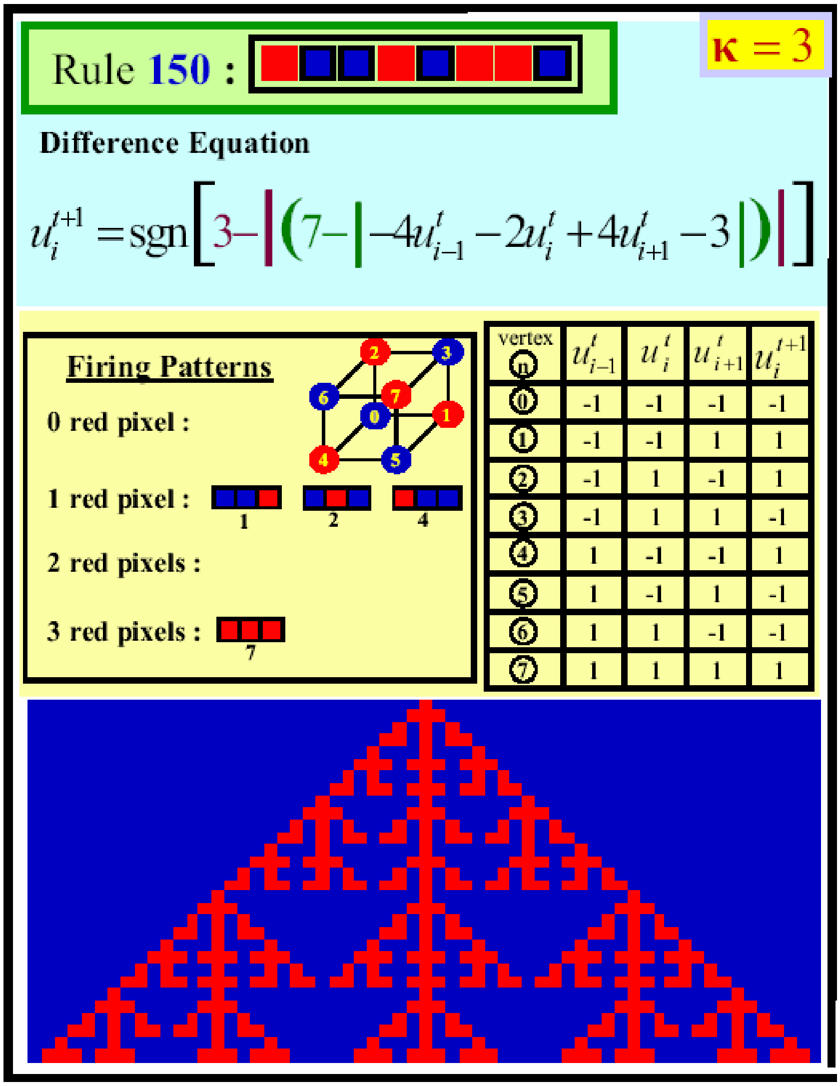

Fig. 4. Truth table, Boolean cube, difference equation, and space-time pattern of local rule $\boxed{150}$.

4. Global Analysis of Local Rules $\boxed{150}$ and $\boxed{105}$

The *truth table*, *Boolean cube*, and "Difference Equation" defining the local rules $\boxed{150}$ and $\boxed{105}$ along with a space-time pattern (with a single red-pixel initial state) exhibited in Table 5 of [Chua *et al.*, 2003] is, reproduced in Figs. 4 and 5, respectively, for the readers convenience. For this paper, it is more instructive to recast the Difference Equations defining $\boxed{150}$ and $\boxed{105}$ as follow:

$$\text{Rule } \boxed{150} \qquad \boxed{x_i^{t+1} = x_{i-1}^t \oplus x_i^t \oplus x_{i+1}^t} \tag{61}$$

$$\text{Rule } \boxed{105} \qquad \boxed{x_i^{t+1} = \overline{x_{i-1}^t \oplus x_i^t \oplus x_{i+1}^t}} \tag{62}$$

where $\oplus$ is the mod 2 sum defined in Table 24, and the bar on top denotes *complementation*. The alert reader will notice that we list $\boxed{150}$ ahead of $\boxed{105}$, counter to our style. This is done to avoid clutter where formula (61) for $\boxed{150}$ is clearly simpler than formula (62) for $\boxed{105}$. Yet, as will be shown in Sec. 4.3, these two rules are related via a global alternating transformation $\widetilde{\boldsymbol{T}}$ where $\boxed{105} = \widetilde{\boldsymbol{T}}(\boxed{150})$, and $\boxed{150} = \widetilde{\boldsymbol{T}}^{-1}(\boxed{105})$, so that it suffices to study only $\boxed{150}$.[13]

[13]Unlike the *Viererqruppe* transformations $T^\dagger$, $\overline{T}$ and T^* in [Chua *et al.*, 2004], which are defined for *all* 256 rules, the *alternating transformation* in Sec. 4.2 is defined only for rules $\boxed{150}$ and $\boxed{105}$.

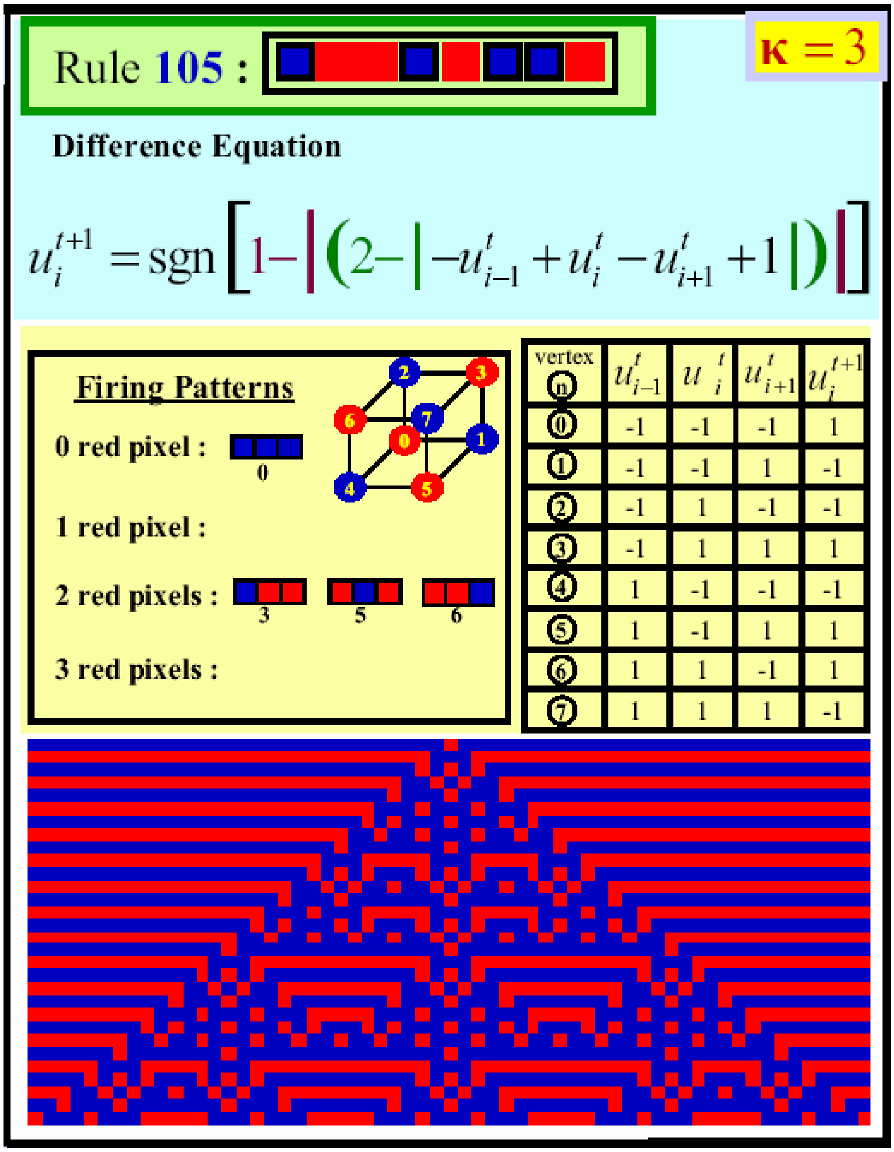

Fig. 5. Truth table, Boolean cube, difference equation, and space-time pattern of local rule $\boxed{105}$.

4.1. *Rules $\boxed{150}$ and $\boxed{105}$ are composed of Isles of Eden if L is not divisible by 3*

Theorem 6. *Every bit string of rules $\boxed{150}$ and $\boxed{105}$ is an* Isle of Eden *if, and only if, $L/3$ is not an Integer.*

Proof. We will present proof only for rule $\boxed{150}$ since rules $\boxed{150}$ and $\boxed{105}$ are globally quasi-equivalent via the *alternating* transformation $\widetilde{\boldsymbol{T}}$ to be defined in Sec. 4.3.

Just like rule $\boxed{90}$, each arbitrary bit string $\boldsymbol{x^t}$ at time t maps into $\boldsymbol{x^{t+1}}$ at time $t+1$ of rule $\boxed{150}$ via an $L \times L$ *circulant* local time-1 state transition matrix; namely,

$$\underbrace{\begin{bmatrix} x_0^{t+1} \\ x_1^{t+1} \\ x_2^{t+1} \\ \vdots \\ x_{L-2}^{t+1} \\ x_{L-1}^{t+1} \end{bmatrix}}_{\boldsymbol{x^{t+1}}} = \underbrace{\begin{bmatrix} 1 & 1 & 0 & 0 & 0 & \cdots & 1 \\ 1 & 1 & 1 & 0 & 0 & \cdots & 0 \\ 0 & 1 & 1 & 1 & 0 & \cdots & 0 \\ \vdots & & & & \ddots & & \vdots \\ 0 & 0 & 0 & \cdots & 1 & 1 & 1 \\ 1 & 0 & 0 & \cdots & 0 & 1 & 1 \end{bmatrix}}_{\boldsymbol{M}(\boxed{150})} \underbrace{\begin{bmatrix} x_0^t \\ x_1^t \\ x_2^t \\ \vdots \\ x_{L-2}^t \\ x_{L-1}^t \end{bmatrix}}_{\boldsymbol{x^t}} \mod (2) \quad (63)$$

Here, the *addition* operation in the matrix multiplication is *mod (2)* sum $\oplus$. It is easy to verify that the above $L \times L$ matrix $\boldsymbol{M}(\boxed{150})$ can be decomposed into the sum of three matrices

$$\boxed{\boldsymbol{M}(\boxed{150}) = \boldsymbol{M}^0 + \boldsymbol{M} + \boldsymbol{M}^{L-1}} \tag{64}$$

where $M^0 = \mathbf{1}$ is an $L \times L$ *identity* matrix,

$$M^{L-1} = \underbrace{M \bullet M \bullet \cdots M}_{L-1 \text{ times}} \tag{65}$$

and

$$\boldsymbol{M} \triangleq \begin{bmatrix} \mathbf{0} & 1 & \mathbf{0} & \mathbf{0} & \cdots & \mathbf{0} \\ \mathbf{0} & \mathbf{0} & 1 & \mathbf{0} & \cdots & \mathbf{0} \\ \mathbf{0} & \mathbf{0} & \mathbf{0} & 1 & \cdots & \mathbf{0} \\ \vdots & & & & & \vdots \\ \mathbf{0} & \mathbf{0} & \mathbf{0} & \cdots & \mathbf{0} & 1 \\ 1 & \mathbf{0} & \mathbf{0} & \cdots & \mathbf{0} & \mathbf{0} \end{bmatrix} \tag{66}$$

It follows from well-known results on *eigenvalues* of *circulant* matrices [Davis, 1979] that the eigenvalues of $\boldsymbol{M}(\boxed{150})$ in Eq. (64) are given by the sum of the eigenvalues of $\boldsymbol{M}^0$, $\boldsymbol{M}$ and $\boldsymbol{M}^{L-1}$, respectively; namely,

$$\lambda_k = 1 + \exp\left(2\pi i \frac{k}{L}\right) + \exp\left(2\pi i (L-1)\frac{k}{L}\right) \tag{67}$$

where $k = 0, 1, \ldots, L-1$.

It is easily verified that if $L \equiv 0 \bmod (3)$, i.e. if L is divisible by 3, then there must exist some $k \in \{1, 2, \ldots, L-1\}$ such that $\lambda_k = 0$. However, if $L \equiv 1, 2 \bmod (3)$, i.e. if L is *not* divisible by 3, then for *any* $k \in \{0, 1, \ldots, L-1\}$, $\lambda_k \neq 0$.

It follows from the property

$$\det \boldsymbol{M} = \lambda_0 \cdot \lambda_1 \cdots \lambda_{L-1}$$

that if L is not divisible by 3, then $\det \boldsymbol{M}(\boxed{150}) \neq 0$. This implies that every bit string in this case has a *unique* preimage, and hence is an *isle of Eden*.

On the other hand, if L is divisible by 3, then every bit string has a multiple preimage, implying that it *cannot* be an isle of Eden. Such a bit string must necessarily lie on a basin tree, or on an attractor. ■

As illustrations of Theorem 6, Tables 37 and 38 exhibit a list of the period "T" of at least one period-T *isle of Eden* for $L \neq 0 \bmod (3)$, and at least one period-T *attractor*, if $L \equiv 0 \bmod (3)$, of local rule $\boxed{150}$ and $\boxed{105}$, respectively. Those "blank" rectangles in these two tables without any entry imply that the period of either an isle of Eden, or an attractor for the particular L is larger than the threshold set by our program. Indeed, Table 28 suggests that the period T of this set of L's (e.g. $L = 47, 49, 53, 55, 67, 69$, etc.) could be astronomically large, and may never be found by brute-force simulations.

4.2. *Global state-transition formula for Rules* $\boxed{150}$ *and* $\boxed{105}$

The state transition formulas given in Figs. 4 and 5 are *local in time*. Our next theorem gives an explicit formula for rule $\boxed{150}$, and for rule $\boxed{105}$, which is *global in time*.

Theorem 7. Global state-transition Formula for rules $\boxed{150}$ and $\boxed{105}$.

Each pixel x_i^n of rules $\boxed{150}$ and $\boxed{105}$ at time $n > 1$ is determined from "$n+1$" initial pixels $x_{i-n}^0, x_{i-n+2}^0, \ldots, x_{i+n-2}^0, x_{i+n}^0$ at $t = 0$ via the following corresponding "Composite Binomial formulas":

Rule $\boxed{150}$

$$\boxed{x_i^n = \sum_{k=0}^{n} \frac{n!}{k!(n-k)!} \sum_{j=0}^{k} \frac{k!}{j!(k-j)!} \bullet x_{i-n+2k-j}^0 \bmod (2)} \tag{68}$$

Rule $\boxed{105}$

$$\boxed{\begin{aligned} x_i^n &= \alpha_n + (-1)^n \sum_{k=0}^{n} \frac{n!}{k!(n-k)!} \bullet \sum_{j=0}^{k} \frac{k!}{j!(k-j)!} \bullet x_{i-n+2k-j}^0 \bmod (2) \\ &\text{where} \quad \alpha_n \triangleq \frac{1}{2}[1-(-1)^n]. \end{aligned}} \tag{69}$$

Table 39 exhibits the detailed expansion of the global state transition formula for rule $\boxed{150}$ for $n = 1, 2, \ldots, 8$. The corresponding formula in *mod (2) coefficients* are shown in Table 40. These coefficients are repacked into a Pascal's like a triangle in Table 41. Table 42 shows the space-time patterns generated from applying the global and local state transition formulas for rule $\boxed{150}$ when the initial configuration consists of a single red center pixel. Table 43 shows corresponding space-time patterns when a *random* initial configuration is used.

The corresponding illustrations for rule $\boxed{105}$ are shown in Tables 44–48, respectively.

Table 37. Period "T" of Isles of Eden and attractors of local rule $\boxed{150}$.

L	Isle of Eden	Attractor
1		
2		
3		T = 1
4	T = 2	
5	T = 3	
6		T = 1
7	T = 7	
8	T = 4	
9		T = 7
10	T = 6	
11	T = 31	
12		T = 1
13	T = 21	
14	T = 14	
15		T = 15
16	T = 8	
17	T = 15	
18		T = 7
19	T = 511	
20	T = 12	
21		T = 63
22	T = 62	
23	T = 2047	
24		T = 2
25	T = 1023	

L	Isle of Eden	Attractor
26	T = 42	
27		T = 511
28	T = 28	
29	T = 16383	
30		T = 15
31	T = 31	
32	T = 16	
33		T = 31
34	T = 30	
35	T = 4095	
36		T= 14
37	T = 29127	
38	T = 1022	
39		T = 4095
40	T = 24	
41	T = 1023	
42		T = 63
43	T = 127	
44	T = 124	
45		T = 4095
46	T = 4094	
47		
48		T = 4
49		
50	T = 2046	

Table 37. (*Continued*)

L	Isle of Eden	Attractor
51		$T = 255$
52	$T = 84$	
53		
54		$T = 511$
55		
56	$T = 56$	
57		$T = 511$
58	$T = 32766$	
59		
60		$T = 30$
61		
62	$T = 62$	
63		$T = 63$
64	$T = 32$	
65	$T = 63$	
66		$T = 31$
67		
68	$T = 60$	
69		
70	$T = 8190$	
71		
72		$T = 28$
73	$T = 511$	
74	$T = 58254$	
75		

L	Isle of Eden	Attractor
76	$T = 2044$	
77		
78		$T = 4095$
79		
80	$T = 48$	
81		
82	$T = 2046$	
83		
84		$T = 126$
85	$T = 255$	
86	$T = 254$	
87		
88	$T = 248$	
89	$T = 2047$	
90		$T = 4095$
91	$T = 4095$	
92	$T = 8188$	
93		$T = 1023$
94		
95		
96		$T = 8$
97		
98		
99		$T = 32767$
100	$T = 4092$	

Table 37. (*Continued*)

L	Isle of Eden	Attractor
101		
102		$T = 255$
103		
104	$T = 168$	
105		$T = 4095$
106		
107		
108		$T = 1022$
109	$T = 262143$	
110		
111		
112	$T = 112$	
113	$T = 16383$	
114		$T = 511$
115		
116	$T = 65532$	
117		$T = 4095$
118		
119		
120		$T = 60$
121		
122		
123		
124	$T = 124$	
125		

L	Isle of Eden	Attractor
126		$T = 63$
127	$T = 127$	
128	$T = 64$	
129		$T = 127$
130	$T = 126$	
131		
132		$T = 62$
133	$T = 262143$	
134		
135		
136	$T = 120$	
137		
138		
139		
140	$T = 16380$	
141		
142		
143		
144		$T = 56$
145	$T = 16383$	
146	$T = 1022$	
147		
148	$T = 116508$	
149		
150		

Table 37. (*Continued*)

L	Isle of Eden	Attractor
151	T = 32767	
152	T = 4088	
153		
154		
155		
156		T= 8190
157		
158		
159		
160	T = 96	
161		
162		
163		
164	T = 4092	
165		
166		
167		
168		T = 252
169		
170	T = 510	
171		T = 511
172	T = 508	
173		
174		
175		
176	T = 496	
177		
178	T = 4094	
179		
180		T = 8190
181		
182	T = 8190	
183		
184	T = 16376	
185	T = 262143	
186		T = 1023
187		
188		
189		
190		
191		
192		T = 16
193		
194		
195		T = 4095
196		
197		
198		T = 32767
199		
200	T = 8184	

Table 37. (*Continued*)

L	Isle of Eden	Attractor
204		$T = 510$
205	$T = 1023$	
208	$T = 336$	
210		$T = 4095$
216		$T = 2044$
217	$T = 32767$	
218	$T = 524286$	
224	$T = 224$	
226	$T = 32766$	
228		$T = 1022$
232	$T = 131064$	
234		$T = 4095$
240		$T = 120$
241	$T = 4095$	
248	$T = 248$	
252		$T = 126$
254	$T = 254$	
255		$T = 255$
256	$T = 128$	
257	$T = 255$	
258		$T = 127$
260	$T = 252$	
264		$T = 124$
266	$T = 524286$	
272	$T = 240$	

L	Isle of Eden	Attractor
273		$T = 4095$
280	$T = 32760$	
288		$T = 112$
290	$T = 32766$	
292	$T = 2044$	
296	$T = 233016$	
302	$T = 65534$	
304	$T = 8176$	
312		$T = 16380$
315		$T = 4095$
320	$T = 192$	
328	$T = 8184$	
336		$T = 504$
340	$T = 1020$	
341	$T = 1023$	
342		$T = 511$
344	$T = 1016$	
352	$T = 992$	
356	$T = 8188$	
360		$T = 16380$
364	$T = 16380$	
368	$T = 32752$	
370	$T = 524286$	
372		$T = 2046$
384		$T = 32$

Table 37. (*Continued*)

L	Isle of Eden	Attractor
390		$T = 4095$
396		$T = 65534$
400	$T = 16368$	
408		$T = 1020$
410	$T = 2046$	
416	$T = 672$	
420		$T = 8190$
432		$T = 4088$
434	$T = 65534$	
436	$T = 1048572$	
448	$T = 448$	
452	$T = 65532$	
455	$T = 4095$	
456		$T = 2044$
464	$T = 262128$	
468		$T = 8190$
480		$T = 240$
482	$T = 8190$	
496	$T = 496$	
504		$T = 252$
508	$T = 508$	
510		$T = 255$
511	$T = 511$	
512	$T = 256$	
513		$T = 511$
514	$T = 510$	

L	Isle of Eden	Attractor
516		$T = 254$
520	$T = 504$	
528		$T = 248$
532	$T = 1048572$	
544	$T = 480$	
546		$T = 4095$
560	$T = 65520$	
565	$T = 16383$	
576		$T = 224$
580	$T = 65532$	
584	$T = 4088$	
585		$T = 4095$
592	$T = 466032$	
604	$T = 131068$	
608	$T = 16352$	
624		$T = 32760$
630		$T = 4095$
640	$T = 384$	
656	$T = 16368$	
672		$T = 1088$
680	$T = 2040$	
682	$T = 2046$	
683	$T = 2047$	
684		$T = 1022$
688	$T = 2032$	
704	$T = 1984$	

Table 37. (*Continued*)

L	Isle of Eden	Attractor
712	T = 16376	
720		T = 32760
728	T = 32760	
736	T = 65504	
740	T = 1048572	
744		T = 4092
768		T = 64
780		T = 8190
792		T = 131068
800	T = 32736	
816		T = 2040
819		T = 4095
820	T = 4092	
832	T = 1344	
840		T = 16380
864		T = 8176
868	T = 131068	
896	T = 896	
904	T = 131064	
910	T = 8190	
912		T = 4088
928	T = 524256	
936		T = 16380
960		T = 480
964	T = 16380	
992	T = 992	

Table 38. Period "T" of Isles of Eden and attractors of local rule $\boxed{105}$.

L	Isle of Eden	Attractor
1		
2		
3		$T = 2$
4	$T = 2$	
5	$T = 6$	
6		$T = 2$
7	$T = 14$	
8	$T = 4$	
9		$T = 14$
10	$T = 6$	
11	$T = 62$	
12		$T = 2$
13	$T = 42$	
14	$T = 14$	
15		$T = 30$
16	$T = 8$	
17	$T = 30$	
18		$T = 14$
19	$T = 1022$	
20	$T = 12$	
21		$T = 126$
22	$T = 62$	
23	$T = 4094$	
24		$T = 4$
25	$T = 2046$	
26	$T = 42$	
27		$T = 1022$
28	$T = 28$	
29	$T = 32766$	
30		$T = 30$
31	$T = 62$	
32	$T = 16$	
33		$T = 62$
34	$T = 30$	
35	T = 8190	
36		$T= 28$
37	$T = 58254$	
38	$T = 1022$	
39		$T = 8190$
40	$T = 24$	
41	$T = 2046$	
42		$T = 126$
43	$T = 254$	
44	$T = 124$	
45		$T = 8190$
46	$T = 4094$	
47		
48		$T = 8$
49		
50	$T = 2046$	

Table 38. (*Continued*)

L	Isle of Eden	Attractor
51		$T = 510$
52	$T = 84$	
53		
54		$T = 1022$
55		
56	$T = 56$	
57		$T = 1022$
58	$T = 32766$	
59		
60		$T = 60$
61		
62	$T = 62$	
63		$T = 126$
64	$T = 32$	
65	$T = 126$	
66		$T = 62$
67		
68	$T = 60$	
69		
70	$T = 8190$	
71		
72		$T = 56$
73	$T = 1022$	
74	$T = 58254$	
75		

L	Isle of Eden	Attractor
76	$T = 2044$	
77		
78		$T = 8190$
79		
80	$T = 48$	
81		
82	$T = 2046$	
83		
84		$T = 252$
85	$T = 510$	
86	$T = 254$	
87		
88	$T = 248$	
89	$T = 4094$	
90		$T = 8190$
91	$T = 8190$	
92	$T = 8188$	
93		$T = 2046$
94		
95		
96		$T = 16$
97		
98		
99		$T = 65534$
100	$T = 4092$	

Table 38. (*Continued*)

L	Isle of Eden	Attractor
101		
102		$T = 510$
103		
104	$T = 168$	
105		$T = 8190$
106		
107		
108		$T = 2044$
109	$T = 524286$	
110		
111		
112	$T = 112$	
113	$T = 32766$	
114		$T = 1022$
115		
116	$T = 65532$	
117		$T = 8190$
118		
119		
120		$T = 120$
121		
122		
123		
124	$T = 124$	
125		

L	Isle of Eden	Attractor
126		$T = 126$
127	$T = 254$	
128	$T = 64$	
129		$T = 254$
130	$T = 126$	
131		
132		$T = 124$
133	$T = 524286$	
134		
135		
136	$T = 120$	
137		
138		
139		
140	$T = 16380$	
141		
142		
143		
144		$T = 112$
145	$T = 32766$	
146	$T = 1022$	
147		
148	$T = 116508$	
149		
150		

Table 38. (*Continued*)

L	Isle of Eden	Attractor
151	$T = 65534$	
152	$T = 4088$	
153		
154		
155		
156		$T = 16380$
157		
158		
159		
160	$T = 96$	
161		
162		
163		
164	$T = 4092$	
165		
166		
167		
168		$T = 504$
169		
170	$T = 510$	
171		$T = 1022$
172	$T = 508$	
173		
174		
175		

L	Isle of Eden	Attractor
176	$T = 496$	
177		
178	$T = 4094$	
179		
180		$T = 16380$
181		
182	$T = 8190$	
183		
184	$T = 16376$	
185	$T = 524286$	
186		$T = 2046$
187		
188		
189		
190		
191		
192		$T = 32$
193		
194		
195		$T = 8190$
196		
197		
198		$T = 65534$
199		
200	$T = 8184$	

Table 38. (*Continued*)

L	Isle of Eden	Attractor
204		$T = 1020$
205	$T = 2046$	
208	$T = 336$	
210		$T = 8190$
216		$T = 4088$
217	$T = 65534$	
218	$T = 524286$	
224	$T = 224$	
226	$T = 32766$	
228		$T = 2044$
232	$T = 131064$	
234		$T = 8190$
240		$T = 240$
241	$T = 8190$	
248	$T = 248$	
252		$T = 252$
254	$T = 254$	
255		$T = 510$
256	$T = 128$	
257	$T = 510$	
258		$T = 254$
260	$T = 252$	
264		$T = 248$
266	$T = 524286$	
272	$T = 240$	

L	Isle of Eden	Attractor
273		$T = 8190$
280	$T = 32760$	
288		$T = 224$
290	$T = 32766$	
292	$T = 2044$	
296	$T = 233016$	
302	$T = 65534$	
304	$T = 8176$	
312		$T = 32760$
315		$T = 8190$
320	$T = 192$	
328	$T = 8184$	
336		$T = 1008$
340	$T = 1020$	
341	$T = 2046$	
342		$T = 1022$
344	$T = 1016$	
352	$T = 992$	
356	$T = 8188$	
360		$T = 32760$
364	$T = 16380$	
368	$T = 32752$	
370	$T = 524286$	
372		$T = 4096$
384		$T = 64$

Table 38. (*Continued*)

L	Isle of Eden	Attractor
390		$T = 8190$
396		$T = 131068$
400	$T = 16368$	
408		$T = 2040$
410	$T = 2046$	
416	$T = 672$	
420		$T = 16380$
432		$T = 8176$
434	$T = 65534$	
436	$T = 1048572$	
448	$T = 448$	
452	$T = 65532$	
455	$T = 8190$	
456		$T = 4088$
464	$T = 262128$	
468		$T = 16380$
480		$T = 480$
482	$T = 8190$	
496	$T = 496$	
504		$T = 504$
508	$T = 508$	
510		$T = 510$
511	$T = 1022$	
512	$T = 256$	
513		$T = 1022$
514	$T = 510$	

L	Isle of Eden	Attractor
516		$T = 508$
520	$T = 504$	
528		$T = 496$
532	$T = 1048572$	
544	$T = 480$	
546		$T = 8190$
560	$T = 65520$	
565	$T = 32766$	
576		$T = 448$
580	$T = 65532$	
584	$T = 4088$	
585		$T = 8190$
592	$T = 466032$	
604	$T = 131068$	
608	$T = 16352$	
624		$T = 65520$
630		$T = 8190$
640	$T = 384$	
656	$T = 16368$	
672		$T = 2016$
680	$T = 2040$	
682	$T = 2046$	
683	$T = 4094$	
684		$T = 2044$
688	$T = 2032$	
704	$T = 1984$	

Table 38. (*Continued*)

L	Isle of Eden	Attractor
712	$T = 16376$	
720		$T = 65520$
728	$T = 32760$	
736	$T = 65504$	
740	$T = 1048572$	
744		$T = 8184$
768		$T = 128$
780		$T = 16380$
792		$T = 262136$
800	$T = 32736$	
816		$T = 4080$
819		$T = 8190$
820	$T = 4092$	
832	$T = 1344$	
840		$T = 32760$
864		$T = 16352$
868	$T = 131068$	
896	$T = 896$	
904	$T = 131064$	
910	$T = 8190$	
912		$T = 8176$
928	$T = 524256$	
936		$T = 32760$
960		$T = 960$
964	$T = 16380$	
992	$T = 992$	

Table 39. Global state-transition formula for rule $\boxed{150}$ for $1 \le n \le 8$.

n	$x_i^n = \sum\limits_{k=0}^{n} \frac{n!}{k!(n-k)!} \sum\limits_{j=0}^{k} \frac{k!}{j!(k-j)!} \cdot x_{i-n+2k-j}^0 \quad \mathbf{mod}(\mathbf{2})$
1	$x_i^1 = x_{i-1}^0 + x_i^0 + x_{i+1}^0 \quad \mathbf{mod}(\mathbf{2})$
2	$x_i^2 = x_{i-2}^0 + 2x_{i-1}^0 + 3x_i^0 + 2x_{i+1}^0 + x_{i+2}^0 \quad \mathbf{mod}(\mathbf{2})$
3	$x_i^3 = x_{i-3}^0 + 3x_{i-2}^0 + 6x_{i-1}^0 + 7x_i^0 + 6x_{i+1}^0 + 3x_{i+2}^0 + x_{i+3}^0 \quad \mathbf{mod}(\mathbf{2})$
4	$x_i^4 = x_{i-4}^0 + 4x_{i-3}^0 + 10x_{i-2}^0 + 16x_{i-1}^0 + 19x_i^0$ $+16x_{i+1}^0 + 10x_{i+2}^0 + 4x_{i+3}^0 + x_{i+4}^0 \quad \mathbf{mod}(\mathbf{2})$
5	$x_i^5 = x_{i-5}^0 + 5x_{i-4}^0 + 15x_{i-3}^0 + 30x_{i-2}^0 + 45x_{i-1}^0 + 51x_i^0$ $+45x_{i+1}^0 + 30x_{i+2}^0 + 15x_{i+3}^0 + 5x_{i+4}^0 + x_{i+5}^0 \quad \mathbf{mod}(\mathbf{2})$
6	$x_i^6 = x_{i-6}^0 + 6x_{i-5}^0 + 21x_{i-4}^0 + 50x_{i-3}^0 + 90x_{i-2}^0 + 126x_{i-1}^0 + 141x_i^0$ $+126x_{i+1}^0 + 90x_{i+2}^0 + 50x_{i+3}^0 + 21x_{i+4}^0 + 6x_{i+5}^0 + x_{i+6}^0 \quad \mathbf{mod}(\mathbf{2})$
7	$x_i^6 = x_{i-7}^0 + 7x_{i-6}^0 + 28x_{i-5}^0 + 77x_{i-4}^0 + 161x_{i-3}^0$ $+266x_{i-2}^0 + 357x_{i-1}^0 + 393x_i^0 + 357x_{i+1}^0 + 266x_{i+2}^0$ $+161x_{i+3}^0 + 77x_{i+4}^0 + 28x_{i+5}^0 + 7x_{i+6}^0 + x_{i+7}^0 \quad \mathbf{mod}(\mathbf{2})$
8	$x_i^6 = x_{i-8}^0 + 8x_{i-7}^0 + 36x_{i-6}^0 + 112x_{i-5}^0 + 266x_{i-4}^0 + 504x_{i-3}^0$ $+784x_{i-2}^0 + 1016x_{i-1}^0 + 1107x_i^0 + 1016x_{i+1}^0 + 784x_{i+2}^0$ $+504x_{i+3}^0 + 266x_{i+4}^0 + 112x_{i+5}^0 + 36x_{i+6}^0 + 8x_{i+7}^0 + x_{i+8}^0 \quad \mathbf{mod}(\mathbf{2})$

The formal proof of Eq. (68) is given below. A similar proof involving more messy expressions can be given for Eq. (69). We omit the proof to avoid clutter. A different and more illuminating proof follows as a *Corollary* to the $\boxed{105} \rightleftarrows \boxed{150}$ *Alternating Symmetry Duality* given in the *Appendix*.

Proof of Global State-Transition Formula (68) for $\boxed{150}$. Apply *mathematical induction* as follow:

(a) Applying $n = 1$ in Eq. (68), we obtain

$$x_i^1 = x_{i-1}^0 + x_i^0 + x_{i+1}^0 \bmod (2) \tag{70}$$

which is Eq. (61) for $t = 0$.

(b) Assuming Eq. (68) is true for $n = m$ (*induction hypothesis*), namely,

$$x_i^m = \sum_{k=0}^{m} \frac{m!}{k!(m-k)!} \sum_{j=0}^{k} \frac{k!}{j!(k-j)!} \bullet x_{i-m+2k-j}^0 \bmod (2) \tag{71}$$

We must show that incrementing "m" to "$m+1$" in Eq. (71) gives Eq. (68) with $n = m + 1$. Rewriting Eq. (70) as a mapping from m to $m + 1$, we have

$$\begin{aligned} x_i^{m+1} &= x_{i-1}^m + x_i^m + x_{i+1}^m \bmod (2) \\ &= \sum_{k=0}^{m} \frac{m!}{k!(m-k)!} \sum_{j=0}^{k} \frac{k!}{j!(k-j)!} \bullet x_{(i-1)-m+2k-j}^0 \end{aligned} \tag{72}$$

Table 40. Mod (2) global state-transition formula in terms of *mod (2)* coefficients for rule $\boxed{150}$ for $1 \leq n \leq 8$.

n	$x_i^n = \sum_{k=0}^{n} \frac{n!}{k!(n-k)!} \sum_{j=0}^{k} \frac{k!}{j!(k-j)!} \cdot x_{i-n+2k-j}^0 \quad \mathbf{mod(2)}$
1	$x_i^1 = x_{i-1}^0 + x_i^0 + x_{i+1}^0 \quad \mathbf{mod(2)}$
2	$x_i^2 = x_{i-2}^0 + x_i^0 + x_{i+2}^0 \quad \mathbf{mod(2)}$
3	$x_i^3 = x_{i-3}^0 + x_{i-2}^0 + x_i^0 + x_{i+2}^0 + x_{i+3}^0 \quad \mathbf{mod(2)}$
4	$x_i^4 = x_{i-4}^0 + x_i^0 + x_{i+4}^0 \quad \mathbf{mod(2)}$
5	$x_i^5 = x_{i-5}^0 + x_{i-4}^0 + x_{i-3}^0 + x_{i-1}^0 + x_i^0 + x_{i+1}^0 + x_{i+3}^0 + x_{i+4}^0 + x_{i+5}^0 \quad \mathbf{mod(2)}$
6	$x_i^6 = x_{i-6}^0 + x_{i-4}^0 + x_i^0 + x_{i+4}^0 + x_{i+6}^0 \quad \mathbf{mod(2)}$
7	$x_i^6 = x_{i-7}^0 + x_{i-6}^0 + x_{i-4}^0 + x_{i-3}^0 + x_{i-1}^0 + x_i^0 + x_{i+1}^0 + x_{i+3}^0 + x_{i+4}^0 + x_{i+6}^0 + x_{i+7}^0 \quad \mathbf{mod(2)}$
8	$x_i^6 = x_{i-8}^0 + x_i^0 + x_{i+8}^0 \quad \mathbf{mod(2)}$

Table 41. Mod (2) coefficients for global-transition formula for $\boxed{150}$ for $1 \leq n \leq 8$.

n	-8	-7	-6	-5	-4	-3	-2	-1	0	1	2	3	4	5	6	7	8
1	0	0	0	0	0	0	0	1	1	1	0	0	0	0	0	0	0
2	0	0	0	0	0	0	1	0	1	0	1	0	0	0	0	0	0
3	0	0	0	0	0	1	1	0	1	0	1	1	0	0	0	0	0
4	0	0	0	0	1	0	0	0	1	0	0	0	1	0	0	0	0
5	0	0	0	1	1	1	0	1	1	1	0	1	1	1	0	0	0
6	0	0	1	0	1	0	0	0	1	0	0	0	1	0	1	0	0
7	0	1	1	0	1	1	0	1	1	1	0	1	1	0	1	1	0
8	1	0	0	0	0	0	0	0	1	0	0	0	0	0	0	0	1

Table 42. Space-time pattern of $\boxed{150}$ calculated from a single red center pixel via (a) global state-transition formula, and (b) local state-transition formula.

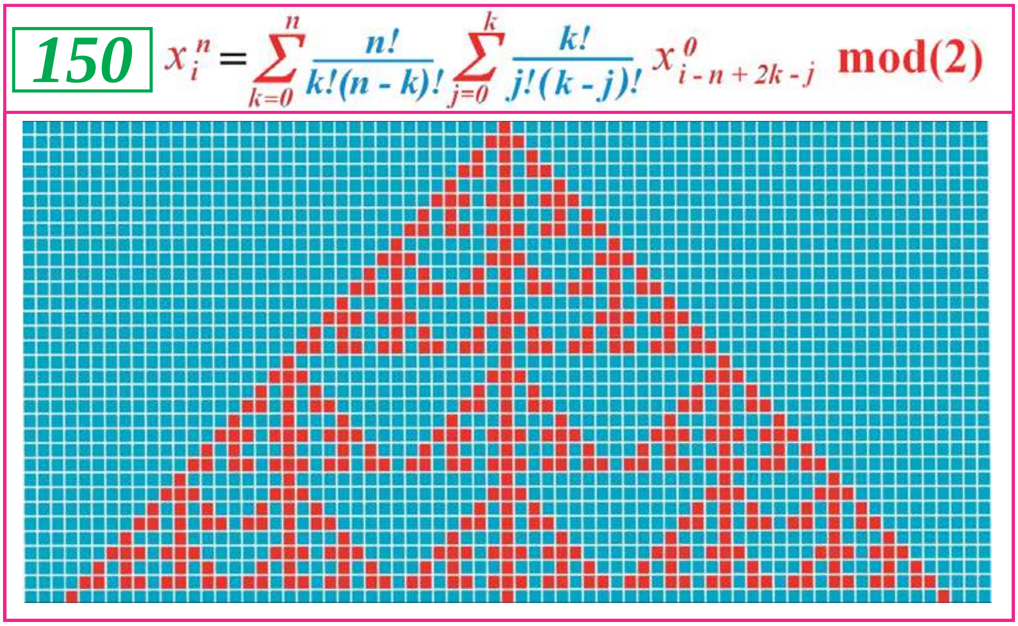

(a)

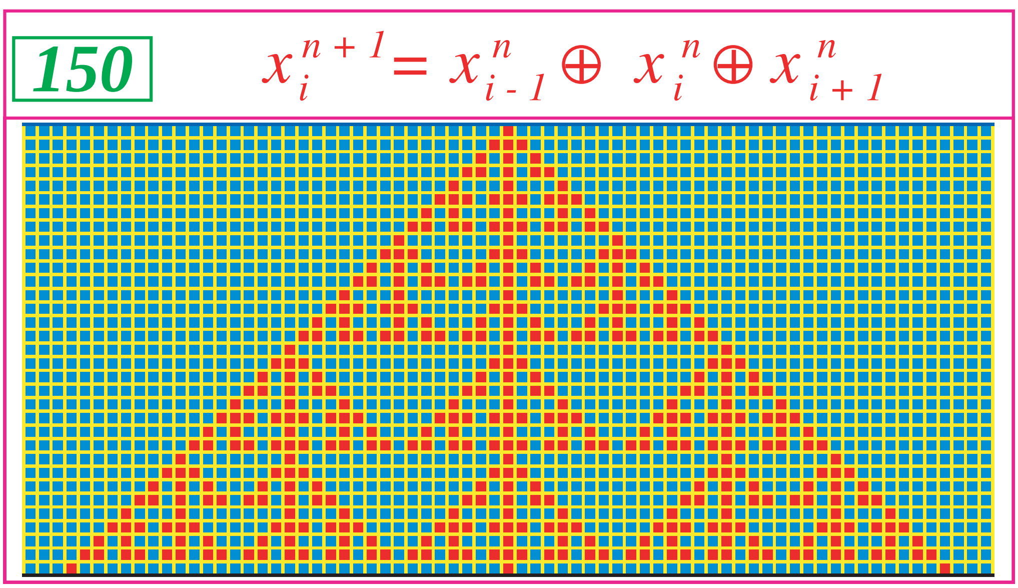

(b)

Table 43. Space-time patterns of $\boxed{150}$ from a *random* initial configuration calculated from the global and local state-transition formula, respectively, of rule $\boxed{150}$.

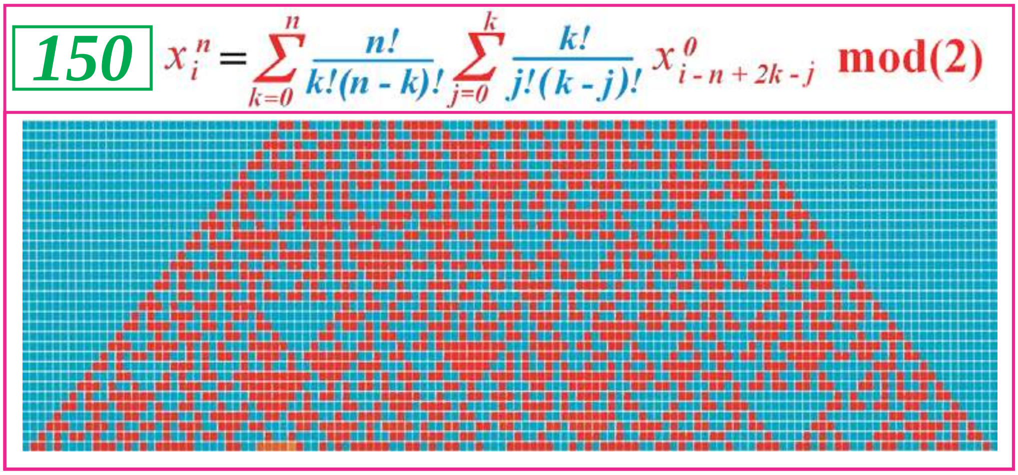

(a)

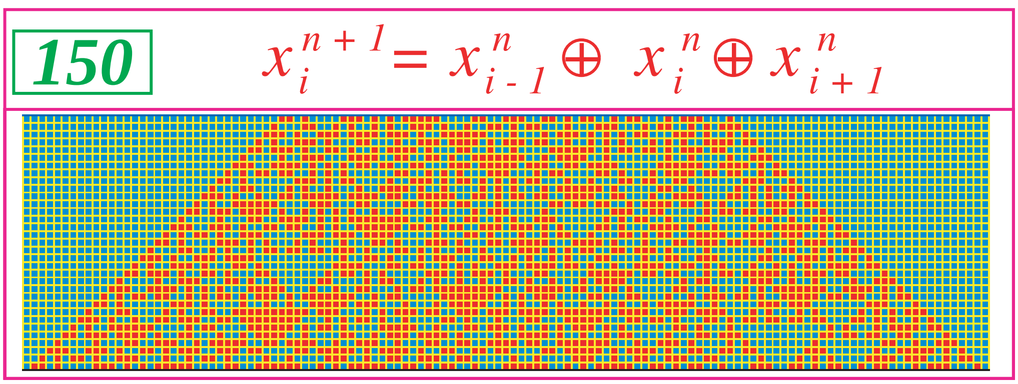

(b)

$$+ \sum_{k=0}^{m} \frac{m!}{k!(m-k)!} \sum_{j=0}^{k} \frac{k!}{j!(k-j)!} \bullet x^0_{i-m+2k-j} \tag{73}$$

$$+ \sum_{k=0}^{m} \frac{m!}{k!(m-k)!} \sum_{j=0}^{k} \frac{k!}{j!(k-j)!} \bullet x^0_{(i+1)-m+2k-j} \bmod (2) \tag{74}$$

(b.1) Changing symbol "m" in Eq. (73) to $m' + 1$ gives

$$x_i^{m+1} = \sum_{k=0}^{m} \frac{m!}{k!(m-k)!} \sum_{j=0}^{k} \frac{k!}{j!(k-j)!} \bullet x^0_{i-1-m+2k-j} \tag{75}$$

$$+ \sum_{k=0}^{m'+1} \frac{(m'+1)!}{k!(m'+1-k)!} \sum_{j=0}^{k} \frac{k!}{j!(k-j)!} \bullet x^0_{i-m'-1+2k-j} \tag{76}$$

$$+ \sum_{k=0}^{m} \frac{(m)!}{k!(m-k)!} \sum_{j=0}^{k} \frac{k!}{j!(k-j)!} \bullet x^0_{i+1-m+2k-j} \bmod (2) \tag{77}$$

Observe that if we substitute $k = m+1$ in Eq. (75) we would get a *zero* because $(m-k)!$ in the denominator gives, in this case, a singularity $(-1)!$ Consequently, the term at $k = m+1$ vanishes and does not affect our derivation. Hence, let us expand the external sum in Eq. (75) from $k = 0$ to $k = m+1$. We omit also in Eq. (76) the prime in m' for convenience.

Table 44. Mod (2) global state-transition formula for rule $\boxed{105}$ for $1 \le n \le 8$.

n	$x_i^n = \alpha_n + (-1)^n \sum_{k=0}^{n} \frac{n!}{k!(n-k)!} \sum_{j=0}^{k} \frac{k!}{j!(k-j)!} \cdot x^0_{i-n+2k-j}$ **mod(2)**
1	$x_i^1 = 1 - x^0_{i-1} - x^0_i - x^0_{i+1}$ **mod(2)**
2	$x_i^2 = x^0_{i-2} + 2x^0_{i-1} + 3x^0_i + 2x^0_{i+1} + x^0_{i+2}$ **mod(2)**
3	$x_i^3 = 1 - x^0_{i-3} - 3x^0_{i-2} - 6x^0_{i-1} - 7x^0_i - 6x^0_{i+1} - 3x^0_{i+2} - x^0_{i+3}$ **mod(2)**
4	$x_i^4 = x^0_{i-4} + 4x^0_{i-3} + 10x^0_{i-2} + 16x^0_{i-1} + 19x^0_i$ $+16x^0_{i+1} + 10x^0_{i+2} + 4x^0_{i+3} + x^0_{i+4}$ **mod(2)**
5	$x_i^5 = 1 - x^0_{i-5} - 5x^0_{i-4} - 15x^0_{i-3} - 30x^0_{i-2} - 45x^0_{i-1} - 51x^0_i$ $-45x^0_{i+1} - 30x^0_{i+2} - 15x^0_{i+3} - 5x^0_{i+4} - x^0_{i+5}$ **mod(2)**
6	$x_i^6 = x^0_{i-6} + 6x^0_{i-5} + 21x^0_{i-4} + 50x^0_{i-3} + 90x^0_{i-2} + 126x^0_{i-1} + 141x^0_i$ $+126x^0_{i+1} + 90x^0_{i+2} + 50x^0_{i+3} + 21x^0_{i+4} + 6x^0_{i+5} + x^0_{i+6}$ **mod(2)**
7	$x_i^6 = 1 - x^0_{i-7} - 7x^0_{i-6} - 28x^0_{i-5} - 77x^0_{i-4} - 161x^0_{i-3}$ $-266x^0_{i-2} - 357x^0_{i-1} - 393x^0_i - 357x^0_{i+1} - 266x^0_{i+2}$ $-161x^0_{i+3} - 77x^0_{i+4} - 28x^0_{i+5} - 7x^0_{i+6} - x^0_{i+7}$ **mod(2)**
8	$x_i^6 = x^0_{i-8} + 8x^0_{i-7} + 36x^0_{i-6} + 112x^0_{i-5} + 266x^0_{i-4} + 504x^0_{i-3}$ $+784x^0_{i-2} + 1016x^0_{i-1} + 1107x^0_i + 1016x^0_{i+1} + 784x^0_{i+2}$ $+504x^0_{i+3} + 266x^0_{i+4} + 112x^0_{i+5} + 36x^0_{i+6} + 8x^0_{i+7} + x^0_{i+8}$ **mod(2)**

$\alpha_n = (1-(-1)^n)/2$

Let us combine Eqs. (75) and (76):

$$x_i^{m+1} = \sum_{k=0}^{m+1} \left(\frac{(m)!}{k!(m-k)!} + \frac{(m+1)!}{k!(m+1-k)!} \right) \bullet \sum_{j=0}^{k} \frac{k!}{j!(k-j)!} \bullet x^0_{i-m-1+2k-j} + \sum_{k=0}^{m} \frac{(m)!}{k!(m-k)!} \sum_{j=0}^{k} \frac{k!}{j!(k-j)!} \bullet x^0_{i+1-m+2k-j} \text{ mod } (2) \tag{78}$$

The sum of the two binomial coefficients contained between the large parentheses in the first sum is

$$\frac{(m)!}{k!(m-k)!} + \frac{(m+1)!}{k!(m+1-k)!} = \frac{(m)!}{k!(m+1-k)!}\big((m+1-k) + (m+1)\big) = \frac{(m)!}{k!(m+1-k)!}(2m+2-k)$$

In this case Eq. (78) can be recast as follows:

$$x_i^{m+1} = \sum_{k=0}^{m+1} \frac{\big(2(m+1)-k\big)(m)!}{(k)!(m+1-k)!} \bullet \sum_{j=0}^{k} \frac{k!}{j!(k-j)!} \bullet x^0_{i-m-1+2k-j} + \sum_{k=0}^{m} \frac{(m)!}{k!(m-k)!} \sum_{j=0}^{k} \frac{k!}{j!(k-j)!} \bullet x^0_{i+1-m+2k-j} \text{ mod } (2) \tag{79}$$

Separating terms with factors $2(m+1)$ and $(-k)$ we obtain

Table 45. Mod (2) global state-transition formula in terms of *mod (2)* coefficients for rule $\boxed{105}$ for $1 \le n \le 8$.

n	$x_i^n = \alpha_n + (-1)^n \sum_{k=0}^{n} \frac{n!}{k!(n-k)!} \sum_{j=0}^{k} \frac{k!}{j!(k-j)!} \cdot x^0_{i-n+2k-j}$ $\mathbf{mod(2)}$
1	$x_i^1 = 1 - x^0_{i-1} - x^0_i - x^0_{i+1}$ $\mathbf{mod(2)}$
2	$x_i^2 = x^0_{i-2} + x^0_i + x^0_{i+2}$ $\mathbf{mod(2)}$
3	$x_i^3 = 1 - x^0_{i-3} - x^0_{i-2} - x^0_i - x^0_{i+2} - x^0_{i+3}$ $\mathbf{mod(2)}$
4	$x_i^4 = x^0_{i-4} + x^0_i + x^0_{i+4}$ $\mathbf{mod(2)}$
5	$x_i^5 = 1 - x^0_{i-5} - x^0_{i-4} - x^0_{i-3} - x^0_{i-1} - x^0_i - x^0_{i+1} - x^0_{i+3} - x^0_{i+4} - x^0_{i+5}$ $\mathbf{mod(2)}$
6	$x_i^6 = x^0_{i-6} + x^0_{i-4} + x^0_i + x^0_{i+4} + x^0_{i+6}$ $\mathbf{mod(2)}$
7	$x_i^6 = 1 - x^0_{i-7} - x^0_{i-6} - x^0_{i-4} - x^0_{i-3} - x^0_{i-1} - x^0_i - x^0_{i+1} - x^0_{i+3} - x^0_{i+4} - x^0_{i+6} - x^0_{i+7}$ $\mathbf{mod(2)}$
8	$x_i^6 = x^0_{i-8} + x^0_i + x^0_{i+8}$ $\mathbf{mod(2)}$

$\alpha_n = (1 - (-1)^n)/2$

Table 46. Mod (2) coefficients for global-transition formula for $\boxed{105}$ for $1 \le n \le 8$.

n	-8	-7	-6	-5	-4	-3	-2	-1	0	1	2	3	4	5	6	7	8
1	1	1	1	1	1	1	1	0	0	0	1	1	1	1	1	1	1
2	0	0	0	0	0	0	1	0	1	0	1	0	0	0	0	0	0
3	1	1	1	1	1	0	0	1	0	1	0	0	1	1	1	1	1
4	0	0	0	0	1	0	0	0	1	0	0	0	1	0	0	0	0
5	1	1	1	0	0	0	1	0	0	0	1	0	0	0	1	1	1
6	0	0	1	0	1	0	0	0	1	0	0	0	1	0	1	0	0
7	1	0	0	1	0	0	1	0	0	0	1	0	0	1	0	0	1
8	1	0	0	0	0	0	0	0	1	0	0	0	0	0	0	0	1

Table 47. Space-time pattern of $\boxed{105}$ calculated from a single red center pixel via (a) global state transition function, and (b) local state transition function.

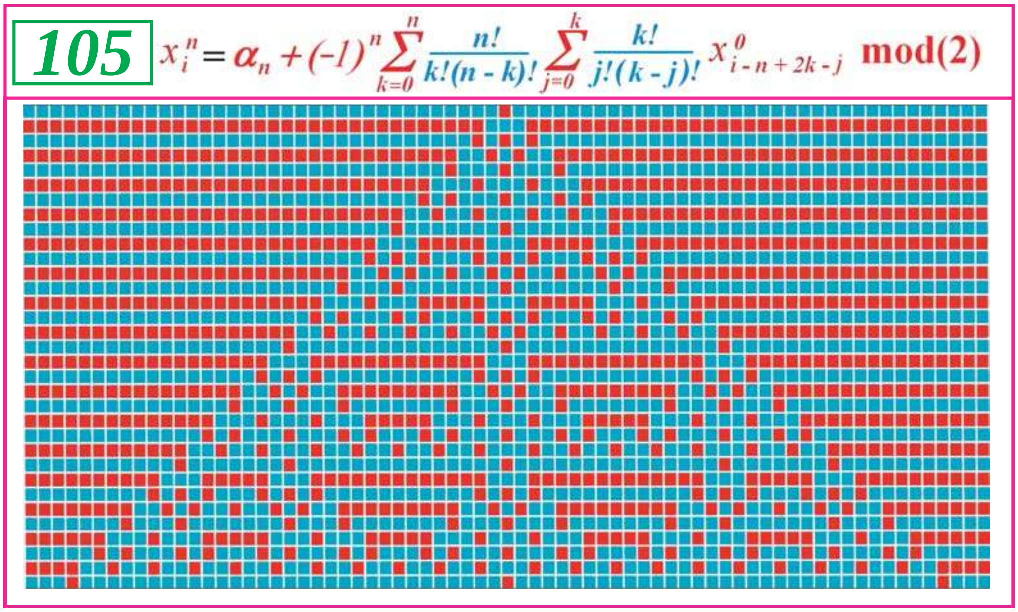

(a)

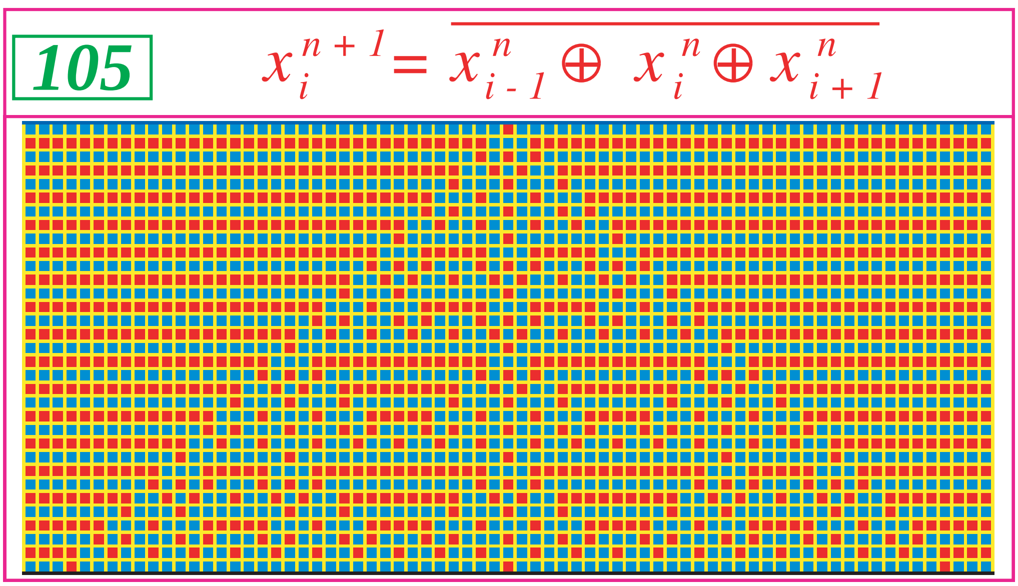

(b)

Table 48. Space-time patterns of $\boxed{105}$ from a *random* initial configuration calculated from the global and local state transition formula, respectively, of rule $\boxed{105}$.

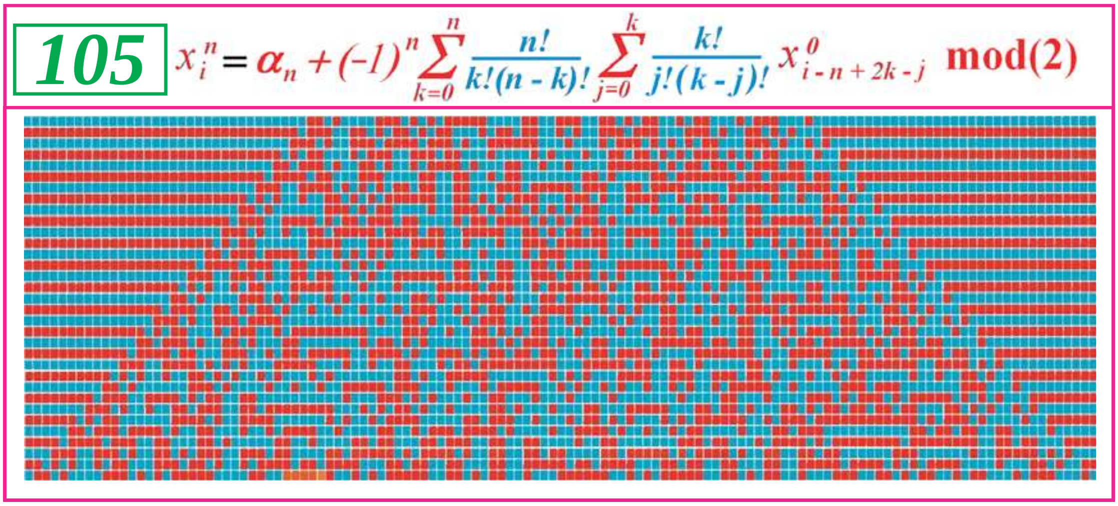

(a)

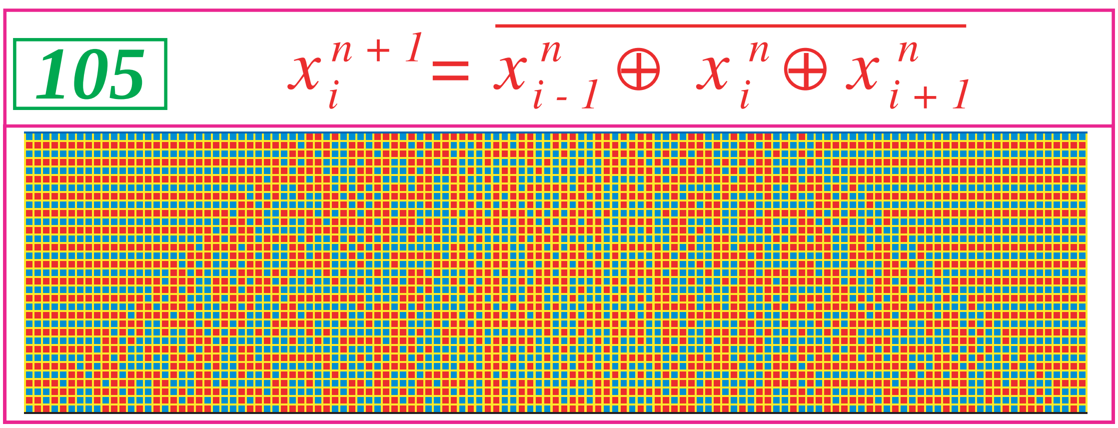

(b)

$$x_i^{m+1} = 2\left(\sum_{k=0}^{m+1} \frac{(m+1)!}{(k)!(m+1-k)!} \sum_{j=0}^{k} \frac{k!}{j!(k-j)!} \bullet x^0_{i-m-1+2k-j}\right) \tag{80}$$

$$+ \sum_{k=0}^{m+1} \frac{(-k) \bullet (m)!}{(k)!(m+1-k)!} \sum_{j=0}^{k} \frac{k!}{j!(k-j)!} \bullet x^0_{i-m-1+2k-j} \tag{81}$$

$$+ \sum_{k=0}^{m} \frac{(m)!}{k!(m-k)!} \sum_{j=0}^{k} \frac{k!}{j!(k-j)!} \bullet x^0_{i+1-m+2k-j} \text{ mod } (2) \tag{82}$$

The first term (80) vanishes under operation **mod (2)** because the multiplier 2 gives rise to all even coefficients. However, let us retain this term until the final computations. The remaining terms are Eqs. (81) and (82).

(b.2) Let us now replace symbol "k" in Eq. (82) by $k' - 1$:

$$x_i^{m+1} = \{\text{Eq. (80)}\} + \left(\sum_{k=0}^{m+1} \frac{(m)!}{(m+1-k)!} \sum_{j=0}^{k} \frac{(-k)}{j!(k-j)!} \bullet x^0_{i-m-1+2k-j} \right.$$

$$\left. + \sum_{k'=1}^{m+1} \frac{(m)!}{(m-k'+1)!} \sum_{j=0}^{k'-1} \frac{1}{j!(k'-1-j)!} \bullet x^0_{i-m-1+2k'-j} \right) \bmod (2) \tag{83}$$

Here we cancel, for convenience, the factorials $k!$ and $(k'-1)!$ from both denominator and numerator. Also we transpose the factor $(-k)$ in the first term, see Eq. (81), to the inner sum.

Now by omitting the prime in k' we can combine the two sums as follows:

$$\sum_{k=0}^{m+1} \frac{(m)!}{(m+1-k)!} \sum_{j=0}^{k} \left(\frac{(-k)}{j!(k-j)!} + \frac{1}{j!(k-1-j)!} \right) \bullet x^0_{i-m-1+2k-j} \bmod (2) \tag{84}$$

The sum of the two binomial coefficients in Eq. (84) gives

$$\frac{-k}{j!(k-j)!} + \frac{1}{j!(k-1-j)!} = \frac{-k+(k-j)}{j!(k-j)!} = \frac{-1}{(j-1)!(k-j)!}.$$

As a result, Eq. (84) transforms to

$$-\sum_{k=0}^{m+1} \frac{(m)!}{k!(m-k+1)!} \sum_{j=0}^{k} \left(\frac{k!}{(j-1)!(k-j)!} \right) \bullet x^0_{i-(m+1)+2k-j} \bmod (2).$$

Here we reinsert the factorial $k!$ in the denominator and in the numerator again.

(b.3) Let us now replace k by $k' + 1$, and j by $j' + 1$ to obtain

$$-\sum_{k'=-1}^{m} \frac{(m)!}{(k'+1)!(m-k')!} \sum_{j'=-1}^{k'} \frac{(k'+1)!}{(j')!(k'-j')!} \bullet x^0_{i-(m+1)+1+2k'-j'} \bmod (2).$$

Replacing m on the right by $m' + 1$ we get

$$-\sum_{k'=-1}^{m'+1} \frac{(m'+1)!}{(k')!(m'+1-k')!} \sum_{j'=-1}^{k'} \frac{(k')!}{(j')!(k'-j')!} \bullet x^0_{i-(m'+1)+2k'-j'} \bmod (2).$$

Observe that at $k' = -1$ and at $j' = -1$, the factorials $(k')!$ and $(j')!$ represented in the denominator are singular, i.e. they are equal to $(-1)!$ Hence, terms with these factorials vanish. Omitting the primes in the symbols m', k' and $j'$and recalling term (80) we obtain finally

$$x_i^{m+1} = 2 \left(\sum_{k=0}^{m+1} \frac{(m+1)!}{(k)!(m+1-k)!} \sum_{j=0}^{k} \frac{k!}{(j)!(k-j)!} \bullet x^0_{i-(m+1)+2k-j} \right)$$

$$- \sum_{k=0}^{m+1} \frac{(m+1)!}{(k)!(m+1-k)!} \sum_{j=0}^{k} \frac{(k)!}{(j)!(k-j)!} \bullet x^0_{i-(m+1)+2k-j} \bmod (2)$$

$$= \sum_{k=0}^{m+1} \frac{(m+1)!}{(k)!(m+1-k)!} \sum_{j=0}^{k} \frac{k!}{(j)!(k-j)!} \bullet x^0_{i-(m+1)+2k-j} \bmod (2) \tag{85}$$

The result is precisely Eq. (71) with m replaced by $m+1$, in the *induction hypothesis* in Eq. (71). ■

4.3. *Rules* $\boxed{150}$ *and* $\boxed{105}$ *are globally quasi-equivalent*

It follows from the *global state transition formulas* (68) for rule $\boxed{150}$ and (69) for rule $\boxed{105}$ that they are *globally equivalent* in the sense that their *space-time* evolution patterns from *any initial bit string* can be derived from each other via the following *affine transformation*

$$\underbrace{\begin{bmatrix} x_0^n(\boxed{105}) \\ x_1^n(\boxed{105}) \\ x_2^n(\boxed{105}) \\ \vdots \\ x_{L-1}^n(\boxed{105}) \end{bmatrix}}_{\boldsymbol{x}(\boxed{105})} = \alpha_n \mathbf{1} + (-1)^n \underbrace{\begin{bmatrix} 1 & \mathbf{0} & \mathbf{0} & \cdots & \mathbf{0} \\ \mathbf{0} & 1 & \mathbf{0} & \cdots & \mathbf{0} \\ \mathbf{0} & \mathbf{0} & 1 & \cdots & \mathbf{0} \\ \vdots & & & \ddots & \vdots \\ \mathbf{0} & \mathbf{0} & \mathbf{0} & \cdots & 1 \end{bmatrix}}_{\widetilde{\boldsymbol{T}} \triangleq (-1)^n \mathbf{1}} \underbrace{\begin{bmatrix} x_0^n(\boxed{150}) \\ x_1^n(\boxed{150}) \\ x_2^n(\boxed{150}) \\ \vdots \\ x_{L-1}^n(\boxed{150}) \end{bmatrix}}_{\boldsymbol{x}(\boxed{150})} \tag{86}$$

where

$$\alpha_n \triangleq \frac{1-(-1)^n}{2} \tag{87}$$

and $\mathbf{1}$ denotes the unit (identity) matrix.

The *inverse* affine transformation is given by:

$$\underbrace{\begin{bmatrix} x_0^n(\boxed{150}) \\ x_1^n(\boxed{150}) \\ x_2^n(\boxed{150}) \\ \vdots \\ x_{L-1}^n(\boxed{150}) \end{bmatrix}}_{\boldsymbol{x}(\boxed{150})} = \alpha_n \mathbf{1} + (-1)^n \underbrace{\begin{bmatrix} 1 & \mathbf{0} & \mathbf{0} & \cdots & \mathbf{0} \\ \mathbf{0} & 1 & \mathbf{0} & \cdots & \mathbf{0} \\ \mathbf{0} & \mathbf{0} & 1 & \cdots & \mathbf{0} \\ \vdots & & & \ddots & \vdots \\ \mathbf{0} & \mathbf{0} & \mathbf{0} & \cdots & 1 \end{bmatrix}}_{\widetilde{\boldsymbol{T}} = (-1)^n \mathbf{1}} \underbrace{\begin{bmatrix} x_0^n(\boxed{105}) \\ x_1^n(\boxed{105}) \\ x_2^n(\boxed{105}) \\ \vdots \\ x_{L-1}^n(\boxed{105}) \end{bmatrix}}_{\boldsymbol{x}(\boxed{105})} \tag{88}$$

Observe that the inverse matrix $\widetilde{\boldsymbol{T}}$ is *itself*.

An analysis of the above global equivalence transformation shows that $\widetilde{\boldsymbol{T}}$ effectively leaves *even-numbered* rows unchanged while complementing the color of all *odd-numbered* rows, for *the same* initial configuration. An example illustrating this transformation is given in Figs. 4 and 5. Consequently, we will henceforth christened $\widetilde{\boldsymbol{T}}$ as an *alternating transformation*. Observe that since $\widetilde{\boldsymbol{T}}$ depends on the *iteration number* "n", it does *not* defined a *topological conjugacy* between the space-time patterns of the two local rules $\boxed{105}$ and $\boxed{150}$. The global quasi-equivalence transformation $\widetilde{\boldsymbol{T}}$ is therefore *weaker* than the three *topologically conjugate* transformations $\boldsymbol{T}^\dagger$, $\overline{\boldsymbol{T}}$ and $\boldsymbol{T}^*$ from the *Vierergruppe* defined in [Chua *et al.*, 2004]. In particular, the number of *connected* components and the *minimal period* of corresponding attractors of $\boxed{105}$ and $\boxed{150}$ *are not* preserved by $\widetilde{\boldsymbol{T}}$, as is evident from the basin-tree diagrams of rules $\boxed{105}$ and $\boxed{150}$. On the other hand, the alternating transformation $\widetilde{\boldsymbol{T}}$ is *not only a bijection* but it also preserves certain qualitative properties; e.g. *gardens of Eden* maps onto *gardens of Eden, transient* bit strings maps onto *transient* bit strings, some *connected period-T* orbits of $\boxed{105}$ maps onto *two disconnected period-$\frac{T}{2}$* orbits of $\boxed{150}$, etc.

In terms of the *real* variables $u_i^n = 2x_i^n - 1$ defined in Eq. (4) of [Chua *et al.*, 2005a], Eq. (88) assumes the following more compact form:

$$\underbrace{\begin{bmatrix} u_0^n(\boxed{105}) \\ u_1^n(\boxed{105}) \\ u_2^n(\boxed{105}) \\ \vdots \\ u_{L-1}^n(\boxed{105}) \end{bmatrix}}_{\boldsymbol{u}(\boxed{105})} = \underbrace{(-1)^n \begin{bmatrix} 1 & 0 & 0 & \cdots & 0 \\ 0 & 1 & 0 & \cdots & 0 \\ 0 & 0 & 1 & \cdots & 0 \\ \vdots & & & \ddots & \vdots \\ 0 & 0 & 0 & \cdots & 1 \end{bmatrix}}_{(-1)^n \mathbf{1}} \underbrace{\begin{bmatrix} u_0^n(\boxed{150}) \\ u_1^n(\boxed{150}) \\ u_2^n(\boxed{150}) \\ \vdots \\ u_{L-1}^n(\boxed{150}) \end{bmatrix}}_{\boldsymbol{u}(\boxed{150})} \tag{89}$$

where

$$\widetilde{\boldsymbol{T}} = \begin{bmatrix} (-1)^n & 0 & 0 & \cdots & 0 \\ 0 & (-1)^n & 0 & \cdots & 0 \\ 0 & 0 & (-1)^n & \cdots & 0 \\ & \vdots & & & \\ 0 & 0 & 0 & \cdots & (-1)^n \end{bmatrix} \tag{90}$$

is the *alternating* transformation.

5. Concluding Remarks

We cannot overemphasize the usefulness of the *basin tree diagrams* presented in Tables 14–23. Indeed, Theorems 3–5 originated from conjectures suggested by Tables 18, 19 and 23. Space limitation precludes a more detailed analysis of the other tables. They will be the subject of future papers.

We wish to remark that in order to make use of the "empty" spaces in these basin-tree diagrams, we have inserted typical space-time patterns, along with their associated *Bernoulli* $\phi_{n-\tau} \mapsto \phi_n$ *return maps*. These maps typically indicate the associated Bernoulli *velocity* σ, the Bernoulli *return time* τ and the Bernoulli *complementation sign* β. Unlike the elementary Bernoulli σ_τ-shifts studied in Parts IV and VI, where these parameters do *not* depend on L, we now find them to depend crucially on L. Moreover, both $|\sigma|$ and τ can assume arbitrarily large values as $L \to \infty$.

The *period* T associated with each σ and τ of the *complex* and *hyper* Bernoulli rules listed in Tables 11 and 12 is generally equal to $T = \tau L$, if $T_0 \triangleq \tau L/|\sigma|$ is not an integer, or $T = \tau L/|\sigma|$ if $|\sigma| \geq 2$. The presence of *symmetry* in a period-T bit string can reduce the *minimal* period T further by a factor of "m" for bit strings made of m identical substrings.

For those space-time patterns which do not exhibit a Bernoulli shift with $|\sigma| > 0$, we can generalize our definition of "Bernoulli σ_τ-shift" to include $\sigma = 0$ for all such *period-*T orbits. In this case, the *return map* $\phi_{n-\tau} \mapsto \phi_n$ will consist of points lying on the *diagonal* line $\phi_n = \phi_{n-\tau}$. We usually include such a graph whenever space permits.

We note also that the period "T" of rules $\boxed{90}$, $\boxed{150}$ and $\boxed{105}$ exhibit a *scale free* property as $L \to \infty$. For example, for $L = 2^m$, the *period* of rule $\boxed{90}$ is always equal $T = 1$ with $\underbrace{0\ 0\ \cdots\ 0}_{L \text{ bits}}$ as its global *fixed point* attractor. To its immediate left $(L = 2^m - 1)$ and immediate right $(L = 2^m + 1)$, the period-T orbits have *equal period* $T = 2^m - 1$, at *any scale* $L \to \infty$. To illustrate the *scale-free distribution* of the period "T" of rule $\boxed{90}$, Fig. 6 shows a plot of log T as a function of log L of the data listed in Table 25. Observe the six *period-1 red stars* on the horizontal axis $(T = 1)$ are located at $L = 2^m$, $m = 2, 3, 4, 5$; namely, $L = 4, 8, 16, 32, 64$, as predicted by Theorem 3. Observe that all data points from Table 25 lie along straight lines with a slope equal to "*one*".

The distributions of the *period* T of rules $\boxed{150}$ and $\boxed{105}$ are plotted in Figs. 7 and 8, respectively, as a function of the *string length* $L = I + 1$, in base-10 logarithmic scales. The data are extracted from Table 37 for rule $\boxed{150}$, and from Table 38 for rule $\boxed{105}$, respectively. Data points corresponding to *isles of Eden* are shown as *blue dots*. Those

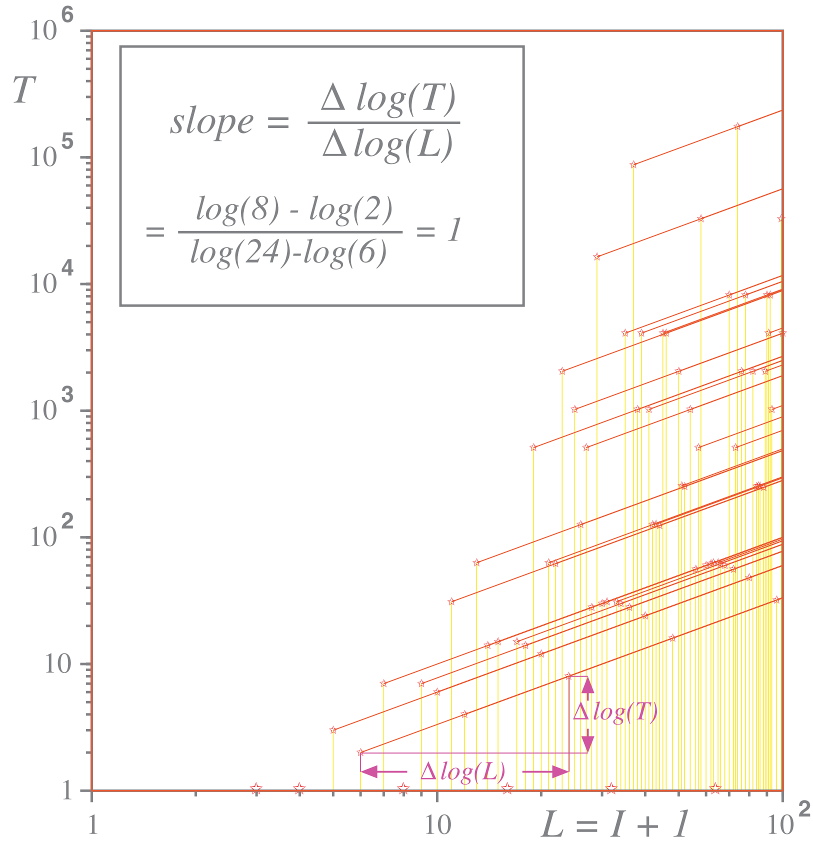

Fig. 6. Relationship between the *period* T and the *length* $L = I + 1$ of *attractors* of rule $\boxed{90}$ plotted in base-10 logarithmic scales.

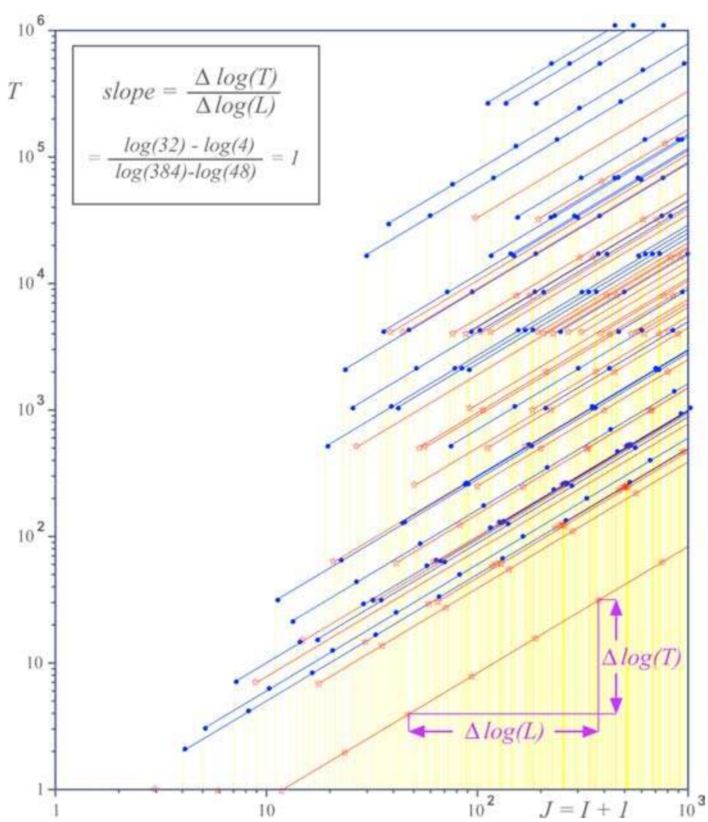

Fig. 7. Relationship between the *period* T and the *length* $L = I + 1$ of *isles of Eden* (plotted as *blue dots*), and *attractors* (plotted as *red stars*) of rule $\boxed{150}$.

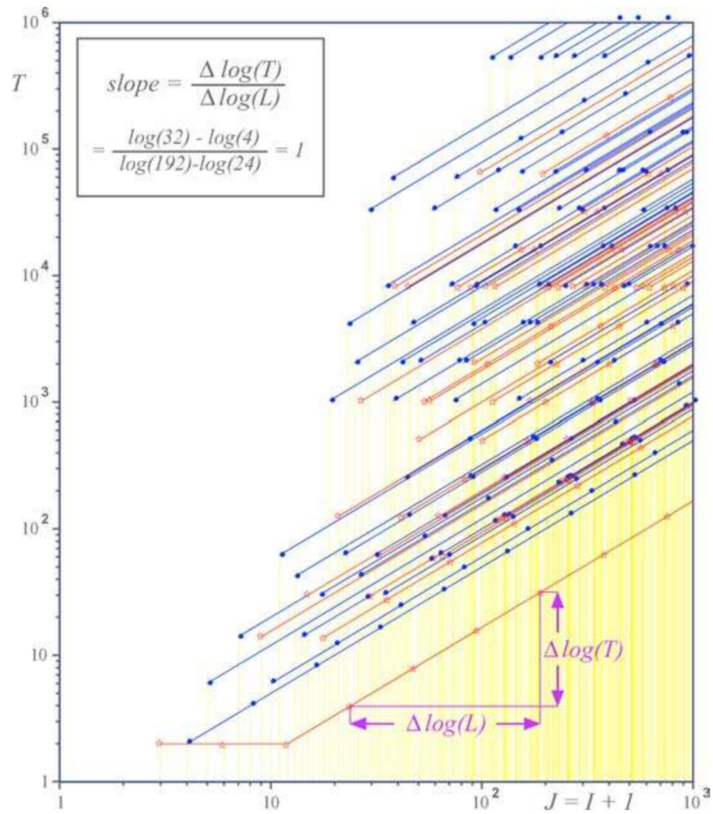

Fig. 8. Relationship between the *period* T and the *length* $L = I + 1$ of *isles of Eden* (plotted as *blue dots*), and attractors (plotted as *red stars*) of rule $\boxed{105}$.

corresponding to *attractors* are shown as *red stars*. Again, the *scale-free* distributions are clearly seen from the parallel straight lines where these data points are located.

References

Adamatzky, A. [2007] "Book review on a nonlinear dynamics perspective of Wolfram's new kind of science," *J. Cellular Automata*, in press.

Chua, L. O. & Roska, T. [2002] *Cellular Neural Networks and Visual Computing* (Cambridge University Press, Cambridge).

Chua, L. O., Yoon, S. & Dogaru, R. [2002] "A nonlinear dynamics perspective of Wolfram's new kind of science. Part I: Threshold of complexity," *Int. J. Bifurcation and Chaos* **12**, 2655–2766.

Chua, L. O., Sbitnev, V. I. & Yoon, S. [2003] "A nonlinear dynamics perspective of Wolfram's new kind of science. Part II: Universal neuron," *Int. J. Bifurcation and Chaos* **13**, 2377–2491.

Chua, L. O., Sbitnev, V. I. & Yoon, S. [2004] "A nonlinear dynamics perspective of Wolfram's new kind of science. Part III: Predicting the unpredictable," *Int. J. Bifurcation and Chaos* **14**, 3689–3820.

Chua, L. O., Sbitnev, V. I. & Yoon, S. [2005a] "A nonlinear dynamics perspective of Wolfram's new kind of science. Part IV: From Bernoulli shift to $1/f$ spectrum," *Int. J. Bifurcation and Chaos* **15**, 1045–1183.

Chua, L. O., Sbitnev, V. I. & Yoon, S. [2005b] "A nonlinear dynamics perspective of Wolfram's new kind of science. Part V: Fractals everywhere," *Int. J. Bifurcation and Chaos* **15**, 3701–3849.

Chua, L. O. [2006] *A Nonlinear Dynamics Perspective of Wolfram's New Kind of Science*, Vol. I (World Scientific, Singapore).

Chua, L. O., Sbitnev, V. I. & Yoon, S. [2006] "A nonlinear dynamics perspective of Wolfram's new kind of science. Part VI: From time-reversible attractors to the arrow of time," *Int. J. Bifurcation and Chaos* **16**, 1097–1373.

Chua, L. O. [2007] *A Nonlinear Dynamics Perspective of Wolfram's New Kind of Science*, Vol. II (World Scientific, Singapore).

Chang, J. & Muthuswamy, B. [2007] "Extracting optimal CNN templates for linearly-separable one-dimensional cellular automata," *Int. J. Bifurcation and Chaos* **17**, 749–779.

Davis, P. J. [1979] *Circulant Matrices* (Wiley-Interscience, NY).

Garay, B. M. & Hofbauer, J. [2003] "Robust permanence for ecological differential equations, minimax, and discretizations," *SIAM J. Math. Anal.* **34**, 1007–1039.

Walker, C. [1971] "Behavior of a class of complex systems: The effect of system size on properties of terminal cycles," *J. Cybern.* **1**, 55–67.

Walker, C. C. & Aadryan, A. A. [1971] "Amount of computation preceding externally detectable steady state behavior in a class of complex systems," *J. Bio-Med. Comput.* **2**, 85–94.

Wolfram, S. [2002] *A New Kind of Science* (Wolfram Media, Inc., Champaign, IL).

Wuensche, A. & Lesser, M. [1992] *The Global Dynamics of Cellular Automata* (Addison-Wesley Publishing Company, Reading, MA).

Appendix

$\boxed{105} \rightleftarrows \boxed{150}$ *Alternating Symmetry Duality*

The bit strings $\{x_0^n, x_1^n, x_2^n, \ldots, x_I^n\}$ and $\{y_0^n, y_1^n, y_2^n, \ldots, y_I^n\}$ generated respectively by rules $\boxed{150}$ and $\boxed{105}$ from *the same* initial state $\{z_0^0, z_1^0, z_2^0, \ldots, z_I^0\}$ obey the following *alternating symmetry relations*:

$$\boxed{\begin{aligned} y_i^n &= \alpha_n + (-1)^n x_i^n \qquad &\text{(A.1)} \\ x_i^n &= \alpha_n + (-1)^n y_i^n \qquad &\text{(A.2)} \end{aligned}}$$

Proof. Bit string $\{x_0^n, x_1^n, x_2^n, \ldots, x_I^n\}$ evolves under rule $\boxed{150}$ via the formula

$$x_i^{n+1} = x_{i-1}^n + x_i^n + x_{i+1}^n \mod (2) \tag{A.3}$$

Bit string $\{y_0^n, y_1^n, y_2^n, \ldots, y_I^n\}$ evolves under rule $\boxed{105}$ via the formula

$$y_i^{n+1} = 1 - (y_{i-1}^n + y_i^n + y_{i+1}^n) \mod (2) \tag{A.4}$$

Changing the symbol "y" in Eq. (A.4) into "x" by applying Eq. (A.1) and invoking the identity $(3\alpha_n) \bmod (2) = \alpha_n \bmod (2)$ we obtain

$$\begin{aligned} &\alpha_{n+1} + (-1)^{n+1} x_i^{n+1} \\ &\quad = 1 - (3\alpha_n + (-1)^n x_{i-1}^n + (-1)^n x_i^n \\ &\qquad + (-1)^n x_{i+1}^n) \mod (2) \\ &\quad = (1 - \alpha_n) - (-1)^n (x_{i-1}^n + x_i^n + x_{i+1}^n) \mod (2) \end{aligned} \tag{A.5}$$

Consider the following two cases:

(a) Assume n is even in Eq. (A.5).

In this case $\alpha_n = 0$ and $\alpha_{n+1} = 1$. Equation (A.5) reduces to:

$$1 - x_i^{n+1} = 1 - (x_{i-1}^n + x_i^n + x_{i+1}^n) \mod (2) \tag{A.6}$$

Hence,

$$x_i^{n+1} = (x_{i-1}^n + x_i^n + x_{i+1}^n) \mod (2) \tag{A.7}$$

(b) Assume n is odd in Eq. (A.5).

In this case $\alpha_n = 1$ and $\alpha_{n+1} = 0$. Equation (A.5) reduces to:

$$x_i^{n+1} = (x_{i-1}^n + x_i^n + x_{i+1}^n) \mod (2) \tag{A.8}$$

Hence, both Eqs. (A.7) and (A.8) are identical to Eq. (A.3).

Following the same procedure let us change the symbol "x" in Eq. (A.3) into "y" by applying Eq. (A.2) to obtain

$$\begin{aligned} &\alpha_{n+1} + (-1)^{n+1} y_i^{n+1} \\ &\quad = (3\alpha_n + (-1)^n y_{i-1}^n + (-1)^n y_i^n \\ &\qquad + (-1)^n y_{i+1}^n) \mod (2) \\ &\quad = \alpha_n + (-1)^n (y_{i-1}^n + y_i^n + y_{i+1}^n) \mod (2) \end{aligned} \tag{A.9}$$

Again, we must consider two cases:

(a) Assume n is even in Eq. (A.9).

In this case $\alpha_n = 0$ and $\alpha_{n+1} = 1$. Equation (A.9) reduces to:

$$1 - y_i^{n+1} = (y_{i-1}^n + y_i^n + y_{i+1}^n) \mod (2) \tag{A.10}$$

Hence,

$$y_i^{n+1} = 1 - (y_{i-1}^n + y_i^n + y_{i+1}^n) \mod (2) \tag{A.11}$$

(b) Assume n is odd in Eq. (A.9).

In this case $\alpha_n = 1$ and $\alpha_{n+1} = 0$. Equation (A.9) reduces to:

$$0 + y_i^{n+1} = 1 - (y_{i-1}^n + y_i^n + y_{i+1}^n) \mod (2) \tag{A.12}$$

Hence, both Eqs. (A.11) and (A.12) are identical to Eq. (A.4). ■